Investigating the role of iASPP in cutaneous disorders

Zinaida Dedeić

A thesis submitted for the degree of
Doctor of Philosophy

Merton College
Ludwig Institute for Cancer Research
Nuffield Department of Clinical Medicine
University of Oxford

Trinity Term 2014

Investigating the role of iASPP in cutaneous disorders

Zinaida Dedeić, Merton College
DPhil in Clinical Medicine, Trinity Term 2014

Abstract

Desmosomes are intercellular junctions that anchor intermediate filaments to the sites of intercellular contacts. They are critical for maintaining the integrity of tissues that experience constant mechanical and structural stresses, like the skin and heart. Perturbation of desmosomal adhesion can lead to devastating epidermal and myocardial diseases. However, little is known about the regulators of desmosomes and the role of desmosomes in cell signalling events.

Recent work has suggested that iASPP, an inhibitor of the p53 family of proteins, localises at the intercalated discs where desmosomes reside. However, its role at the desmosomes has remained elusive. Thus, in this thesis, it was investigated whether iASPP is a dual function protein that links desmosome adhesion to gene expression and if desmosome-related diseases develop in the absence of iASPP. iASPP was found to be a novel regulator of desmosomes, co-localising with them by physically interacting with the desmosomal components desmoplakin and K5 intermediate filaments. Loss of iASPP resulted in increased phosphorylation and solubilisation of desmoplakin, leading to the formation of K5 aggregates. This culminated in disrupted intercellular adhesion and enhanced cellular migration. Consistent with the role of iASPP in the maintenance of desmosomal adhesion integrity, focal palmoplantar keratoderma was observed in iASPP-deficient mice — a disorder often associated with desmosome dysfunction. This was accompanied by disrupted intracellular signalling, as exemplified by the disrupted expression of differentiation markers; an increase in the thickness of cell layers expressing differentiation marker K1 was noted, and K5 and K6 cells were ectopically expressed throughout the diseased palmoplantar epidermis. Impaired intercellular adhesion and migration had consequences for wound healing, as iASPP-deficient mice exhibited delayed wound closure. Furthermore, defects in eyelid closure in iASPP-deficient mice were found to be due to increased apoptosis. The localisation of apoptotic cells at the leading edge of the eyelid epidermis implied that apoptosis might have occurred due to a loss of cell-matrix or cell-cell contact, i.e. anoikis. Taken together, these results suggest that iASPP is involved in pathological (palmoplantar keratoderma), physiological (wound healing) and developmental processes (embryonic eyelid closure) through its regulation of desmosomes and their dynamics. Therefore, iASPP represents a new candidate gene in cutaneous disorders and could be implicated in a variety of epidermal and myocardial diseases.

Declaration

All the material presented in this thesis is the result of my own work, except where specifically indicated here and in the corresponding sections:

1. The transmission electron microscopy of epidermal desmosomes from iASPP$^{+/+}$ and iASPP$^{\Delta 8/\Delta 8}$ littermates illustrated in Figure 3.3A in Chapter III was done by Dr Mario Notari and Prof. David Ferguson.
2. The bar graph in Figure 3.3D in Chapter III representing keratin aggregation in primary keratinocytes includes four independent experiments, where two of those experiments were performed by a former laboratory member Dr Ying Hu and two were performed by me. Values obtained from all four experiments are represented. The bar graph also includes data from a different cell line, namely IMOK. This experiment was performed solely by me.
3. The wound healing procedure on iASPP-deficient mice only, reported in Figure 4.2 of Chapter IV required the experiment to be performed using sterile technique. This made it necessary to seek help from laboratory members to perform the procedure under aseptic conditions. Therefore, I made the wound incisions while fellow laboratory member Kathryn Chung assisted me in performing the procedure by monitoring the depth of anaesthesia in animals undergoing the procedure and by helping me achieve sterile technique.
4. The Home Office encourages us to reduce the number of animals used in the studies. To observe this practice in the table included as part of the Figure 5.5 in Chapter V, some of the animals included in the count were maintained by fellow laboratory member Kathryn Chung.

Contributions by the aforementioned colleagues are clearly indicated in the text of the thesis at the relevant points. None of the work presented in this thesis has been accepted or submitted for any degree, diploma or certificate or other qualification in this University or elsewhere. This thesis does not exceed 50,000 words, exclusive of bibliography, as recommended by the Medical Sciences Division.

Zinaida Dedeić 2014

Acknowledgments

First and foremost, I would like to express my gratitude to my supervisor Prof. Xin Lu for guiding, challenging and inspiring me over the past four years and for giving me this great opportunity to complete my DPhil in her laboratory. I also wish to acknowledge the financial support I received from the Ludwig Institute for Cancer Research and Nuffield Department of Clinical Medicine, without which this DPhil would not have been possible.

I would like to extend my gratitude to my examiners Professors Elizabeth Robertson and David Kelsell for their time and effort.

A massive thank you to the current and past members of the Lu and other laboratories on the first floor of the Ludwig Institute for providing a supportive, fun and educational environment to work in. In particular, thanks go to Luca Tordella, Ewa Dudziec, Emma Morris from Banbury, Sofaia Koch, Chris Royer, Anna Banana, Mario Notari, Gopi Sutendra, Paul Miller, Liz Slee, Emmanoula Repapi, Anna Grawenda, Jorge Zeron, Beatriz Diez and Katrin Bagola. A special mention goes to Kath Chung, with whom I have overlapped during my entire DPhil and have shared many excitements and commiserations over research projects and results.

I wish to acknowledge the colleagues who helped me during various stages of my DPhil. Mario Notari and Ying Hu for providing guidance during the first year of my studies. Gopi Sutendra for his valuable advice, suggestions and critical reading of parts of my thesis. Paul Miller for reading and commenting on parts of my thesis, and for his engaging scientific and non-scientific discussions over the past few years. I would also like to thank Sasha Aljakna, Ellen Leffler and Marsha Wallace for their useful suggestions on sections of my thesis.

Thanks must also be given to Mark Shipman, for his help with microscopy and image analysis, Indi Ratnayaka, for her assistance with histology, and Claire Beveridge, for critical reading of this thesis. Many thanks to Ludwig's past and present support and administration team including Alex Ward, Neil Carveth, Jan Twitchen, Evelyn Harvey, Mark McDermott, James Hall and Stan Ng. Special thanks to Veronica Counsell for her help and for being a constant source of support and encouragement.

I must thank my family; my parents Šemso and Ćama, siblings Edo, Dita and Aljo, siblings in law Adela and Sajo, nephews Rijo and Hamza and nieces Rijalda and Penny for their love, encouragement and support. I am very grateful to my parents for always believing in me and letting me wander off 13 years ago into the big world certain that I will make the best of it.

Lastly, but by no means least, my deepest gratitude goes to my husband Danny Wilson for his unconditional love, tireless patience, enthusiasm, support and encouragement, which has helped me to stay positive and excited during sometimes infuriating and demanding times. Thanks also go to him for reading and giving suggestions on parts of my thesis, and for asking my parents in-law Brian and Janty to kindly read sections of it as well.

I am indebted to you all for your invaluable contributions without which this DPhil would not have been achievable. Thank you all very much.

Glossary of acronyms

ADAM17	A disintegrin and metalloproteinase 17
APS	Ammonium persulphate
ARVC	Arrhythmogenic right ventricular cardiomyopathy
ASPP	Apoptosis stimulating proteins of p53
ASPP1	Apoptosis stimulating proteins of p53 1
ASPP2	Apoptosis stimulating proteins of p53 2
BBP	Bcl-2 binding protein
Bcl2	B-cell lymphoma 2
BPAG1e	Bullous pemphigoid antigen 1e
BPAG2	Bullous pemphigoid antigen 2
BrdU	Bromodeoxyuridine
Ca^{+2}	Calcium
cDNA	Complementary DNA
Cre/*LoxP*	Cyclisation recombination/locus of X-over P
C-terminus	Carboxy terminus
DAPI	4',6-diamidino-2-phenylindole
DBD	DNA-binding domain
DMEM	Dulbecco's modified Eagle's medium
DMSO	Dimethyl sulfoxide
DNA	Deoxyribonucleic acid
dNTP	Deoxyribonucleotide phosphate
DSP	Desmoplakin
DSC	Desmocollin
DSG	Desmoglein
E-cadherin	Epithelial cadherin
EDTA	Ethylene diamine tetraacetic acid
EGF	Epidermal growth factor
EGFR	Epidermal growth factor receptor
EGTA	Ethylene glycol tetraacetic acid
ERK1/2	Extracellular signal-related protein 1/2
FBS	Fetal bovine serum
g	Gramme
GFP	Green fluorescence protein
GSR	Glycine–serine–arginine-rich domain
H&E	Haematoxylin and eosin
HB-EGF	Heparin binding EGF-like growth factor
HCM	High calcium media
I	Insoluble
IA	Intercellular anchor
iASPP	Inhibitory apoptosis stimulating proteins of p53
iASPP CreER	$iASPP^{loxP/loxP}$ $Cre^{+}ER^{T}$
ICS	Intracellular catenin-binding segment

IF	Intermediate filament
IMOK	Immortalised mouse oral keratinocytes
IP	Immunoprecipitation
K1	Keratin 1
K5	Keratin 5
K6	Keratin 6
K10	Keratin 10
K16	Keratin 16
K17	Keratin 17
kDa	Kilodalton
L	Linker region
L	Litre
LCM	Low calcium media
LEF	Lymphoid enhancer-binding factor
M	Molar
µg	Microgramme
mg	Milligramme
min	Minute
µl	Microlitre
ml	Millilitre
mM	Millimolar
MEF	Mouse embryo fibroblast
NaOH	Sodium hydroxide
N-cadherin	Neuronal cadherin
NFκB	Nuclear factor of kappa light polypeptide gene enhancer in B-cells
N-terminus	Amino terminus
OD	Oligomerisation domain
PBS	Phosphate buffered saline
P-cadherin	Placental cadherin
PCR	Polymerase chain reaction
pERK1/2	Phosphorylayed extracellular signal-related protein 1/2
PG	Plakoglobin
PKA	Protein kinase A
PKC	Protein kinase C
PKP	Plakophilin
PP1	Protein phosphatase 1
PPK	Palmoplantar keratoderma
PRD	Plakin repeat domain
RaDAR	RanGDP Ankyrin Repeat
RAI	RelA-associated inhibitor
RNA	Ribonucleic acid
RT-qPCR	Real time quantitative polymerase chain reaction
RV	Right ventricle
S2849	Serine 2849
S2849G	Serine 2849 –> Glycine

S	Serine
S	Soluble
SAM	Sterile alpha-motif
SCC	Squamous cell carcinoma
SDS-PAGE	Sodium dodecyl sulfate-polyacrylamide gel electrophoresis
SEM	Standard error of the mean
SH3	Src homology domain 3
siRNA	Small interfering RNA
SPPK	Striate palmoplantar keratoderma
TAD	Transactivation domain
TBS	Tris-buffered saline
TCF	T-cell factor
TGFα	Transforming growth factor alpha
TID	Transcription inhibitory domain
TL	Total lysate
TM	Transmembrane domain
TNFR	Tumour necrosis factor receptor
TPA	12-O-tetradecanoyl-13-phorbol acetate
TUNEL	Terminal deoxynucleotidyl transferase dUTP nick end labelling
Ub	Ubiquitin
UV	Ultraviolet
VE-cadherin	Vascular endothelial cadherin
WH	Woolly hair
Wnt	Wingless-type
Y	Tyrosine

Table of contents

List of figures

List of tables

Chapter I: General Introduction

Overview and significance

For proper development and healthy functioning, skin and heart tissue must be supple yet maintain sufficient strength to cope with the persistent mechanical forces that they endure. Their ability to withstand this mechanical exertion relies heavily on the maintenance of intact and robust intercellular adhesions. Perturbations of intercellular connectivity due to genetic mutations in adhesion components can lead to epidermal and myocardial conditions including cancer, in both animal models and humans. These conditions are particularly prominent when genetic mutations occur in components of desmosome junctions, thereby impairing the integrity of cell-cell adhesion (Lai-Cheong *et al.*, 2007; Nitoiu *et al.*, 2014).

Desmosomes are a type of cellular interaction that join adjacent cells together and link the plasma membrane to the stress-bearing intermediate filament cytoskeleton. In so doing, they connect the intermediate filament network across many cells and distribute structural stresses throughout the tissue. In the skin, desmosomes form part of the body's physical barrier to the external environment, and provide resistance to mechanical strains endured during development, activity, homeostasis and wound healing (Al-Jassar *et al.*, 2013). In the heart, desmosomes are required to maintain tissue integrity for the potentiation of mechanical and electrical activity, thereby allowing the heart to perform its spatiotemporal coordinated contractions (Delmar and McKenna, 2010).

Mutations in desmosomal junction components in both humans and genetically engineered mice can lead directly to life-threatening diseases, including arrhythmogenic right ventricular cardiomyopathy (ARVC) and cutaneous disorders associated with tissue fragility (Al-Jassar *et*

al., 2013; Brooke *et al.*, 2012; Nitoiu *et al.*, 2014). The incidence of ARVC reaches 500 in 100,000 in parts of Europe, notably Northern Italy and Germany, and has attracted considerable attention as a major cause of sudden death in young athletes. To date, most of the genetic mutations that lead to ARVC have been found in desmosome components, leading clinicians and researchers to call ARVC "the disease of the desmosome" (Herren *et al.*, 2009).

Desmosome-mediated adhesion therefore helps to maintain tissue architecture, integrity and healthy function. Yet the function of desmosomes extends beyond their roles in adhesion and the maintenance of structural tissue integrity. Desmosome components are active participants in processes of tissue morphogenesis and homeostasis. During wound healing and morphogenetic developmental processes desmosomes are remodelled to facilitate cell migration (Garrod *et al.*, 2005). Loss of desmosome molecules can affect multiple cellular events, including proliferation, apoptosis and migration (Dusek *et al.*, 2007a; Wan *et al.*, 2007; Weiske *et al.*, 2001). Furthermore, the expression patterns of individual desmosome components within the skin is specialized across cell types, implicating these components in differentiation-specific functions that transcend their roles in adhesion (Dusek *et al.*, 2007b).

Desmosomes are thought to play an important role in suppressing tumour growth and its progression to malignancy. The expression of desmosome components is altered in many types of carcinoma, and experimental studies have shown that the induction of desmosome adhesion in invasive cancer cell lines can mitigate invasive behaviour (Tselepis *et al.*, 1998). It is postulated that the earliest steps in cancer dissemination and metastasis involve the dissolution of desmosome junctions, followed by disassembly of other intercellular adhesions, allowing cancerous cells to dissociate from the tissue and travel to other sites in the body (Chun and Hanahan, 2010; Dusek and Attardi, 2011).

Desmosome components are involved in signalling pathways that regulate apoptosis, proliferation and migration, events that are critical for controlling tumour progression and cardiocutaneous disorders. Understanding the link between desmosome dysfunction and the regulation of these cellular processes is an important avenue for research into these diseases. Desmosome function has been the focus of extensive research, but continued work in this area suggests that additional regulators of desmosomes exist. Further research is required to elucidate these novel desmosomal proteins and their roles in adhesion, signalling and the regulation of cellular processes. These novel genes represent candidates that may fill gaps in our knowledge as to how desmosomal genes switch between their adhesive and signalling functions. Pursuing this line of research has great potential for improving our biological understanding of cell adhesion and signalling, as well as identifying new avenues for pharmaceutical research directed towards the management of cancer progression and cardiocutaneous diseases.

Here it is proposed that the Apoptosis Stimulating Protein of P53 (ASPP) family, in particular the inhibitory ASPP (iASPP) protein, provides such a link. Several observations support this proposition. Firstly, iASPP deficiency resembles deficiencies in desmosome components and is associated with cardiocutaneous disorders (Herron *et al.*, 2005; Simpson *et al.*, 2009a). Secondly, iASPP localises to myocardial intercalated discs where desmosomes reside, and its loss in mice has been found to lead to ARVC (Notari, 2012). Thirdly, iASPP shuttles between cell compartments including the nucleus, cytoplasm and cell-cell junctions, and is involved in gene regulation (Chikh *et al.*, 2011; Notari *et al.*, 2011). Finally, loss of junctional iASPP and its increased nuclear expression has been linked to prostate cancer progression and poor clinical outcome (Morris, 2013). Taken together, these observations suggest that iASPP might be a good candidate for explaining the link between desmosome adhesion and intracellular signalling. It follows that understanding the molecular mechanisms by which iASPP participates

in desmosome regulation and gene expression could contribute to the development of future therapeutic and diagnostic tools for the management of desmosome-related disorders. The focus of this thesis is, therefore, to explore and establish the role of iASPP in the regulation of desmosome adhesion and gene expression using a combination of microscopic, functional and molecular techniques.

In the subsequent sections of this chapter, background material concerning skin structure and homeostasis is presented. This is followed by a description of cellular junctions that hold the skin together, with a focus on desmosomes. The regulation of desmosome assembly and the players involved are discussed, and mutations that lead to desmosome-related diseases are highlighted. This concludes with the introduction of the ASPP protein family and their roles in development, cell-cell junctions, and tumourigenesis.

Background

1.1 Mammalian skin: an overview

The skin represents the largest and most multifaceted organ of the body. It covers the outside of the body, protecting it from fluid loss, microbial incursion and mechanical trauma, and keeps our internal systems intact (Fuchs, 2007). Moreover, the skin senses the environment and communicates this information to the brain, resulting in our perception of pain, pleasure, temperature and form (Lumpkin and Caterina, 2007). The skin consists of three layers: the epidermis, dermis and hypodermis. The separation between the epidermis and dermis is provided by a basement membrane, which is a composite of proteins secreted by both epidermal and hypodermal cells. The dermis and hypodermis are composed of connective tissue, hair follicles, various glands, nerves and blood vessels. They are important in absorbing mechanical stress, providing nourishment to the skin and in regulating internal organ and body temperature (Blanpain and Fuchs, 2006). The epidermis fulfils the skin's role as a primary physical barrier that protects our body from dehydration, noxious stimuli and microbial assaults. Subjected to a plethora of harmful agents, the epidermis must maintain itself and preserve its barrier function. It accomplishes this by undergoing continual self-renewal to replenish lost or old cells by a process of homeostasis, and resurfaces wound sites in cases of injury (Blanpain and Fuchs, 2009; Fuchs, 2007; Koster and Roop, 2007). During the homeostatic process, proliferative cells lying on top of the basement membrane migrate outwards and undergo terminal differentiation and stratification, to be ultimately discarded from the skin’s surface (Koster and Roop, 2007).

1.1.1 Epidermal stratification

Epidermal stratification is a process by which layers of epithelial cells are formed and maintained atop a basement membrane. These epithelial layers are divided into: basal, spinous, granular, and the outermost cornified layer. Each layer contains cells, namely keratinocytes, with different proliferative capacities, gene expression profiles and adhesive properties (Figure 1.1).

The basal layer consists of highly proliferative keratinocytes that are characterised by the expression of p63, keratin 5 (K5) and keratin 14 (K14). K5 and K14 assemble into organised but relatively sparse filaments that attach to the basement membrane and adjacent cells via hemidesmosomes and desmosomes, respectively (Fuchs, 1990). A subset of basal cells detaches from the basement membrane and progresses upwards to form the spinous layer.

Keratinocytes in the spinous layer exit the cell cycle and switch their production of keratins, downregulating K5 and K14 and upregulating their expression of keratin 1 (K1) and keratin 10 (K10). In comparison with basal cells, filaments formed by K1 and K10 in spinous cells are denser and make up a considerable volume of cytoplasmic contents. These filaments connect to desmosomes, which are also more abundant in the spinous layer, forming a robust cell-cell junction network that is able to resist mechanical stress. Downregulation of p63 is apparent in this layer (Blanpain *et al.*, 2007; Fuchs and Green, 1980; Koster and Roop, 2007). The expression of other keratins such as keratin 6 (K6), keratin 16 (K16) and keratin 17 (K17) can be observed in the spinous layer, although only during wound healing, which is characterised by hyperproliferation and cell migration (Mazzalupo *et al.*, 2003). Cells in the upper spinous layers produce lamellar granules that contain lipids and glycoproteins (e.g. corneodesmosin). The contents of these granules are released in the intercellular space only once spinous cells reach

the cornified layer (Swartzendruber *et al.*, 1989). Upper spinous cells transit outwards and differentiate further, forming granular layers.

Granular keratinocytes are characterised by the synthesis of electron dense keratohyalin granules, which are composed of profilaggrin, loricrin and keratins. Other proteins produced in granular cells include transglutaminases and proteins such as: envoplakin, periplakin, involucrin, small proline-rich protein (SPR) and loricrin, which form the cornified envelope of the future cornified cell. Processing of profilaggrin into filaggrin marks the transit of granular cells into the cornified layer. Processed filaggrin packs keratin filaments into dense macrofibrillar cables (Candi *et al.*, 2005; Resing *et al.*, 1985).

The cornified layer of cells is formed in the final step of epidermal stratification. In this layer, calcium-activated transglutaminases cross-link the envelope proteins to generate a tough proteinaceous envelope that encloses the keratin macrofibrillar cables. This envelope serves as a scaffold for lipids and glycoproteins extruded from the lamellar bodies. The lipids glue together the envelope proteins, generating a continuous and impermeable surface coat on the epidermis (Candi *et al.*, 2005; Eckert *et al.*, 2005; Kalinin *et al.*, 2002; Segre, 2003). To finalise the process, the cornified cells degrade intracellular components, including the nucleus. Therefore, the major constituents of the cornified cell are tightly packed keratin macrofibrillar cables that are enclosed by a cornified envelope, which is held together, in part, by corneodesmosomes. The cornified layer cells are eventually shed from the surface but are continuously replenished by differentiating cells from underneath, ensuring maintenance of the barrier function (Blanpain and Fuchs, 2009; Fuchs, 2007).

The induction of epidermal stratification is triggered by an increasing calcium gradient from basal cells outwards. This gradient also promotes the formation and reinforcement of cell-cell adhesions (Celli *et al.*, 2010; Koster and Roop, 2007; Savignac *et al.*, 2011).

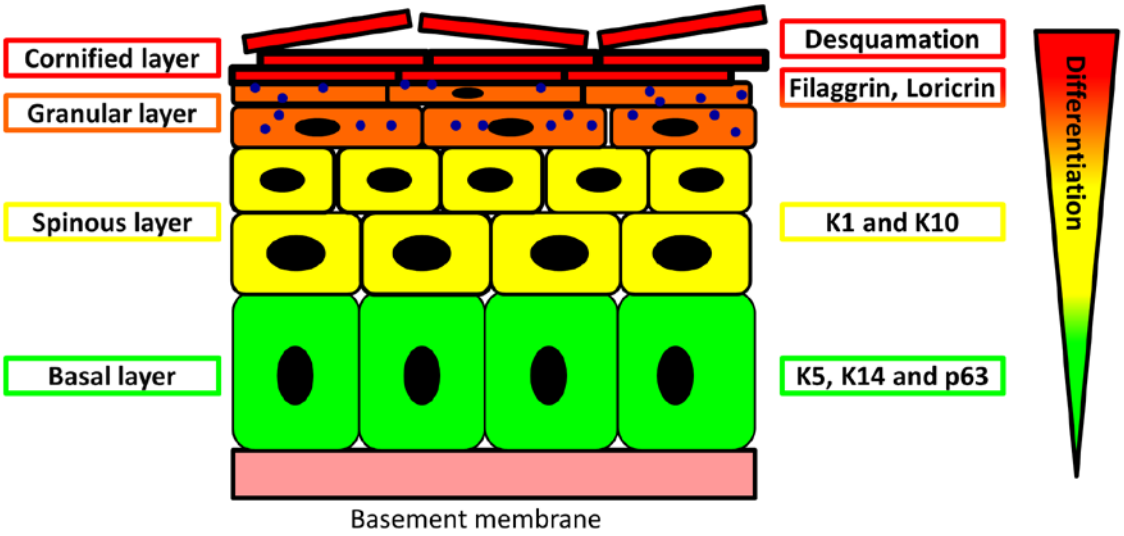

Figure 1.1 Epidermal stratification and the expression of layer-specific protein markers
The epidermis is composed of a number of stratified cell layers: basal, spinous, granular and cornified. Each layer is characterised by a different protein expression profile, indicated on the right-hand side of the respective cellular layer. Proliferative cells of the basal layer are responsible for replenishing cells lost during the process of desquamation at the cornified layer.

1.1.2 p63: a master regulator of epidermal stratification

The coordination of changes in gene expression that accompany epidermal stratification is tightly controlled by transcription factors. A key transcriptional regulator of epidermal stratification is p63, a member of the tumour suppressor p53 family comprising p53 and p73, in addition to p63. The essential role of p63 in epidermal development and homeostasis is evidenced by the developmental defects observed in humans and animal models with dysfunctional p63. Craniofacial and skeletal abnormalities, together with a complete lack of all stratified epithelia and its derivatives, can be observed in p63-deficient mice. As a consequence of absent epithelial stratification and concurrent barrier dysfunction, these mice die from dehydration hours after birth (Mills *et al.*, 1999; Yang *et al.*, 1999). Similarly, human patients carrying mutations in the p63 gene present with ectrodactyly, ectodermal dysplasia and cleft lip, and ankyloblepharon-ectodermal dysplasia-clefting syndrome (Celli *et al.*, 1999; Koster, 2010)). In addition, Yang *et al.* have identified about 5,800 target sites that p63 has the potential to bind to. These targets included genes that regulate proliferation, apoptosis, differentiation and cell-cell adhesion (Yang *et al.*, 2006). This study, and the array of phenotypes observed in both human and mice, emphasise the multitude of processes that p63 may regulate. However, the molecular mechanisms that p63 utilises to regulate these processes are still under investigation, complicated due to the existence of at least six different p63 isoforms.

1.1.2.1 The isoforms and architecture of p63

The p63 isoforms can be classified into two categories: TAp63 and ΔNp63. They result from transcription from two different promoters. TAp63 isoforms contain a transactivation domain (TAD), DNA-binding domain (DBD) and oligomerisation domain (OD). ΔNp63 isoforms differ from TAp63 isoforms in that their N-terminus is shorter and lacks the main TAD domain, but

contains an alternative transactivation domain (Duijf *et al.*, 2002). At the C-terminus, both TAp63 and ΔNp63 isoforms can be alternatively spliced to generate α, β and ɣ variants (Figure 1.2A (Yang *et al.*, 1998)). The longest α variant of both TAp63 and ΔNp63 isoforms contains a sterile-alpha motif (SAM) and a transcription inhibitory domain (TID). The SAM motif mediates protein-protein interactions and has been implicated in development. Mutations in the SAM domain of p63 have been reported in patients with ankyloblepharon-ectodermal dysplasia-clefting syndrome (Fomenkov *et al.*, 2003). The TID domain in the C-terminus inhibits transcription by binding to and masking a few residues in the TAD domain of TAp63 isoforms (Straub *et al.*, 2010).

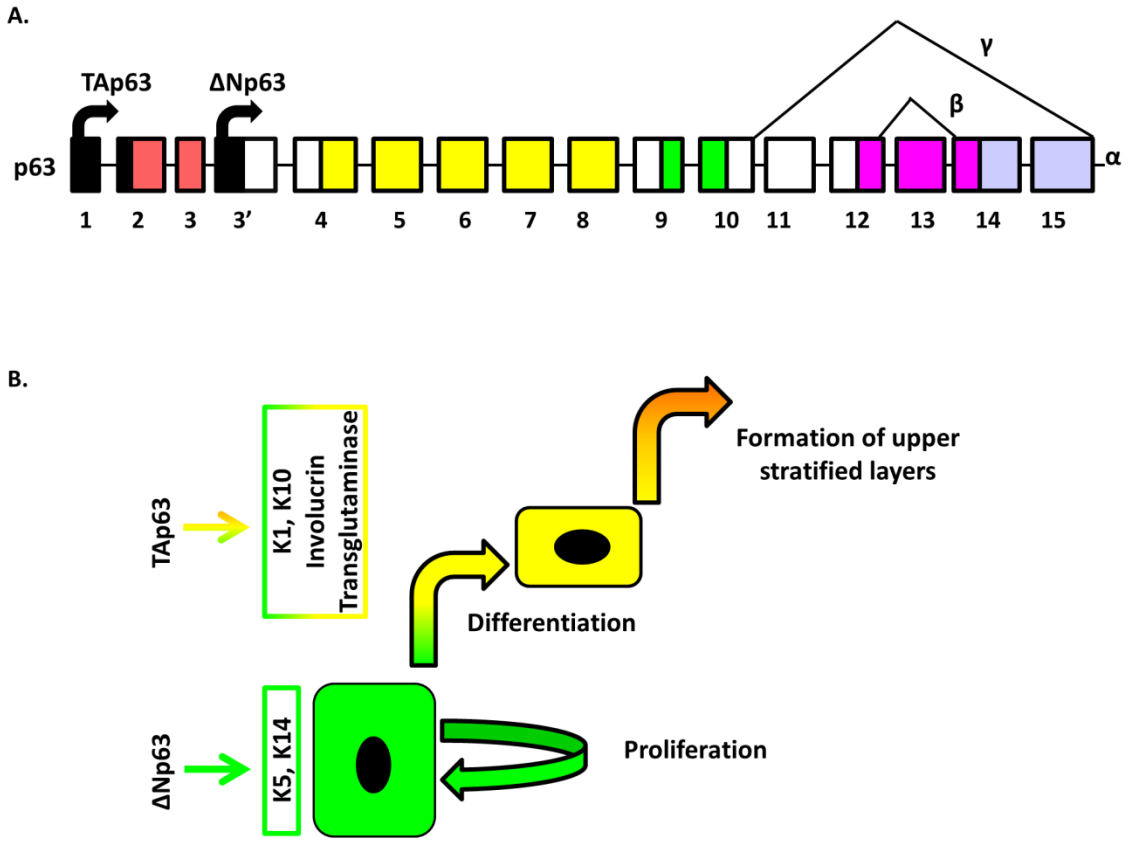

Figure 1.2 The p63 isoforms and their proposed functions

A. p63 contains two alternative promoters: the first is proximal to the transactivation domain (TAD, in orange) and transcribes the TAp63 isoforms, while the second one lies just after the TAD and transcribes the isoforms with truncated TAD, termed ΔNp63 isoforms. Each isoform has three splice variants α, β, and γ, resulting from alternative splicing of its C-terminus. All isoforms contain a DNA-binding domain (DBD, in yellow), and oligomerisation domains (OD in green). The α isoform of both TAp63 and ΔNp63 contain a sterile alpha motif (SAM in pink), and transcription inhibitory domain (TID in purple). **B.** Both TAp63 and ΔNp63 isoforms are necessary for epidermal development. ΔNp63 isoforms are believed to regulate the proliferation of basal cells and the expression of basal cell markers (K5, K14), while TAp63 isoforms are thought to facilitate epidermal differentiation through the regulation of differentiation markers (K1, K10, involucrin, transglutaminases). Adapted from Candi *et al.,* 2006.

1.1.2.2 Function of the p63 isoforms in epidermal stratification

Over the past ten years, great strides have been made in deciphering the individual functions of the TAp63 and ΔNp63 transcripts. This has been done using animal models in which individual p63 isoforms were ablated or introduced in a p63-deficient background (Candi *et al.*, 2006; Romano *et al.*, 2012; Su *et al.*, 2009). Candi *et al.* neatly showed that, by introducing ΔNp63α into p63-deficient mice, they were able to partially reverse the phenotype of p63-deficient mice and substantially rescue the development of the basal layer. In contrast, the introduction of TAp63α in p63-deficient mice was insufficient to reverse the phenotype, and no epidermal development was observed. Introduction of both ΔNp63α and TAp63α in p63-deficient mice resulted in the formation of both the basal and spinous layers. These results suggested that ΔNp63α promotes the proliferation of progenitor cells and formation of the basal layer, while TAp63α regulates differentiation of the stratified epidermis. Examination of transcriptional targets of either ΔNp63α or TAp63α corroborated this hypothesis. ΔNp63α was found to mainly regulate the expression of basal keratinocyte markers such as K14 and K5, while TAp63α was shown to mediate the expression of differentiation markers including K1, K10, involucrin and profilaggrin (Candi *et al.*, 2006). Similar findings were reported by Romano *et al.*, which showed that the ablation of ΔNp63α in mice resulted in a poorly developed stratified epidermis and lack of epidermal derivatives, a phenotype observed in mice lacking all p63 isoforms (Romano *et al.*, 2012). The emerging theme from these studies is that both TA- and ΔN-isoforms are important in epidermal development; ΔNp63 is thought to regulate progenitor cell expansion and early development of the epidermis, while TAp63 is believed to direct differentiation of the stratified epidermis (Figure 1.2B). This is further supported by the expression profile of p63 isoforms. ΔNp63 is expressed earlier in development than TAp63, and ΔNp63 is the prevailing isoform in the basal layer of the epidermis, where progenitors reside (Candi *et al.*, 2006; Laurikkala *et al.*, 2006). Recently, Su *et al.* generated mice lacking the

TAp63 isoforms. These mice underwent normal epidermal development; however, in early adulthood they started to suffer from blistering and ulceration of the skin, and an inability to heal wounds. These results suggested that TAp63 is dispensable for the early development of the skin but is critical for the maintenance of the adult epidermis through regulation of the proliferation of adult tissue stem cells. This hypothesis was further reinforced by the discovery that epidermal cells lacking TAp63 initially hyperproliferate before succumbing to senescence. This was proposed to cause depletion of the stem cell pool, with life-threatening consequences for wound healing due to the lack of stem cells needed to help regenerate them. Indeed, these mice suffered from non-healing wounds (Su *et al.*, 2009). These results are in agreement with studies performed by Candi *et al.* in that they suggest that ΔNp63 is a master regulator of the early development of the epidermis. However, they question the role of TAp63 in epidermal differentiation, particularly because TAp63 has very limited expression in the epidermis (Laurikkala *et al.*, 2006; Truong *et al.*, 2006). Perhaps TAp63 is necessary for adult tissue maintenance, regulation of the adult stem cell proliferation and their subsequent differentiation. Further studies are needed to decipher the physiological roles of all of the p63 isoforms, to clarify precisely when in epidermal development TAp63 and ΔNp63 are necessary. Conditional isoform-specific mouse mutants in which TAp63 and ΔNp63 are deleted at specific developmental stages would provide a useful tool to address this.

1.1.2.3 Functions of p63 beyond the regulation of epidermal stratification

In the past decade, it has become clear that p63 regulates cell survival and cell adhesion genes in addition to genes involved epidermal differentiation. This is critical in epidermal homeostasis, as is the regulation of progenitor cell expansion and their differentiation. For example, overexpression or ablation of p63 in mammary epithelial cells and keratinocytes results in the upregulation or downregulation of many cell-cell and cell-matrix adhesion

components. Not surprisingly, loss of p63 leads to anoikis, i.e. cell-detachment-induced death, while ectopic expression of either p63 isoform is able to suppress it (Carroll *et al.*, 2006).

p63 regulates the expression of Perp, a transmembrane protein that localises to desmosomes in epithelial tissues. Loss of Perp leads to neonatal lethality due to morphological abnormalities in desmosomal adhesion, and consequent intraepithelial blistering in the skin and oral mucosa. Besides the adhesion defect, hyperproliferation can be observed in these mice, indicating the reciprocal relationship between adhesion and proliferation (Ihrie *et al.*, 2005; Marques *et al.*, 2006).

1.2 Epidermal stratification and cell-cell adhesions

For epidermal stratification and homeostasis to proceed efficiently, a switch in the expression of keratins along the stratified layers must be accompanied by a switch in the expression of cellular junction components. This repertoire of compositional and structural differences is considered to be tailored to suit the function of each layer. Perturbations in the expression profile of either keratins or junctional components can lead to skin diseases, often with the involvement of other organs (Christiano, 1997).

1.2.1 Cellular adhesions in the epidermis

There are five main types of cellular adhesion that help maintain the unity of the epithelial sheet during stratification. They are continually adjusted during this process and include: focal adhesions and hemidesmosomes, adherens junctions, desmosomes, gap junctions and tight junctions (Figure1.3).

Focal adhesions and hemidesmosomes are present in basal cells and connect basal cells and their cytoskeleton to the basement membrane. Hemidesmosomes attach keratin filaments to the basement membrane via plakin proteins such as plectin and bullous pemphigoid antigen 1e (BPAG1e), and a transmembrane protein BPAG2 that directly binds to α6β4 integrins. Focal adhesions couple the basement membrane to actin filaments via numerous proteins including plectin, paxillin and vinculin, which directly or indirectly interact with α3β1 integrins (Tsuruta *et al.*, 2011). Focal adhesions and hemidesmosomes are thought to control the differentiation of basal cells as a loss of adhesion to the basement membrane is thought to lead to differentiation (Fuchs and Raghavan, 2002; Watt, 2002).

Adherens junctions draw adjacent cells together and link actin cytoskeleton bundles to membrane-associated adhesion sites. They are present throughout the epidermis, but are denser in the basal layer and absent from the cornified layer (Fuchs and Raghavan, 2002; Simpson *et al.*, 2011). The formation of adherens junctions is a prerequisite for the establishment of desmosome adhesion (Lewis *et al.*, 1997). Protein families represented in adherens junctions are similar to those that constitute desmosomes. In adherens junctions, extracellular connections between cells are established via classical cadherins such as E-cadherin and P-cadherin. These cadherins associate with the actin cytoskeleton via armadillo proteins, for example β-catenin and α-catenin, and other adapter proteins including afadin and nectin (Niessen, 2007).

Desmosomes pin stress-resisting keratin filaments to the cell-cell contacts, allowing mechanical and structural strain to be distributed throughout the tissue. They are present in all epidermal layers, but are more numerous in the spinous and granular layers and disassemble in the final stages of differentiation (Skerrow *et al.*, 1989; White and Gohari, 1984).

Gap junctions facilitate electrical and chemical coupling between cells. They are composed of oligomers of six connexins (CXs). In the skin, CX26, CX43, CX30, CX30.3, and CX31 are represented (Mese *et al.*, 2007). They are present in the basal, spinous and granular layers of human and murine epidermis but not in the cornified layer (Caputo and Peluchetti, 1977; Risek *et al.*, 1992).

Tight junctions mediate the paracellular transport of solutes. Although distributed throughout the epidermis, they are essential in the granular layer for the establishment of an impervious barrier (Green *et al.*, 2010; Morita and Miyachi, 2003). The protein composition of tight

junctions consists of transmembrane proteins claudins and occludins, that link to the actin cytoskeleton via zonula occludens (ZO) proteins ZO1, ZO2 and ZO3 (Niessen, 2007).

Together, all of these adhesions contribute towards a physiologically and mechanistically functional polarised epithelial-cell sheet. Although these adhesions are important for tissue integrity and function, desmosomes are considered to be the most specialised for mechanical stability. Unlike other intercellular junctions, desmosomes are able to acquire a strongly adhesive state. This state is required to help load bearing tissues, such as the heart and skin, resist shearing forces that can perturb tissue integrity by disconnecting cells (Brooke *et al.*, 2012; Garrod and Chidgey, 2008). Furthermore, desmosomes link to the stress-bearing intermediate filament cytoskeleton, which adds another degree of support for tissue integrity. Intermediate filaments prevent cell breakage under mechanical load. Therefore, desmosome-intermediate filaments together form a resilient structural framework that is able to withstand mechanical trauma. To date, the vast majority of identified skin fragility disorders that are accompanied by heart diseases result from mutations in desmosome components (Lai-Cheong *et al.*, 2007). The greater part of the studies outlined in this thesis focuses on desmosomal junctions, so in the interests of brevity, the following sections will concentrate on describing desmosomes, their architectural components and how they are regulated or disrupted in human disease.

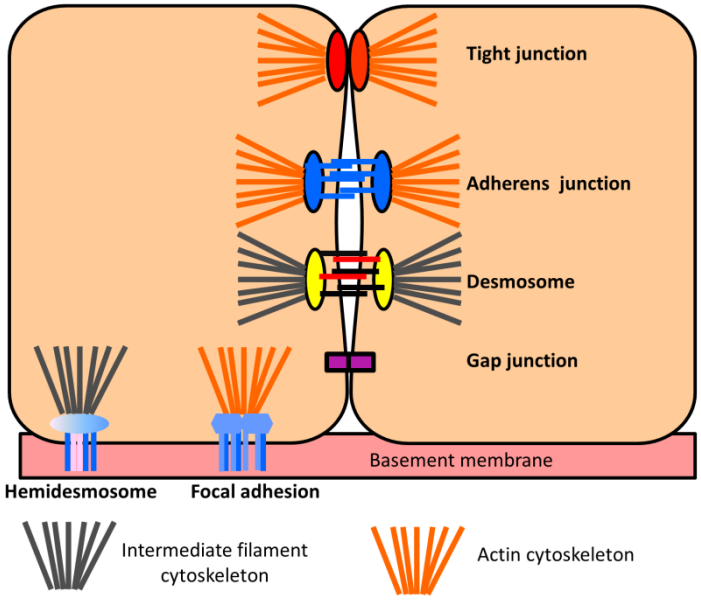

Figure 1.3 Cell adhesions in epithelial cells

Basal cells of the epidermis establish connections to the basement membrane via hemidesmosomes and focal adhesions. Intercellular adhesion occurs via tight junctions, adherens junctions and desmosomes. Cells are electrically and chemically coupled via gap junctions. Tight junctions, adherens junctions and focal adhesions adhere to the actin cytoskeleton, while desmosomes and hemidesmosomes adhere to resilient intermediate filaments (keratin filaments) in epithelial cells. Adapted from Jefferson *et al.,* 2004.

1.3 The desmosome and its structural components

Desmosome junctions exist in tissues that bear high mechanical strain, such as the skin and the ever-pumping heart. On the extracellular side, desmosomes connect to adjoining cells, while on the intracellular side they link to resilient intermediate filaments. This allows desmosomes to link intermediate filaments across many cells within a tissue, imparting mechanical resilience to the entire tissue. The type of intermediate filament that the desmosome attaches to within a cell is based on the filament type represented within a particular cell: desmosomes attach to keratin filaments in epithelial cells and desmin filaments in cardiomyocytes (Bazzi and Christiano, 2007).

The durability and tensile strength of desmosomes is dependent on the strength of their components. The intercellular components include transmembrane desmosomal cadherins, while the intracellular components include intermediate filaments, desmosomal armadillos and plakins (Figure 1.4 and Figure 1.5 (Garrod and Chidgey, 2008)). The importance of individual desmosomal constituents is highlighted when specific genetic, immunological- or toxin-mediated targeting disrupts the tissue architecture and integrity. Structural and functional description of these junctional components will be outlined in the sections that follow.

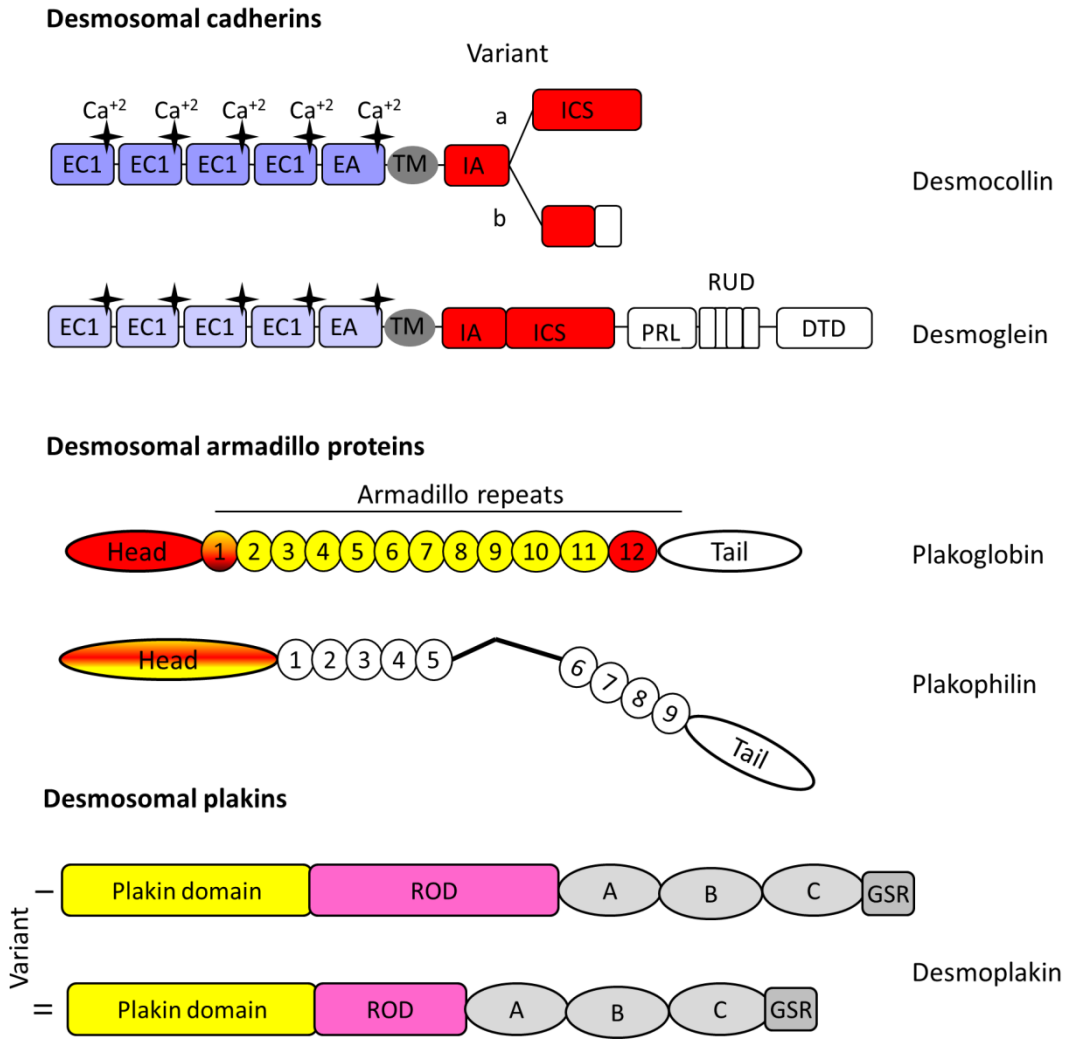

Figure 1.4 Desmosomal proteins and their structures

Desmosomal proteins belong to three families: cadherins (desmogleins and desmocollins), armadillos (plakophilins and plakoglobin) and plakins (desmoplakin). They are equipped with various domains which participate in protein-protein interactions. In their N-termini, desmosomal cadherins contain four extracellular cadherin repeats (EC1–EC4) interspersed with calcium binding sites and an extracellular anchor (EA). These extracellular domains (blue) mediate adhesion with cadherins on the opposing cells. In the central region they contain a transmembrane domain (TM), and at the C-termini they contain an intracellular anchor domain (IA, red) and an intracellular cadherin-like sequence motif (ICS, red) that mediates interactions with armadillo proteins. Armadillo proteins, plakoglobin and plakophilins contain head and tail domains that are spanned by armadillo repeats. There are twelve armadillo repeats in plakoglobin and nine in plakophilins. The head domain of plakophilin is thought to mediate all of its interactions. The central armadillo repeats of plakoglobin (yellow) are thought to bind to desmoplakin, while its head domain (red) in the N-terminus is believed to mediate interactions with cadherins. Desmoplakin is a core component of desmosomes. It has a central α-helical coiled-coil rod domain (pink) which is involved in protein dimerisation. In the N-terminus, a globular plakin domain (yellow) exists and binds to armadillo proteins. At the C-terminus there are three plakin-repeat domains (A, B, C) and a glycine–serine–arginine-rich domain (GSR) which participate in the interaction with the intermediate filaments. There are two splice isoforms of desmoplakin, I and II, where the second isoform has a shorter α-helical rod domain. Matching colours represent regions that proteins of different families use to interact with one another. Adapted from Thomasson *et al.,* 2010.

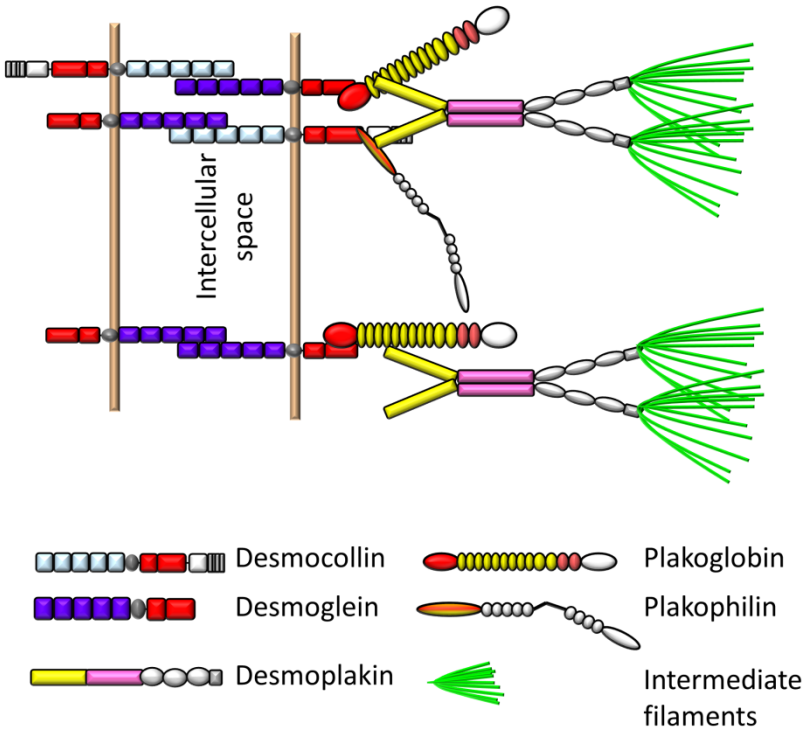

Figure 1.5 Organisation of principal desmosome components within a desmosome
Schematic representation of extracellular and intracellular interactions between desmosomal components. Transmembrane desmosomal cadherins, desmoglein and desmocollin, form extracellular connections with desmosomal cadherins of opposing cells, while attaching to the armadillo proteins (plakoglobin and plakophilins) inside the cell. Plakoglobin and plakophilins interact with desmoplakin, which is anchored to the intermediate filaments. Plasma membranes of opposing cells are represented in beige, with indicated intercellular space. Adapted from Dubash *et al.,* 2011.

1.3.1 Desmosomal cadherins

Desmosomal cadherins are calcium-dependent transmembrane components of desmosomes that act as the principal linkers between opposing cells. They consist of desmogleins and desmocollins. To date, there are four known isoforms of desmogleins (1-4) and three desmocollins (1-3) in humans. Desmocollins are present in two variants: 'a' and 'b'. The main domains characterising their structure include:

(i) a series of five extracellular domains interspersed with calcium binding sites, which are thought to be important for the interaction with cadherins on opposing cells

(ii) a short transmembrane domain (TM)

(iii) a cytoplasmic tail containing an intercellular anchor (IA) and an intercellular cadherin like sequence (ICS) that mediates interaction with desmosomal armadillos (Al-Amoudi *et al.*, 2007; Dusek *et al.*, 2006; Garrod *et al.*, 2002; North *et al.*, 1999).

Desmogleins and desmocollins are expressed in a stratification- and tissue-specific manner. In the epidermis, in particular, all seven cadherins are expressed with each cadherin having different expression profiles (Figure 1.6). For example, desmocollin 3 and desmoglein 3 are predominant in the basal and first suprabasal layers, while desmocollin 1 and desmoglein 1 are expressed in the upper suprabasal layers, with the highest expression in the most differentiated layers. Although not completely understood, this highly patterned expression profile is deemed to be multi-purpose. It is thought to mediate cell relationships during tissue morphogenesis and homeostasis, and is also believed to be involved in the epidermal differentiation process (Garrod and Chidgey, 2008; Green and Simpson, 2007). Both views are supported by genetic manipulation studies. One example where specific expression of desmocollins and desmogleins guides cell positioning is in the alveoli of the mammary gland. Alveoli consist of the luminal cells that express desmocollin 2 and desmoglein 2, which are

surrounded by myoepithelial cells that express desmocollin 3 and desmoglein 3. Ablation of adhesion between desmoglein 2 and desmocollin 2, or desmoglein 3 to desmocollin 3, in 3-D alveoli cultures has been shown to disrupt the patterning of luminal and myoepithelial cells (Runswick *et al.*, 2001). This study showed that desmosomes regulate cell positioning during morphogenesis. Additional studies have also provided evidence for the role of desmosomes in the regulation of differentiation. For example, ectopic expression of desmoglein 3 and desmocollin 3 in the uppermost layers of the epidermis perturbs differentiation and results in phenotypes such as skin flaking, acanthosis, hyperproliferation and a loss of barrier function (Elias *et al.*, 2001; Merritt *et al.*, 2002). This highlights the importance of the highly specific expression profile of cadherins in epidermal differentiation.

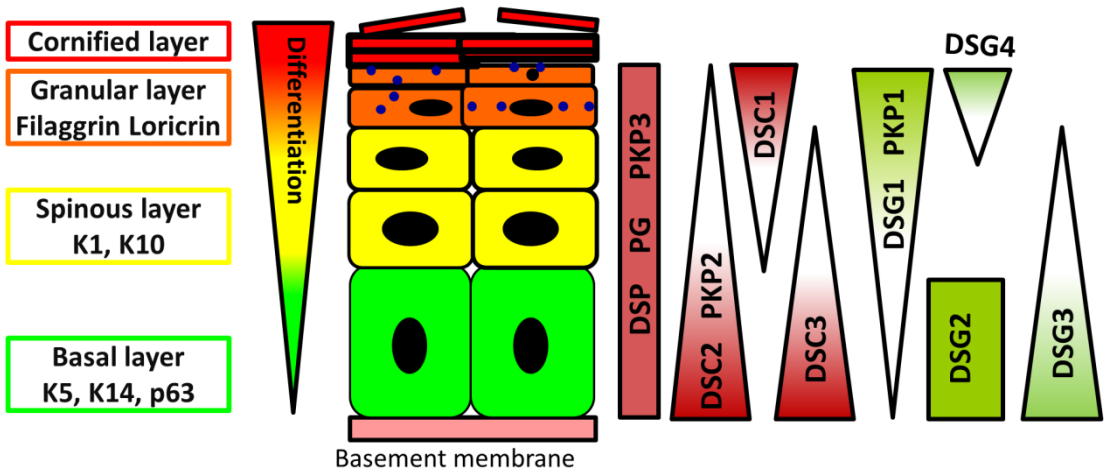

Figure 1.6 Expression patterns of individual desmosome components in the epidermis
Indicated on the right is the distribution of desmosome components: desmogleins 1-4 (DSG1-4), desmocollins 1-3 (DSC1-3), plakoglobin (PG), plakophilin (PKP1-3) and desmoplakin (DSP). Having a customised expression profile is particularly important during keratinocyte differentiation. Adapted from Delva *et al.,* 2009.

1.3.2 Desmosomal armadillo proteins

Desmosomal armadillo proteins are essential building blocks of desmosomes that couple cadherins to plakin proteins and intermediate filaments. They consist of two subclasses of proteins: ɣ-catenin (plakoglobin) and plakophilins (1-4), where plakophilins 1 and 2 have isoforms termed “a” and “b”. Although the structural domains of both plakoglobin and plakophilins have been delineated, the functionality of the domains in plakophilins require further investigation (Bass-Zubek *et al.*, 2009; Neuber *et al.*, 2010).

Structurally, armadillo proteins contain a N-terminus head domain and a C-terminus tail domain that is flanked by twelve or nine armadillo repeats depending on the armadillo subclass. In plakoglobin, the N-terminus and the armadillo repeats close to the C-terminus associate with cadherins, whereas central armadillo repeats associate with plakin proteins, specifically desmoplakin (Kowalczyk *et al.*, 1997; Smith and Fuchs, 1998; Wahl *et al.*, 1996). In plakophilins, the head domain is thought to mediate all protein-protein interactions with desmosomal components. Beside their ability to bind cadherins and link them to plakin proteins, armadillos can bind to each other and mediate lateral interactions. This increases the density of desmosome complexes and their tethering to intermediate filaments, intensifying the sturdiness of the tissue (Bass-Zubek *et al.*, 2009; Bornslaeger *et al.*, 2001; Chen *et al.*, 2002; Kowalczyk *et al.*, 1999).

Similar to cadherins, the expression of armadillo proteins is differentiation- and tissue-specific. Ascending up the epidermal layers, increased expression of plakophilin 1, decreased expression of plakophilin 2 and widespread expression of plakoglobin and plakophilin 3 has been reported (Figure 1.6; (Desai *et al.*, 2009; Moll *et al.*, 1997; Neuber *et al.*, 2010). The significance of this patterned expression profile in cellular processes such as proliferation,

apoptosis and adhesion is unclear. In addition to junctional localisation, shuttling of plakoglobin and plakophilin 1 or 2 to other subcellular compartments including the nucleus is prominent (Bass-Zubek *et al.*, 2009; Hatzfeld, 2007; Neuber *et al.*, 2010). Analogous to β-catenin (the adherens junction's armadillo protein), which translocates between subcellular compartments and has a clear cell signalling role, it has been postulated that plakoglobin and plakophilin 1-2 also participate in signalling events. In contrast to plakoglobin, current understanding of the roles of nuclear plakophilins is largely speculative and their nuclear functions are only just being unravelled.

1.3.2.1 Plakoglobin in intracellular signalling

Plakoglobin is homologous to β-catenin, a well-known regulator in the Wingless-type (Wnt)/β-catenin signalling pathway that also helps maintain the integrity of adherens junctions. In the canonical Wnt/β-catenin signalling pathway, the absence or presence of Wnt signals regulate the degradation or nuclear translocation of β-catenin, respectively. Once in the nucleus, β-catenin associates with T-cell/lymphoid enhancer factors (TCF/LEF) to mediate the expression of Wnt-target genes (Li *et al.*, 2006; Novak and Dedhar, 1999). Plakoglobin can also bind TCF/LEF factors and regulate the Wnt pathway (Zhurinsky *et al.*, 2000). In some cases, plakoglobin induces Wnt signalling and in other cases it represses it (Maeda *et al.*, 2004; Yang *et al.*, 2012). Whether it acts as an activator or repressor of the Wnt pathway appears to be context-dependent. Overexpression of plakoglobin can enhance the nuclear translocation of β-catenin and its association with TCF/LEF factors. It has been suggested that plakoglobin executes this task by interfering with the proteasome degradation of β-catenin, therefore, allowing β-catenin to go into the nucleus and activate signalling. However, others have suggested that plakoglobin interferes with β-catenin's activation of TCF/LEF regulated genes. For example, treatment of cells with the tyrosine phosphatase inhibitor peroxovanadate results in the translocation of plakoglobin and β-catenin from cell-cell junctions to the nucleus.

This translocation is associated with enhanced plakoglobin and diminished β-catenin binding to TCF/LEF, and subsequent downregulation of TCF/LEF-reporter activity (Hu *et al.*, 2003).

The repression of the Wnt/β-catenin pathway by plakoglobin is particularly prominent in cardiomyocytes in which desmoplakin has been silenced using a desmoplakin-specific small interfering RNA (siRNA). In these desmoplakin-deficient cardiomyocytes, nuclear accumulation of plakoglobin together with the downregulation of Wnt activity, and the ensuing upregulation of adipogenic and fibrogenic genes, has been observed. These results are recapitulated *in vivo* in mice heterozygous for desmoplakin where myocardium fibrosis, adipocyte overabundance and cardiomyocyte apoptosis, together with cardiac malfunction and ventricular arrhythmias, can be observed (Garcia-Gras *et al.*, 2006). These features are highly reminiscent of the phenotype observed in patients with ARVC (Herren *et al.*, 2009). Therefore, disruption of desmoplakin can lead to a nuclear accumulation of plakoglobin that can induce signalling, resulting in ARVC pathogenesis. These results suggest that desmosome components are not just structural guardians of tissue integrity, but also have cell-signalling functions. Expanding our understanding of plakoglobin regulation and cell compartment expression could, thus, offer clues for the development of new therapeutic strategies for ARVC.

1.3.3 Plakin proteins: desmoplakin

The plakin family of proteins consists of large, multidomain proteins that clamp the intermediate filament cytoskeleton to cell-cell and cell-matrix adhesion sites. Desmosomal plakin proteins include desmoplakin, plectin, periplakin and envoplakin. Based on animal models in which genes encoding these proteins have been ablated, desmoplakin is the only obligatory protein for anchorage functions (Ruhrberg *et al.*, 1997; Sonnenberg and Liem, 2007).

Structural domains of desmoplakin include a coiled-coil rod domain positioned amid the N- and C-terminal globular domains (Green *et al.*, 1990). The N-terminus, comprised of spectrin repeats and a Src homology 3 domain (SH3), binds the armadillo proteins plakoglobin and plakophilin and therefore targets desmoplakin to the plasma membrane (Sonnenberg and Liem, 2007). The rod domain contains heptad motifs that are thought to facilitate parallel dimerisation of desmoplakin proteins (O'Keefe *et al.*, 1989). The C-terminus, containing three plakin repeats (A, B and C) and glycine-serine-arginine rich domains, associates with intermediate filaments (Choi *et al.*, 2002; Delva *et al.*, 2009; North *et al.*, 1999; Smith and Fuchs, 1998). Both the N- and C-termini are essential for proper desmosomal function, as mutations in either domain can lead to structural instability of the whole intermediate filament-desmosome network (Sonnenberg and Liem, 2007; Stappenbeck *et al.*, 1993). Glycine-serine-arginine rich domains at the very end of the C-terminus contain phosphorylation sites thought to be involved in the regulation of desmoplakin localisation and interactions, and thus adhesion (Garrod and Chidgey, 2008; Stappenbeck *et al.*, 1994).

Desmoplakin is alternatively spliced to yield two isoforms, namely desmoplakin I (332 kDa) and desmoplakin II (259 kDa), where desmoplakin II is characterised by a truncated rod domain and

is unable to form dimers *in vitro* compared to desmoplakin I (Angst *et al.*, 1990; Green *et al.*, 1992; O'Keefe *et al.*, 1989). More recently a splice variant of desmoplakin I, termed desmoplakin Iα, has been described and is thought to have considerably lower expression levels than the predominant desmoplakin I/II isoforms (Cabral *et al.*, 2010b). Analysis of epithelial cell lysates on a western blot using anti-desmoplakin antibodies usually results in only a doublet band being observed, representing the predominant isoforms. The desmoplakin Iα isoform is either co-migrating with desmoplakin II (Cabral *et al.*, 2010b), or its protein expression is tightly regulated so that it is detectable only under certain unknown circumstances.

Desmoplakin I/II are abundant in all types of epithelia. In the heart, desmoplakin I is the predominantly expressed isoform (Al-Jassar *et al.*, 2013; Angst *et al.*, 1990; Sonnenberg and Liem, 2007). Unlike desmogleins and desmocollins, desmoplakin is uniformly expressed in the epidermal layers, suggesting an obligatory function in desmosome adhesion.

The importance of desmoplakin is highlighted by studies using genetically engineered mice lacking desmoplakin, as well as human patients with mutations in the desmoplakin gene. Genetically engineered mice lacking desmoplakin die *in utero* at embryonic day 6.5 as a result of an inability to extend their egg cylinder. Elongation of the egg cylinder requires a burst of proliferation followed by orchestrated changes in cellular organisation, while maintaining cellular connections. Not only do desmoplakin-mutant embryos suffer frail cellular adhesions, but they also show impaired cellular proliferation and a fragile surface endoderm that is unable to keep up with the organisational changes that accompany the elongation process. These mice die, partially as a result of the surface endoderm succumbing to organisational mechanical stress (Gallicano *et al.*, 1998). To circumvent early embryonic lethality and to study the importance of desmoplakin for the integrity and development of specific tissues,

conditional mouse models were developed. Cardiac-targeted ablation of desmoplakin led to embryonic lethality due to defective heart morphogenesis with adipocytes dispersed between disorganised cardiomyocytes (Garcia-Gras *et al.*, 2006). Epidermis-specific deletion of desmoplakin resulted in skin fragility, characterised by disrupted desmosome-intermediate filament association and the formation of perinuclear keratin aggregates (Vasioukhin *et al.*, 2001). Vasioukhin *et al*. therefore demonstrated that maintaining a normal desmosome-intermediate filament association is critical in conferring skin integrity.

The significance of desmoplakin for tissue integrity is also highlighted by desmoplakin mutations in human patients. Such patients develop a range of debilitating diseases including palmoplantar keratodermas and cardiomyopathies (Lai Cheong *et al.*, 2005), discussed further in section 1.5 of this chapter. Aberrant association between desmosomes and intermediate filaments has been reported in some of these patients. For example, a recessive 7901delG mutation in the desmoplakin gene, producing desmoplakin protein lacking a plakin repeat C and the extreme tail region, was reported in patients diagnosed with palmoplantar keratoderma, woolly hair and dilated cardiomyopathy. Histopathological analysis of patients' palmoplantar epidermis revealed large intercellular spaces and a collapsed keratin filament network, highlighting the importance of desmoplakin in attaching intermediate filaments to the desmosomes and in maintaining tissue integrity (Norgett *et al.*, 2000).

1.3.4 Intermediate filaments

Intermediate filaments in conjunction with desmosomes span numerous cells, organising these cells into tissues and providing them with mechanical support. The ability of intermediate filaments to contribute to the mechanical stability of cells and tissues lies in their visco-elastic properties. Studies using electron and atomic force microscopy show that intermediate filaments are endowed with high elasticity, extensibility and shear moduli, and can be exposed

to high shearing forces before breaking. This is in contrast to actin and microtubule extensibility, which break under small mechanical strains (Herrmann *et al.*, 2007; Kreplak and Fudge, 2007).

There are about 70 intermediate filament genes divided into six subtypes (I-VI) with each type having tissue-, cell- and development-specific expression patterns. Encoded by 54 genes, the type I and type II keratin proteins account for the majority of intermediate filaments (Godsel *et al.*, 2008; Szeverenyi *et al.*, 2008)). In heart and skin tissue respectively, type III desmin and pairs of type I and II keratins are the prominent filaments. Type I (acidic) and II (basic) keratins are expressed as obligate heterodimers in epithelial cells in a differentiation-specific manner. As mentioned previously, keratins K14 and K5 are abundant in the basal, while K10 and K1 are broadly expressed in the suprabasal epidermal layers (Fuchs and Weber, 1994).

Structurally desmin and keratins have similar building elements. They both contain an α-helical rod domain, which facilitates the formation of resilient coiled-coil bundles, and N- and C-termini that contain phosphorylation sites thought to mediate protein interactions and filament dynamics (Godsel *et al.*, 2008; Letai *et al.*, 1992; Omary *et al.*, 2004). Specifically, the N-terminal domain of type II keratins (K1, K2, K5 and K6) associates with the C-terminus of desmoplakin, thereby establishing a connection between desmosomes and intermediate filaments and maintaining the integrity of the cells and epithelial sheet (Kouklis *et al.*, 1994; Stappenbeck *et al.*, 1993). Similar to mutations in desmosomal core components, malfunctioning of intermediate filaments leads to severe impairment of tissue integrity. Often, epidymolitic disease and muscular dystrophies are presented in patients with less stable intermediate filaments (Haines and Lane, 2012). The spectrum of disease associated with mutations in desmosomal components will be briefly discussed in the following sections.

1.3.5 Further desmosome components and their intracellular signalling roles

While the aforementioned desmosomal proteins are thought to be the core constituents of the desmosome, other proteins that assist desmosome maintenance and/or assembly have been identified. These include Perp, pinin, corneodesmosin, kazrin and erbin. While not fully understood, we have some insight into their functions that pertains not only to their intercellular adhesion roles, but also to their signalling roles.

Corneodesmosin is a secreted protein of the cornified envelope that is associated with the maturation of desmosomes into corneodesmosomes. It is essential for the formation of an impervious epidermal barrier. Consistent with this, corneodesmosin-deficient animal models suffer from lethal epidermal tearing in response to mechanical strain. Reduction in corneodesmosin levels is necessary for the shedding of uppermost skin cells to occur (Jonca *et al.*, 2002; Leclerc *et al.*, 2009; Simon *et al.*, 2001). Whether or not corneodesmosin downregulation and subsequent cell desquamation have proliferation inductive properties has not been studied.

Pinin has dual roles in adhesion and signalling. For example, it localises to desmosomes where it is thought to strengthen the integrity of desmosome-intermediate filament connections in epithelial cells. Its loss results in weakened cell adhesions (Ouyang and Sugrue, 1996). It is also found in the nucleus, where it participates in pre-mRNA splicing and transcriptional repression (Alpatov *et al.*, 2004; Wang *et al.*, 2002).

Kazrin is yet another dual action protein that supports cell-cell junction integrity, as well as participating in cell signalling. It assists its interacting partner in the cornified envelope, periplakin, in integrating cytoskeletal networks and linking them to the plasma membrane.

Loss of kazrin results in impaired differentiation and increased proliferation (Sevilla *et al.*, 2008).

Erbin is another desmosomal component implicated in cell signalling. It interacts with the desmosomal components plakophilin 4 and desmoglein 1, as well as with epidermal growth factor 2 (EGFR2). Its interaction with plakophillin is thought to be important for maintaining epithelial sheet integrity (Jaulin-Bastard *et al.*, 2002), while its interaction with desmoglein 1 is thought to mediate differentiation by suppressing ERK signalling (Harmon *et al.*, 2013).

Finally, Perp, which has been mentioned previously as a p63-transcritional target, has an important role in desmosome integrity. Perp-deficient mice have fewer desmosomes, and aberrant association of intermediate filaments with cell-cell adhesion sites. Owing to disrupted desmosomal morphology, Perp-deficient mice develop intraepithelial blistering and die neonatally (Ihrie *et al.*, 2005). In addition to anomalous adhesion, enhanced proliferation can be seen in the epithelia of these mice. Whether Perp acts only as a structural constituent of desmosomes, or plays a role in desmosome formation and maintenance needs further verification. It is likely that Perp has both roles, given that Ihrie *et al.* observed increased distribution of non-ionic-detergent soluble desmosome proteins in Perp-deficient keratinocytes (Ihrie *et al.*, 2005).

Given the importance of desmosomal adhesion, and the fact that new desmosome-related genes are continually being identified, it is tempting to suggest that additional Perp-like proteins that might take part in regulating desmosome assembly, function and coupling to intracellular signalling are widely present in desmosomes.

1.4 Desmosome dynamics

Epithelial tissues undergo constant remodelling in response to injury or homeostasis in general; cell junctions need to be disassembled and assembled to facilitate the healthy progression of these physiological and developmental processes. Understanding the dynamics of desmosome components is therefore vital for our perception of how these processes go awry in disease, and development of new treatment strategies (Green and Simpson, 2007). While the previous sections focused on desmosome composition and the distribution and structural domains of desmosome components, the following sections will concentrate on the regulation of desmosome assembly.

1.4.1 Desmosome assembly

The process by which desmosomal components are assembled into functional organelles has been the focus of much research in the field since the 1980s. The general view today is that desmosome assembly and disassembly is regulated by calcium levels, posttranslational modifications and, as already mentioned, cross-talk with adherens junctions.

Calcium signalling is thought to trigger the formation of cellular junctions *in vitro*. In the absence of calcium, junctions either fail to form or are disassembled. *In vitro* assays, in which extracellular calcium is switched from low to high levels, offered the earliest insights into how desmosomal components are assembled into desmosomes (Hennings and Holbrook, 1983; Pasdar and Nelson, 1989; Penn *et al.*, 1989; Watt *et al.*, 1984). In Madin-Darby Canine Kidney epithelial (MDCK) cells, it was observed that under low calcium conditions desmosomal components are synthesised but fail to assemble into membrane-bound desmosomes, and are soluble in non-ionic detergents. Accordingly, switching calcium from low to more physiological levels results in the establishment of cell-cell contacts and the incorporation of desmosomal

components into desmosomes at these sites. It appears that, as these components are assembled into desmosomes, they become insoluble in non-ionic detergent (Pasdar and Nelson, 1988, 1989; Penn *et al.*, 1987; Penn *et al.*, 1989). These studies offered a limited understanding of how desmosome components assemble into desmosomes but have stirred further investigation.

In an elegant calcium switch assay, Sullivan and colleagues showed that desmosome assembly occurs in two stages. In the first stage occurring within 30 minutes of calcium addition, small vesicles primarily carrying cadherin proteins desmocolin 2 and E-cadherin are dispatched from the golgi to the cell surface. The majority of these vesicles are internalised and the few that are retained are thought to serve as nucleation points for desmosome assembly. In the second stage occurring within 60 minutes of calcium addition, larger vesicles containing desmogleins, plakoglobin, β-catenin and E-cadherin are targeted to the basolateral surface where desmocollin 2 is retained (Figure, 1.7; (Burdett and Sullivan, 2002)). Burdett *et al.* proposed that plakin proteins, in particular desmoplakin, assemble into desmosomes in a subsequent stage (Figure1.7). This is supported by a study by Pasdar *et al.*, which showed that prior to assembly into desmosomes, desmoplakin and desmoglein have differential cytoplasmic distributions and associate with different cytoskeletal networks; desmoplakin associates with intermediate filaments while desmoglein associates with the microtubule network (Pasdar *et al.*, 1991). In further support, desmosome-like structures assembled normally in skin with deletion of desmoplakin, although intermediate filament attachments were absent (Vasioukhin *et al.*, 2001). In addition, studies in Dr Green's laboratory have confirmed that desmoplakin fuses with nascent desmosomes after desmocollins and desmogleins have established the precursor desmosomal structure. Using time-lapse imaging they monitored GFP-tagged desmoplakin during desmosome assembly in an A431 epidermoid carcinoma cell line. From these studies it was deduced that desmoplakin recruitment to desmosomes occurs

in three temporally and spatially coordinated phases. In the first phase, rapid accumulation of desmoplakin along the newly established cell-cell border can be observed. This is followed by a second phase in which plakophilin- and desmoplakin-containing punctae appear in the cytoplasm. Finally, in a third phase, these cytoplasmic particles migrate using an actin-myosin mechanism to desmoplakin clusters at nascent cell-cell contacts (Godsel *et al.*, 2005). In the paper by Godsel *et al.*, it was also noted that desmoplakin interacts with intermediate filaments in the cytoplasmic punctae, and that this interaction is required for desmoplakin to assemble into desmosomes. However, this interaction needs to be flexible and dynamic. Enhancing the cytoplasmic interaction between desmoplakin and intermediate filaments through the S2849G mutation of desmoplakin has a negative effect on desmosome assembly, and initially results in desmoplakin accumulation in the cytoplasm. However, once the S2849G desmoplakin mutant is assembled into desmosomes it leads to less dynamic and more hyperadhesive desmosome adhesion (Bass-Zubek *et al.*, 2008; Stappenbeck *et al.*, 1994).

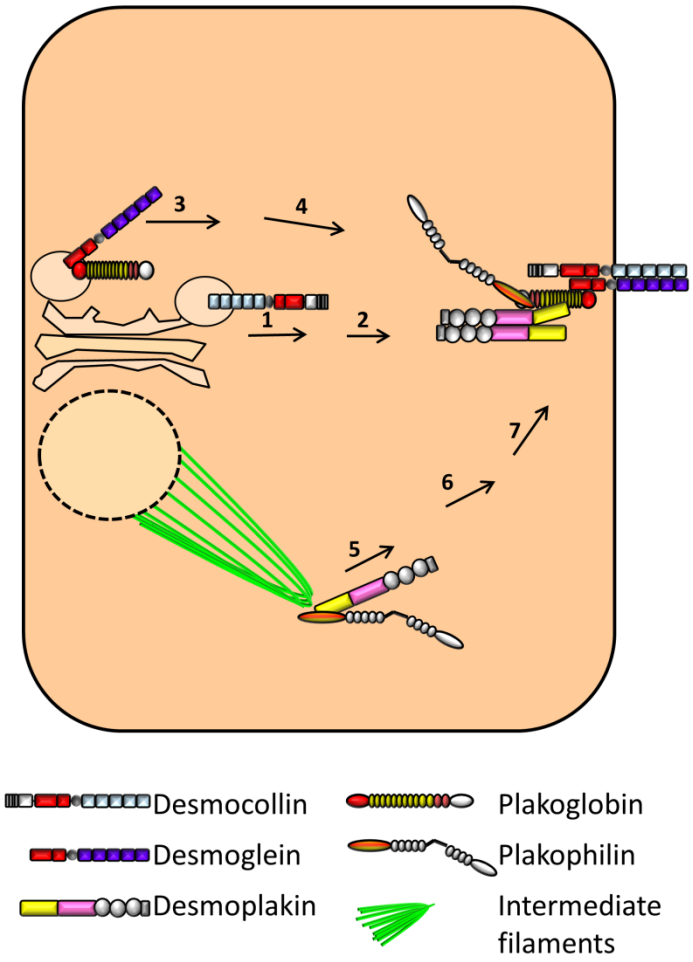

Figure 1.7 Assembly of desmosomal components into desmosomes at the cell membrane
Trafficking of cytoplasmic desmosomal components to the cell membrane is schematically represented. Desmocollin-containing vesicles are thought to be the first ones to shuttle from the golgi network to the plasma membrane where they create docking sites for the second round of vesicles containing desmoglein and plakoglobin. Although not represented in the scheme, these vesicles rely on the microtubule network for their journey to the plasma membrane. Subsequently, a pool of desmoplakin and plakophilin moves to desmosome nucleation sites at the plasma membrane. Their journey to the membrane is dependent on the actin cytoskeleton (not shown). The structure bounded by a dotted line represents the nucleus and the layered structure above it is the golgi apparatus. Adapted from Green and Simpson, 2007.

Posttranslational modifications are thought to play an important role in desmoplakin's assembly into desmosomes (Yin and Green, 2004). This has been investigated by a number of research teams whose work is briefly discussed here. Calcium influx, which triggers the formation of cell-cell junctions, is also known to induce PKCα (Sheu *et al.*, 1989). PKCα is thought to be the main transducer of the signal for the initiation of cell-cell junction formation during the calcium switch. Indeed, activation of PKCα by TPA is sufficient to induce cellular-junction formation in low calcium conditions, recapitulating the dynamics of junction formation seen by switching from low to physiological calcium levels (Nagao *et al.*, 1989). Likewise, inhibition of PKCα inhibited junction assembly and desmoplakin recruitment to the cell membrane in a squamous epithelial cell line during the calcium switch (Bass-Zubek, 2008). PKCα is thought to mediate desmoplakin translocation to cell junctions by phosphorylating its C-terminus, specifically the serine 2849 (S2849) domain. Mutating this domain to unphosphorylatable S2849G impairs desmoplakin's assembly into desmosomes, while enhancing its interaction with intermediate filaments in cytoplasmic punctae (Stappenbeck *et al.*, 1994). As mentioned, inhibition of PKCα has a similar effect during the calcium switch (Bass-Zubek *et al.*, 2008). Collectively, studies in Dr Green's laboratory suggest that plakophilin brings PKCα to cytoplasmic punctae containing desmoplakin, wherein PKCα phosphorylates desmoplakin and recruits intermediate filaments to it, following which the whole complex is transported to cell-cell junctions (Bass-Zubek *et al.*, 2008; Stappenbeck *et al.*, 1994; Yin and Green, 2004).

Once the cell-cell junctions are formed, PKCα-activation appears to have a reverse function and induces the disassembly of cell-cell junctions (Amar *et al.*, 1999; Garrod *et al.*, 2005; Wallis *et al.*, 2000). This raises new questions about what happens to desmosomes after they have assembled. Furthermore, given that phosphorylation is responsible for the initiation of desmosome assembly, additional questions also come to mind: such as what is the role of

phosphatases in desmosome adhesion, specifically once the desmosomes have formed? Toivola *et al.* have shown that protein phosphatases play an important role in maintaining the organisation of, and interactions between, desmoplakin and intermediate filaments. Blocking of protein phosphatase type 1 (PP1) and type 2A (PP2A) by microcystin-LR in hepatocytes leads to an aberrant distribution of desmoplakin (symptomatic of desmosome disassembly), and increased solubility and disorganisation of intermediate filaments (Toivola *et al.*, 1997). This study suggests that protein phosphatases are important in the maintenance of cell adhesions. In the third chapter of this thesis, findings related to desmoplakin's phosphorylation status and its junctional localisation will be outlined.

1.4.2 Modulation of desmosome adhesiveness and desmosome disassembly

Desmosome maturation

The research team in Prof. Garrod's laboratory has investigated what happens to desmosomes after their initial assembly. His group coined the concept of desmosome maturation and calcium independence (hyperadhesion), and described it as a progressive process whereby desmosomes mature over few days upon calcium addition to become hyperadhesive in *in vitro* systems. The hyperadhesive state is characterised by a stable and strong adhesion that is resistant to perturbation by chelation of calcium (Kimura *et al.*, 2007). This state is also developmentally regulated. Desmosomes in the epidermis adopt a calcium-independent state between embryonic day 14 and 19 (75% and 100% calcium-independence, respectively), and this remains their standard state in adult tissues (Garrod, 2010; Kimura *et al.*, 2012).

Desmosomes are not locked into the hyperadhesive state. In cases of injury and wounding of epithelial sheets *in vitro* and *in vivo,* desmosomes revert to a calcium-dependent unrestrictive state (Figure 1.8). This is a remarkable feature of desmosomes, which allows cells to

participate in morphogenetic movements for tissue remodelling during wound healing. Therefore, malleable adhesion appears to be crucial for sustaining tissue integrity (Garrod, 2010; Garrod *et al.*, 2005; Thomason *et al.*, 2012; Thomason *et al.*, 2010; Wallis *et al.*, 2000). The strength of adhesion is thought to be modulated by PKCα, although there are suggestions that other protein kinases might also be involved. Activation of PKCα is sufficient to render calcium-independent desmosomes calcium-dependent. Similarly, inhibition of PKCα can induce loosely-adherent desmosomes to become hyperadhesive (Kimura *et al.*, 2007; Wallis *et al.*, 2000). Not surprisingly, therefore, PKCα activity is attenuated as desmosomes mature. It is, however, re-activated and recruited to the cell membranes of cells participating in wound closure, where it is thought to mediate cell adhesion and cell migration (Garrod *et al.*, 2005; Wallis *et al.*, 2000). Together, these studies suggest that phosphorylation of desmosomal components plays an important role in desmosome adhesiveness (Kimura *et al.*, 2007).

Desmosome disassembly

Proteolytic cleavage of desmosome components is thought to facilitate desmosome disassembly and/or remodelling during apoptosis, differentiation and wound healing. In apoptotic cells, desmoplakin, desmogleins, desmocollins, plakoglobin and plakophilins are cleaved by caspases, a process necessary for apoptosis to proceed (Brancolini *et al.*, 1998; Dusek *et al.*, 2006; Weiske *et al.*, 2001). The extracellular domains of desmogleins and desmocollins can also be cleaved by metalloproteinases, which leads to their internalisation and the dismantling of desmosomes (Cirillo *et al.*, 2007). Abnormal cleavage of desmosome complex constituents leads to skin fragility diseases, and can facilitate the spread of cancer. For example, exfoliative toxin A produced by *Staphylococcus aureus* cleaves desmoglein 1, leading to extreme blistering of the skin (Amagai *et al.*, 2000). Netherton syndrome, characterised by scaly and inflamed skin with defective barrier function, also results from the

abnormal cleavage of desmoglein 1 and desmocollin 1 (Descargues *et al.*, 2005; Descargues *et al.*, 2006). Matrix metalloproteinases are often upregulated during cancer invasion and can facilitate tumour spreading by cleaving desmosome components, leading to desmosome dissolution and enhanced migration.

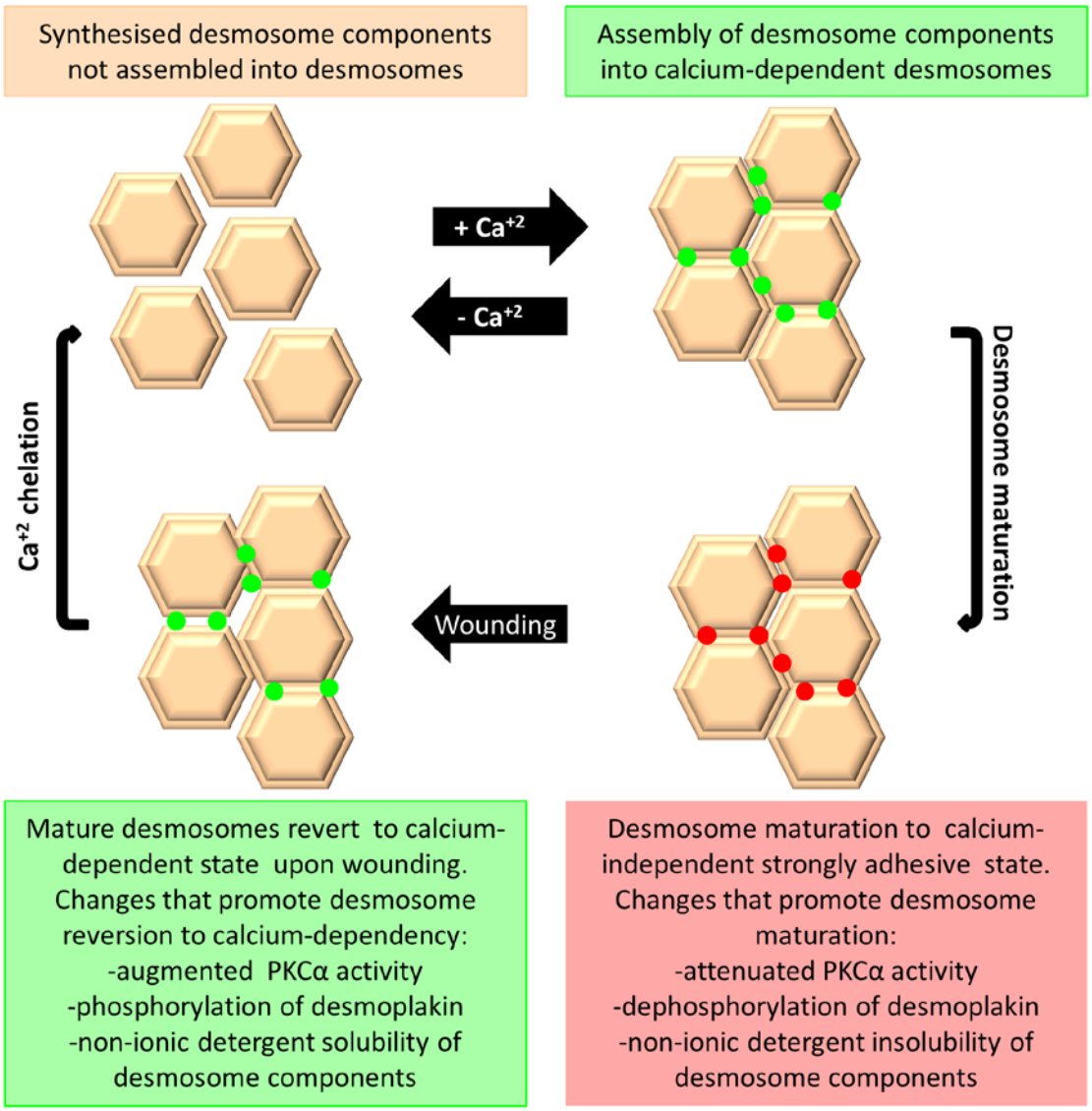

Figure 1.8 Schematic representation of desmosome assembly and dynamics
Calcium signalling induces cell-cell junction formation and the assembly of desmosome components into desmosomes (green punctae). Once desmosomes have assembled, they mature to become strongly adhesive and insensitive to calcium chelation (red punctae). Dephosphorylation of desmosome components might promote the formation of this highly adhesive state. Wounding and other stimuli like PKCα activation can trigger desmosomes to revert to their dynamic calcium-chelation-dependent state. The features accompanying desmosome maturation or their reversion to a less adhesive calcium-independent state are outlined in the lower red and green boxes, respectively. Adapted from Green and Simpson, 2007.

1.5 Diseases of desmosomes

Given the wide distribution of desmosomes, their multiprotein complexes and their role in maintaining tissue integrity, it is not surprising that a myriad of diverse human diseases result from mutations in desmosome components (McGrath, 2005). These diseases are also seen in genetically engineered mice carrying similar mutations (Brooke *et al.*, 2012; Thomason *et al.*, 2010). Not surprisingly, stress-bearing organs that rely on mechanical resilience, such as the skin and heart, are most commonly affected by these mutations. Diseases associated with desmosomal malfunction include skin blistering or fragility, skin dysplasia, palmoplantar keratoderma, woolly hair, nail abnormalities, keratosis, and cardiomyopathies. The correlation between genotypes and phenotypes manifested in the skin and heart, and the underlying molecular pathogenic mechanisms, have been studied, among others, by the groups of Professors David Kelsell and John McGrath. A table listing the diseases and their genetic basis is included below. Desmosome-related diseases in humans result from both autosomal recessive and autosomal dominant mutations. Although not in every case, recessive mutations often lead to a phenotype that affects more than one organ, such as the skin, heart and hair (Figure 1.9).

Note that in the table and figure represented below (Table 1, Figure 1.9), mutations in some desmosomal components have a tendency to cause epidermal diseases without cardiac features and vice versa. This is likely due to tissue-specific distribution of different desmosomal components. For example, out of the three plakophilins, only plakophilin 2 is expressed in the cardiac tissue, while all three are present in skin. Therefore, it is expected that mutations in plakophilins 1 and 3 would not affect cardiac development and function. Similarly, all desmosomal cadherins are represented in the skin, whereas desmoglein 2 and desmocollin 2

are the main desmosomal cadherins in myocardial desmosomes (Bolling and Jonkman, 2009; Whittock, 2003).

Desmosome component	Human disease	Phenotype of mutant mice
Desmoplakin	Palmoplantar keratodermas, skin and nail fragility, woolly hair, epidermolysis bullosa, ARVC or other cardiomyopathies (Alcalai *et al.*, 2003; Bauce *et al.*, 2005; Jonkman *et al.*, 2005; Norgett *et al.*, 2000; Uzumcu *et al.*, 2006; Whittock *et al.*, 1999).	Embryonic lethality at egg cylinder stage, heart defects (Gallicano *et al.*, 2001; Gallicano *et al.*, 1998).
Desmoglein 1	Palmoplantar keratoderma, scaled skin syndrome, hypotrichosis, allergies, pemphigus foliaceous and bullous impetigo (Amagai *et al.*, 2000; Hunt *et al.*, 2001; Kljuic *et al.*, 2003b; Rickman *et al.*, 1999; Samuelov *et al.*, 2013; Warren *et al.*, 2000).	N/A
Desmoglein 2	ARVC (Awad *et al.*, 2006a; Jimenez-Jaimez *et al.*, 2014; Pilichou *et al.*, 2006; Syrris *et al.*, 2007).	Embryonic lethality shortly after implantation (Eshkind *et al.*, 2002).
Desmoglein 3	Antibodies to desmoglein 3 in patients with pemphigus vulgaris-like skin disease (Arteaga *et al.*, 2002).	Postnatal suprabasilar acantholysis of skin and oral mucosa, hair loss and eye lesions (Koch *et al.*, 1998; Koch *et al.*, 1997).
Desmoglein 4	Hypotrichosis: hair follicle abnormalities with sparse hair and epidermal hyperproliferation (Kljuic *et al.*, 2003a).	Lanceolate hair (Kljuic *et al.*, 2003a)
Desmocollin 1	Antibodies to desmocollin 1 lead to subcorneal pustular dermatosis (Hashimoto *et al.*, 1997).	Open-eyelids at birth, epidermal fragility, barrier defects and abnormal differentiation (Chidgey *et al.*, 2001).
Desmocollin 2	ARVC, palmoplantar keratoderma and woolly hair (Al-Sabeq *et al.*, 2014; Heuser *et al.*, 2006; Simpson *et al.*, 2009b; Syrris *et al.*, 2006).	N/A
Desmocollin 3	Hypotrichosis with large fluid vesicles in the skin (Ayub *et al.*, 2009).	Pre-implantation and pre-desmosome formation embryonic lethality (Den *et al.*, 2006).
Plakoglobin	ARVC, palmoplantar keratoderma, woolly hair, alopecia and acantholytic epidermolysis bullosa (Asimaki *et al.*, 2007; Cabral *et al.*, 2010a; Erken *et al.*, 2011; McKoy *et al.*, 2000).	Embryonic lethality between E10.5 and birth, heart defect, skin blistering and acantholytic cornea (Bierkamp *et al.*, 1996; Ruiz *et al.*, 1996).
Plakophilin 1	Ectodermal dysplasia, skin fragility, dystrophic nails and woolly hair (McGrath *et al.*, 1999; McGrath *et al.*, 1997; Whittock *et*	N/A

	al., 2000).	
Plakophilin 2	ARVC (Awad *et al.*, 2006b; Gerull *et al.*, 2004).	Embryonic lethality at E11 and heart defects (Grossmann *et al.*, 2004).
Plakophilin 3	N/A	Mild defects in hair follicle morphogenesis (Schmidt and Koch, 2007).
Perp	N/A	Neonatal lethality, epithelial blistering (Ihrie *et al.*, 2005).
Keratin 1	Epidermolytic hyperkeratosis, palmoplantar keratodermas	N/A
Keratin 5	Epidermolysis bullosa simplex diseases, palmoplantar keratoderma	Neonatal lethality, epidermolysis bullosa and cytolysis of basal cells (Peters *et al.*, 2001).
Keratin 6	Focal palmoplantar keratoderma, nail dystrophy	K6 (a&b)—25% survival rate, tongue lesions, nail dystrophy, cell lysis during migration during wound healing (Wojcik *et al.*, 2001; Wong *et al.*, 2000).
Keratin 10	Epidermolytic hyperkeratosis, palmoplantar keratodermas	Epidermolytic hyperkeratosis and acanthosis (Reichelt *et al.*, 1997).
Keratin 14	Epidermolysis bullosa simplex diseases, epidermal hyperpigmentation and palmoplantar keratodermas	Epidermolysis bullosa, cytolysis of basal cells, skin fragility and increased neonatal mortality (Lloyd *et al.*, 1995).

Table 1 Diseases caused by mutations in desmosome components in both human and genetically engineered mouse models

Diseases associated with desmosome mutations are reviewed in papers by Nitoiu *et al.,* 2014, Schmidt *et al.,* 2007, and McGrath *et al.,* 2005. Human diseases associated with keratin mutations were obtained from the Intermediate Filament Database, http://www.interfil.org/ (Szeverenyi *et al.*, 2008). N/A means that no mutations in the genes have been reported to date. ARVC stands for arrhythmogenic right ventricular cardiomyopathy.

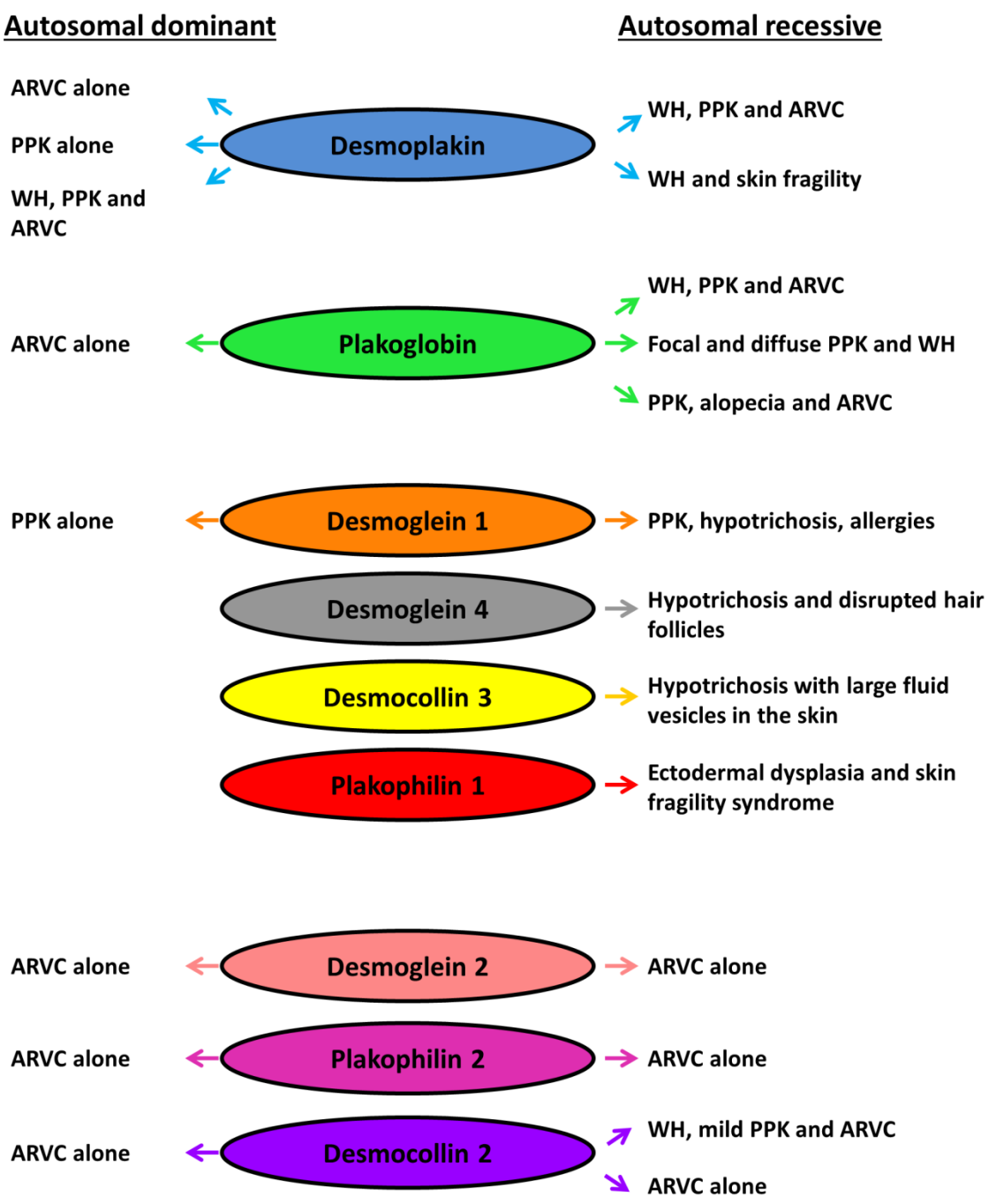

Figure 1.9 Schematic representation of the autosomal dominant and recessive disease phenotypes resulting from reported mutations in selected desmosomal components
WH stands for woolly hair and PPK for palmoplantar keratoderma. References cited in Table 1 were used to generate the figure. Adapted from Brooke *et al.,* 2012.

Palmoplantar keratoderma is one of the diseases associated with desmosome dysfunction. A clinical feature of palmoplantar keratoderma at the histological level is the thickening of the epidermis—acanthosis (basal and spinous layers) and hyperkeratosis (granular and cornified layers)—of the palms and soles. The pattern of thickening ranges from focal and punctate to diffuse. As the name suggests, focal thickening affects only a limited area of the palmoplantar surface, often the sites that are exposed to mechanical trauma. On the other hand, diffuse thickening affects the whole palmoplantar surface (Itin and Fistarol, 2005). At the microscopic level, increased intercellular spaces between keratinocytes, known as acantholysis, can be observed in the affected skin when compared to unaffected control skin. This has been reported in palmoplantar keratoderma resulting from mutations in the desmoglein gene (Wan *et al.*, 2004). Studies by Armstrong *et al.* and Whittock *et al.* showed that mutations resulting in desmoplakin haploinsufficiency lead to focal palmoplantar keratoderma in humans. They also revealed other microscopic features of the disease, which included (i) weakening of intercellular junctions as represented by a widening of intercellular spaces and (ii) perturbations of desmosome-intermediate filament interactions as represented by the formation of cytoplasmic keratin aggregates and irregular or absent connections between desmosomes and intermediate filaments (Armstrong *et al.*, 1999; Whittock *et al.*, 1999). Furthermore, *in vitro* modelling of these mutations, together with a cyclic mechanical stretch assay and a dispase mechanical dissociation procedure, confirmed that intercellular adhesions are weakened in the presence of these mutations. Monolayers of keratinocytes carrying these mutations more easily succumb to fragmentation upon mechanical stress (Cabral *et al.*, 2012).

ARVC is another typical disease of desmosome dysfunction. As most of the identified mutations causing ARVC have been in desmosome genes, ARVC has been termed the 'disease of the desmosome' (Herren *et al.*, 2009). If ARVC presents on its own, it is commonly of autosomal dominant inheritance. However, if the skin, heart and hair are involved, it is likely to

be of recessive inheritance. Indeed, a recessively inherited syndrome with a triad of phenotypic features: woolly hair, ARVC and palmoplantar keratoderma, was reported in families from the Greek island Naxos (Protonotarios *et al.*, 1986). As it was the first case report of the disease, it was given the name Naxos disease. However, the disease was later observed in other countries (Bukhari and Juma'a, 2004; Kilic *et al.*, 2007; Norgett *et al.*, 2000; Tosti *et al.*, 1994). In the general population, ARVC afflicts 1 in 5,000 people. Its clinical features include defects in the electrical conduction of the heart with life threatening arrhythmias, dilation of the right ventricle, thinning of the right ventricular wall and replacement of the myocardium with fibrous and adipose tissue. Patients often die young of sudden cardiac arrest. The disease mainly results from mutations in the desmosomal components, and the ensuing compromised cell-cell adhesion integrity (Awad *et al.*, 2008). Fibro-fatty deposits are thought to result from the misregulation of Wnt/β-catenin signalling due to the aberrant localisation of plakoglobin. Displacement of plakoglobin from desmosomes to the nucleus in ARVC cases is thought to inhibit the Wnt/β-catenin pathway (Garcia-Gras *et al.*, 2006). The repression of this pathway results in the switch of the transcriptional programme from myogenesis to adipogenesis (Ross *et al.*, 2000).

1.5.1 Diseases of desmosome dynamics

As already mentioned, desmosome are not locked into a static and hyperadhesive state; their adhesiveness is readjusted during tissue modelling or remodelling that necessitates cell rearrangement and movement, such as wound healing or embryonic eyelid closure. Therefore, perturbation of desmosome dynamics can impede wound healing, embryonic eyelid closure and many other morphological processes.

Wound healing requires rapid regeneration of the epithelium to seal the exposed wound site. This involves cell proliferation and the migration of epithelial cells to cover the wound surface. The remodelling of otherwise highly restrictive desmosomes is instrumental in the facilitation of cell motility (Coulombe, 2003; Croft and Tarin, 1970; Garrod *et al.*, 2005; Krawczyk and Wilgram, 1973). Loss of desmosomes might be predicted to impede wound closure, as compromised cell-cell adhesions might obstruct the coordinated migration of cells resurfacing the wound. However, this has not been studied extensively due to the fatal consequences of ablating individual desmosomal components in mice. In some instances, the issue of lethality was circumvented by using conditional knockout mouse strains. One such example is conditional Perp-deficient mice. These mice display delayed wound closure due to compromised cell-cell adhesion (Beaudry *et al.*, 2010). Additionally, it is not surprising that wound closure defects can be observed in animal models possessing mutations that affect desmosome dynamics. Indeed, mice lacking PKCα, a regulator of desmosome adhesiveness, display delayed wound re-epithelisation as a result of retained desmosomal hyperadhesiveness (Thomason *et al.*, 2012).

Embryonic eyelid closure, which happens in both humans and mice, is another situation in which timely modulation of desmosome hyper-adhesiveness is required. In mice, the process

can be monitored easily. It occurs between embryonic day E11.5 and E14.5, when the surface ectoderm undergoes extensive proliferation and morphological changes resulting in the formation of an eyelid groove with a protruding eyelid edge. Eyelid development continues when the epidermal layers at the opposing developing eyelids start to elongate and migrate towards the centre of the cornea. Finally, the epithelial layers from opposing eyelids meet and fuse at about E16.5. Following this fusion, the dermis migrates towards the junction between opposing eyelid epithelia (Findlater *et al.*, 1993; Mine *et al.*, 2005). Desmosomes, along with other cell-cell adhesions, are thought to facilitate the fusion between opposing eyelids. After approximately 12 days of postnatal development, eyelid adhesion breaks due to epithelial cell apoptosis and necrosis at the junction, permitting normal ocular function. Failure to undergo embryonic eyelid closure leads to severe ocular lesions (Findlater *et al.*, 1993; Harris and McLeod, 1982). Germline deletion of desmosomal components leads to early embryonic lethality, making it difficult to examine whether embryonic eyelid closure has been compromised. One exception is in desmocollin 1-deficient mice, which survive into adulthood and have impaired embryonic eyelid closure and the open-eyelids at birth phenotype (Chidgey *et al.*, 2001). Whether such open eyes at birth result from a failure of epithelial sheets to proficiently migrate or fuse requires further investigation.

1.5.2 Desmosomes and cancer

While clearly important in maintaining the integrity and plasticity of adult tissues, the role of desmosomes in cancer progression is just starting to emerge. Cancer progression relies on the attenuation of cell-cell adhesions and the enhancement of growth, migration and anti-apoptotic pathways. This allows cancerous cells to survive and acquire more migratory and invasive phenotypes (Hanahan and Weinberg, 2000).

The roles of adherens junction components in cancer progression are well established. Some components, like E-cadherin, that mainly participate in intercellular adhesion are often downregulated, while other components, like β-catenin, that have a dual role in adhesion and cell signalling are often upregulated. This upregulation of β-catenin results from mutations in the β-catenin degradation complex or from a stabilising mutation in β-catenin itself. These mutations lead to enhanced β-catenin signalling and reduced cell-cell adhesion, resulting in the activation of anti-apoptotic, cell cycle progression, and pro-motility genes (Conacci-Sorrell *et al.*, 2002; Vasioukhin, 2012).

The role of desmosome components in cancer progression is less well understood, and there is no clear trend towards up or downregulation (Chidgey and Dawson, 2007). For example, desmoplakin is often downregulated in breast carcinomas, and its loss in pancreatic neuroendocrine tumours is thought to promote invasion independent of adherens junctions (Chun and Hanahan, 2010; Davies *et al.*, 1999). Desmoglein 2 is reported to be downregulated in gastric and pancreatic cancer, while it is upregulated in squamous cell carcinoma of the skin (Biedermann *et al.*, 2005; Kurzen *et al.*, 2003; Ramani *et al.*, 2008; Yashiro *et al.*, 2006). Furthermore, epidermal growth factor receptor (EGFR) is overexpressed in many head and neck carcinomas, and is known to perturb desmosome adhesion by stimulating the

degradation of desmoglein 2 and altering desmoplakin and plakoglobin interactions (Lorch *et al.*, 2004; Yin *et al.*, 2005a). Plakoglobin, like β-catenin, has both cell adhesion and cell signalling roles, and increases in its nuclear levels can lead to the transactivation of Wnt signalling and tumour progression (Conacci-Sorrell *et al.*, 2002). Plakoglobin has been shown to facilitate the transformation of rat epithelial cells by inducing the expression of the *myc* gene (Kolligs *et al.*, 2000). Furthermore, plakoglobin participates in the regulation of cell motility, and the regulation of pro-survival signals by inducing the expression of the *bcl-2* gene (Hakimelahi *et al.*, 2000). These studies illustrate potential avenues by which disruption of desmosomes and desmosome-related cell signalling can lead to tumour progression and metastasis.

1.6 Novel desmosome regulators implicated in desmosome-like diseases: ADAM 17, EGFR and iASPP

Around 30-50% of patients with desmosome-like cardiocutaneous disorders have mutations in the established desmosome components (Marcus *et al.*, 2013). The causative genes for the other 50% of patients remain obscure, suggesting the existence of novel desmosome regulators. In support of this, Djabali *et al.* identified two Arab families with the cardiocutaneous Naxos syndrome, in whom mutations in desmoplakin, desmogleins, desmocollins, plakoglobin and plakophilins were excluded (Djabali *et al.*, 2002). Identification of these novel genes and whether they cause disease by affecting desmosome function warrants investigation.

A number of genes influencing desmosome dynamics have recently been identified. These include A Disintegrin and Metalloproteinase 17 (ADAM17), Epidermal Growth Factor Receptor

(EGFR), and the previously-mentioned PKCα. ADAM17, an extracellular domain sheddase, is thought to regulate desmosome disassembly by mediating the cleavage of desmoglein 2 and its subsequent internalisation. Patients with loss-of-function mutations in ADAM17 manifest cardiomyopathy, inflammatory skin and bowel syndrome partly as a result of defective desmoglein 2 cleavage, and disrupted desmosomes (Blaydon *et al.*, 2011). A similar phenotype is observed in loss-of-function mouse mutants, which in addition display the open-eyelids at birth phenotype (Brandl *et al.*, 2010; Hassemer *et al.*, 2010; Peschon *et al.*, 1998). ADAM17 is thought to facilitate the cleavage of EGFR ligands (TGFα, EGF, and HB-EGF) and therefore mediate EGFR signalling. EGFR activation leads to a series of phosphorylation events that signal for the internalisation and cleavage of desmoglein 2, resulting in the dismantling of desmosomes. Accordingly, inhibition of EGFR leads to increased intercellular adhesive strength and an accumulation of desmoglein 2 at the cell membrane, by interfering with ADAM17's cleavage of desmoglein 2. Therefore, ADAM17 and EGFR are thought to act cooperatively to regulate desmosome dynamics (Klessner *et al.*, 2009; Lorch *et al.*, 2004). Anti-EGFR cancer treatments in patients have dermatological side effects including dry, irritated and itchy skin (Lacouture, 2006). Furthermore, EGFR mediates the phosphorylation of plakoglobin, decreasing its association with desmoplakin, followed by the loss of adhesive strength and increased nuclear β-catenin activity on TCF/LEF reporters (Miravet *et al.*, 2003; Yin *et al.*, 2005a).

The phenotypes exhibited by ADAM17-deficient mice are also observed in mouse models lacking HB-EGF, TGFα and iASPP (Table 2), suggesting that there might be additional regulators of desmosomes. As HB-EGF and TGFα participate in the EGFR pathway, iASPP and its role in desmosome regulation is of particular interest for delineating novel desmosome regulators. The interest in the link between iASPP and desmosomes has been further fuelled by recent findings in our laboratory, showing that iASPP localises to desmosomes in the intercalated

discs of the heart and that a loss of iASPP in mice leads to ARVC (Notari, 2012). Furthermore, iASPP is known to participate in gene regulation, hence iASPP could be a dual function protein, just like β-catenin or plakoglobin, which is able to link desmosomes to intracellular signalling. Investigations into the participation of iASPP in desmosome regulation could therefore provide an explanation for the observed differentiation defects that arise as a result of various mutations in desmosome components. Therefore, the role of iASPP in desmosomes warrants further investigation.

Component	Phenotype in mutant mice
ADAM17	ADAM17 mice with inactivating metalloproteinase activity mutations die perinatally. Phenotypes include open-eyelids at birth, eye defects, hair follicle abnormalities, abnormal myocardial development and epithelial dysgenesis in multiple organs such as the intestine, lung and non-glandular stomach (Peschon *et al.*, 1998; Shi *et al.*, 2003).
HB-EGF	HB-EGF-deficient mice exhibit perinatal lethality due to heart defects, hypoplastic lungs, open-eyelids at birth and delayed wound healing (Iwamoto *et al.*, 2003; Mine *et al.*, 2005; Shirakata *et al.*, 2005). HB-EGF mice lacking the transmembrane domain and containing the active cleaved form of HB-EGF have severe epidermal hyperplasia with abnormal differentiation and hyperplastic hearts (Yamazaki *et al.*, 2003).
TGFα	TGFα-deficient mice have wavy fur, hair follicle abnormalities, eye abnormalities and open-eyelids at birth (Berkowitz *et al.*, 1996; Luetteke *et al.*, 1993; Mann *et al.*, 1993).
iASPP	iASPP-deficient mice have cardiac defects, hair follicle abnormalities, open-eyelids at birth, wavy and woolly coats and abnormal skin differentiation (Herron *et al.*, 2005; Notari *et al.*, 2011).

Table 2 Potential regulators of desmosomes and their dynamics

1.7 iASPP and the ASPP protein family

1.7.1 Structure and binding partners of ASPP proteins

iASPP is a member of the ASPP protein family, which also comprises ASPP1 and ASPP2. iASPP is the most evolutionarily conserved member of the family, conserved across animal phyla as diverse as nematodes and chordates. ASPP1 and ASPP2 evolved later in mammalian development (Bergamaschi *et al.*, 2003). The ASPP proteins gained their earliest recognition for their ability to regulate the activity of the p53 family members: p53, p63 and p73. Specifically, they are responsible for regulating pro-apoptotic genes in conjunction with p53 family members, explaining the etymology of their name: Apoptosis Simulating Proteins of P53. Their name also reflects the structural domains found in their C-termini—ankyrin repeats, SH3 and proline rich domains. iASPP and ASPP2 both have shorter variants deprived of the first 123 and 477 amino acids, respectively, at their N-termini (Figure 1.10). These shorter variants are termed BBP (1005aa) for ASPP2, and RAI (403aa) for iASPP. BBP results from alternative splicing of the third exon of full-length ASPP2 (Takahashi *et al.*, 2004). The longer variants, termed ASPP2 (1128aa) and iASPP (828aa), are thought to be the predominant forms *in vivo* (Samuels-Lev *et al.*, 2001).

The C-termini are highly homologous between the family members and form the basis for interaction with a number of proteins, including the p53 protein family (p53, p63 and p73) (Robinson *et al.*, 2008), Bcl2 (Naumovski and Cleary, 1996), relA/p65 (Yang *et al.*, 1999) and PP1 (Llanos *et al.*, 2011). The ankyrin repeats in the C-termini contain a RanGDP binding code, which is thought to facilitate the nuclear entry of these proteins using a newly identified RanGDP-Ankyrin-Repeat (RaDAR) pathway (Lu *et al.*, 2014). These proteins also contain a conserved nuclear exclusion signal at their N-termini, which is required for their cytoplasmic

expression. In the absence of the N-termini, these proteins localise exclusively to the nucleus (Slee *et al.*, 2004). For example, RAI (which lacks the N-terminus) is mainly present in the nucleus and has a stronger inhibitory effect on p53-mediated apoptosis compared to full-length iASPP (Bergamaschi *et al.*, 2003).

Apart from the nuclear exclusion signal, the N-terminus is divergent between the evolutionarily older and younger siblings. ASPP1 and ASPP2 share homology in their N-termini (Bergamaschi *et al.*, 2003). The N-termini of ASPP1 and ASPP2 contain a ubiquitin-like fold used for binding to active GTP-bound RAS (Wang *et al.*, 2013). Moreover, the N-terminus of ASPP2 contains a coiled-coil domain thought to be important for the interaction between ASPP2 and the tight junction protein Par3 (Sottocornola *et al.*, 2010). Not much is known about the function of iASPP's N-terminus. iASPP can be found at the desmosomes within the intercalated discs in heart tissue (Notari, 2012). What regulates the expression of iASPP at the desmosomes is not known. Given that the N-terminus of iASPP differs from that of ASPP2, it is likely that iASPP localises to the desmosome using its N-terminus. Since ASPP proteins have distinct functions depending on their subcellular localisation, it would be of great value to uncover the factors that regulate the intracellular translocations of these proteins. Recently, it was demonstrated that cyclinB/cyclin-dependent kinase 1 phosphorylation of serine 84 and 113 of iASPP prevents its dimerisation, and facilitates its nuclear entry by unmasking the C-terminus, which contains the nuclear inclusion sequence (Lu *et al.*, 2013).

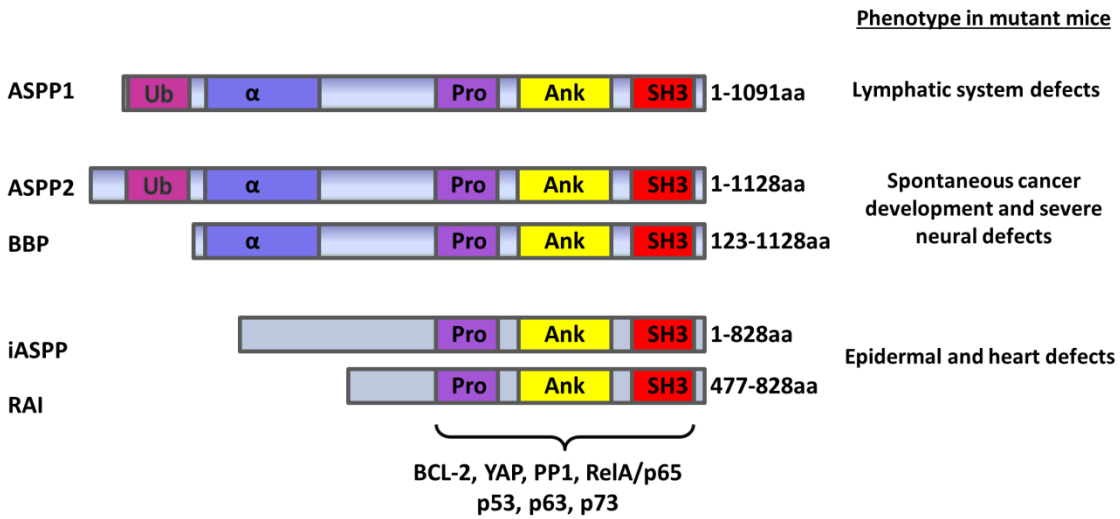

Figure 1.10 The ASPP family members and their architecture

The ASPP family comprises three members: ASPP1, ASPP2 and iASPP. ASPP2 and iASPP have splice variants: BBP (Bcl-2 binding protein) for ASPP2, and RAI (RelA/p65 inhibitor) for iASPP. On the right, the amino acid length of each protein is indicated. Structural domains with which ASPP proteins are equipped include a proline-rich region (Pro, purple), an ankyrin repeat region (Ank, yellow) and a Src homology domain 3 (SH3, red). ASPP1 and ASPP2 also contain an alpha helical coiled-coil (α, blue) and a ubiquitin-like fold (Ub, pink). ASPP1, ASPP2 and iASPP have different developmental functions, exemplified by the phenotypes observed in mouse models in which each gene is deleted. ASPP1 plays a pivotal role in the development of the lymphatic system, ASPP2 has a key role in neural development and tumour suppression, while iASPP has a role in heart and epidermal development.

1.7.2 Developmental functions of ASPP family members

The numerous binding partners of the ASPP proteins and their broad subcellular localisation suggest that the repertoire of ASPP protein functions is wide-ranging. Indeed, mice lacking individual ASPP proteins exemplify the non-redundant and broad functions these proteins have in development.

ASPP1 has been mainly studied by Hirashima *et al.*, who have shown it to be an endothelial-specific marker with a p53-independent function in lymphogenesis (Hirashima *et al.*, 2004; Hirashima *et al.*, 2008). Their ASPP1-deficient mice display subcutaneous embryonic oedema, delayed lymphatic vessel formation and disordered draining lymphatic vessels. In a p53-deficient background, ASPP1-deficient mice do not show any exacerbation or alleviation of the lymphogenic phenotype, confirming that the role of ASPP1 in lymphogenesis is p53-independent (Hirashima *et al.*, 2008).

ASPP2 exon3-deficient mice, generated in our laboratory, reveal the key roles that ASPP2 plays in the development of the central nervous system and retina. Consistent with this, ASPP2 has been found to be highly expressed in the spinal cord, brain and optic cup from E9 onwards. ASPP2 mutant mice on a mixed 129SvxC57BL/6J background die perinatally from severe hydrocephalus and neural tube closure defects. On a Balb/c background, these mice survive past the weaning age and display similar, but slightly ameliorated, phenotypes. These include hydrocephalus, neuroepithelial abnormalities and retinal dysplasia (Sottocornola *et al.*, 2010; Vives *et al.*, 2006). Investigation into the molecular function of ASPP2 in the neuroepithelium has revealed that ASPP2 localises with the Par complex at the tight junctions of the mouse neuroepithelium. Loss of ASPP2 in the mutant mice results in the disrupted integrity of tight junctions in the choroid plexus, leading to the development of hydrocephalus. From this data,

ASPP2 was reported to be a gatekeeper of tight junction integrity in the neuroepithelium. The N-terminus of ASPP2, which is not conserved in iASPP, is thought to mediate its interaction with the Par complex (Sottocornola *et al.*, 2010). This suggests that ASPP2 and iASPP are likely to have distinctive roles in neuroepithelial polarity and development. Vives *et al.* and Kampa *et al.* have shown that the loss of one copy of ASPP2 is sufficient to induce the development of spontaneous tumours in mice. Tumours developed range from lymphomas, fibroblastic sarcomas, squamous cell carcinomas and lung adenocarcinomas. ɣ-irradiation accelerated the age of onset of lymphomas in ASPP2 heterozygous mice (Kampa *et al.*, 2009; Vives *et al.*, 2006). These studies suggests that ASPP2 has tumour suppressive functions *in vivo*.

iASPP-deficient mice have highlighted the functions of iASPP in the development of the heart and skin. Herron and colleagues have shown that iASPP is predominantly expressed in the skin, heart, lung, testis and intestines. Its loss in mice leads to phenotypes such as wavy hair, epidermal defects, cardiomyopathy and open-eyelids at birth. These mice also die suddenly between three to six months of age (Herron *et al.*, 2005; Notari *et al.*, 2011).

It has been shown that iASPP regulates skin development by modulating the activity of p63, a master regulator of epithelial stratification, to regulate genes required for proliferation and differentiation. Loss of iASPP leads to modest thickening of the epidermis associated with increased differentiation and decreased proliferation (Chikh *et al.*, 2011; Notari *et al.*, 2011).

Studies focused on the heart phenotype have revealed that iASPP-deficient mice suffer from ARVC. Fibrofatty deposits were observed in the hearts of iASPP-deficient mice, and the integrity of the intercalated discs of the heart was compromised. In accordance, iASPP was observed at the intercalated discs of mouse hearts together with N-cadherin, desmoplakin, plakoglobin and Connexin 43. Disrupted expression patterns in these proteins was observed in

iASPP-deficient mice (Notari, 2012). Moreover, the hearts of iASPP-deficient mice displayed irregular electrical conduction.

While these studies have uncovered some of the functions of iASPP, many questions remain. In humans, the phenotypic triad of ARVC (or ARVC-like disease), palmoplantar keratoderma and woolly hair are observed in patients with Carvajal syndrome and Naxos disease. These diseases are thought to be diseases of desmosome dysfunction, and affected individuals often harbour mutations in desmoplakin, plakoglobin and desmocollin 2 (Keller *et al.*, 2012; McKoy *et al.*, 2000; Norgett *et al.*, 2000; Saffitz, 2009). However, case reports suggest the existence of other causative genes for Naxos disease in two Arab families and in one Spanish patient, since these patients do not show mutations in well-established desmosomal components (Alonso-Orgaz *et al.*, 2007; Djabali *et al.*, 2002). Moreover, only 50% of ARVC cases are due to mutations in desmosome components, suggesting that other genes might be involved in the progression of the disease in the remaining 50% of patients (den Haan *et al.*, 2009). This suggests that iASPP could be a candidate gene regulating desmosomes and preventing the development of ARVC. Although Dr Notari has reported that iASPP localises to the intercalated discs of the heart and maintains their integrity, the molecular mechanisms by which it performs this function are not clear. Whether iASPP participates in desmosome assembly and maturation is unknown. Moreover, the question of whether iASPP interacts with desmosome components in the epidermis remains to be tested. Furthermore, neither Herron *et al.* nor Notari *et al.* have investigated whether iASPP-deficient mice display palmoplantar keratoderma. If iASPP participates in desmosome function, it would not be surprising to observe palmoplantar keratoderma in iASPP-deficient mice, since palmoplantar keratoderma is a common phenotype in humans and animal models harbouring desmosomal mutations. Additionally, the question of whether desmosome dynamics are altered in these mice requires further investigation. Embryonic eyelid closure requires the migration of keratinocytes at the eyelid fronts and

desmosome re-adjustment is necessary for migration to occur. Therefore, it would be interesting to test whether desmosome dynamics are compromised in these mice.

1.7.3 Cancer-related functions of the ASPP proteins

The best-characterised function of the ASPP proteins is their ability to regulate p53-dependent apoptosis without affecting p53-dependent cell cycle arrest. ASPP1 and ASPP2 are thought to enhance the p53-dependent transactivation of apoptotic genes (*BAX, PUMA, PIG3*), while iASPP is thought to inhibit it (Figure 1.11) (Bergamaschi *et al.*, 2004; Samuels-Lev *et al.*, 2001). The ability of ASPP proteins to regulate the apoptotic function of p53, a major tumour suppressor and the most frequently deregulated gene in cancer (Hainaut and Hollstein, 2000), indicates that these proteins are likely to be implicated in tumourigenesis. Indeed, expression profiling of many cancer samples has yielded significant insight into the role of the ASPP proteins in the initiation and development of cancer. Based on deregulated apoptosis, dysregulation of ASPP family mRNA and protein expression in these cancer samples, proto-oncogenic functions have been ascribed to iASPP while tumour suppressive functions have been ascribed to ASPP1 and ASPP2 (Bergamaschi *et al.*, 2003; Trigiante and Lu, 2006).

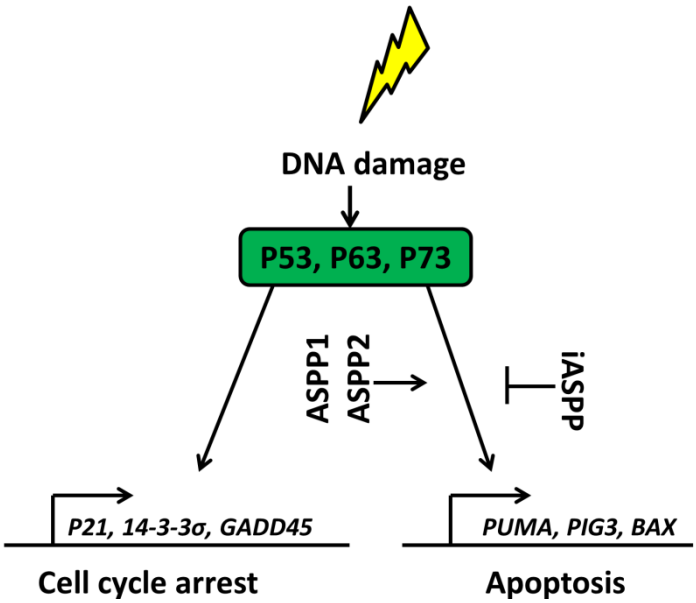

Figure 1.11 ASPP proteins selectively regulate the p53-apoptotic response
Stress signals induce the expression of the transcription factors P53, P63, P73 and E2F. E2F factors activate the expression of the ASPP family members, which in turn are able to cooperate with p53 family members to selectively regulate the apoptotic response. ASPP1 and ASPP2 enhance the binding of p53 family members to the promoters of pro-apoptotic genes such as *BAX, PUMA* and *PIG3*, while iASPP has an opposing function and inhibits the p53-dependent transactivation of pro-apoptotic genes. Adapted from Trigiante and Lu, (2006).

ASPP1 is considered to be a tumour suppressor and it is well known that its expression levels are often downregulated in various cancers. ASPP1 levels are lowered in leukaemia cell lines (Liu *et al.*, 2004), acute lymphoblastic leukaemia (Agirre *et al.*, 2006), non-small cell lung carcinoma (Su *et al.*, 2014), endometrial endometrioid adenocarcinoma (Liu *et al.*, 2010), gestational trophoblastic disease (Mak *et al.*, 2011) and hepatocellular carcinomas (Zhao *et al.*, 2010). ASPP1 downregulation in cancer appears to occur via epigenetic silencing through the methylation of its promoter (Agirre *et al.*, 2006; Mak *et al.*, 2011; Zhao *et al.*, 2010).

ASPP2 is also considered to be a tumour suppressor and its expression profile follows a similar trend to ASPP1 in cancer samples. ASPP2 downregulation has been reported in breast tumours (Samuels-Lev *et al.*, 2001), breast cancer cell lines (Liu *et al.*, 2005), lung cancer cell lines (Mori *et al.*, 2004), hepatocellular carcinomas (Zhao *et al.*, 2010), lymphoma (Lossos *et al.*, 2002), myeloid and lymphoid leukaemia (Schittenhelm *et al.*, 2013) and choriocarcinoma (Mak *et al.*, 2013). Reduced levels of ASPP2 have also been associated with poor clinical outcome in lymphoma (Lossos *et al.*, 2002), breast cancer (Cobleigh *et al.*, 2005; Sgroi *et al.*, 1999) and leukaemia patients (Schittenhelm *et al.*, 2013). The main mechanisms of ASPP2 downregulation are promoter methylation and loss-of-function mutations (Park *et al.*, 2010; Schittenhelm *et al.*, 2013; Zhao *et al.*, 2010). Furthermore, the R181K and R181L mutations observed in breast and cervical tumours render p53 unable to promote apoptosis. These residues are also important for the interaction with ASPP2, and their mutation from arginine to lysine or leucine prevents ASPP2 from binding p53 and transactivating pro-apoptotic genes (Samuels-Lev *et al.*, 2001; Trigiante and Lu, 2006). These mutations also weaken the affinity of ASPP1 for p53. Additional support for the role of ASPP1 and ASPP2 in tumour suppression is the finding that exogenous expression of ASPP1 or ASPP2 can hinder the transforming activity of oncogenic RAS and adenovirus E1A in rat fibroblasts. Further suppression of the

transformative capacities of RAS and E1A is obtained when p53 is co-expressed with ASPP2, suggesting that p53 and ASPP2 act alongside each other to enhance p53's tumour-suppressive function (Iwabuchi *et al.*, 1998).

iASPP has proto-oncogenic properties as suggested by multiple lines of evidence. Consistent with this, overexpression of iASPP can be seen in human breast carcinomas (Bergamaschi *et al.*, 2003), non-small lung cancers (Chen *et al.*, 2010), hepatocellular carcinomas (Lu *et al.*, 2010), prostate cancers (Zhang *et al.*, 2011), endometrial endometrioid adenocarcinoma (Liu *et al.*, 2010), leukaemia cell lines and leukaemias (Zhang *et al.*, 2005). A recent DPhil graduate in our laboratory, Dr Emma Morris, has shown that increased nuclear and decreased junctional expression of iASPP associates with higher grade and more invasive prostate cancer with a poor clinical outcome (Morris, 2013). This suggests that iASPP's expression pattern and levels could be used as a prognostic marker for prostate cancer. Moreover, these results also imply that sequestration of iASPP in cell-cell junctions may serve to limit the non-junctional pool of iASPP available for signalling. Increased iASPP signalling can have oncogenic effects, such as the inhibition of apoptosis in cancerous cells. Indeed, cell lines overexpressing iASPP are more resistant to apoptosis induced by the DNA-damaging reagent cisplatin and UV radiation (Bergamaschi *et al.*, 2003). Furthermore, iASPP cooperates with the RAS and E1A oncoproteins in their transformation of rat fibroblasts (Bergamaschi *et al.*, 2003). These anti-apoptotic and transformative roles, together with broad and frequent overexpression of iASPP in cancer samples, implicate iASPP as a proto-oncogene. However, further studies are needed to confirm its oncogenic properties.

1.7.4 Regulation of expression of ASPP family members

ASPP1 and ASPP2 expression is regulated through epigenetic DNA modification, transcriptional regulation and posttranslational modification. In cancer samples, as outlined in section 1.7.3, ASPP1 and ASPP2 are mainly downregulated through abnormal methylation of their promoters (Agirre *et al.*, 2006; Mak *et al.*, 2011; Schittenhelm *et al.*, 2013; Zhao *et al.*, 2010). At a transcriptional level, ASPP1 and ASPP2 are regulated by the E2F family of transcription factors. Genotoxic events induce E2F factors to participate in the induction of cell apoptosis in a p53-dependent or p53-independent manner. Overexpression of E2Fs leads to increased expression of ASPP1 and ASPP2 at both the mRNA and protein level, illustrating another possible route by which E2F could mediate p53-dependent apoptosis (Chen *et al.*, 2005; Fogal *et al.*, 2005). Furthermore, the induction of inflammation results in increased ASPP2 expression. This is thought to be regulated by inflammation-driven STAT1 (signal transduced and activator of transcription) expression and its subsequent binding to the ASPP2 promoter to induce its transcription (Turnquist *et al.*, 2014). At a post-translational level, ubiquitination of the central region of ASPP2 leads to its proteasomal degradation (Zhu *et al.*, 2005).

iASPP has been found to be overexpressed in many cancers. However, what regulates its expression remains poorly understood. To date, only two studies have examined its regulation at the transcriptional level. Lu *et al.* have reported that, in hepatocellular carcinoma, iASPP overexpression is driven by the binding of the Nuclear Factor Kappa B (NF-kB) transcription factors p65/p50 to iASPP's promoter regions, inducing its transcription (Lu *et al.*, 2010). Chikh *et al.* showed that iASPP contains binding sites for p53-family members in its promoter, and that iASPP is a direct transcriptional target of p63. Accordingly, overexpression or depletion of p63 led to the induction or downregulation of iASPP, respectively. They also reported that

iASPP indirectly regulates p63's translation by inhibiting the expression of two miRNAs, namely miR-720 and miR-574-3p, which would otherwise suppress p63's translation (Chikh *et al.*, 2011). These interesting findings explain the mechanism by which a loss of iASPP leads to increased differentiation of the epidermis, i.e. by regulating p63-dependent control of differentiation (Chikh *et al.*, 2011; Notari *et al.*, 2011). An aspect of iASPP's regulation that needs to be addressed is the question of what mediates its localisation. iASPP can be found in all compartments of the cell: the nucleus, cytoplasm and cell-cell junctions. In the nucleus, as mentioned previously, it inhibits p53 protein family-mediated apoptosis and modulates p63-dependent differentiation. Its functions in the cytoplasm and at cell-cell junctions remain elusive.

1.8 Aims of the study

Mutations in desmosome components often lead to a phenotypic triad of woolly hair, ARVC and palmoplantar keratoderma. Moreover, processes that require efficient desmosome modelling and remodelling are often affected when the dynamics of desmosome components are compromised. One such process requiring desmosome remodelling is wound healing. iASPP-deficient mice have three main macroscopic abnormalities: wavy hair, enlarged abnormal hearts, and open-eyelids at birth. A recent graduate from our laboratory, Dr Notari, has shown that the heart phenotype mimics the ARVC phenotype observed in human patients. Dr Notari also noted that iASPP localises to the intercalated discs of the heart, where desmosome components reside. Consistent with this, iASPP loss resulted in a diminished integrity of intercalated discs alongside decreased expression of desmoplakin, N-cadherin and connexion 43 at the intercalated discs. Furthermore, iASPP is known for its regulation of epidermal differentiation through its mediation of p63 stratification-related activities. These findings suggest that iASPP is a potential regulator of desmosomes that links cell adhesion to intracellular signalling. Therefore, the aim of this study was to investigate whether iASPP is a dual function protein that links desmosome adhesion to gene expression and, if so, whether desmosome-related diseases develop in the absence of iASPP. This aim was addressed using three approaches.

First, as desmosome dysfunction is often associated with palmoplantar keratoderma, the question of whether the loss of iASPP in iASPP-deficient mice leads to the development of palmoplantar keratoderma was examined. This was investigated by histologically examining the palms and soles of the feet. Common features of palmoplantar keratoderma were looked for, such as increased intercellular spacing and thickening of the epidermis. Aspects of epidermal differentiation were also examined to determine whether intracellular signalling

was affected by ablation of iASPP. Further, *in vitro* techniques were employed to examine whether iASPP interacts with desmosome components, and whether intercellular adhesions were compromised upon iASPP loss. The localisation and solubility of desmosome components in the presence or absence of iASPP was also examined.

Second, the role of iASPP in processes that require the modulation of desmosome adhesiveness was studied. In particular, the role of iASPP in wound healing was investigated. This was investigated both *in vivo* in animal models and *in vitro* using keratinocytes. As loss of desmosome adhesion is known to affect proliferation and cell migration, the effect of iASPP depletion on these processes was also examined.

Third, since iASPP-deficient mice have the open-eyelids at birth phenotype, and the ablation of the desmosome component desmocollin 1 in mice causes the same phenotype, the molecular mechanisms by which loss of iASPP leads to this phenotype were investigated. Cellular processes that could impede eyelid closure such as proliferation, apoptosis and migration were investigated. As iASPP is known to regulate the apoptotic activities of p53 family members, we investigated whether the deficit in eyelid closure in iASPP-deficient mice was p53 or p63 dependent.

In summary, this study aimed to achieve new insights into the roles of iASPP in pathological, physiological and developmental processes and the regulation of desmosome adhesion.

Chapter II: Materials and methods

2.1 Materials

2.2 Methods

Chapter II: Materials and methods

All chemicals purchased from the companies outlined in the text below were prepared, maintained and stored according to the manufacturers' instructions. Catalogue numbers and manufacturer information are provided in the materials section. The methods section describes the protocols followed to perform the experiments.

2.1 Materials

2.1.1 Reagents for cell culture

Cell lines

Name	Tissue Type/Origin
IMOK	Immortalised Mouse Oral Keratinocytes; Ludwig Institute for Cancer Research, University of Oxford, UK; Described in (Parikh *et al.*, 2008)
MCF10a	Human fibrocystic mammary tissue cells; Ludwig Institute for Cancer Research, University of Oxford, UK
UT-SCC-74A	Human squamous cell carcinoma of the head and neck; Dr S. Feller, University of Oxford, UK
Primary dermal fibroblasts	Dermis from pups at P2; Ludwig Institute for Cancer Research, University of Oxford, UK
Primary mouse keratinocytes	Epidermis from pups at P2; Ludwig Institute for Cancer Research, University of Oxford, UK

Table 3 A list of cell lines used during the course of research

Chelating resin

Chelex® 100 resin (BioRad, cat. no. 142-2842) was used to remove calcium from fetal bovine serum (FBS) for the preparation of calcium-free media for keratinocyte cultures.

Cell passaging components

Cells were expanded by trypsinising an attached confluent sheet of cells using 1 X 0.05% Trypsin-EDTA (Gibco, cat. no. 25300-054) and splitting them 1:2 for IMOK and MCF10A, or 1:4 for other cell lines.

DharmaFECT® transfection reagent I was used for the transfection of siRNAs into cells (cat.no. T-2001). 40 nM final siRNA concentration with 2 µl of transfection reagent and 80,000 cells in 1 ml media was the optimal condition for transfection for a single well in a 24-well plate.

Ethylene glycol tetraacetic acid (EGTA)

190 g of EGTA (Sigma, cat. no. E4378) was added to 900 ml of water and, while stirring, the pH was adjusted to 8.0 with pellets of sodium hydroxide (NaOH, >4 g). The final volume was brought up to 1 L with water.

Freezing media for cell storage

An attached confluent sheet of cells was trypsinised and detached using 1 X 0.05% Trypsin-EDTA. Subsequently, cells were spun down and incubated in the freezing media described below.

10% (v/v) Dimethyl sulfoxide (DMSO, Sigma, cat. no. D8418)

90% (v/v) FBS

Growth media

Growth media for primary keratinocytes

Defined keratinocyte serum-free media

Keratinocyte growth media (KGM, Gibco, cat. no. 10744-019)

100 units/ml penicillin and 100 µg/ml streptomycin (Gibco, cat. no. 15070)

Low calcium media (LCM)

Eagle's minimum essential medium (EMEM), calcium-free (BioWhittaker, cat. no. 06-174G), supplemented with:

4% (v/v) FBS (Sigma, cat. no. F4135), chelated

0.05 mM Calcium

100 units/ml penicillin and 100 µg/ml streptomycin

For better cell growth the following supplements were added:

0.4 µg/ml Hydrocortisone (Sigma, cat. no. H-0888)

5 µg/ml Insulin (Sigma, cat. no. I-1882)

10 ng/ml Epidermal growth factor (EGF, Peprotech cat. no. AF-100-15)

10^{-10} M Cholera toxin (Sigma, cat. no. C-8052)

100 units/ml penicillin and 100 µg/ml streptomycin

High calcium media (HCM)

Prepared by adding extra calcium to a final concentration of 1.5 mM.

Growth media for the Immortalised Mouse Oral Keratinocytes (IMOK) cell line

EMEM, calcium free

4% (v/v) FBS, chelated

100 units/ml penicillin and 100 µg/ml streptomycin

Growth media for the MCF10a cell line

Dulbecco's Modified Eagle's Medium: Nutrient mixture F12 (DMEM: F-12, Gibco, cat.no.12634-010)

5 % (v/v) Horse serum (Gibco, cat. no. 26050)

10 µg/mL Insulin

20ng/mL EGF

100ng/mL Cholera toxin

0.5 µg/mL Hydrocortisone

100 units/ml penicillin and 100 µg/ml streptomycin

Growth media for other cell lines – Complete DMEM

DMEM (Lonza, cat. no. LZBE12-604F)

5 % (v/v) FBS

2 mM $_{L}$-Glutamine (Gibco, cat. no. 25030)

100 units/ml penicillin and 100 µg/ml streptomycin

2.1.2 Reagents for DNA- and RNA-based techniques

Agarose gels for DNA electrophoresis

Agarose (Fisher Scientific, cat. no. BP1356) was dissolved at a concentration of 1% (w/v) in 1 X TAE buffer and, upon solidification, was used to separate DNA fragments by electrophoresis. Ethidium bromide (Sigma, cat. no. E1510), a fluorescent DNA-intercalating reagent, was added to the agarose gel at a final concentration of 0.4 μg/ml, and DNA was visualised using a UV transilluminator (BioDoc-It System, UVP).

DNA amplification primers

Unless otherwise stated, Eurofins MWG Operon synthesised the primers. The lyophilised primers were dissolved in TE buffer at a concentration of 100 μM. The lists of primers used in PCR or RT-qPCR are listed in the sections describing the method used to carry out PCR or RT-qPCR.

DNA Marker

DNA fragment size was determined using commercially available 1kb HyperLadder I ladder (Bioline Reagents Ltd., cat.no. BIO-33053).

GNT-K buffer for DNA isolation from tissues

50 mM KCl

1.5 mM MgCl

10 mM Tris-HCl (pH 8.5)

0.01% Gelatine

0.45% NP-40

0.45% Tween®-20

100 μg/ml Proteinase K

Real-time quantitative PCR (RT-qPCR)

cDNA levels were quantified using the QuantiTect SYBR Green PCR kit (Qiagen, cat. no. 204143). RT-qPCR was used to determine whether iASPP was deleted at the mRNA level in primary cell lines used in the studies presented in this thesis.

RNA isolation

Isolation of RNA from tissues and cells was carried out using the RNeasy Mini Kit (Qiagen, cat. no. 74106). The exact composition of the reagents provided in the kit is proprietary, and therefore not listed in this thesis.

RNA to cDNA conversion

cDNA was prepared from RNA using the SuperScript® First Stand Synthesis System (Invitrogen, cat. no. 11904-018). Components included: Oligo(dT)12-18 (0.5 μg/μL), 10 X RT buffer [200 mM Tris-HCl (pH 8.4), 500 mM KCl], 25 mM $MgCl_2$, 0.1 M DTT, 10 mM dNTPmix (10 mM each dATP, dCTP, dGTP, dTTP), SuperScript II RT (50 units/μL), RNaseOUT. Recombinant ribonuclease inhibitor (40 units/μL), *E. coli* RNase H (2 units/μL), DEPC-treated water, control RNA (50 ng/μL), control primer A (10μM), control primer B (10μM).

Removal of DNA contamination during RNA purification

An RNase-Free DNase set (Qiagen, cat. no. 79254) was used to remove DNA contamination during RNA purification. The components included:

DNaseI stock solution: 1500 Kunitz units DNaseI in 550 μl RNase-free water

10 μl of stock solution in 70 μl RDD buffer was used per single RNA isolation reaction.

TAE X 50 (Tris-Acetate-EDTA) running buffer, pH 8.5

242 g Tris base

57.1 ml Glacial acetic acid

100 ml 0.5 M EDTA

Dissolved in 1 L of water. Working solution was 1 X.

TE Buffer

10 mM Tris-HCl, pH 8

1 mM EDTA

2.1.3 Reagents for protein-based techniques

Antibodies

PRIMARY ANTIBODIES				
Antigen	**Antibody Clone**	**Host/Type**	**Source/Product code**	**Application**
Actin	C4	mouse mAb	Santa Cruz/sc-47778	WB (1:2000)
β-tubulin	TUB2.1	mouse mAb	Abcam/ab11308	WB (1:2000)
β-catenin	-	rabbit pAb	Abcam/ab2365	IF (1:100), WB (1:1000)
β-catenin	6B3	rabbit mAb	Cell Signalling/9582S	IF (1:50), WB (1:1000)
BrdU	BU1/75	rat mAb	Abcam/ab6326	IF (1:250)
iASPP	LX128.5	mouse mAb	Ascite	WB (1:1000)
iASPP	LX49.3	mouse mAb	Ascite	ICC/IF (1:250), WB (1:1000)
iASPP	N1	rabbit pAb	Ascite	WB (1:1000), IP
Cyclin-D1	DCS-6	mouse mAb	Abcam/ab10540	IF (1:200)
Desmoglein 1/2	DG 3.10	mouse mAb	Progen Scientific/ 61002	IF (1:200), WB (1:500)
Desmoplakin 1/2	H300	rabbit pAb	Santa Cruz/sc-33555	IF (1:100), WB (1:1000), IP
Desmoplakin 1	DP2.17	mouse mAb	Progen Scientific/61024	WB (1:500)
Desmoplakin 1/2	DP-2.15/-2.17/-2.20	mouse mAb	Progen Scientific/65146	IF(1:10)
Desmoplakin 1/2	DP2.15	mouse mAb	Progen Scientific/61003	WB (1:500)
Desmoplakin phospho-Ser2849	pSer2849	rabbit pAb	LifeSpan Biosciences/LS-C209392	WB (1:500) IF (1:50)
Plakoglobin	-	rabbit pAb	Abcam/ab15153	IF (1:100), WB (1:1000)
Keratin 1	AE1	mouse mAb	Abcam/ab9286	IHC (1:400)
Keratin 1	AF-109	rabbit pAb	Covance/PRB-165P	IF (1:500), WB (1:2000)
Keratin 14	AF-64	rabbit pAb	Covance/PRB-155P	IF (1:500), WB (1:2000)
Keratin 5	AF-138	rabbit pAb	Covance/PRB 160P	IF (1:500), WB (1:2000)
Keratin 5	AE-16	goat pAb	Santa Cruz/sc-17090	WB (1:1000), IP
Keratin 6	-	rabbit pAb	Covance/PRB-169P	WB (1:1000), IF (1:500)
Ki67	-	rabbit pAb	Abcam (ab15580)	IHC (1:400)
Myc-tag	9E10	mouse mAb	Ascite	WB (1:1000)
Myc-tag	-	rabbit pAb	Abcam/ab9106	WB (1:1000)
P53	DO-1	mouse mAb	Santa Cruz (sc-126)	ICC/IF (1:200)

P53	CM5	rabbit pAb	Leica/NCL-p53-CM5p	IF (1:100)
P63	4A4	mouse mAb	Santa Cruz (sc-8431)	IHC/ICC/IF (1:400), WB (1:1000)
P63	H137	rabbit pAb	Santa Cruz/sc-8343	ICC/IF (1:200)
PERP		rabbit pAb	Abcam/ab5986	IF, WB
PKCα	-	rabbit pAb	Cell Signalling/2056S	WB (1:1000)
PKCα/β p-Thr638/641	-	rabbit pAb	Cell Signalling/9375	WB (1:1000), IF (1:50)
PKC substrate phospho	-	rabbit pAb	Cell Signalling/9375	WB (1:1000)
Plectin	E398P	rabbit pAb	Abcam/83497	
PP1 α	C19	goat pAb	Santa Cruz/sc-6104	WB (1:1000)
PP1	E9	mouse mAb	Santa Cruz/sc-7482	WB (1:1000)
V5-tag	SV5-Pk1	mouse mAb	Serotec	ICC/IF (1:400), WB (1:1000)
V5-tag	-	rabbit pAb	Abcam (ab9116)	ICC/IF (1:400), WB (1:1000)
Vimentin	RV202	mouse mAb	Abcam (ab8978)	IHC (1:400)
ZO-1	--	rabbit pAb	Invitrogen/61-7300	WB(1:1000)
ZO-1	--	rabbit pAb	Invitrogen/33-9100	IF (1:100)

Table 4 A list of primary antibodies used in protein-based techniques in this study

SECONDARY ANTIBODIES			
Ab name	host	Source/cat.no.	applications
Alexa Fluor® 488 F(ab')2 fragment anti-rabbit IgG (H+L)	goat	Invitrogen/A11070	IF (1:400)
Alexa Fluor® 488 F(ab')2 fragment anti-mouse IgG (H+L)	goat	Invitrogen/A11017	IF (1:400)
Alexa Fluor® 546 F(ab')2 fragment anti-rabbit IgG (H+L)	goat	Invitrogen/A11071	IF (1:400)
Alexa Fluor® 546 anti-mouse IgG (H+L)	goat	Invitrogen/A11003	IF (1:400)
Alexa Fluor® 647 F(ab')2 fragment anti-rabbit IgG (H+L)	goat	Invitrogen/21246	IF (1:400)
Alexa Fluor® 647 F(ab')2 fragment anti-mouse IgG (H+L)	goat	Invitrogen/21237	IF (1:400)
Alexa Fluor® 488 Anti-Mouse IgG (H+L)	donkey	Invitrogen/A21202	IF (1:400)
Alexa Fluor® 488 Anti-Goat IgG (H+L)	donkey	Invitrogen/A11055	IF (1:400)
Alexa Fluor® 488 Anti-Rabbit IgG (H+L)	donkey	Invitrogen/A21206	IF (1:400)
Alexa Fluor® 546 Anti-Rabbit IgG (H+L)	donkey	Invitrogen/A10040	IF (1:400)
Alexa Fluor® 647 Anti-Rabbit IgG (H+L)	donkey	Invitrogen/A31573	IF (1:400)
Alexa Fluor® 647 anti-mouse IgG (H+L)	donkey	Invitrogen/A31571	IF (1:400)
Anti-Goat Immunoglobulins/HRP	rabbit	Dako/P0449	WB (1:2000)
Anti-Rabbit Immunoglobulins/HRP	swine	Dako/P0217	WB (1:2000)
Anti-Mouse Immunoglobulins/HRP	rabbit	Dako/P0161	WB (1:2000)
Biotinylated Anti-Mouse IgG	goat	Vector Labs/BA-9200	IHC (1:250)
Biotinylated Anti-Rabbit IgG	goat	Vector Labs/BA-1000	IHC (1:250)
Biotinylated Anti-Goat IgG	rabbit	Vector Labs/BA-9500	IHC (1:250)

Table 5 A list of secondary antibodies used in protein-based techniques in this study
For double-immunostaining assays, secondary antibodies raised in goat were used. For triple immunostaining assays, secondary antibodies raised in donkey were used.

Ammonium Persulphate (APS)

10% (w/v) stock solution was prepared in water and used within three weeks of preparation.

Blocking solution

5% (w/v) skimmed milk powder (Marvel) or 3% (w/v) bovine serum albumin (BSA, Sigma, cat.no. A7906) in Tris-buffered saline and Tween 20 (1X TBS-T) was used for blocking of protein membranes.

Citric acid buffer 100 mM (10X), pH 6.0

19.2 g of citric acid was dissolved in 1 L of water to make 10X stock solution. The pH was adjusted to 6.0 with NaOH.

Ethylene diamine tetraacetic acid (EDTA), 0.5 M, pH 8.0, solution

181.6 g of EDTA was added to 800 ml of water and, while stirring, the pH was adjusted to 8.0 with pellets of NaOH (about 20 g NaOH). The final volume was brought up to 1 L with water.

Fluorescence mounting media

Fluoromount G (Southern Biotech, cat. no. 0100-01)

ProLong® Gold Antifade Reagent (Life Technologies, cat. no. P36934)

NETN buffer

50mM Tris pH 8.0

150mM NaCl

1mM EDTA

1% (v/v) NP-40

COmplete™ protease and PhosSTOP phosphatase inhibitor cocktails from Roche (cat. no.11 830 145 001 and 04 906 837 001, respectively) were added to the buffer before use.

Paraformaldehyde Stock Solution, 20%, pH 7.4

A 20% paraformaldehyde stock solution was prepared by dissolving 20 g of paraformaldehyde powder in 700 ml of heated PBS. Dissolution was facilitated by adding a few drops of NaOH. The volume was brought up to 1 L with heated PBS. The solution was stored at -20°C. The working concentration was 4% (v/v) in PBS.

Phosphate buffered saline (PBS), pH 7.0

12.5 mM NaCl

1 mM Sodium dihydrogen phosphate, NaH_2PO_4

1.6 mM Disodium dihydrogen phosphate, Na_2HPO_4

Ponceau S staining solution

Ponceau solution was obtained from Sigma (cat. no. P7170).

Protein G sepharose beads

The beads were stored in 20% ethanol at 4˚C. Pharmacia Biotech beads were initially used. Due to non-specific binding of these beads to various proteins, their use was discontinued and a switch was made to beads from Roche (cat. no. 05 015 952 001).

Protein molecular weight markers

A New England Biolabs prestained protein marker (cat. no. P7708S) was used as a size standard for SDS-polyacrylamide gel electrophoresis.

Polyacrylamide gel preparation

Stacking Gel		Resolving Gels			
4	**Acrylamide %**	6	8	10	12
1.3 ml	**Acrylamide/Bis**	2 ml	2.7 ml	3.3 ml	4.0 ml
--	**1.5M Tris-HCl pH 8.8**	2.5 ml	2.5 ml	2.5 ml	2.5 ml
2.5 ml	**1.0M Tris-HCl pH 6.8**	--	--	--	--
100 µl	**10% SDS**	100 µl	100 µl	100 µl	100 µl
100 µl	**10% APS**	100 µl	100 µl	100 µl	100 µl
10 µl	**TEMED**	10 µl	8 µl	5 µl	5 µl
6.1 ml	**Distilled Water**	5.3 ml	4.6 ml	4.0 ml	3.3 ml
10 ml	**Total Volume**	10 ml	10 ml	10 ml	10 ml

Table 6 Recipes for the preparation of stacking and resolving SDS-polyacrylamide gels

Polyacrylamide gel solution

30% Acrylamide concentrate (Bis-Acrylamide Ratio 37.5:1) from Severn Biotech Ltd. (cat. no. 20-2100-10) was used in the preparation of polyacrylamide gels.

RIPA buffer

150 mM NaCl

1% (v/v) NP-40

0.1% (w/v) SDS

50 mM Tris base

COmpleteTM protease and PhosSTOP phosphatase inhibitor cocktails were added to the buffer just before use.

SDS-PAGE 10X running buffer

720 g Glycine

150 g Tris

50 g SDS

Dissolved in 5 L of water. 1x solution was used experimentally.

SDS-PAGE 10X transfer buffer

725 g Glycine

145 g Tris

Solubilised in 5L of water. 20% ethanol was added to 1X buffer during protein transfer.

SDS-PAGE 2X loading dye

100mM Tris-HCl, pH 6.8

4% (w/v) SDS

20% (v/v) Glycerol

0.2% (w/v) Bromophenol Blue

5% (v/v) β-mercaptoethanol added just before use

SDS-PAGE 5X loading dye

250mM Tris-HCl

10% (w/v) SDS

50% (v/v) Glycerol

12.5% (v/v) β-mercaptoethanol (added before use)

0.5%(w/v) Bromophenol blue

Stripping buffer

15.5 ml of 1 M Tris-HCl, pH 6.7 (62.5 mM)

1.75 ml of β-mercaptoethanol (100 mM)

5 g SDS (2%)

Suspended in 250 ml of water.

Tris buffered saline tween 10X (TBS-T), pH 7.6

121 g Tris base

36.53 g NaCl

250 ml Tween 20

Solubilised in 5 L of water. The solution was used at 1 x concentration.

Tris-HCl, 1.5 M, pH 8.8

181.7 g of Tris base was dissolved in 1 L of water, and the pH adjusted to 8.8 using HCl.

Tris-HCl, 0.5 M, pH 6.8

60.6 g of Tris base was suspended in 1 L of water, and the pH adjusted to 6.8 using HCl.

TEMED

The solution was purchased from Fisher Scientific (cat. no. T/P190/04).

Urea buffer

8 M Urea

1 M Thiourea

0.5 % (w/v) CHAPS 3(-[(3-cholamidopropyl)-dimethylammonio]-1-propane sulfonate

50 mM DTT

24 mM Spermine

Water

Nanopure water (Type I), generated from the MilliQ water system, was used for all procedures.

2.2 Methods

2.2.1 Animal procedures

Breeding and handling of mouse colonies

All animals were maintained at the Wellcome Trust Centre for Human Genetics, Oxford. They were kept in individually ventilated cages (IVCs) to provide a clean environment. All procedures were performed in accordance with the project license approved by the UK Government Home Office (PIL: 30/9255; PPL: 30/2862).

Generation of the iASPP$^{\Delta 8/\Delta 8}$ and tamoxifen-inducible conditional iASPP$^{\Delta 8/\Delta 8}$ CreER mice used in this study has been previously described (Notari *et al.*, 2011). iASPP$^{+/+}$ and iASPP$^{\Delta 8/\Delta 8}$ mice were of mixed genetic background C57BL/6J and 129Sv. iASPP$^{flox/flox}$ conditional mice were crossed with R26Cre^{+}-ER^{T} mice (obtained from Prof. Anton Berns) on a Balb/c background to allow for the deletion of exon 8 upon treatment with tamoxifen (Sigma, cat. no. T5648) or 4-hydroxytamoxifen (4-OHT) (Sigma, cat. no. 6278) in primary cell lines, enabling the generation of iASPP$^{\Delta 8/\Delta 8}$ CreER mice or cells. Genotyping was done using polymerase chain reaction (PCR) primers for wild type allele I8 (5'-CCGAATTGGAGAAGTGAAGC- 3') and E8 (5'-AGAGCAGCCTCAGAGCATGG -3'), lox allele FLP2 (5'-CCGAATTGGAGAAGTGAAGC-3') and FRNT9 (5'GGGTAGGAAAAAGGGCTGAG3') and deletion allele I8 and FLP2. Cre transgene was genotyped using Cre-F (5'-CATTTGGGCCAGCTAAACAT-3') and Cre-R (5'-ATTCTCCCACCGTCAGTACG-3').

Balb/c-p63 heterozygous mice were kindly provided by Prof. Frank McKeon, Harvard Medical School, USA. p63$^{+/-}$ and iASPP$^{+/\Delta 8}$ heterozygous mice were crossed to generate double heterozygotes, which were subsequently intercrossed to generate compound genotypes. The

following primers were used to genotype p63 transgenic mice: 5'-TTCTCAGATGGTACCGCTCC-3' (exon 3), 5'-GGTGCTTTGAGGCCCGGATC-3' (exon 4), and 5'-TACCCGCTTCCATTGCTCAG-3' (neomycin resistance gene).

Balb/c-p53$^{+/-}$ mice were kindly shared by Prof. Tyler Jacks, Massachusetts Institute of Technology, USA and were intercrossed with 129Sv x C57BL/6J-iASPP$^{+/\Delta 8}$ mice to generate double heterozygotes on a mixed background. Further crossing of double heterozygotes was done to generate compound genotypes. The following primers: 5'-CACAGCGTGGTGGTACCTTA-3' (exon 6), 5'-TAAGGATAGGTCGGCGGTTC-3' (exon 7), and 5'-CATCGCCTTCTATCGCCTTC-3' (neomycin resistance gene) were used to genotype p53 transgenic mice.

K14-iASPP$^{\Delta 8/\Delta 8}$ embryos were generated by intercrossing parents with the K14-iASPP$^{+/\Delta 8}$ genotype and collecting embryos from the pregnant mother at the desired age. Embryos were genotyped for iASPP using the primers described for iASPP$^{\Delta 8/\Delta 8}$ mice. The initial generation of K14-iASPP$^{+/\Delta 8}$ mice was done by Kathryn Chung, a fellow graduate student. This was done by crossing mice with *loxP*-flanked exon 8 of iASPP with mice expressing Cre-recombinase under the K14 promoter (K14-Cre). Both mouse strains were on a C57BL/6J background. The resulting mice had specific deletion of iASPP in K14-expressing tissues. K14-Cre was genotyped using Cre-R (5'-ATTCTCCCACCGTCAGTACG-3') and K14-1 (5'-GCTCTCTGTCACCCTGGCTA-3').

Conditional iASPP$^{F811A/F811A}$ knock-in mice were engineered in the inGenoius Targeting Laboratory and were generated on a C57BL/6J and 129Sv genetic background. These mice were created by mutating iASPP's PP1-binding site at F811 to F811A in the endogenous exon 12. Subsequently, an artificial fusion of wildtype exons 12 and 13 plus a stop codon, flanked by *LoxP* sites, was inserted before the mutant exon 12. In succession, Dr Elizabeth Slee crossed these mice to R26Cre^{+}-ER^{T} mice to provide conditional iASPP$^{F811A/F811A}$ knock-in mice, which

were maintained and used in this study. It is expected that in the absence of activated Cre, the wildtype iASPP is expressed, as the stop codon lies before the mutant exons. Upon Cre activation, the artificial exon 12 and 13 plus the stop codon is floxed out, resulting in the expression of exons 12 and 13 carrying the F811A mutation. R26Cre^{+}-ER^{T} mice were provided by Prof. Anton Berns, Netherlands Cancer Institute, Amsterdam, The Netherlands (Vooijs *et al.*, 2001).

BrdU incorporation *in vivo* and cell cycle analysis

Mice were intraperitoneally injected with 50 µg/g body weight BrdU, 2 hours prior to euthanasia, to assess proliferation rate. The immunofluorescence technique described below, using the anti-BrdU antibody, was used to localise BrdU-positive cells. The number of cells that had incorporated BrdU were counted using ImageJ and divided by the total number of DAPI-positive cells in the area. In wound healing samples, BrdU-positive cells were counted in epidermal wound edges expressing migration marker K6 using ImageJ. Proliferation was assessed in a minimum of three animals, and three sections per animal.

DNA extraction for genotyping

Mouse ears were punched and the acquired tissues were digested overnight at 55°C in 200 µl of GNT-K buffer. The following day, proteinase K was de-activated by boiling the digested sample at 95°C for 10 minutes. 1 µl of the sample was used for PCR analysis. For genotyping of embryos, a small piece of tail was clipped and digested as described above.

Haematoxylin and eosin staining

4 µm thick tissue sections were processed for haematoxylin & eosin (H&E) staining following the outlined deparaffinisation and rehydration steps.

1. Deparaffinise in Histoclear I and II (5 minutes each)

2. Rehydrate by immersing slides in:
    a. EtOH 100% (5 minutes)
    b. EtOH 100% (5 minutes)
    c. EtOH 90% (3 minutes)
    d. EtOH 95% (3 minutes)
3. Rinse slides in distilled water (5 minutes)
4. Stain slides in haematoxylin (5 minutes)
5. Rinse slides in running tap water until water is clear
6. Decolourise slides in acid alcohol (1 second)
7. Rinse slides in tap water (5 minutes)
8. Counterstain slides in eosin (5 minutes)
9. Dehydrate slides through successive immersion in:
    a. EtOH 70 % (30 seconds)
    b. EtOH 90% (30 seconds)
    c. EtOH 100 % (1 minute)
    d. EtOH 100 % (2 minutes)
10. Clear slides in Histoclear I and II (5 minutes)
11. Mount slides with Vectashield®

PCR conditions

All genotyping PCR reactions worked under the following PCR conditions:

1. 94°C 5 minutes
2. 94°C 30 seconds
3. 60°C 30 seconds
4. 72°C 1 minute
5. GO 30X to step 2

6. 72°C 5 minutes

Tissue processing for protein-based assays

Embryos at various developmental stages, as well as other dissected tissues (skin and paw skin), were fixed in 4% paraformaldehyde solution overnight and then processed through the following series before being embedded in paraffin for sectioning at 4 μm thickness:

1. 30% ethanol (2 hours)
2. 50% ethanol (2 hours)
3. 70% ethanol (2 hours)
4. 90% ethanol (2 hours)
5. 95% ethanol (2 hours)
6. Absolute ethanol I and II (2 hours each)
7. First clearing agent (Xylene : Ethanol-1:1, 2 hours)
8. Xylene (2 hours)
9. Wax I and II at 58°C (2 hours each)

Wound healing

Six to eight week old iASPP$^{+/+}$and iASPP$^{\Delta 8/\Delta 8}$ mice were intraperitoneally injected with 1 mg/kg Metacam 30 minutes prior to wounding. Mice were anaesthetised by isoflurane inhalation and the dorsal side was shaved and sterilised with Hibiscrub. A full thickness excisional wound was made on the middle paravertebral region of the mouse using a biopsy punch of 6 mm diameter (Stiefel, cat. no. BC-BI-2000). The wound closure process was monitored by measuring the wound area (length and breadth, area of an ellipse) every other day, and was represented as the percentage of the initial wound area. Data is presented as mean value ± 2 standard errors of the mean (SEM). Statistical analysis between two groups was performed using the Mann-Whitney U-test and $p<0.05$ was considered statistically significant. Note that six to eight week old mice were recruited for wound healing study because their hair is at a

telogen phase (resting hair cycle). Active hair cycling (anagen hair phase) can affect blood vasculature and the skin immune system, which could affect wound healing.

The wound healing procedure required the experiment to be performed using sterile technique. This made it necessary to seek help from laboratory members to perform the procedure under aseptic conditions. Therefore, Kathryn Chung provided assistance during the execution of the procedure (on iASPP-deficient mice only) by monitoring the depth of anaesthesia in animals undergoing the procedure and by helping me achieve sterile technique.

2.2.2 Cell culture methods

Culture of primary keratinocytes and other cell lines

Isolation and culture of primary keratinocytes from iASPP$^{\Delta 8/\Delta 8}$ CreER and iASPP$^{+/+}$ CreER mice was performed following the protocol described previously (Lichti *et al.*, 2008). Briefly, skin was isolated from pups at postnatal day 2 and floated over 0.25% trypsin-EDTA overnight at 4°C. The following day, the epidermis was peeled off and triturated in low calcium media containing calcium-free EMEM with 8% calcium-stripped FBS, 50 µg/ml Gentamicin and 0.05 mM calcium. The cells were seceded from the resulting suspension using a 100 µm cell strainer (BD Falcon cat. no. 352360) and plated on rat collagen type I (BD Bioscience, cat. no. 354249) coated plastic dishes or cover slips. iASPP deletion was induced by adding 1 µM 4-OHT to the cells for 4 days. To improve cell growth, cell lines were sometimes grown in the enriched media mentioned in the materials section. This media was used only for the first two days after isolation. Induction of cell-cell adhesion of cells was stimulated by supplementing the media with calcium to a final concentration of 1.5 mM for the indicated time period. Increasing calcium concentration leads to the differentiation of keratinocytes (Hennings and Holbrook, 1983; Hennings *et al.*, 1980). The cells were maintained in a Heraeus incubator at 35°C in the presence of 7% CO_2.

MCF10a cells were maintained in Dulbecco's modified Eagle's medium/F12 containing 5% horse serum, 20 ng/ml EGF, 0.5 mg/ml hydrocortisone, 100 ng/ml cholera toxin, 10 µg/ml insulin and 100 U/ml penicillin/streptomycin solution. The cells were maintained in a Heraeus incubator at 37°C in the presence of 10% CO_2.

Other cell lines were maintained in Complete DMEM (refer to the materials section).

Calcium chelation from FBS

Chelating resin, designed for the removal of metal cations at appropriate pH values, was used to chelate calcium cations from FBS. Briefly, 80g chelating resin (see the materials section) was poured into 1 L of double distilled water, and the pH value adjusted to 7.5 with HCl. Upon reaching pH 7.5, the resin was filtered through Whatman filter paper. 500 ml of FBS was mixed with the resin and the mixture was stirred for at least 4 hours in a glass beaker. FBS was subsequently filter sterilised through a 0.45 µM filter, and then a 0.22 µM filter in a cell culture hood. Calcium depleted FBS was aliquoted and stored at -80°C.

Calcium switch assay

Confluent primary keratinocytes were maintained in high calcium media for either 2 or 6 days. The media was then either left or replaced with low calcium media containing 3mM EGTA for 90 minutes. The cells were subsequently stained for desmoplakin following the immunocytochemistry protocol described below. Calcium switch protocol has been described before elsewhere (Merritt *et al.*, 2006).

Cell passaging and freezing

Cells reaching 90-100% confluence were washed twice with 1X PBS and incubated with 2-4 ml pre-warmed 0.05% Trypsin-EDTA at 37°C, until cells detached from the dish surface. Trypsin was next inhibited by the addition of growth medium. The cells were subsequently pelleted. They were either resuspended in growth medium and plated at a desired density, or were resuspended in 1 ml of Freezing Medium and placed in cryovials (Corning, cat. no. 377267). The cryovials were placed in a Nalgen Cryo container in a -80°C freezer (New Brunswick Scientific) for at least 24 hr, before being transferred to a liquid nitrogen tank for long-term storage. The IMOK cell line adhered tightly to the dishes and the use of 0.25% Trypsin-EDTA at 37°C for 5 minutes was necessary to detach them.

Dispase mechanical dissociation assay

Keratinocytes were seeded in 6-well plates and allowed to reach confluence. Confluent keratinocyte cultures were switched from 0.05 mM to 1.5 mM calcium for 24 hours, before being rinsed in PBS and incubated with 2.4 U/ml dispase (Roche, cat. no. 04942078001) for 30 minutes at 37°C. Released monolayers were carefully rinsed in PBS, transferred to 15 ml conical tubes containing 2 ml PBS and subjected to orbital rotation (20 rpm) for 5 minutes. Fragments were visualised with a dissecting microscope (Leica M165C) and images were obtained with Jenoptik CF Scan or HP Scanjet 5590P. ImageJ cell counter function was used to count the number of fragments, and fragments smaller than 4 pixels in diameter (~area 1700 μm^2) were excluded from the quantification. Images were processed in Adobe Photoshop CS3. Data are expressed as the average number of fragments in 3 experiments ± 2SEM. Statistical analysis was done using the Unpaired Student's *t* test and significance was defined as $p<0.05$. The same protocol was used for the dispase assay with the UT SCC74A cell line transfected with the appropriate siRNA for 72 hours.

***In vitro* wound healing assay**

iASPP$^{+/+}$ and 4OHT-induced iASPP$^{\Delta 8/\Delta 8}$keratinocytes were grown to confluence. The cells were washed, and wounded by scratching a monolayer with a disposable pipette tip. The cell were washed and incubated in appropriate media. Wound closure was followed, and images were taken every 20 minutes for 48 hours using timelapse video microscopy. The wound healing closure was calculated as the percentage of the remaining wound area versus the original wound area using ImageJ. The average percentage of wound area closed by iASPP$^{+/+}$ or 4OHT-induced iASPP$^{\Delta 8/\Delta 8}$keratinocytes within 8 hours of wound closure was quantified. Statistical analysis between two groups was done using an Mann-Whitney's U test and $p<0.05$ was considered statistically significant.

***In vitro* motility behaviour assay**

iASPP$^{+/+}$ and 4OHT-induced iASPP$^{\Delta 8/\Delta 8}$ keratinocytes were grown in keratinocyte defined medium. Under these conditions, cells formed cell contacts leading to the formation of cell clusters. The motility behaviour of cells was followed for 48 hours using timelapse video microscopy. To avoid the effect of proliferation on cell motility, cells were treated with 1 ng/ml mitomyocin C for 1 hour. Before timelapse monitoring, cells were rinsed with PBS and incubated in the above mentioned media. ImageJ's cell tracking plugin was used to analyse the speed and the distance (µm) moved by individual cells (n=7 cells x 3 cell clusters x 3 replicates). The mean distance travelled by iASPP$^{+/+}$ or 4OHT-induced iASPP$^{\Delta 8/\Delta 8}$ cells was calculated and the statistical significance of the difference in the means of the two samples was assessed using an Unpaired Student's *t*-test.

2.2.3 DNA- and RNA-based methods

RNA extraction and reverse transcription

RNA was extracted from cells or tissues using the Qiagen RNeasy mini kit following the manufacturer's instructions. The optional step involving treatment with DNase I (refer to the materials section) to eliminate possible genomic DNA contamination was performed. 500 ng of RNA was used to generate cDNA using the SuperScript® First Stand Synthesis System following the manufacturer's instructions (refer to the materials section).

RT-qPCR

The QuantiTect SYBR Green PCR kit was used to perform real-time quantitative PCR using the 7500 real time PCR system (Applied Biosystem). Each reaction was performed in triplicate per cDNA sample in a final volume of 25 µl. Reaction constituents were:

Reagent	Per reaction (µl)
2 x SYBR Green reagent	12. 5
Forward/Reverse primer mix (100 µM)	0.125 (0.3 µM final concentration)
RNAse-free water	11.375
cDNA	1 (≤500 ng per reaction)

Table 7 RT-qPCR reaction set up

The following thermal cycle was used for all of the samples:

1. 95°C 10 minutes
2. 95°C 30 seconds
3. 55°C 40 seconds (temperature adjusted based on primer annealing temperature)
4. 72°C 40 seconds
5. Go 40X to step 2

To detect the efficiency of iASPP deletion, RNA was collected from iASPP$^{+/+}$ and 4OHT-induced iASPP$^{\Delta 8/\Delta 8}$keratinocytes and converted to cDNA. To determine mRNA levels of iASPP in iASPP$^{+/+}$

and 4OHT-induced iASPP$^{\Delta 8/\Delta 8}$keratinocytes, the generated cDNA was used to perform RT-qPCR using a 5'-AGACTCCAGCACCTCAACAGA-3' forward primer and 5'-GACCGTGCCTTCATCTGC-3'reverse primer. As a positive control, RT-qPCR was performed using cDNA prepared from iASPP$^{+/+}$ and iASPP$^{\Delta 8/\Delta 8}$ keratinocytes, utilising the same primers. GAPDH was used as an internal control. The expression level of iASPP and GAPDH mRNA was analysed based on the $\Delta\Delta C_T$ method described by Schmittgen and Livak (Schmittgen and Livak, 2008). The efficiency of the iASPP deletion at the mRNA level in iASPP$^{\Delta 8/\Delta 8}$ and 4OHT-induced iASPP$^{\Delta 8/\Delta 8}$ keratinocytes is shown below (Table 8). Although iASPP mRNA levels were higher in 4OHT-induced iASPP$^{\Delta 8/\Delta 8}$ keratinocytes compared to iASPP$^{\Delta 8/\Delta 8}$ keratinocytes, the levels were barely detectable in either.

Sample	ΔC_T	$\Delta\Delta C_T$	Fold change = $2^{\wedge(-\Delta\Delta C_T)}$
iASPP$^{\Delta 8/\Delta 8}$	14.5	8.4	1.2E-11
4OHT-induced iASPP$^{\Delta 8/\Delta 8}$	41	36	4.1E-5

Table 8 4-OHT deletion efficiency of iASPP
C_T values represent the fractional PCR cycle number at which the reporter fluorescence exceeded the background level. ΔC_T = (C_T gene of interest − C_T internal control). $\Delta\Delta C_T$ = [(ΔC_T sample A) − (ΔC_T sample B)]. Sample A represents iASPP levels in either 4OHT-induced iASPP$^{\Delta 8/\Delta 8}$ or iASPP$^{\Delta 8/\Delta 8}$ keratinocytes, and sample B represents iASPP levels in vehicle-treated iASPP$^{+/+}$ or iASPP$^{+/+}$ keratinocytes.

siRNA-induced gene silencing

A number of siRNA oligos purchased from Dharmacon were used to silence the expression of genes of interest in keratinocytes (Table 9). IMOK cells were transiently transfected with a combination of oligos using DharmaFECT I transfection reagent, following manufacturer's instructions. Briefly, 2µl of DharmaFECT I transfection reagent was added to 98 µl of HBSS and incubated for 5 minutes at room temperature. 1.75 µl of 20 µM siRNA diluted in 98.25µl of HBSS was combined with the transfection reagent-containing mixture and left to incubate for 20 minutes. Cells were trypsinised, and 80,000 cells in 800 µl of media were merged with

transfection mixture and plated in the well of a 24-well plate. The extent of silencing was assessed 72 hours post-transfection.

siRNA Oligos	Catalogue number	Target sequences
miASPP On-Target plus set of 4	LU-060065-01-0002	UGGUACAGCAGGCGGUGAA CCGAAGGCCUGGAACGAGU UGACAGGCGUUCUGACGUU CCGCCAAAGUGGACGAAUU
hiASPP On-Target plus set of 4	LU-003815-00-002	AGUAAAGUCUAGCAGGAUA GCACGGGUGUUGGCGGAAA GCAGACGUCGAGCAGAGUA UCGAGAAGUGCGACCCUUA
mDesmoplakin On-Target plus set of 4	LU-040653-01-0002	AGGAAGAUAGAGUCGAAA CGGACAUUCAUGCGAGAUA CCGAAGAAGCCAUCCGCAA CGGUUGACAUGGCGUAUAA
mKeratin 5 On-Target plus set of 4	LU-048162-01-0002	GAUCUGAAAUUGACAACGU AGGCAUGAGCUUCGGCAGU CUACAUUUGUGUUGCACGU GGAGAGUAGUCUAGACCAU
mPkcα	LU-040348-00-0002	GGACGACUCGGAAUGACUU UAACAUAGACCAAUCUGAU GAAGGGUUCUCGUAUGUCA CAGCAAGUCGGGAAAUUUA
Scrambled	D-001220-01-05	Proprietary

Table 9 siRNA oligos used in this study and their target sequences
A letter in front of the gene name refers to the species: m=mouse, h=human.

2.2.3 Protein-based methods

Immunoblotting and electrophoresis

Cells were grown in appropriate media in 6-well plates until confluence. Primary keratinocytes were grown in low 0.5 mM calcium media (LCM). Upon confluence, cells were switched to high 1.5 mM calcium media (HCM) for 24 hours. Cells were rinsed in ice-cold PBS and the soluble protein fraction was obtained by lysing cells in NETN buffer and shaking the lysates at 4°C for 30 minutes. The lysates were pelleted for 15 minutes at 14,000g, and the insoluble protein pool was obtained by solubilising the pellet in UREA buffer. If cell lysates were not fractionated into soluble and insoluble pools, the lysis buffer of choice was UREA buffer. Protein concentration was measured using the Bradford's method and 5x SDS sample buffer was added to both the soluble and insoluble pools, and samples were boiled at 95°C for 10 minutes. Equal amounts of protein were loaded onto acrylamide gels, or when indicated on a PhosTag gel, and gels were run at 130V for 1.5 hours in 1x running buffer using the Biorad running system. The proteins were then transferred from the polyacrylamide gel onto nitrocellulose membrane for 2.5 hours at a constant voltage of 75 V. Membranes were blocked in 5% milk in TBST, or for cell signalling antibodies in 3% BSA in TBST. Membranes were incubated with primary antibody for 4 hours at room temperature or overnight at 4°C. After 5x 5 minutes washing in TBST, membranes were incubated in secondary antibody for 1 hour at room temperature. The results were visualised by enhanced chemoluminescence detection using X-ray films (Fujifilm). If membranes were to be probed with another primary antibody, the membrane was immediately re-probed or incubated with stripping buffer for 30 min at 55°C. Succeeding these steps, the membrane was re-blocked before being incubated with another primary antibody.

Immunofluorescence assay on cells

Cells were seeded onto glass coverslip in 24-well plates or in a plastic Ibidi plate of high optical quality. Once experimental procedures were completed, cells were fixed for 15 minutes in 4% paraformaldehyde and then permeabilised with 0.5% Triton X-100 for 15 minutes at 4°C. Unspecific binding of antibodies was blocked by incubating cells in 5% normal goat serum in PBS for 30 minutes. Primary antibodies diluted in blocking solution were applied to cells for 1 hour (refer to the materials section for antibody dilutions). Protein expression was detected by appropriate Alexa®Fluor secondary antibodies. DAPI was used as a nuclear marker.

Immunofluorescence assay on tissue sections

4 μm thick paraffin sections were processed for immunofluorescence. The samples were de-paraffinised and hydrated following the first 3 steps outlined in the haematoxylin and eosin procedure above. Subsequently, antigen retrieval in 10 mM sodium citrate buffer (pH 6) at 95°C for 15 minutes (30 minutes for BrdU and cleaved Cas3 staining) was carried out. The samples were washed three times in PBS before blocking the non-specific binding of the antibodies with 5% goat serum for 30 minutes. Primary antibody diluted in blocking solution was applied to the samples overnight at 4°C. After three washes in PBS for 5 minutes each, secondary antibodies diluted in blocking solution were applied to the samples for 1 hour. The samples were washed in PBS and mounted in Fluoromount G.

Immunoprecipitation

Cells were grown in 15 cm dishes and, upon confluence, lysed in NETN buffer containing protease and phosphatase inhibitors. Lysates were pre-cleared by adding 30 µl Protein G-agarose beads per 2 mg of protein lysate, and rotating the mixture for 1 hour at 4°C. The beads intended for immunoprecipitation were blocked with DMEM containing 5% FBS for 1 hour, and were subsequently washed three times in NETN. 2mg of protein lysate was incubated with 30

µl of pre-blocked beads and 3 µg of antibody, and the mix was rotated overnight at 4°C. The following day, beads were rinsed 3X in lysis buffer and resuspended in 5 x SDS-sample buffer. The samples were boiled and resolved on SDS-PAGE.

Protein concentration determination

The protein concentration of cell and tissue lysates was determined using BioRad (Bradford) protein assay. Six dilutions of bovine serum albumin (BSA) were used to establish a standard curve at an absorbance of 595nm. Dilutions of BSA in 1x BioRad assay reagent (cat. no. 500-0006) were pipetted into a 96-well plate along with 1 µL of cell lysates dissolved in 200 µL of 1x BioRad assay reagent. The plate was read in a spectrophotometer (Anthus Labtech Instrument, using Magellan software) at an absorbance of 595nm, and the concentration of the cell lysate extrapolated.

TUNEL assay

The terminal deoxynucleotidyl transferase d-UTP nick end labelling (TUNEL) assay was carried out on paraffin-embedded embryonic or wound healing tissue from iASPP$^{+/+}$ and iASPP$^{\Delta 8/\Delta 8}$ mice. Three sections from each sample were analysed (1 in every 10 sections). The TUNEL assay was performed according to manufacturer's instructions (Millipore, cat. no. S7165). Cells were also stained for nuclear marker DAPI. TUNEL- and DAPI-positive cells were counted using ImageJ.

Chapter III: iASPP is a regulator of desmosomes and its deficiency leads to cutaneous disorders

Chapter III: iASPP is a regulator of desmosomes and its deficiency leads to cutaneous disorders

3.1 Introduction

Desmosomes are adhesive intercellular junctions. They are found at cell-cell interfaces, where they provide tethering sites for intermediate filaments. As they connect adjacent cells together they also interconnect their intermediate filament cytoskeletons, forming a large mechanically resilient network that spans multiple layers of cells. Such intercellular connectivity allows for structural stresses to be distributed evenly across the entire tissue. Desmosomes are present in tissues such as the epidermis and heart muscle that are assailed by persistent mechanical forces. In these tissues, they have a central role in withstanding mechanical stress and maintaining the structural integrity of the tissue (Garrod and Chidgey, 2008).

The adhesive complex of desmosomes is mainly composed of proteins from three families: cadherins, armadillo proteins and plakins. Cadherins are represented by desmogleins and desmocollins; armadillo proteins are represented by plakoglobin and plakophilins; and finally, desmoplakin is the main and obligate plakin protein involved in desmosome adhesion (Godsel *et al.*, 2004). When desmosome adhesion is compromised due to genetic mutations in desmosome components, a number of pathological conditions ensue including epidermal thickening of palms and soles (palmoplantar keratoderma), woolly hair, impaired wound healing and ARVC (Beaudry *et al.*, 2010; Kottke *et al.*, 2006). Both autosomal recessive and dominant mutations in desmoplakin have been reported. Dominant mutations have been found in patients with palmoplantar keratoderma or ARVC, while recessive mutations have been linked to patients presenting with a phenotypic triad of woolly hair, palmoplantar keratoderma and dilated cardiomyopathy or ARVC (Alcalai *et al.*, 2003; Armstrong *et al.*, 1999;

Norgett *et al.*, 2000; Whittock *et al.*, 1999). A similar tripartite pathological disorder that affects the skin, hair and heart is observed in patients with a homozygous C-terminus truncation of plakoglobin (McKoy *et al.*, 2000). Evidence points to extended functions of desmosomes beyond mere adhesive and structural properties. The dissociation of desmosomes leads to the succumbing of cells to the effects of mechanical strain, which evokes proliferation and differentiation (Lechler and Fuchs, 2007; Wan *et al.*, 2004). However, it is unclear how the integrity of junctions is sensed and how this signal is transduced to the nucleus to mediate gene expression.

The armadillo protein of the adherens junctions, β-catenin, is known to have a dual function in cell-cell adhesion and gene transcription. The main stable pool of β−catenin is found in cell-cell adhesion complexes, where it is bound to E-cadherin on one side and the actin binding protein α-catenin on the other. Disruption of adherens junctions leads to the translocation of β-catenin to the nucleus, where it associates with LEF/TCF factors to regulate the expression of a diverse set of genes involved in proliferation, survival, migration and differentiation (Stadeli *et al.*, 2006; Stockinger *et al.*, 2001). Aberrant activity of β-catenin in the nucleus can lead to hyperproliferation and tumour development (Beronja *et al.*, 2013). These reports portray β-catenin as a multifunctional protein that senses the integrity of cell-cell adhesions, and conveys the message to the nucleus where it regulates gene expression. A β-catenin-like signalling molecule may sense the integrity of desmosomes and transduce it to the nucleus to mediate gene transcription in response to mechanical stress. Elucidation of such a molecule would further modify the view of desmosomes being merely structural adhesion points, raising the possibility of more dynamic structures that also participate in gene regulation (Green and Simpson, 2007).

A potential candidate that may link cell adhesion to transcriptional regulation is iASPP. iASPP can shuttle between cellular compartments, just like β-catenin. Its nuclear roles include the suppression of p53-dependent transcription of apoptotic genes (Bergamaschi *et al.*, 2006) and the regulation of p63 to inhibit senescence, differentiation and stratification of the epidermis. Loss of iASPP leads to premature senescence, increased expression of differentiation markers (K1 and loricrin), and decreased expression of proliferation markers (K14 and p63) (Chikh *et al.*, 2011; Notari *et al.*, 2011). Furthermore, immunofluorescence and microscopy studies show that iASPP localises to desmosomes in the heart. Loss of iASPP in mice results in disruption of the integrity of desmosomes in cardiomyocytes, which leads to development of ARVC and sudden death (Notari, 2012). These data implicate iASPP in the regulation of junctional integrity. iASPP-deficient mice, created in our laboratory, also have peculiarly wavy hair. Pathological defects observed in iASPP-deficient mice are highly reminiscent of the phenotypic triad associated with desmosome dysfunction: palmoplantar keratoderma, woolly hair and cardiomyopathies. Whether iASPP-deficient mice suffer from palmoplantar keratoderma has not yet been answered. Moreover, although iASPP appears to be associated with diseases linked to desmosome instability, it remains to be determined whether or not iASPP interacts with desmosome components and is able to regulate their function. Therefore, the aim of this chapter is to investigate whether iASPP-deficient mice develop palmoplantar keratoderma, and by what molecular mechanisms iASPP contributes to the development of this disease.

It is demonstrated here that iASPP-deficient mice present with epidermal thickening on the palms and soles of their paws, similar to patients with palmoplantar keratodermas. Reminiscent of other desmosome components, iASPP localises to cell-cell junctions in response to increased calcium concentration. Junctional iASPP forms an interaction with desmoplakin and K5. Its deficiency enhances the phosphorylation and solubility of desmoplakin resulting in desmosome instability, enhanced susceptibility to mechanical stress, the formation of keratin

aggregates and reduced cell-cell adhesion. This work suggests an important role for iASPP in desmosome regulation, with its suppression associated with pathological epidermal processes.

3.2 Results

3.2.1 iASPP-deficient mice have wavy hair, cardiac defects and focal plantar keratosis

To investigate the role of iASPP *in vivo*, iASPP-deficient mice were generated as previously described by Notari and colleagues (Notari *et al.*, 2011). Briefly, the mouse model was created by deleting *loxP*-flanked exon 8 in the iASPP gene using the Cre/*loxP*-based excision system. Cre-recombinase, driven by a ubiquitously expressed CMV promoter, mediated the excision of the exon, which resulted in a frameshift and a null allele. In this thesis, from now on, iASPP-deficient mice are referred to as iASPP$^{\Delta 8/\Delta 8}$.

To determine the biological role of iASPP, the phenotypes that iASPP$^{\Delta 8/\Delta 8}$ mice exhibit were examined. Intriguingly, wavy/spiky hair, cardiac defects, eye abnormalities and focal palmoplantar keratosis were observed in the iASPP$^{\Delta 8/\Delta 8}$ mice (Figure 3.1). iASPP$^{\Delta 8/\Delta 8}$ mice also died suddenly, probably because of cardiac failure, between 3-6 months of age. The hair, heart and eye abnormalities displayed by iASPP$^{\Delta 8/\Delta 8}$ mice had 100% penetrance. Spontaneous development of focal palmoplantar disorder occurred in 60% of mice (Figure 3.1D). Given that iASPP$^{\Delta 8/\Delta 8}$ mice have heart defects, it is likely that these mice are less motile and do not subject their paws to considerable physical pressure. This could be an explanation for the reduced penetrance of the palmoplantar phenotype. Therefore, it would be interesting to monitor the activity of iASPP$^{\Delta 8/\Delta 8}$ mice and compare it to that of iASPP$^{+/+}$ mice in the future. Altogether, these data suggest that iASPP plays an important role in the development of the heart and epithelial tissues. The features of the phenotypes observed in iASPP$^{\Delta 8/\Delta 8}$ are further explored below.

The hearts isolated from iASPP$^{\Delta 8/\Delta 8}$ mice were enlarged and fibrotic (Figure 3.1C). As previously mentioned, this phenotype has been studied by Dr Mario Notari. Our group believes that these mice share many of the features of ARVC including fibrosis, fatty acid infiltration, arrhythmias and RV-specific dilation (Notari, 2012).

iASPP$^{\Delta 8/\Delta 8}$ mice also display a wide variety of eye anomalies that include clouding, thickening and ulceration of the cornea, small eyes, lens rupture and extrusion. The eye phenotype is likely to be related to impaired embryonic eyelid closure, which is addressed in chapter V of this thesis. An example of a gross eye defect in these mice is shown in Figure 3.1A.

In addition, starting at about 6 weeks of age, iASPP$^{\Delta 8/\Delta 8}$ mice developed progressive plantar and palmer lesions (Figure 3.1B). Keratosis, along with shedding of the cornified envelope, in the areas of the paw epidermis under high physical pressure could be observed in iASPP$^{\Delta 8/\Delta 8}$ mice. These features are indicative of palmoplantar keratoderma, the study of which using histological techniques is outlined in more detail in the following sections.

In summary, iASPP$^{\Delta 8/\Delta 8}$ mice have helped us to discover the important roles iASPP plays in the development of heart and epithelial tissues. The main phenotypes observed in these mice are often associated with desmosome dysfunction such as ARVC, woolly/wavy hair and palmoplantar thickening.

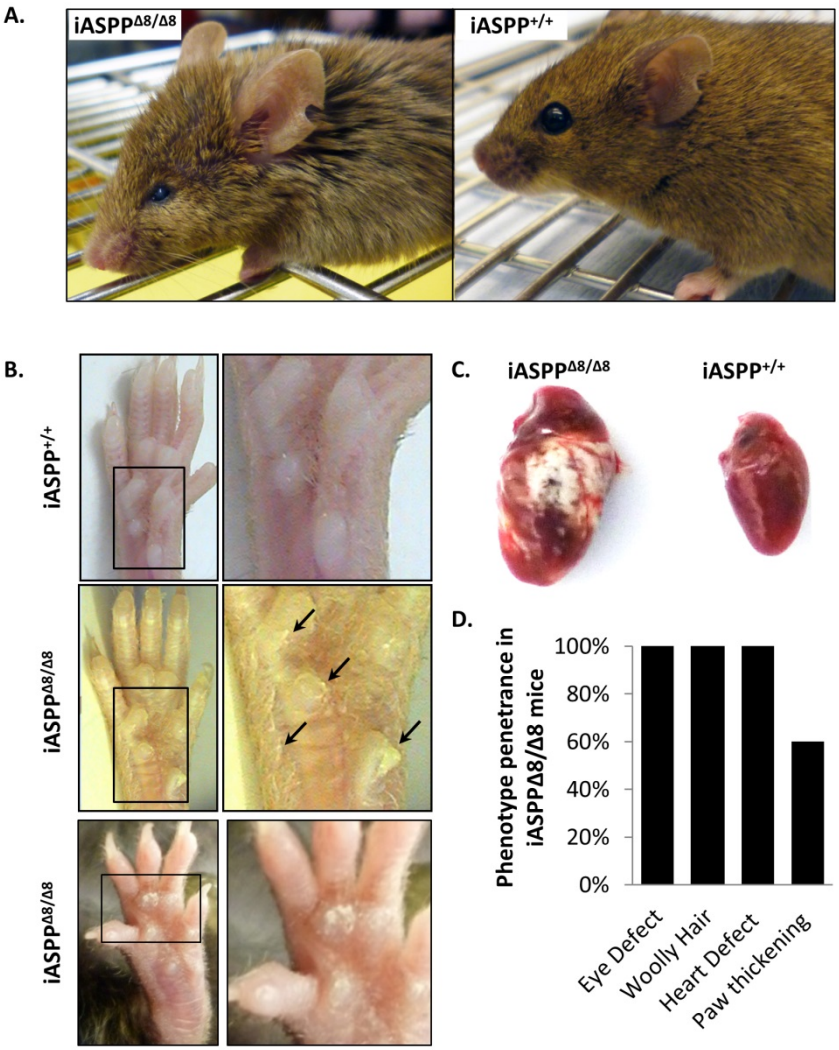

Figure 3.1 iASPP deficiency in mice results in phenotypes in organs exposed to mechanical stress

A. iASPP$^{\Delta 8/\Delta 8}$ mice exhibit eye defects and a woolly/wavy hair phenotype. **B.** iASPP$^{\Delta 8/\Delta 8}$ mice also present with a focal paw thickening phenotype starting at about 6 weeks of age. Keratosis, along with shedding of the cornified envelope (black arrows), of the epidermis in iASPP$^{\Delta 8/\Delta 8}$ mice are indicative of palmoplantar keratoderma. Representative paws of 3 month old iASPP$^{\Delta 8/\Delta 8}$ and iASPP$^{+/+}$ mice are shown. **C.** iASPP$^{\Delta 8/\Delta 8}$ mice have enlarged fibrotic hearts. Hearts from 2 month old iASPP$^{\Delta 8/\Delta 8}$ and iASPP$^{+/+}$ mice photographed next to each other are presented. **D.** Penetrance of various phenotypes in iASPP$^{\Delta 8/\Delta 8}$ mice. Phenotypes associated with iASPP deficiency are highly penetrant. n>50 for eye, hair and heart defects and n=15 for the paw thickening phenotype.

3.2.2 iASPP deficiency causes palmoplantar keratoderma

Since macroscopic features of palmoplantar keratoderma were observed in the iASPP$^{\Delta 8/\Delta 8}$ mice, the phenotype was further confirmed microscopically. Using immunofluorescence assays, iASPP expression in the paws was determined. This was followed by the histological examination of the paws from iASPP$^{+/+}$ and iASPP$^{\Delta 8/\Delta 8}$ mice. Results showed that, moving up the epidermal layers, iASPP expression changed from being predominantly cytoplasmic and nuclear to cytoplasmic and junctional. Moreover, ascending up the epidermis, iASPP expression appeared to decrease (Figure 3.2A). Histological analysis revealed focal thickening of the subcornified and cornified epidermal layers in paws of iASPP$^{\Delta 8/\Delta 8}$ mice compared to iASPP$^{+/+}$controls (Figure 3.2B,C). Moreover, widening of the intercellular spaces could be observed in iASPP$^{\Delta 8/\Delta 8}$ mice (Figure 3.2C'). Interestingly, although thickening of both the subcornified and cornified layers was observed in iASPP$^{\Delta 8/\Delta 8}$ mice, only the difference in the thickening of subcornified layers reached statistical significance compared to iASPP$^{+/+}$ mice (*t*-test, p=0.02 for subcornified layers, p=0.5 for cornified layers). This could be explained by the general expression pattern of iASPP, which appeared to be lower in the upper-granular and cornified layers. However, it appeared that the cornified layer had a differentiation defect and contained cells that had failed to replace the cytoplasm with cross-linked cornified envelope proteins and keratin macrofibrillar cables, which warrants further investigation (Figure 3.2C, black arrows). In summary, these results suggest that iASPP$^{\Delta 8/\Delta 8}$ mice display features of focal palmoplantar keratoderma, including focal thickening of the subcornified layers and increased intercellular spaces between cells.

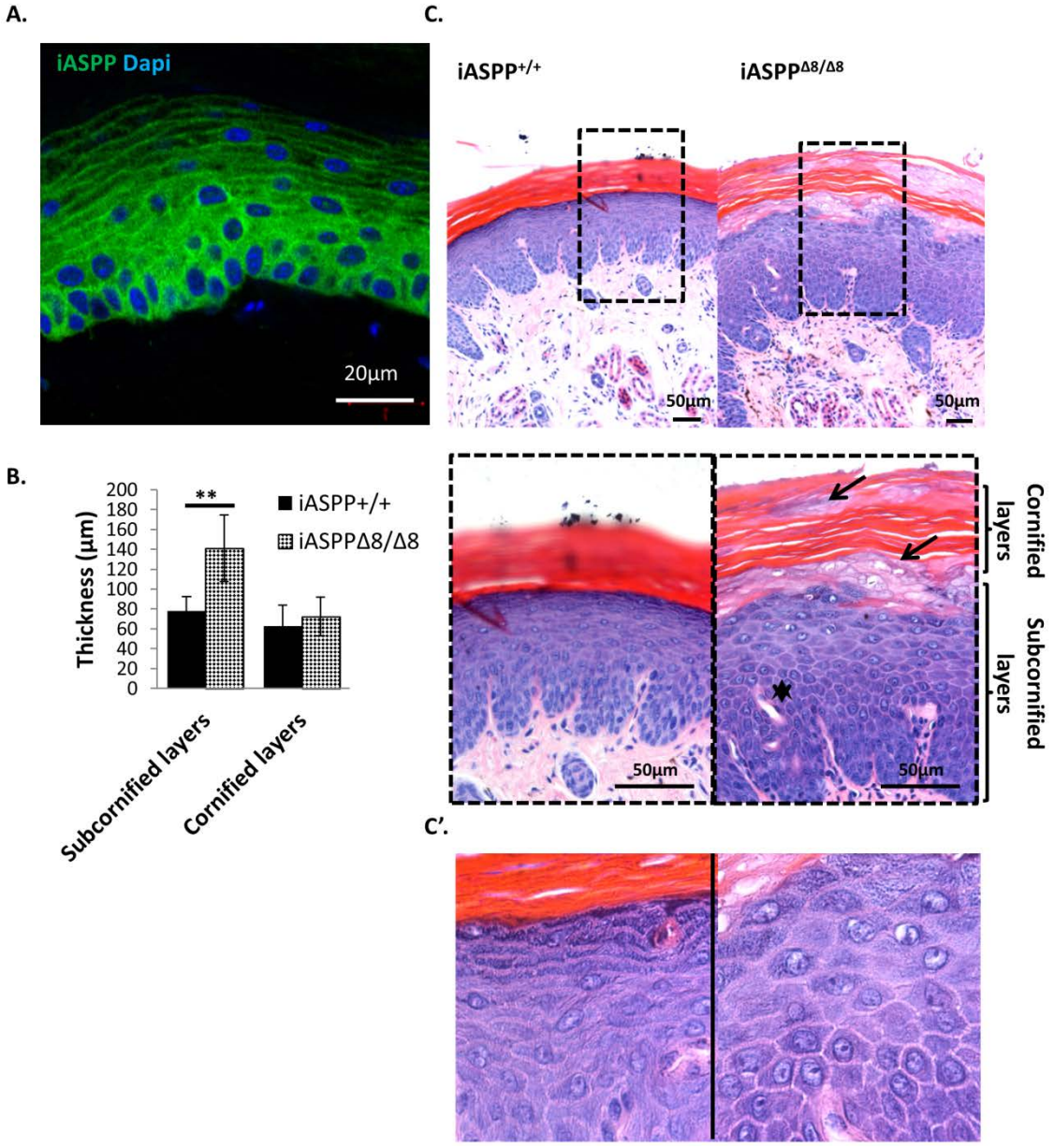

Figure 3.2 iASPP-deficient mice have focal thickening of the paw epidermis

A. Immunofluorescence staining shows iASPP expression at the junctions, in the cytoplasm and a few nuclei in the plantar epidermis of iASPP$^{+/+}$ mice. **B.** Quantification of the thickness of the subcornified and cornified layers in iASPP$^{+/+}$ and iASPP$^{\Delta 8/\Delta 8}$ mice. The unpaired *t*-test was performed to assess whether the difference in paw thickness between iASPP$^{+/+}$ and iASPP$^{\Delta 8/\Delta 8}$ was statistically significant: p=0.02 for the thickness of the subcornified layers, p=0.5 for the thickness of the cornified layers. Error bars are ± 2SEM **C.** Haematoxylin and eosin staining showing thickening of the subcornified and cornified layers of the epidermis in iASPP$^{\Delta 8/\Delta 8}$ mice compared to iASPP$^{+/+}$ mice. Arrows point to cells in the cornified layer that have failed to replace the cytoplasm with cornified envelope proteins and keratins. The star points to the intercellular space in the paw epidermis of iASPP$^{\Delta 8/\Delta 8}$ mice. **C'.** Magnification of **C.** showing widened intercellular spaces in the epidermis of iASPP$^{\Delta 8/\Delta 8}$ mice compared to iASPP$^{+/+}$ controls.

3.2.3 iASPP deficiency causes keratin aggregation

Cytoplasmic keratin aggregates are often present in the affected epidermis of palmoplantar keratoderma patients with desmoplakin mutations (Armstrong *et al.*, 1999). Using electron microscopy, in collaboration with Dr Notari and Prof. Ferguson, it was investigated whether keratin aggregates form in the epidermis obtained from 12-week old iASPP$^{+/+}$ and iASPP$^{\Delta 8/\Delta 8}$ mice. In the epidermis of iASPP$^{\Delta 8/\Delta 8}$ mice, desmosome morphology appeared to be largely unaffected (Figure 3.3A, black box). However, moderate keratin aggregation (Figure 3.3A, red arrowheads) and disruption of keratin filament interaction with desmosomes could be observed (Figure 3.3A lower panel, black arrows). In the epidermis of iASPP$^{+/+}$ mice, these anomalies were rarely seen (Figure 3.3A). One potential explanation for the modest keratin aggregation in the iASPP$^{\Delta 8/\Delta 8}$ mice is that the dorsal skin was used for electron microscopy and not the paws, which may have displayed a stronger phenotype as they are much more exposed to mechanical stress. Furthermore, palmoplantar keratoderma in iASPP$^{\Delta 8/\Delta 8}$ is focal, therefore a more systematic analysis of palmoplantar epidermis needs to be performed in the future. For these reasons, it is also possible that abnormalities in desmosome morphology were not observed.

To provide further evidence that a loss of iASPP leads to the collapse of keratin filaments, immortalised oral mouse keratinocytes (IMOK) were treated with scrambled siRNA or siRNA against iASPP, and were grown in calcium-rich conditions for 24 hours to allow for cell-cell junctions to form. Protein levels of K5 were not altered upon iASPP loss (Figure 3.3B). However, K5 aggregates could be observed specifically in cells lacking iASPP (Figure 3.3C). A similar trend was observed in iASPP$^{\Delta 8/\Delta 8}$ primary keratinocytes. Quantification of the percentage of cells having K5 aggregates in both IMOK and primary keratinocytes is shown in Figure 3.3D. A significant increase in the percentage of cells with keratin aggregation could be

observed between iASPP-deficient cells compared to control cells (*t*-test, *p*=0.01 in IMOK cells, *p*=0.05 in primary keratinocytes). In summary, these results suggest that a loss of iASPP leads to the collapse of keratin filaments and focal thickening of the plantar and palmar epidermis, a phenotype reminiscent of palmoplantar keratoderma in human patients.

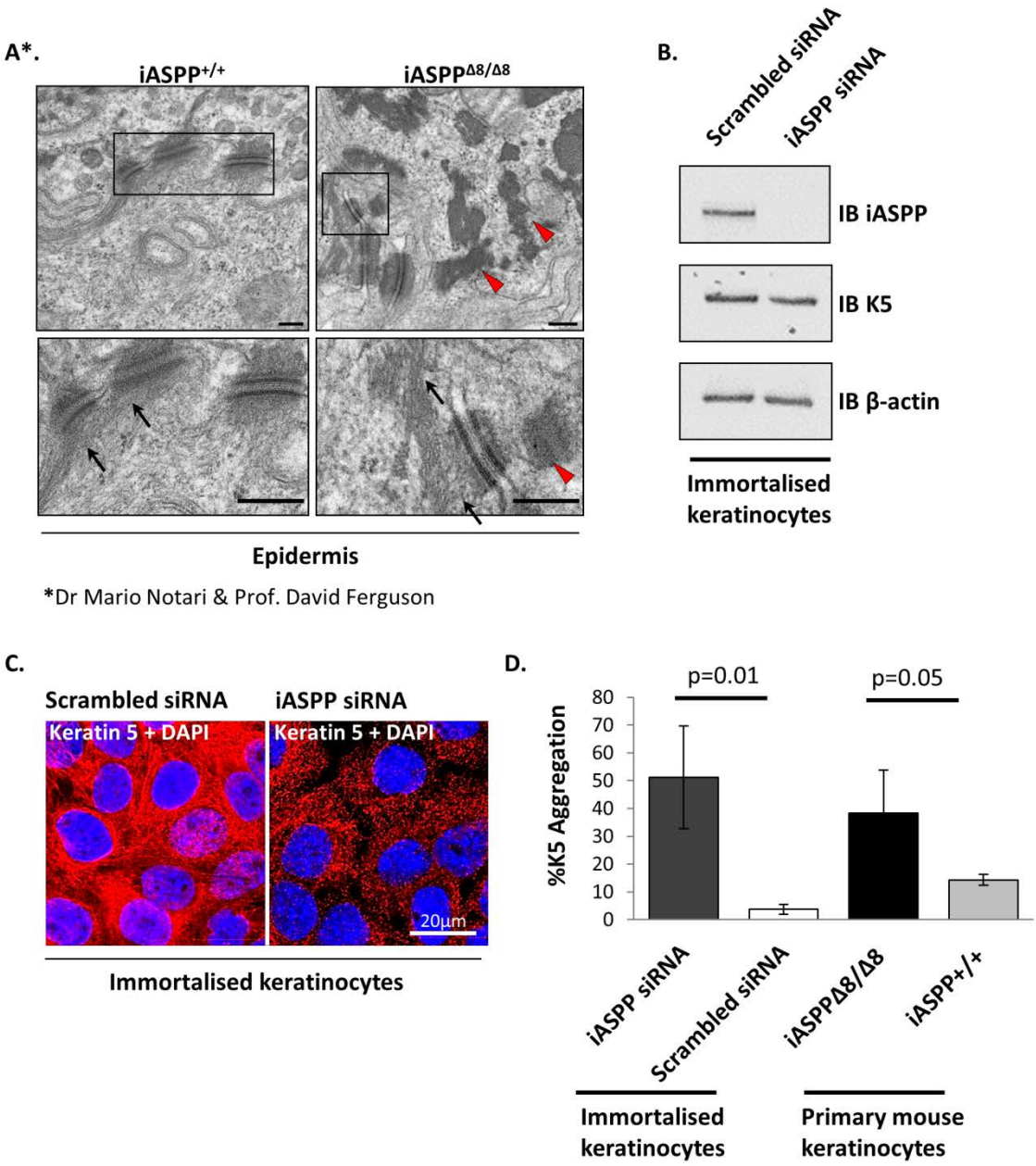

Figure 3.3 Increased keratin aggregation both *in vivo* and *in vitro* in keratinocytes lacking iASPP

A. Transmission electron microscopy of epidermal desmosomes from iASPP$^{+/+}$ and iASPP$^{\Delta 8/\Delta 8}$ mice. Red arrowheads indicate keratin aggregates. Altered interaction between the desmosomes and intermediate filaments (black arrow) can be observed in the epidermis of iASPP$^{\Delta 8/\Delta 8}$ mice. *Experiment was done by Dr Mario Notari and Prof. David Ferguson **B.** Immunoblots showing that a loss of iASPP in immortalised keratinocytes (IMOK) does not affect the levels of K5 **C.** IMOK treated with iASPP siRNA display enhanced K5 aggregation compared to scrambled siRNA-treated cells **D.** Bar graph showing the percentage of iASPP-containing or lacking cells with K5 aggregation. The unpaired *t*-test was performed to test whether the difference in keratin aggregation was significant. Error bar denotes ± 2SEM. The representation of keratin aggregation in IMOK cells is representative of three independent experiments. The representation of keratin aggregation in primary keratinocytes includes four independent experiments, where two of those experiments were performed by a former laboratory member Dr Ying Hu. Values obtained from all four experiments are represented.

3.2.4 iASPP localises to cell-cell junctions and interacts with K5 and desmoplakin

It is now well established that switching calcium levels from low to normal physiological levels (1-2 mM) triggers the translocation of desmosomal components from the cytoplasm to cellular junctions *in vitro* (Watt *et al.*, 1984). Given that a loss of iASPP led to desmosome-related diseases, it was investigated whether iASPP behaves in a similar fashion to desmosome components in response to calcium. A calcium switch assay to study iASPP's localisation following the induction of calcium signaling was performed. Switching calcium levels from 0.5 mM to 1.5 mM resulted in a time-dependent translocation of iASPP from the cytoplasm to cell-cell junctions. Interestingly, a 30 minute exposure of cells to 1.5 mM calcium was sufficient to trigger iASPP to translocate to the cell membrane. After 24 hour exposure to 1.5 mM calcium, iASPP was predominantly junctional, and its localisation at the junctions was maintained for at least 48 hours (Figure 3.4A).

Mutations in desmoplakin, which alter its interaction with keratin filaments, lead to keratin aggregation and palmoplantar keratoderma (Armstrong *et al.*, 1999; Norgett *et al.*, 2000; Whittock *et al.*, 1999). Given that a similar phenotype was observed in the iASPP$^{\Delta 8/\Delta 8}$ mice, it was investigated whether iASPP was located in the same molecular complex as desmoplakin. Using an immunofluorescence assay and high resolution microscopy, co-localisation between iASPP and desmoplakin *in vitro* in primary keratinocytes grown in 1.5 mM calcium media for 24 hours was observed. Co-localisation was also detected *in vivo* in the epidermis of the skin (Figure 3.4B). This interaction was further explored using an immunoprecipitation assay, where interacting partners of iASPP were pulled down using an anti-iASPP antibody. Results showed that desmoplakin is a binding partner of iASPP. The binding of iASPP to the phosphatase PP1, a known interacting partner of iASPP (Llanos *et al.*, 2011), was also detected. As desmoplakin is known to bind K5 filaments, whether iASPP interacts with K5 was also tested. It was found that

iASPP forms interactions with both K5 and desmoplakin (Figure 3.4C). This interaction was further examined by performing a reciprocal immunoprecipitation assay. Goat polyclonal K5 antibody was used to pull down K5 binding partners in IMOK cell lysates. To test whether desmoplakin was required for this interaction, the assay was performed in the presence or absence of a desmoplakin siRNA. It was found that immunoprecipitated K5's binding to iASPP was reduced in the presence of desmoplakin siRNA, suggesting that iASPP's binding to K5 is desmoplakin dependent (Figure 3.4D). In summary, these data show that iASPP localises to the cellular junctions and forms a complex with K5 and desmoplakin. iASPP binding to K5 is enhanced in the presence of desmoplakin.

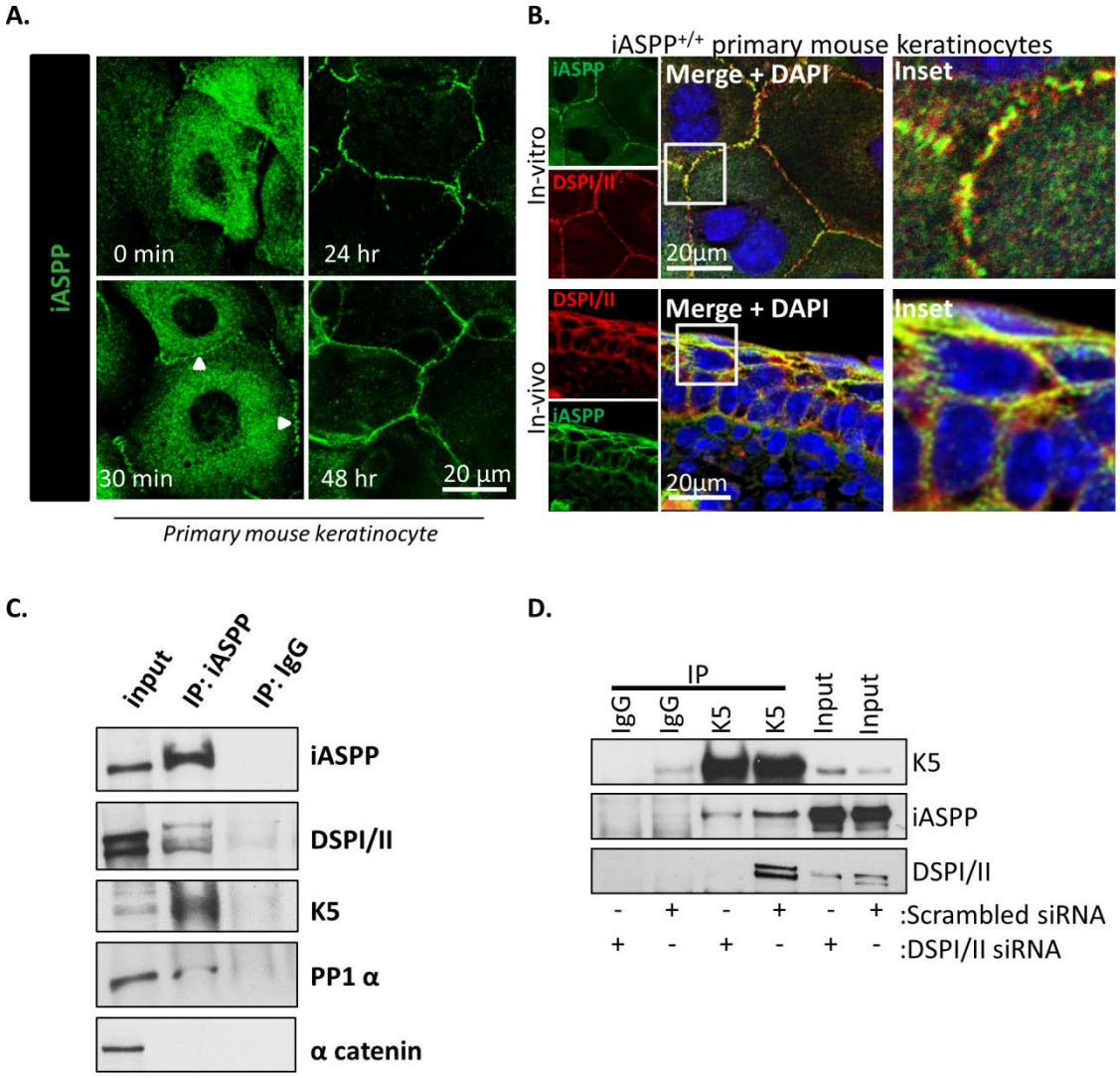

Figure 3. 4 iASPP localises at the cell-cell junctions and interacts with desmoplakin and K5
A. iASPP translocates to the cell-cell junctions upon calcium treatment. Time points indicate the amount of time cells that were exposed to 1.5 mM calcium growth media. Within 30 minutes, iASPP localises to the cell-cell junctions (arrowheads). **B.** Immunofluorescence shows the junctional localisation of iASPP (green) and desmoplakin (DSPI/II, red) in primary mouse keratinocytes (*in vitro*) and epidermis (*in vivo*), where the inset shows their co-localisation (yellow). DAPI is in blue **C.** An immunoprecipitation (IP) assay showing that endogenous iASPP protein interacts with endogenous desmoplakin in keratinocytes grown in 1.5 mM calcium media for 24 hours. Rabbit polyclonal antibody was used to immunoprecipitate iASPP and its binding partners. IgG derived from the rabbit was used as a negative control. PP1 is known to bind iASPP and was used as a positive control. Desmoplakin was detected using a mouse anti-desmoplakin antibody. The antibodies that the membranes were probed with are indicated. **D.** K5 binding to iASPP is reduced in the presence of desmoplakin siRNA. Mouse keratinocytes were treated with scrambled vs. desmoplakin siRNA. K5 was used to immunoprecipitate iASPP and desmoplakin.

3.2.5 Loss of iASPP leads to the disorganisation of desmoplakin distribution

Desmoplakin is an obligatory component of desmosomes. Its role is to link intermediate filaments to the desmosomes at intercellular contact sites. In growth conditions lacking calcium, desmoplakin is solely cytoplasmic and the addition of calcium triggers its junctional localisation. Consistently, withdrawal of calcium after junctions have assembled leads to the relocation of desmoplakin from junctions to the cytoplasm (Pasdar and Nelson, 1988). Given that iASPP was found to interact with desmoplakin, it was investigated whether iASPP is necessary for the junctional localisation of desmoplakin. Using an immunofluorescence assay, desmoplakin localisation was assessed *in vivo* in the plantar epidermis of both $iASPP^{+/+}$ and $iASPP^{\Delta 8/\Delta 8}$ mice, and *in vitro* in keratinocytes isolated from $iASPP^{+/+}$ and $iASPP^{\Delta 8/\Delta 8}$ pups that were grown in 1.5 mM calcium media for 24 hours. Increased numbers of cells with diffuse cytoplasmic desmoplakin staining could be observed in epidermal cells from $iASPP^{\Delta 8/\Delta 8}$ mice compared to $iASPP^{+/+}$ controls. In addition, cytoplasmic punctae, which were positive for desmoplakin, appeared more numerous in the plantar epidermis from $iASPP^{\Delta 8/\Delta 8}$ mice compared to $iASPP^{+/+}$ mice (Figure 3.5A). The localisation of plakoglobin and members of adherens and tight junctions in keratinocytes grown in 1.5 mM calcium media was generally unaffected by iASPP depletion (Figure 3.6). Taken together, these results show that although desmoplakin still localised to cell-cell junctions, it had an increased and disorganised cytoplasmic distribution in $iASPP^{\Delta 8/\Delta 8}$ keratinocytes compared to $iASPP^{+/+}$ keratinocytes (Figure 3.5).

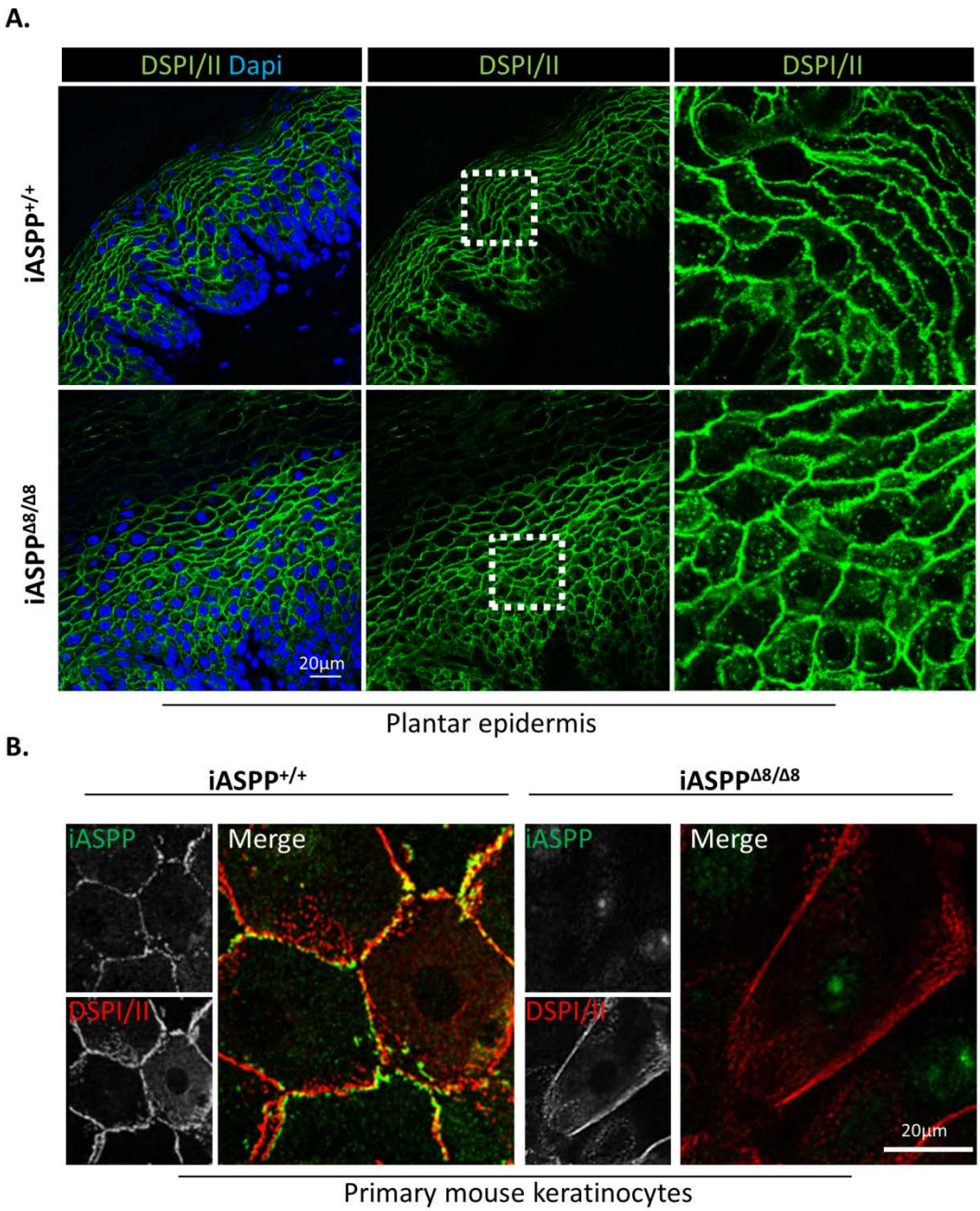

Figure 3.5 iASPP deficiency *in vivo* and *in vitro* results in the disorganized localisation of desmoplakin

A. Desmoplakin (green) was detected by immunofluorescence staining in the plantar epidermis of iASPP$^{+/+}$ and iASPP$^{\Delta 8/\Delta 8}$ mice. Nuclear stain DAPI is in blue. The white box represents the region that is enlarged and shown in the rightmost panel. Note the increased number of cytoplasmic green punctae in cells from iASPP$^{\Delta 8/\Delta 8}$ mice. An increased number of cells with diffuse desmoplakin staining can be also observed in cells lacking iASPP in comparison to cells that do not lack iASPP. **B.** iASPP deficiency in primary keratinocytes results in no detectable levels of iASPP (green) and decreased desmoplakin localisation (red) at the junctions.

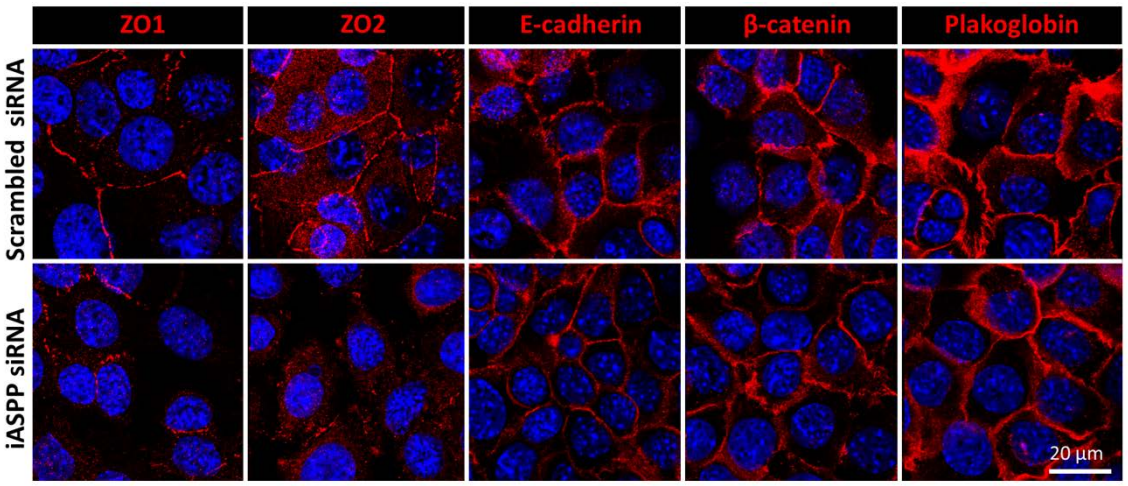

Figure 3.6 iASPP deficiency has no overt effect on the localisation of components of adherens and tight junctions

IMOK keratinocytes were treated with iASPP or scrambled siRNA, and cultured in 1.5 mM calcium conditions for 24 hours prior to immunofluorescence staining using the indicated antibodies. A slight delay in the formation of tight junctions can be observed in 1.5 mM calcium conditions.

3.2.6 iASPP controls the solubility and phosphorylation status of desmoplakin

Desmoplakin that localises to cell-cell junctions is known to be insoluble in lysis buffers containing non-ionic detergents. Accordingly, cytoplasmic desmoplakin has increased solubility in such buffers and this reflects weakened cellular adhesions. Furthermore, PKCα, a serine- and threonine-specific kinase, mediates the phosphorylation and subsequent solubilisation of desmoplakin, ultimately leading to desmosome disassembly (Amar *et al.*, 1999). As iASPP deficiency resulted in increased cytosolic desmoplakin, it is likely that iASPP affects desmoplakin's phosphorylation, solubility and its maintenance at cell-cell junctions. This is explored further in the following sections.

3.2.6.1 iASPP controls the solubility of desmoplakin

To determine if iASPP regulates the solubility of desmoplakin a cell fractionation experiment was performed. iASPP$^{+/+}$ and iASPP$^{\Delta 8/\Delta 8}$ keratinocytes were lysed and solubilised in a buffer containing non-ionic detergent. The lysates were spun and the pellet containing the insoluble proteins further solubilised in urea buffer. For total lysates, cells were directly lysed in urea buffer. Interestingly, in comparison to iASPP$^{+/+}$ keratinocytes, a higher amount of desmoplakin was observed in the soluble fraction of iASPP$^{\Delta 8/\Delta 8}$ keratinocytes, even though the total desmoplakin levels remained similar (Figure 3.7A). In the same experiment, the protein levels of soluble and insoluble plakoglobin, vinculin and keratin 17 were found to be comparable between iASPP$^{+/+}$ and iASPP$^{\Delta 8/\Delta 8}$ keratinocytes (Figure 3.7A'). These data suggest that iASPP specifically prevents the solubilisation of desmoplakin.

Notably, protein levels of many cell-cell adhesion components are regulated at the post-transcriptional level through the control of protein stability. Therefore, it is not surprising that the microarray assay results showed no differences at the mRNA level between iASPP$^{+/+}$ and

iASPP$^{\Delta 8/\Delta 8}$ keratinocytes for any of the desmosome components. Similar results were obtained using an RNA-seq experiment performed by a fellow graduate student Kathryn Chung.

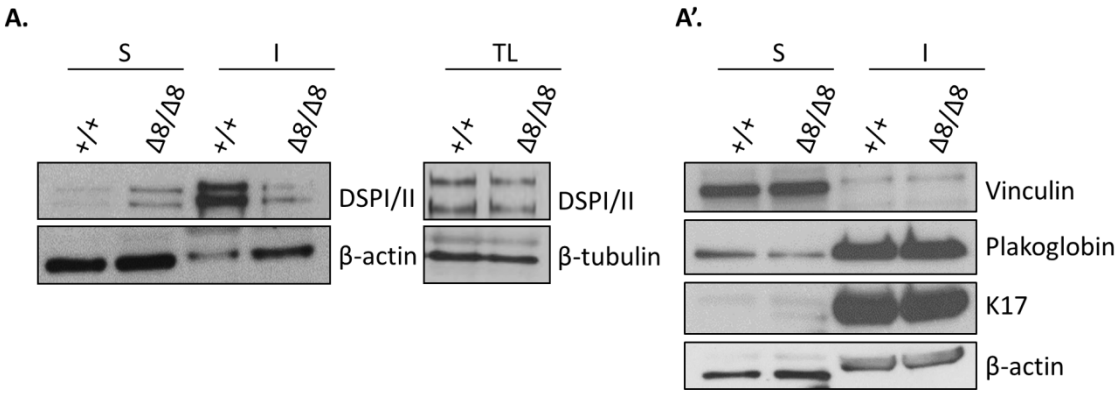

Figure 3.7 iASPP deficiency results in increased desmoplakin solubility
A. Levels of non-ionic detergent soluble and insoluble desmoplakin were examined in primary keratinocytes isolated from conditional iASPP CreER mice treated with vehicle or 4-OHT for four days to induce iASPP deletion. 24 hours prior to lysate collection, the media was switched from low calcium to high calcium to induce cell-cell junction formation. iASPP loss results in increased soluble and decreased insoluble desmoplakin levels. Loss of iASPP does not affect the total levels of desmoplakin in protein lysates collected using urea buffer only. **A'**. In the same experiment, levels of soluble and insoluble plakoglobin, K17 and vinculin are comparable between iASPP$^{+/+}$ and iASPP$^{\Delta 8/\Delta 8}$ keratinocytes. S stands for non-ionic detergent soluble fraction, I stands for non-ionic detergent insoluble fraction, and TL stands for total lysates.

Consistent with the observation that a loss of iASPP results in higher desmoplakin solubility, increased desmoplakin and K5 complex formation was observed in IMOK cells transfected with iASPP siRNA compared to controls (Figure 3.8A). Similar results were found in primary keratinocytes lacking iASPP (Figure 3.8B). Although it might appear that a loss of iASPP resulted in enhanced binding between K5 and desmoplakin, it is important to consider that immunoprecipation is performed on the soluble pool of proteins. Therefore, when normalised to input, the binding of K5 to desmoplakin was comparable between cells that with and without iASPP (Figure 3.8). These results suggest that the affinity of desmoplakin for K5 is unaltered in the absence of iASPP.

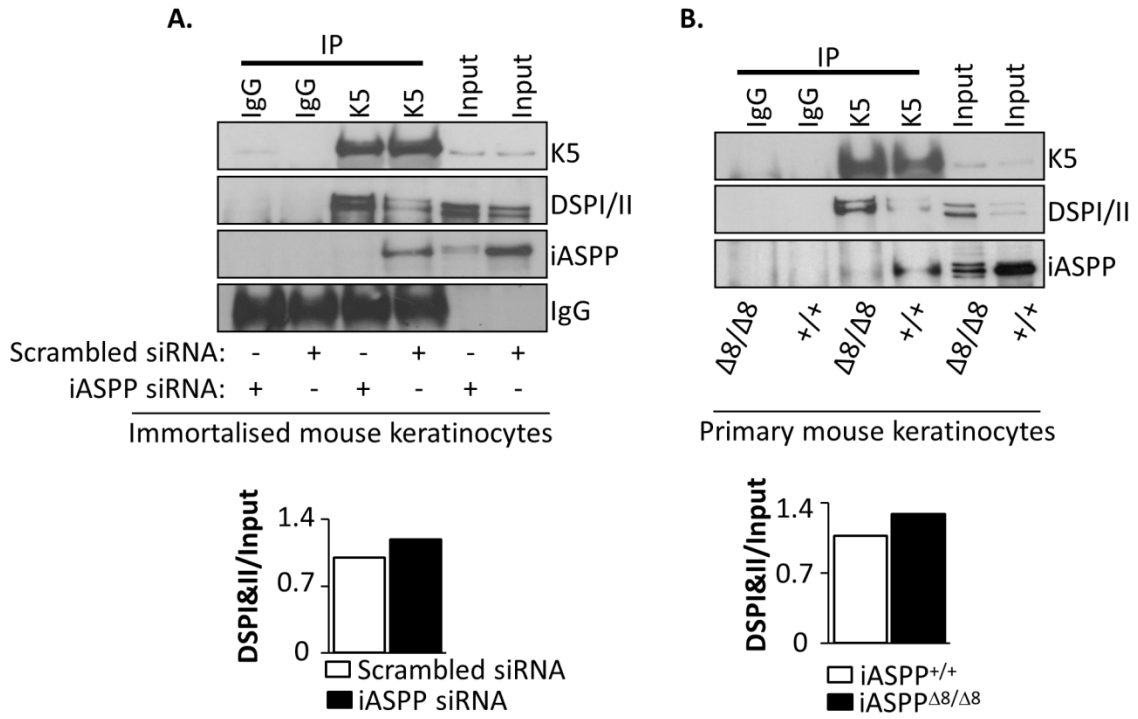

Figure 3.8 iASPP deficiency does not alter the affinity of desmoplakin for K5
K5 was immunoprecipitated from either **A.** immortalised keratinocytes (IMOK) previously treated with scrambled or iASPP siRNA or **B.** primary keratinocytes isolated from iASPP CreER pups in which iASPP has been deleted or not using 4-OHT. In iASPP-deficient keratinocytes compared to controls, immunoprecipitated K5 binds similarly to DSP when normalised to input (see bar charts).

3.2.6.2 iASPP regulates the phosphorylation of desmoplakin

Given that the solubility of desmoplakin is regulated by phosphorylation, whether iASPP influences desmoplakin phosphorylation was tested using a Phos-tag gel, which can detect the overall phosphorylation state of proteins. Results showed that the phosphorylation status of soluble desmoplakin in lysates from iASPP$^{\Delta 8/\Delta 8}$ keratinocytes was enhanced compared to control lysates (Figure 3.9B, white arrowheads, middle blot), while phosphorylation of insoluble desmoplakin was not altered (Figure 3.9B, black arrows, top blot).

Phosphorylation of desmoplakin at residue S2849, a site in close proximity to desmoplakin's keratin binding region, is involved in the modification of desmosome adhesiveness during processes that require cell movement such as wound healing. Specifically, phosphorylation of this site results in weaker cell-cell adhesions that allow cells to migrate more efficiently (Choi *et al.*, 2002; Green and Simpson, 2007; Wallis *et al.*, 2000). Consistent with this, the incorporation of phospho-deficient desmoplakin mutant S2849G into desmosomes increases the adhesiveness and cohesiveness of keratinocyte cell sheets (Bass-Zubek *et al.*, 2008; Dehner *et al.*, 2014; Godsel *et al.*, 2005). Therefore, whether the phosphorylation of S2849 of desmoplakin was altered upon iASPP ablation was examined. An antibody designed by LifeSpan Sciences directed against phospho-S2849 was used to detect phosphorylated desmoplakin in the soluble fractions and total lysates from iASPP$^{+/+}$ and iASPP$^{\Delta 8/\Delta 8}$ keratinocytes. Enriched phosphorylation of S2849 in cells lacking iASPP could be observed (Figure 3.9B). Recognition of phosphorylated desmoplakin was ablated by λ protein phosphatase (λPP) treatment, confirming the specificity of the antibody for the phosphorylated substrate (Figure 3.9C).

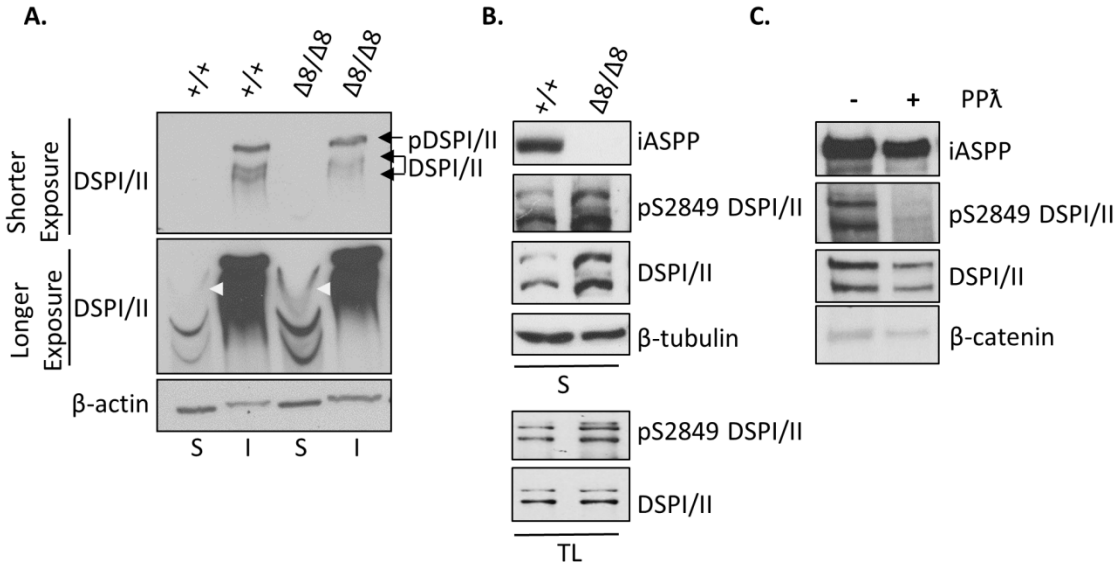

Figure 3.9 iASPP deficiency results in increased desmoplakin phosphorylation

A. Soluble and insoluble protein fractions from primary keratinocytes from iASPP CreER mice, in which iASPP has been accordingly deleted, were loaded on a Phos-tag gel to separate phosphorylated (top band) and unphosphorylated (lower bands) desmoplakin. Phosphorylated and unphosphorylated insoluble desmoplakin is indicated by the black arrows. Increased levels of phosphorylated desmoplakin can be seen in the soluble fraction from iASPP$^{\Delta 8/\Delta 8}$ keratinocytes compared to iASPP$^{+/+}$ keratinocytes (see white arrowheads). β-actin was used as a loading control. **B.** Total and non-ionic detergent-soluble lysates from iASPP$^{+/+}$ and iASPP$^{\Delta 8/\Delta 8}$ keratinocytes, treated with vehicle or 4-OHT respectively, were analysed by western blot. Levels of phosphorylated (p) pS2849 desmoplakin in vehicle-treated iASPP$^{+/+}$ keratinocytes are lower than in 4-OHT-treated iASPP$^{\Delta 8/\Delta 8}$ keratinocytes. **C.** The specificity of the S2849 phospho-specific antibody was tested by treating lysates with ƛPP. Detection of phosphorylated desmoplakin is ablated upon treatment with ƛPP. S stands for non-ionic detergent soluble fraction, I stands for non-ionic detergent insoluble fraction, and TL stands for total lysates.

3.2.7 iASPP deficiency does not alter the phosphorylation status of K5 and K14

Keratin collapse and aggregation can result from either the anomalous interaction of keratins with desmoplakin or from the aberrant posttranslational modification of keratins themselves. Therefore, to rule out the possibility that iASPP deficiency causes keratin collapse by influencing keratin phosphorylation, the phosphorylation status of K5 was examined using a Phos-tag gel. No difference in the phosphorylation of K5 was observed between iASPP$^{+/+}$ and iASPP$^{\Delta 8/\Delta 8}$ keratinocytes (Figure 3.10A). Intriguingly, a drop in the level of keratin phosphorylation was observed as cells were induced to differentiate with the addition of calcium. Note that by 24 hours of growth in calcium, keratinocytes lost the top band on a Phos-tag gel (Figure 3.10A). Therefore, the regulation of keratin phosphorylation might facilitate a change in keratin expression during differentiation. This has not yet been explored, but appears to be independent of iASPP, warranting future investigation.

The effects of iASPP on the phosphorylation of K14 were also examined using phospho-specific antibodies directed against S32 and S33 of K14. These antibodies were kindly provided by Prof. Birgit Lane. No difference in the phosphorylation levels of K14 was observed between iASPP$^{+/+}$ and iASPP$^{\Delta 8/\Delta 8}$ cells (Figure 3.10B). Similar to the trend observed with K5, phosphorylation of K14 was attenuated as cells were directed to differentiate with the addition of calcium for 24 hours. Together, these data indicate that iASPP affects desmosomes and leads to keratin instability by influencing desmoplakin phosphorylation status and solubility. Future studies should address the interesting findings that show a loss of keratin phosphorylation during differentiation.

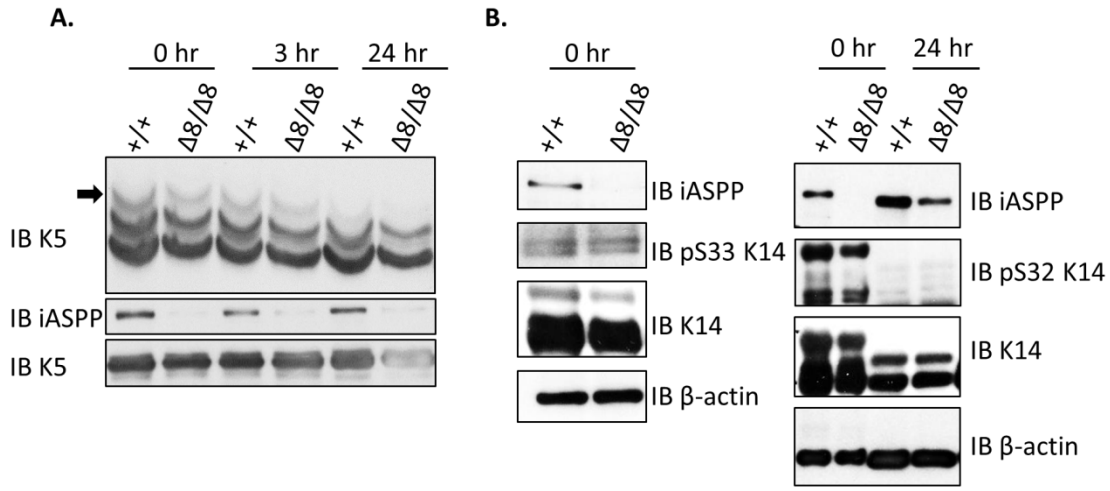

Figure 3.10 Loss of iASPP does not affect the phosphorylation of K5 and K14
A. Levels of phosphorylated K5 are unchanged upon the deletion of iASPP (see arrow pointing to the top band on a Phos-tag gel). Phosphorylation of K5 is reduced as iASPP$^{+/+}$ and iASPP$^{\Delta 8/\Delta 8}$ cells start to differentiate upon calcium addition. Primary keratinocytes, treated or not with 4-OHT to induce deletion of iASPP, were grown in the presence of 1.5 mM calcium for the amount of time indicated. Cells were lysed in non-ionic detergent-containing buffer and lysates were run on a Phos-tag (top panel) and 8% acrylamide gel (second and third panels), followed by the transfer of proteins to a nitrocellulose membrane and its subsequent immunoblotting for the various proteins indicated above. Notice that on the Phos-tag gel, proteins are separated based on their phosphorylation status, resulting in three bands for K5 compared to a single band on the acrylamide gel. **B.** K14 phosphorylation is mostly unaffected by iASPP deletion. Phospho-S32 and S33 antibodies were kindly provided by Prof. Birgit Lane and have been shown to detect phosphorylated K14 (Lane, personal communication). Levels of phosphorylated (p) S32 and S33 are similar between protein lysates isolated from iASPP$^{+/+}$ and iASPP$^{\Delta 8/\Delta 8}$ cells. Levels of pS32 in both iASPP$^{+/+}$ and iASPP$^{\Delta 8/\Delta 8}$ cells are considerably reduced as cells differentiate with the addition of calcium.

3.2.8 iASPP deficiency compromises cell-cell adhesion *in vitro*

Given that increased desmoplakin solubility and keratin disorganisation were observed in iASPP$^{\Delta 8/\Delta 8}$ keratinocytes, it was also likely that the loss of iASPP weakened the adhesive strength of keratinocytes. To test this theory, a dispase mechanical dissociation assay was performed. Dispase disrupts cell-matrix interactions, leaving cell-cell adhesion intact. Therefore, dispase was used to release a cell monolayer from the substrate, which was then placed in a canonical tube and subjected to 5 minutes of orbital rotation in phosphate buffered saline. Dissociation of the monolayer into fragments in response to shear stress is representative of the integrity of adherence. Under these circumstances, the monolayer of iASPP$^{\Delta 8/\Delta 8}$ keratinocytes fragmented more than the monolayer of iASPP$^{+/+}$ keratinocytes (Figure 3.11A, *t*-test, p=0.02). Similar results were obtained using the squamous cell carcinoma cell line UT-SCC74a that was treated with scrambled or iASPP siRNA (Figure 3.11B, *t*-test, p=0.07). In this cell line, high iASPP expression was also observed at cell-cell adhesion sites. Note that results obtained using UT-SCC74a failed to reach statistical significance. This might be because siRNA-mediated deletion of iASPP is less efficient than Cre-mediated deletion of iASPP in primary keratinocytes. Alternatively, the UT-SCC74a cell line could harbour mutations in cell-cell adhesion genes, which might have led to increased fragmentation of monolayers in cells treated with scrambled siRNA, affecting the results of this study. Nonetheless, these results demonstrate that iASPP is important for the integrity of cell adhesions in response to mechanical trauma.

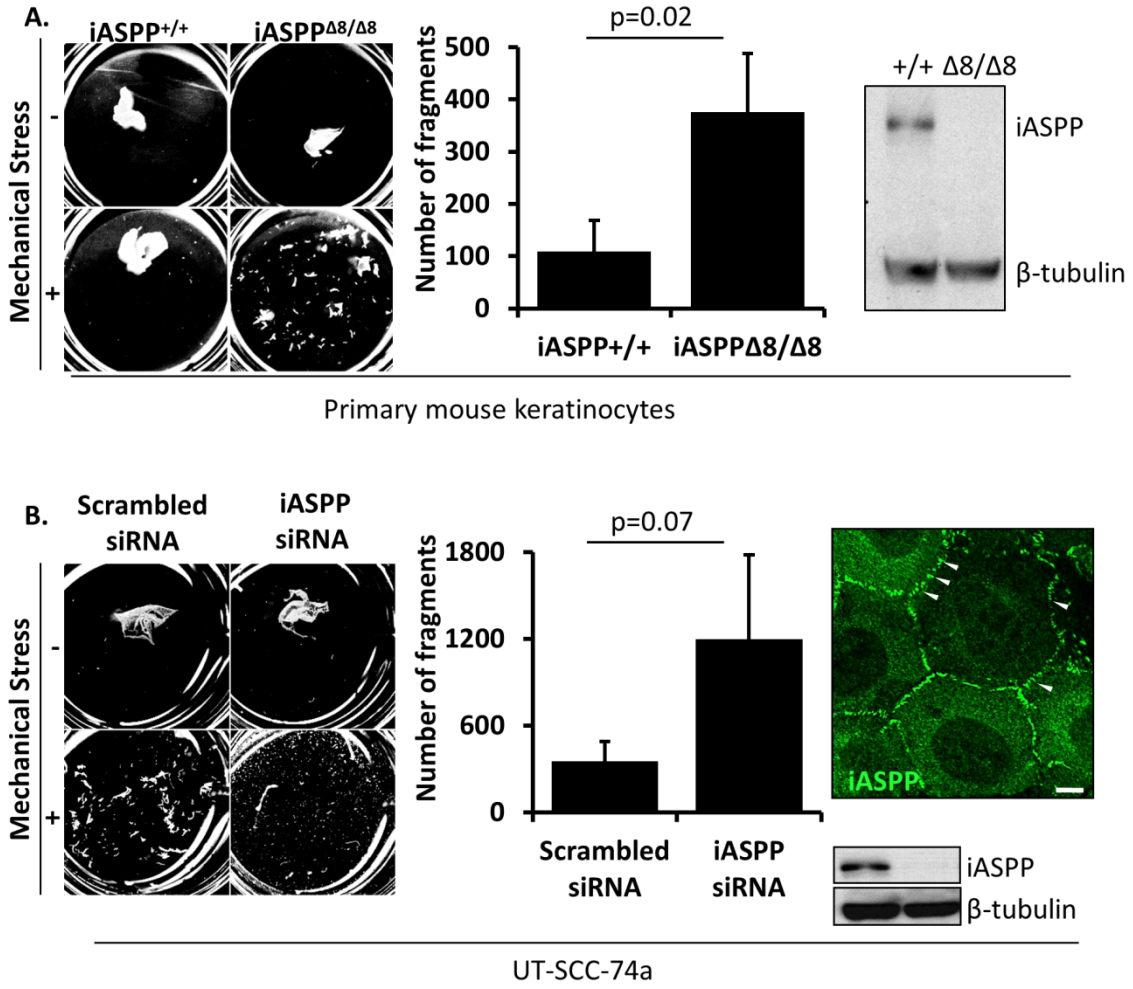

Figure 3.11 Cell-cell adhesions are compromised in iASPP-deficient cells

Loss of iASPP results in weakened cell-cell adhesions in **A.** primary keratinocytes isolated from iASPP$^{+/+}$ and iASPP$^{\Delta 8/\Delta 8}$ mice or **B.** UT-SCC74a cells cultured under high calcium conditions. Confluent monolayers of primary keratinocytes or UT-SCC74a cells were subjected to a dispase mechanical dissociation assay. Representative pictures were taken before and after mechanical stress as indicated. The bar chart shows the number of fragments released as a result of the mechanical stress. Increasing numbers of fragments indicate weaker cell-cell adhesion. Values are means ± 2SEM from three different experiments. *p*=0.07 (UT SCC 74a). Immunofluorescence was carried out using an antibody against iASPP. iASPP localises predominantly at the cell-cell junctions in epithelial UT-SCC74a cells, see **B.** rightmost panel.

3.2.9 iASPP is important for desmosome maturation and hyperadhesion

Previous studies have shown that the phospho-deficient desmoplakin mutant S2849G is associated with stronger intercellular adherence when incorporated into desmosomes. The findings presented above show that a loss of iASPP results in increased desmoplakin phosphorylation and weaker cell-cell adhesions. Therefore, it was hypothesised that iASPP might regulate the acquisition of a highly adhesive desmosome state by modulating the dephosphorylation of desmoplakin. To address this hypothesis, the ability of desmosomes to become highly adhesive in the presence or absence of iASPP was tested. This was done using an elegant calcium chelation assay that determines the adhesiveness of desmosomes. The assay has been developed in Prof. Garrod's laboratory, and takes advantage of the concept that "hyperadhesive" desmosomes can maintain intercellular connectivity even when calcium is chelated below physiological levels (Garrod and Tabernero, 2014).

In MDCK and HaCaT cells, a hyperadhesive desmosome state is acquired after growing cells in high calcium media (HCM) for 4-6 days. This has been determined by the presence of junctional desmoplakin and the resistance of cellular adhesions (at days 4 and 6 cells) to calcium chelation using 3mM EGTA for 90 minutes. The intercellular connectivity of cells grown in HCM for just 2 days has been shown to be very sensitive to the depletion of calcium with EGTA, and results in the dissociation of cell adhesions (Kimura *et al.*, 2007; Wallis *et al.*, 2000).

To examine whether primary keratinocytes have this ability, and to determine whether iASPP might regulate desmosomal acquisition of a hyperadhesive state, keratinocytes were grown in calcium-rich media for 2 or 6 days. Following this, calcium was depleted using EGTA for 90 minutes and cell-cell adhesion integrity was judged by desmoplakin staining. Both $iASPP^{+/+}$ and $iASPP^{\Delta 8/\Delta 8}$ cells grown in HCM formed cell-cell adhesions. However, more cytosolic

desmoplakin was observed in iASPP$^{\Delta 8/\Delta 8}$ keratinocytes (Figure 3.12, panel 2 top and bottom). Following calcium chelation and growth in low calcium media (LCM) for 90 minutes, day 2 and day 6 iASPP$^{\Delta 8/\Delta 8}$ cells lost cell-cell contacts and internalised desmoplakin (Figure 3.12, bottom panels 3 and 4). In contrast, both day 2 and day 6 iASPP$^{+/+}$ cells were resistant to calcium chelation (Figure 3.12, top panels 3 and 4). This suggests that in primary keratinocytes, desmosomes acquire a hyperadhesive state sooner than desmosomes in MDCK and HaCaT cells. These results also demonstrate that a loss of iASPP renders cells unable to form hyperadhesive desmosomes.

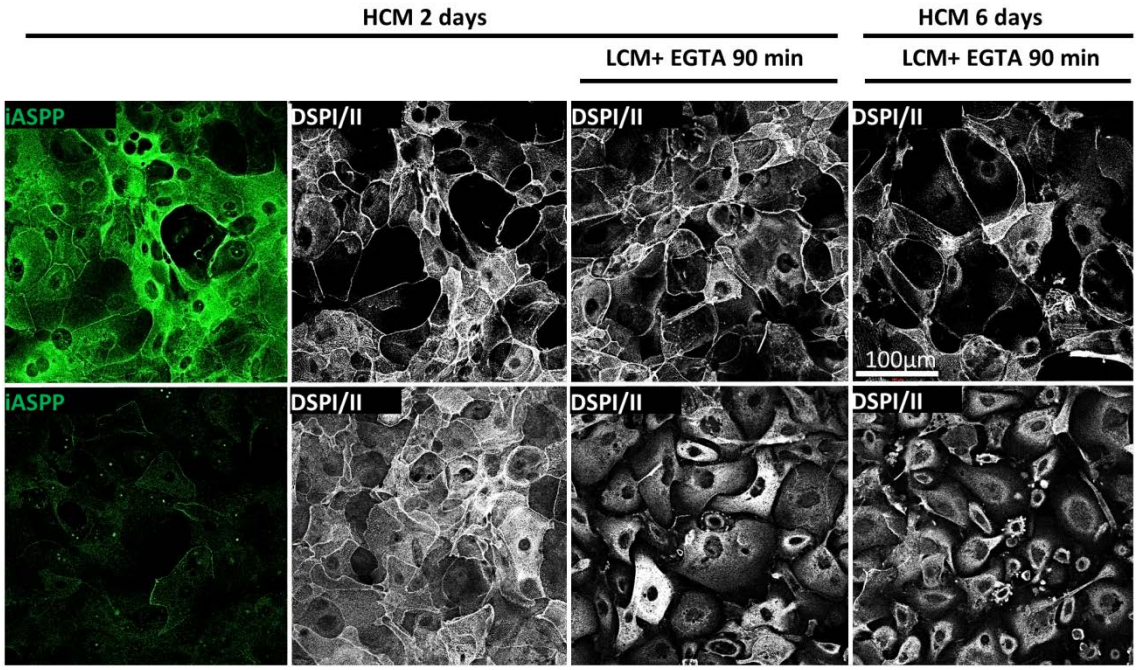

Figure 3.12 iASPP deficiency results in the formation of weakly adhesive desmosomes
Immunostaining for iASPP (green) and desmoplakin (white) in primary keratinocytes cultured at confluence in high calcium medium (HCM) for either 2 or 6 days, which were subsequently subjected to calcium depletion for 90 minutes by switching HCM to low calcium media (LCM) containing 3mM EGTA. Dissolution of desmosomes can be seen in iASPP$^{\Delta 8/\Delta 8}$ keratinocytes that have been treated with 4-OHT to deplete iASPP (lower panels). This was independent of whether they had been grown in HCM for 2 or 6 days, suggesting that iASPP ablation prevents the formation of mature and calcium-independent desmosomes that have higher adhesive strength. Vehicle-treated iASPP$^{+/+}$ keratinocytes are shown in the top panels. 4-OHT-induced iASPP$^{\Delta 8/\Delta 8}$ keratinocytes are shown in the lower panels.

To define the window of time in which desmosomes acquire hyperadhesion, primary keratinocytes were grown in HCM for either 4 or 24 hours and then subjected to calcium chelation. The results presented below show that, after 4 hours in HCM, desmosomes in iASPP$^{+/+}$ cells were sensitive to calcium chelation (Figure 3.13, left panels). By 24 hours, desmosome adhesion in primary keratinocytes appeared stronger and resistant to calcium depletion (Figure 3.13, right panels). These results suggest that calcium independence and hyperadhesion of desmosomes in primary keratinocytes is acquired between 24 and 48 hours of culturing in HCM. Keratinocytes lacking iASPP failed to form hyperadhesive desmosomes at either timepoint. Taken together, these results show that iASPP regulates desmoplakin phosphorylation and solubility, and mediates desmosome maturation.

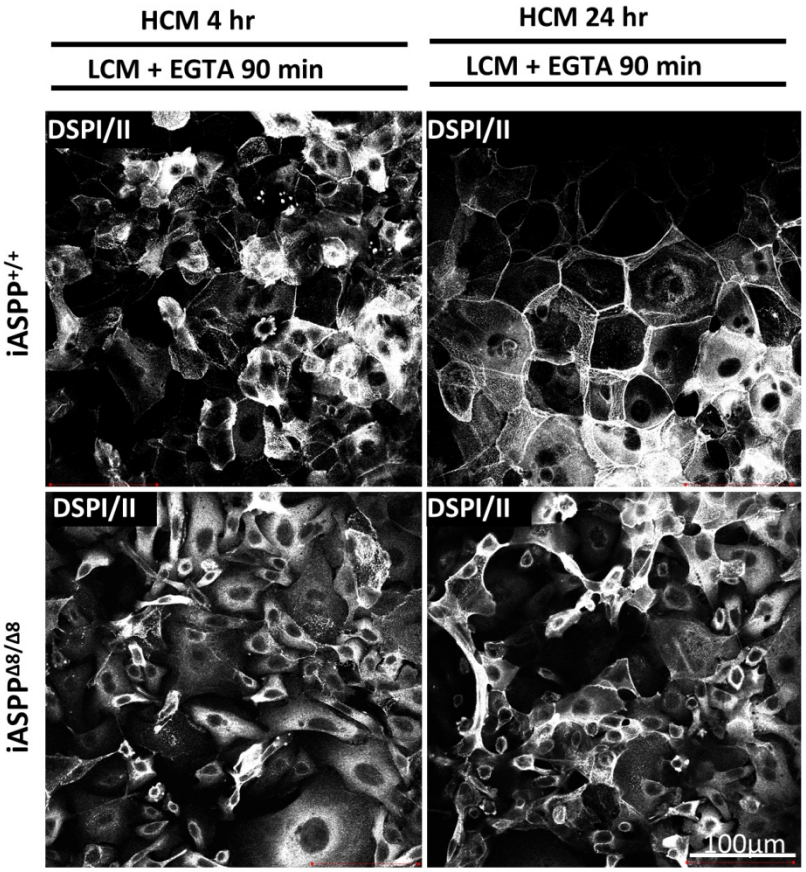

Figure 3.13 Desmosomes in primary keratinocytes become hyperadhesive between 24 and 48 hours in HCM

Primary iASPP$^{+/+}$ keratinocytes were grown in HCM for 4 or 24 hours and then exposed to the calcium chelating agent EGTA for 90 minutes. The loss of cell-cell contact upon calcium chelation was taken as a lack of resistance to calcium chelation, which is suggestive of calcium-dependent and loosely adhesive desmosomes. Maintenance of cell-cell adhesions following calcium depletion was considered to represent hyperadhesive calcium-independent desmosomes. iASPP$^{+/+}$ keratinocytes are shown in the top panels. iASPP$^{\Delta 8/\Delta 8}$ keratinocytes are shown in the bottom panels.

3.2.10 iASPP controls desmoplakin phosphorylation via a PP1-dependent mechanism

iASPP's C-terminus is known to bind PP1, a serine- and threonine-specific phosphatase. Specifically, residue F811 of mouse iASPP is necessary for this interaction (Llanos *et al.*, 2011). Results presented in the previous sections showed that iASPP binds desmoplakin and affects its phosphorylation and solubility. This led to the hypothesis that iASPP's interaction with PP1 might be necessary for the mediation of desmoplakin phosphorylation. To test this hypothesis, we sought to determine whether abrogation of iASPP's interaction with PP1 would recapitulate the desmoplakin phosphorylation phenotype observed when iASPP is ablated. For this purpose, conditional iASPP$^{F811A/F811A}$ knock-in mice were generated, in which a single iASPP mutation (F811A) is knocked-in upon treatment with tamoxifen (Figure 3.14A). This mutation is designed to disrupt the interaction between iASPP and PP1. To confirm this, an immunoprecipitation assay was performed using lysates from dermal fibroblasts from iASPP$^{+/+}$ and iASPP$^{F811A/F811A}$ mutants. Indeed, the results showed that the iASPP$^{F811A/F811A}$ mutant had lower binding affinity for PP1 (Figure 3.14B). Furthermore, the effect of the iASPP$^{F811A/F811A}$ mutant on the phosphorylation status of desmoplakin was examined. The results showed that keratinocytes from iASPP$^{F811A/F811A}$ mice had increased desmoplakin phosphorylation, similar to that observed in iASPP$^{\Delta 8/\Delta 8}$ keratinocytes (Figure 3.14C). Intriguingly, iASPP$^{F811A/F811A}$ keratinocytes did not show increased solubility, suggesting that iASPP controls solubilisation via a PP1-independent mechanism. The N-terminus of desmoplakin is important for its recruitment to desmosomes and this is associated with increased desmoplakin insolubility in non-ionic detergents. Therefore, given that iASPP interacts with desmoplakin, it is likely that this interaction stabilises desmoplakin's interactions with other desmosomal components at the desmosomes, preventing the solubilisation of desmoplakin. In support of this, the junctional localisation of iASPP was not affected by F811A mutation, and K5 aggregates were not observed in iASPP$^{F811A/F811A}$ keratinocytes (Figure 3.14D,E). This suggests that iASPP, besides

mediating desmoplakin phosphorylation, also participates in the strengthening of the interaction of desmoplakin with K5 at the cell-cell junctions. These results suggest that iASPP regulates desmoplakin dephosphorylation in a PP1-dependent mechanism, and mediates the integrity of K5 and desmoplakin interaction at the cell-cell junctions via PP1-independent mechanism.

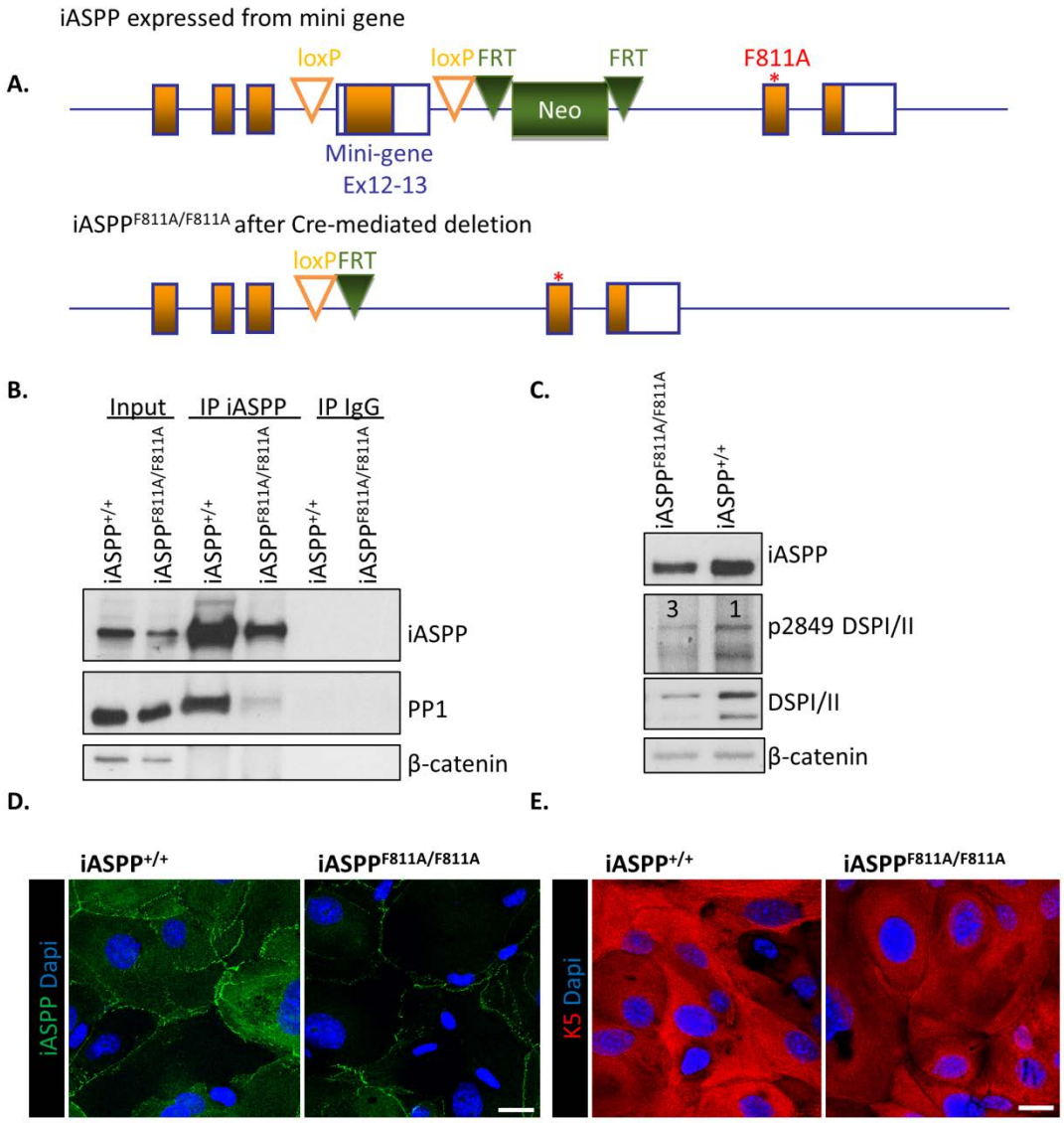

Figure 3.14 iASPP regulates the phosphorylation of desmoplakin in a PP1-dependent mechanism

A. A residue responsible for the interaction between iASPP and PP1, specifically iASPP F811 residue, was mutated to F811A and conditionally knocked-in upon activation of CreER with 4-OHT. **B.** iASPP was immunoprecipitated using a polyclonal rabbit anti-iASPP antibody and immunprecipitated complexes were analysed by western blot to test if PP1 was pulled along. Mouse monoclonal anti-PP1 antibody was used to immunoblot for PP1. Reduced binding between PP1 and iASPP was observed in lysates from iASPP$^{F811A/F811A}$ cells. **C.** Non-ionic detergent-soluble lysates from iASPP$^{+/+}$ and iASPP$^{F811A/F811A}$ keratinocytes, treated with vehicle or 4-OHT respectively, were analysed by western blot. Increased levels of phosphorylated desmoplakin are observed in iASPP$^{F811A/F811A}$ keratinocytes compared to control iASPP$^{+/+}$ keratinocytes. Upon normalisation to desmoplakin I/II, levels of phosphorylated desmoplakin in iASPP$^{F811A/F811A}$ keratinocytes are three times that in iASPP$^{+/+}$ keratinocytes. **D.** Immunoflorescence staining was done to examine the localisation of iASPP in iASPP$^{F811A/F811A}$ keratinocytes. Reduced overall iASPP levels are observed when iASPP is mutated to F811A. **E.** K5 distribution was examined in iASPP$^{+/+}$ and iASPP$^{F811A/F811A}$ keratinocytes. No keratin aggregates can be observed in iASPP$^{F811A/F811A}$ keratinocytes.

3.2.11 Loss of iASPP results in altered keratinocyte differentiation in the plantar epidermis

p63 is a master regulator of the epidermal stratification programme. Its deficiency leads to complete loss of stratified epithelia. iASPP has been shown to be an important regulator of the proliferative potential of p63. Loss of iASPP has been shown to result in premature senescence, increased expression of differentiation markers and decreased expression of proliferation markers in the epidermis (Notari *et al.*, 2011). Given that thickening of the palmoplantar epidermis was observed in iASPP$^{\Delta 8/\Delta 8}$ mice, and that dysfunction of desmosome components is associated with aberrant differentiation, whether or not thickening of the epidermis can be attributed to aberrant differentiation in iASPP$^{\Delta 8/\Delta 8}$ mice was investigated.

Plantar epidermis sections from iASPP$^{+/+}$ and age-matched 3-month old iASPP$^{\Delta 8/\Delta 8}$ mice were subjected to immunofluorescence staining for various markers of epidermal stratification including p63, K5, K1, K6 and loricrin. In the normal plantar epidermis, p63 and K5 expression was observed to be confined to the proliferative basal and the nearest suprabasal layers, in accordance with the published literature (Figure 3.15 and 3.16 first panel). K1 expression was observed to be present throughout the suprabasal layers and was absent from the uppermost layers (Figure 3.16, second panel). Usually, K6 expression is restricted to the follicular epidermis, with the exception of traumatised, diseased and wounded epidermis where broader K6 expression can be seen. In iASPP$^{+/+}$ sections, K6 expression was only observed in the follicular epidermis. Finally, in normal epidermis, loricrin expression was observed in the terminally differentiated uppermost epidermal layers (Figure 3.16, bottom panel). In the plantar epidermis of iASPP$^{\Delta 8/\Delta 8}$ mice, the expression pattern of several stratification markers was altered. p63 had very variable expression, with a lack of expression in some basal layer regions (Figure 3.15, left panel arrowheads) and expanded expression in other regions (Figure

3.15, left panel arrows). Whether or not the absence of p63 in some cells marks the loss of their proliferative capacity requires further investigation. As reported previously, loss of TAp63 can lead to uncontrolled hyperproliferation and exhaustion of the proliferative capacity of adult stems cells, resulting in increased cellular senescence (Su *et al.*, 2009). Whether iASPP is dampening the levels of TAp63 and affecting its regulatory activities needs further analysis. Interestingly, K5 expression was observed in the immediate subcornified layers (Figure 3.16, top panel), suggesting that the cells of the upper layers had adopted the attributes of basal cells. Additionally, K1 had a broadened expression that was associated with thickening of the spinous layers in these mice. K6 expression in the plantar epidermis of iASPP$^{\Delta 8/\Delta 8}$ mice was also broadened, and scattered K6 cells could be seen throughout the epidermis. These results support previous reports showing that iASPP is important in the regulation of differentiation. They also show that iASPP plays an important role in the positioning of cells, since K5-positive cells can be observed ectopically in the upper layers of the affected epidermis in iASPP-deficient mice. It would be interesting to determine whether K5-positive basal cells are able to percolate to the uppermost layers as a result of weakened cell-cell adhesions. Alternatively, suprabasal cells might have failed to downregulate K5.

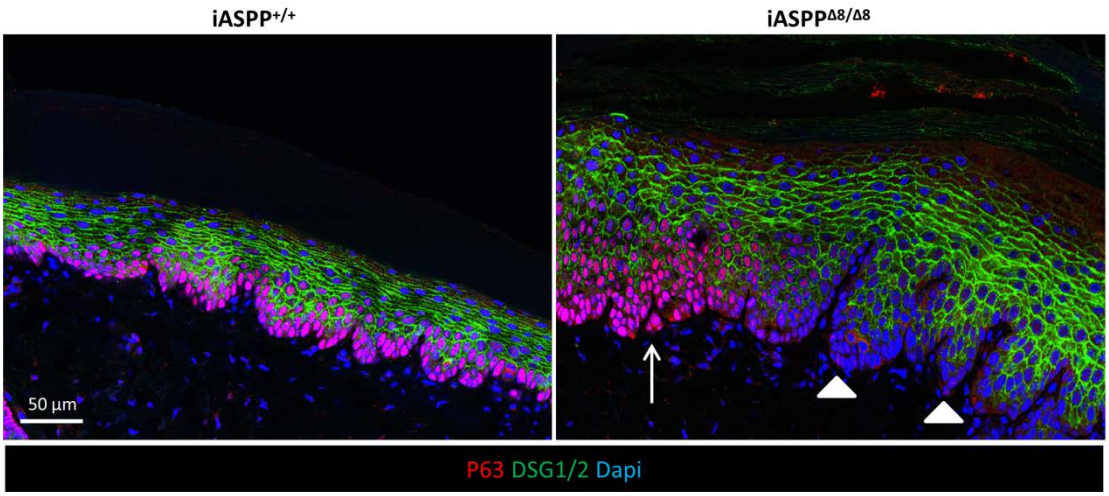

Figure 3.15 p63 expression is altered in the plantar epidermis of iASPPΔ8/Δ8mice
Immunofluorescence staining for p63 (red) and desmoglein 1/2 (DSG1/2, green) was done on sections from iASPP$^{+/+}$ and iASPP$^{\Delta 8/\Delta 8}$ mice. In iASPP$^{+/+}$ epidermis, p63 expression is restricted to the basal and immediate suprabasal layers. In the epidermis of iASPP$^{\Delta 8/\Delta 8}$ mice, p63's expression pattern is variable, with some basal layers cells completely deprived of p63 expression (white arrowheads).

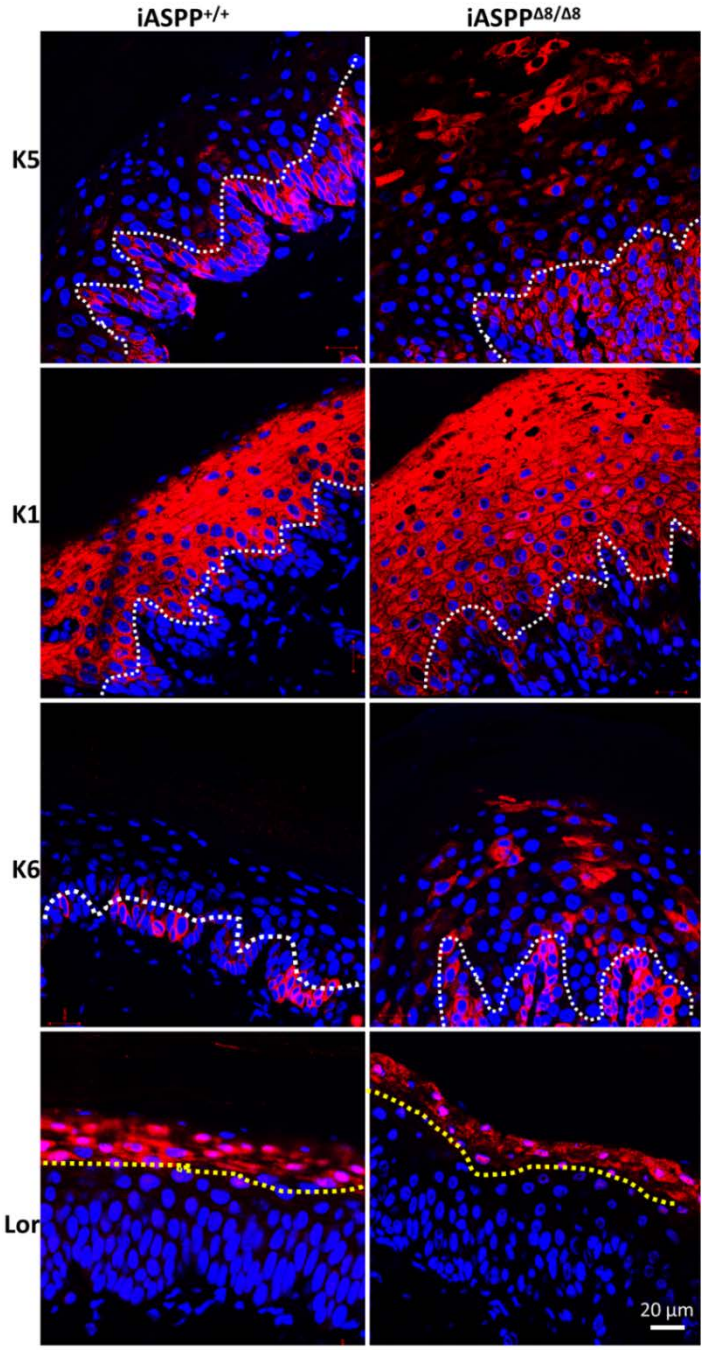

Figure 3.16 Loss of iASPP results in the aberrant expression of epidermal stratification markers

Immunofluorescence staining for K5, K1, K6 and loricrin (all in red) in the plantar epidermis of 3 month old iASPP$^{+/+}$ and iASPP$^{\Delta8/\Delta8}$ mice. K5 was observed only in the basal layer of the control, but extended into the suprabasal layers of iASPP$^{\Delta8/\Delta8}$ epidermis. Scattered K5 positive cells can also be observed in the upper suprabasal layers in iASPP$^{\Delta8/\Delta8}$ mice. Broad expression of K1 was detected in the iASPP$^{\Delta8/\Delta8}$ plantar epidermis. Basal and occasional suprabasal cells displayed K6 expression in the epidermis in iASPP$^{\Delta8/\Delta8}$ mice. Loricrin expression is comparable between iASPP$^{+/+}$ and iASPP$^{\Delta8/\Delta8}$ mice. Nuclei are in blue, stained with DAPI. White dashed lines indicate the boundary between the basal and suprabasal cell layers, while yellow dashed lines indicate boundary of the granular and cornified layers.

3.2.12 Working model for the role of iASPP in desmosome stability

The data presented in this chapter suggests that iASPP localises at cell-cell junctions in response to calcium signalling, where it interacts with desmoplakin and K5. Moreover, the results show that iASPP participates in the regulation of desmoplakin's dephosphorylation, which results in a more stable association of desmoplakin with desmosome components at cell-cell junctions. In the absence of iASPP, cell-cell adhesions are weakened and desmosomes fail to acquire a hyperadhesive state. Moreover, increased desmoplakin solubility and keratin aggregation is observed when iASPP is deleted. Furthermore, iASPP is implicated in the regulation of epidermal stratification, suggesting that iASPP is a dual function protein that is able to link adhesion to cell signalling. These findings have led to the proposal of a working model for the role of iASPP in desmosome stability that is presented below (Figure 3.17).

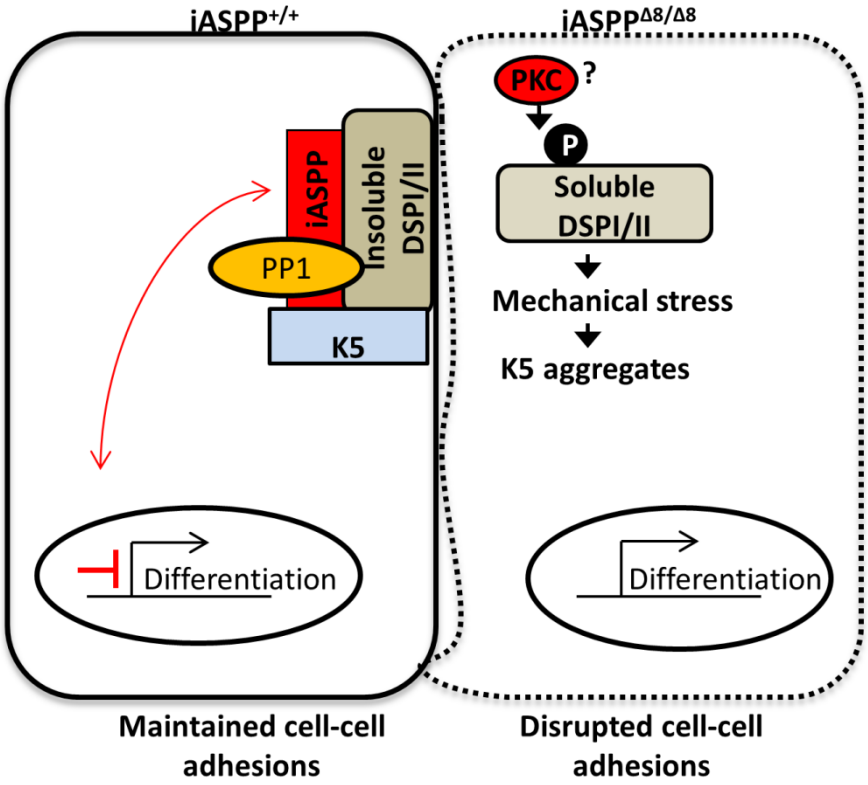

Figure 3.17 Working model for the role of iASPP in desmosome stability
In iASPP$^{+/+}$ keratinocytes, iASPP interacts with desmoplakin and K5. iASPP mediates the dephosphorylation of junctional desmoplakin via a PP1-dependent mechanism and also stabilises the association of desmoplakin with desmosomes at cell-cell junctions. This results in the formation of stable desmosomes and the maintenance of cell-cell junctions. In iASPP$^{\Delta 8/\Delta 8}$ keratinocytes, the interaction between desmoplakin and keratin is altered due to increased phosphorylation of desmoplakin and its increased solubility. This leads to increased susceptibility of the cells to stress, which results in the disruption of cell-cell junctions and the formation of keratin aggregates. It is also likely that iASPP interferes with PKCα's binding to, and phosphorylation of, desmoplakin. This requires further investigation. As iASPP can also translocate to the nucleus to inhibit differentiation, increased differentiation and ensuing thickening of epidermis can be observed in the absence of iASPP.

3.3 Summary and brief discussion

The generation of mice that lack iASPP has been of great importance for our understanding of the physiological functions of iASPP, and the molecular mechanisms by which iASPP participates in the regulation of these functions. The major phenotypes observed in iASPP$^{\Delta 8/\Delta 8}$ mice include woolly/spiky hair, cardiac abnormalities, and eye and epidermal defects. These defects are often linked to desmosome dysfunction. An additional phenotype accompanying aberrant desmosome function is palmoplantar keratoderma. Given that iASPP$^{\Delta 8/\Delta 8}$ mice present with phenotypes associated with diseases of dysfunctional desmosomes, efforts were made to understand whether iASPP mice display palmoplantar keratoderma and whether iASPP is involved in the regulation of desmosomes. A number of microscopic, biochemical and functional assays were used to address this aim.

Firstly, a number of palmar and plantar skin specimens from age-matched iASPP$^{+/+}$ and iASPP$^{\Delta 8/\Delta 8}$ mice were collected and subjected to microscopic analysis. Histological examination of these specimens revealed focal thickening of the palmoplantar epidermis in iASPP$^{\Delta 8/\Delta 8}$ mice compared to iASPP$^{+/+}$ controls. Specifically, significant thickening of the spinous layers and modest thickening of the cornified layers were observed. Electron microscope analysis of dorsal skin epidermis revealed further morphological abnormalities in iASPP$^{\Delta 8/\Delta 8}$ mice that were rarely seen in iASPP$^{+/+}$ mice. Formation of keratin aggregates and disruption of desmosome-keratin filament association was observed in the epidermis of iASPP$^{\Delta 8/\Delta 8}$ mice. However, desmosome morphology appeared normal. The observation that a loss of iASPP led to keratin aggregation was confirmed *in vitro* in keratinocytes. The absence of morphological defects in desmosomes in the EM analysis could be explained by the dynamic nature of iASPP expression, or by the fact that epidermal thickening was not diffuse but rather focal. Therefore, it is likely that keratinocytes analysed using electron microscopy lacked junctional

iASPP expression or had a modest desmosome phenotype. A more thorough analysis of desmosomes in the epidermis is required. As the palmoplantar epidermis is subjected to higher physical trauma, electron microscope analysis of the palmoplantar epidermis might offer better insight into whether desmosome morphology is affected. While characterisation of the palmoplantar epidermis from iASPP$^{\Delta 8/\Delta 8}$ mice could benefit from further study, the data gathered so far indicate that iASPP$^{\Delta 8/\Delta 8}$ mice suffer from focal palmoplantar keratoderma.

Altered desmoplakin function due to homozygous or heterozygous mutations has been associated with palmoplantar keratoderma and the collapse of the keratin network (Armstrong *et al.*, 1999; Norgett *et al.*, 2000; Wan *et al.*, 2004). A propensity for keratin aggregation in the epidermis of iASPP$^{\Delta 8/\Delta 8}$ mice suggests that iASPP participates in the regulation of desmosome integrity. To verify this, it was shown that iASPP was able to interact with desmoplakin and that this interaction had functional significance. In the absence of iASPP, the solubility and phosphorylation of desmoplakin was increased. Increased cytosolic localisation of desmoplakin was also observed both *in vivo* and *in vitro*. These protein modifications and expression changes had functional consequences on desmosome adhesion and maturation. Keratinocyte monolayers with a loss of iASPP expression showed increased susceptibility to mechanical stress. Moreover, intercellular adhesion proved to be weak and highly sensitive to disruption after calcium chelation. These studies confirmed the role of iASPP in the regulation of desmosome integrity. Furthermore, they are in keeping with previous findings showing that the inhibition of PP1 leads to increased phosphorylation of desmoplakin and desmosome disassembly (Toivola *et al.*, 1997). Given that iASPP is also known to regulate epidermal differentiation (Notari *et al.*, 2011), it is not surprising that aberrant differentiation was observed in the palmoplantar epidermis of iASPP$^{\Delta 8/\Delta 8}$ mice. Since desmosomes are key players in sensing structural stresses, the identification of iASPP as a regulator of desmosomes places

it as an exemplar dual function protein that can sense the integrity of junctions and integrate it into the nucleus to regulate gene transcription.

The phosphorylation status of desmoplakin residue S2849 has been shown to play an important role in desmosome maturation and hyperadhesiveness. Compromising the phosphorylation of this site by mutating S2849 to unphosphorylatable S2849G results in the formation of highly adhesive intercellular connections (Godsel *et al.*, 2005). As the serine/threonine-specific phosphatase PP1 is known to bind iASPP, attempts were made to understand whether iASPP could mediate the localisation of PP1 to the desmoplakin adhesion complex. To address this aim, a conditional iASPP$^{F811A/F811A}$ mouse model was generated, in which iASPP's binding to PP1 was abrogated. The generation of these mice was facilitated by the previous discovery in our laboratory that residue F811 of murine iASPP is necessary and sufficient for the interaction of iASPP with PP1 (Llanos *et al.*, 2011). Therefore, the mouse model contained a single mutation, F811A, that altered the PP1 binding site on iASPP. Analysis of the phosphorylation status of desmoplakin in the soluble fraction of proteins from iASPP$^{+/+}$ and iASPPF$^{811A/F811A}$ keratinocytes revealed increased desmoplakin phosphorylation in iASPPF$^{811A/F811A}$ keratinocytes compared to iASPP$^{+/+}$ controls. However, increased solubility of desmoplakin in iASPP$^{F811A/F811A}$ keratinocytes was not observed. These results suggest that iASPP regulates the phosphorylation of desmoplakin in PP1-dependent mechanisms, while it mediates the solubility of desmoplakin in a PP1-independent mechanism. Studies examining whether keratinocytes from iASPP$^{F811A/F811A}$ mice have weakened cell-cell adhesions that are unable to mature are currently under investigation. Further studies are needed to determine if phosphorylation of other sites on desmoplakin are regulated by iASPP/desmoplakin interaction, and how these sites may be important in the regulation of desmoplakin solubility. The possibility that iASPP might prevent kinases such as PKCα from binding and phosphorylating desmoplakin cannot be excluded. Collectively, these studies show that iASPP

is a dual function protein that regulates desmosome integrity and the epidermal differentiation programme.

Chapter IV: Wound healing is delayed in mice deficient of iASPP

Chapter IV: Wound healing is delayed in mice deficient of iASPP

4.1 Introduction

Skin serves as a physical and chemical barrier to the external environment. As the outermost organ, the skin is at high risk for sustaining wounds. Upon wounding, the skin must rapidly repair itself and restore its barrier function. Two important cellular processes contribute to the wound repair. Firstly, a fibroblast-coordinated contraction of dermal tissue occurs beneath the wound site, which helps to draw the wound edges closer together. Second, a keratinocyte-driven re-epithelisation of the wound ensues, which includes a burst of keratinocyte proliferation proximal to the wound margin, modification of the cell-cell adhesion complexes in keratinocytes at the leading edges of the wound, and subsequent migration of those keratinocytes as a cohesive sheet across the wound bed (Coulombe, 2003; Garrod *et al.*, 2005; Martin, 1997). Impairment of any of the outlined processes can hinder wound healing.

Both *in vitro* and *in vivo* studies have shown that desmosome components are involved in the regulation of cellular processes implicated in wound healing such as adhesion, proliferation and migration (Garrod *et al.*, 2005; Thomason *et al.*, 2012; Wallis *et al.*, 2000). For example, in the process of re-epithelisation, desmosome adhesion between adjacent cells at the wound front is loosened during cell migration to become reinforced when the wound site is resurfaced. The inhibition of desmosomes from switching between adhesive states delays wound closure (Thomason *et al.*, 2012). Furthermore, a mutation in the desmosome component Perp delays wound healing *in vivo* by compromising cell-cell adhesion and perturbing the cohesive migration of the epithelial sheet over the wound site (Beaudry *et al.*, 2010). Investigations into the roles of other desmosome components in wound healing *in vivo* have not been carried out, in part due to lethality caused by the ablation of these components

in mouse models. Mice that survive, such as desmocollin 1-deficient mice, have increased cell proliferation in the skin but are unable to efficiently heal scratching lesions, which leads to their exacerbation resulting in ulceration and chronic dermatitis (Chidgey *et al.*, 2001). Loss of other components such as plakophilin 1 and plakoglobin results in increased cell motility *in vitro* (South *et al.*, 2003; Yin *et al.*, 2005b). Whether the increased motility promotes quicker wound healing, or disrupts the cohesive movement of epithelial cells across the wound site and impedes wound healing, remains to be determined. Nonetheless, these reports show that desmosomes are important regulators of a healthy wound healing process.

In the previous chapter, it was shown that iASPP regulates desmosomes and their adhesiveness. iASPP also participates in the maintenance of the proliferative potential of p63-positive cells in the basal layer of the skin epidermis, implicating iASPP in the regulation of proliferation (Notari *et al.*, 2011). In human cancers, which are characterised by increased cellular proliferation and invasiveness, iASPP is often upregulated (Bergamaschi *et al.*, 2003; Liu *et al.*, 2010; Zhang *et al.*, 2005). Since iASPP participates in cellular processes critical for wound re-epithelisation: adhesion, proliferation and invasiveness/migration, the role of iASPP in wound re-epithelisation *in vivo* was investigated in this chapter. To carry out the study, iASPP$^{\Delta 8/\Delta 8}$ mice were used in which incisional wounds were made, and their healing progress monitored relative to iASPP$^{+/+}$ controls. Whether proliferation was affected in sections from these mice was subsequently examined. *In vitro* analyses were used to elucidate whether iASPP affects cell migration.

It is demonstrated here that iASPP$^{\Delta 8/\Delta 8}$ mice have delayed wound healing. This delay is not due a defect in proliferation, but rather due to altered migration. Loss of iASPP affects the migratory behaviour of keratinocytes, and iASPP$^{\Delta 8/\Delta 8}$ cells migrate faster and in a disorganised

manner. Therefore, impeded wound healing in iASPP$^{\Delta 8/\Delta 8}$ mice is at least in part due to an inability of the epithelial sheet to migrate efficiently and cohesively over the wound site.

4.2 Results

4.2.1 iASPP is expressed in the wounded epidermis

To investigate whether iASPP could be important in wound healing, the first step was to determine whether iASPP is expressed in the wounded epidermis. Therefore, iASPP$^{+/+}$ mice were subjected to incisional wounds of 6mm in diameter, and iASPP expression assessed at the wound rim 2, 3, and 6 days after wounding. Strong iASPP expression was observed at the wound edge epidermis of all sections examined. Strong cytoplasmic and modest nuclear iASPP staining was often observed in cells of the basal layers, while more junctional iASPP staining was observed in the cells of upper epidermal layers (Figure 4.1A). The increased iASPP nuclear intensity in the basal layer cells in comparison to subrabasal layer cells was confirmed by quantification of the average nuclear intensity using ImageJ (Figure 4.1B). Lack of iASPP staining was observed in the wound section from iASPP$^{\Delta 8/\Delta 8}$ mice (Figure 4.1A, rightmost panel), confirming the specificity of the antibody for epidermal cells. The extensive expression of iASPP suggests that this protein might be involved in the regulation of the wound healing process. The junctional localisation of iASPP suggests that iASPP might help to keep cells together during the migration of the epithelial sheet over the wound bed. Nuclear iASPP might be regulating the proliferative potential of p63, which has been shown before (Chikh *et al.*, 2011; Notari *et al.*, 2011).

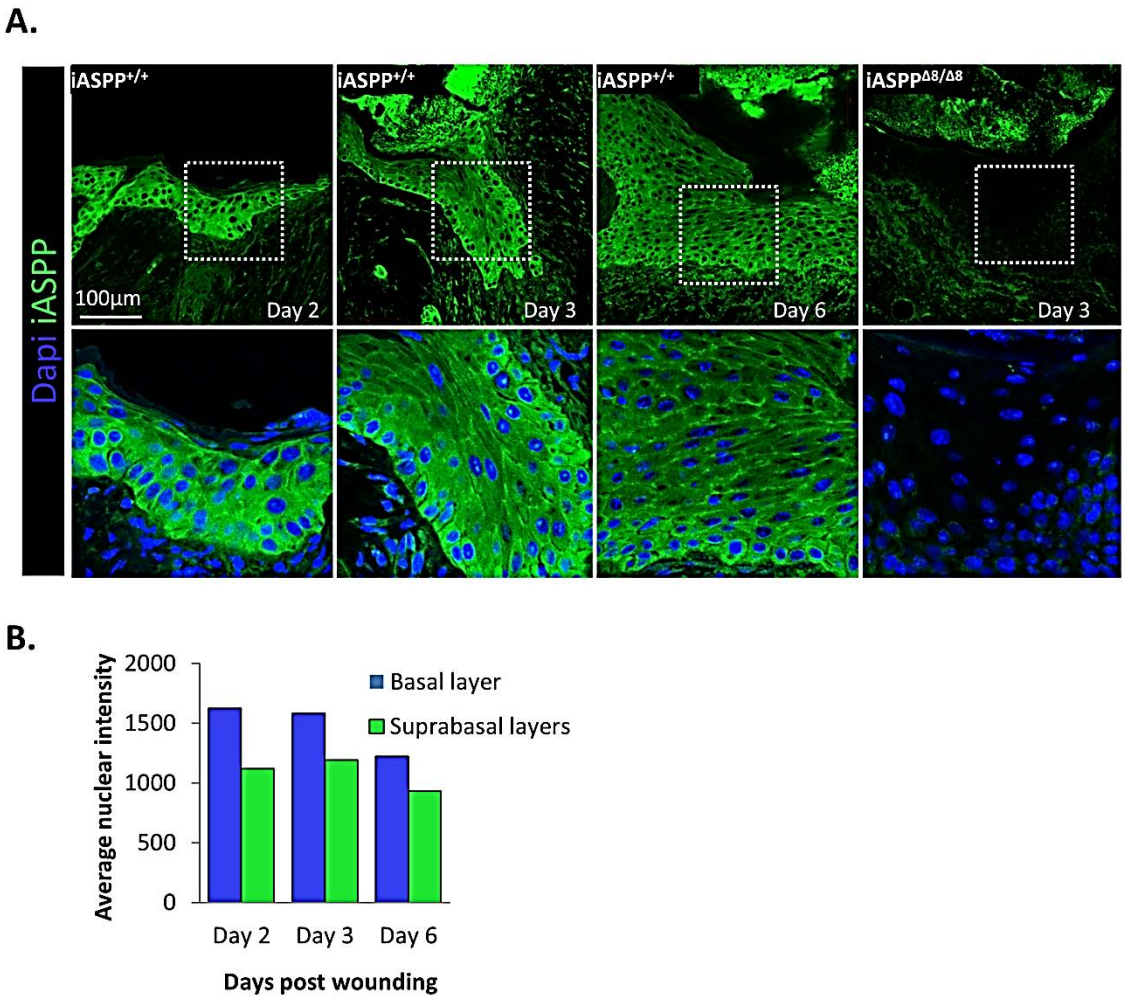

Figure 4.1 iASPP is expressed at the wound edge epidermis

A. Immunofluorescence staining for iASPP (green) at the wound edge epidermis 2, 3 and 6 days after wounding. Strong iASPP expression is observed in the basal layers of all sections. At 3 and 6 days post-wounding, junctional iASPP staining can be observed in the upper epidermal layers. To confirm the specificity of the antibody, a wound section from iASPP$^{\Delta 8/\Delta 8}$ mice at day 3 post-wounding was subjected to immunofluorescence staining. Scale bar for top panel images taken at 20 x magnification is 100 µm. In the bottom panel, squared regions from the upper panel are shown at a higher magnification. Nuclear stain DAPI (blue) is included. **B.** The average nuclear intensity of iASPP in the basal and suprabasal layers was quantified using ImageJ. Basal layer cells were defined as cells in the first epidermal layer, while suprabasal cells were defined as cells outside the first epidermal layer.

4.2.2 iASPP deficiency delays wound healing *in vivo*

After confirming the presence of iASPP expression at the wound site, the role of iASPP in wound healing was investigated *in vivo*. 6 week old iASPP$^{\Delta 8/\Delta 8}$ and iASPP$^{+/+}$ mice were subjected to full skin thickness punch biopsies of 6mm in diameter, and the areas of the wounds measured every other day for 14 days. In the absence of iASPP, wound healing was delayed. iASPP$^{\Delta 8/\Delta 8}$ mice showed significantly larger wounds than iASPP$^{+/+}$ mice at days 2-4 (Figure 4.2; Mann-Whitney's U test, $p<0.001$). By day 6, the wounds of iASPP$^{\Delta 8/\Delta 8}$ mice showed progressed healing but were still significantly larger than the wounds in iASPP$^{+/+}$ mice ($p<0.05$). However, by day 10-14 both iASPP$^{+/+}$ and iASPP$^{\Delta 8/\Delta 8}$ mice had fully closed wounds (Figure 4.2A).

To further assess the wound healing process, histological examination of wound healing sections from both iASPP$^{+/+}$ and iASPP$^{\Delta 8/\Delta 8}$ mice was performed at days 2, 4, and 6 after wounding (Figure 4.3A). These analyses showed wider intercellular spaces between the epithelial cells of the wound margin in iASPP$^{\Delta 8/\Delta 8}$ mice compared to iASPP$^{+/+}$ controls (Figure 4.3B, arrowheads). While widening of the intercellular spaces at the migrating epithelial sheet is a recognised morphological change during wound healing (Odland and Ross, 1968), the extent of widening can have adverse consequences on the healing process. It can prevent the advancing sheet from migrating efficiently and in a well-synchronised manner (Beaudry *et al.*, 2010). The increased widening of the spaces in the advancing epithelium of iASPP$^{\Delta 8/\Delta 8}$ mice is suggestive of disrupted cellular adhesions.

In summary, iASPP$^{\Delta 8/\Delta 8}$ mice exhibited a delay in the initial stages of wound healing and displayed more extensive widening of the intercellular spaces in the migrating epithelial sheet.

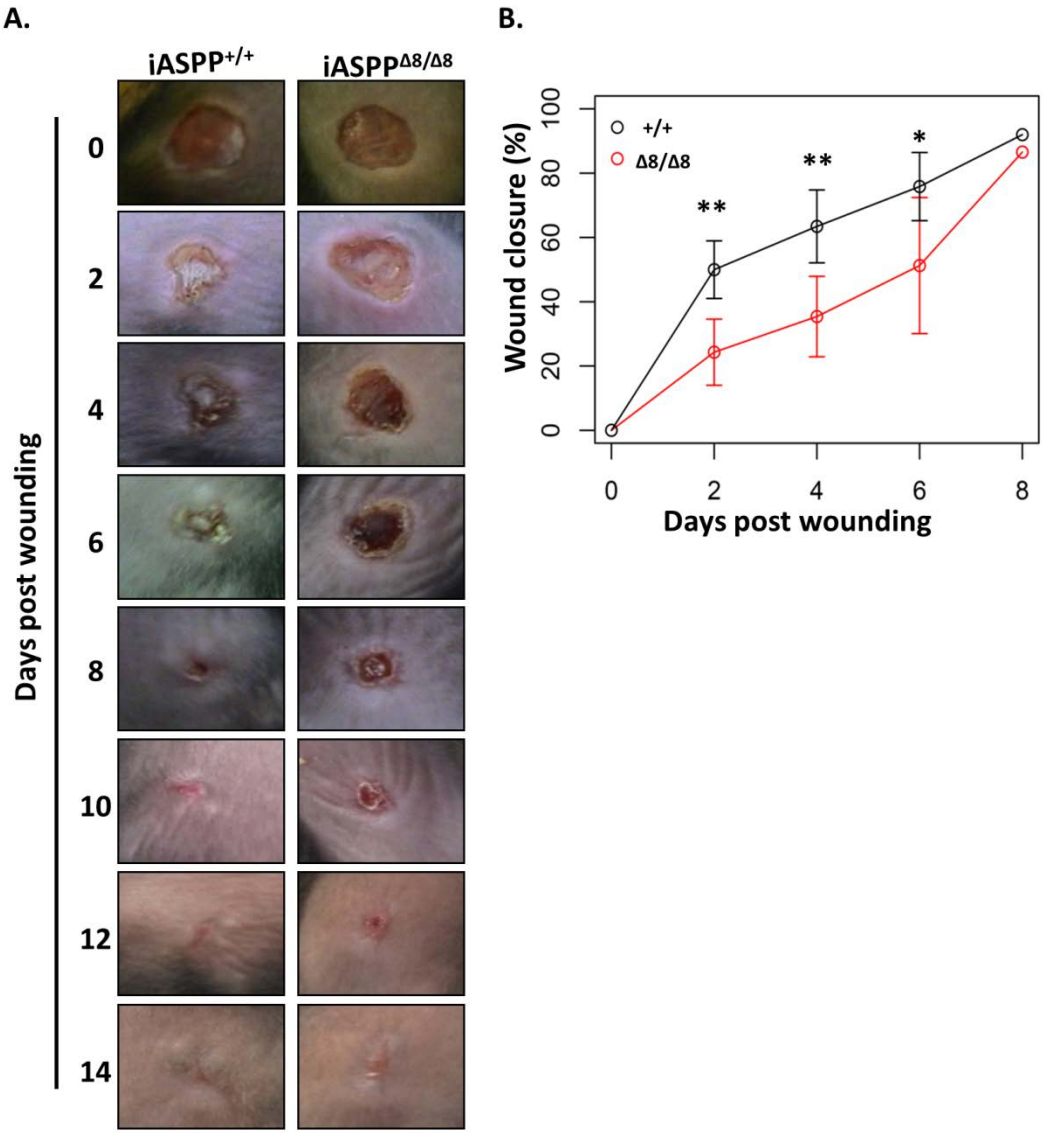

Figure 4.2 Wound healing is delayed in iASPP$^{\Delta 8/\Delta 8}$ mice

A. Representative images of delayed wound healing in iASPP$^{\Delta 8/\Delta 8}$ mice. **B.** Graphical representation showing the average percentage (mean ± 2 SEM) of wound area closed in iASPP$^{+/+}$ and iASPP$^{\Delta 8/\Delta 8}$ mice. **p<0.01, *p<0.05. The number of mice included at time points day 2, day 4 and day 6 for iASPP$^{+/+}$ and iASPP$^{\Delta 8/\Delta 8}$ mice are 11 and 13, 7 and 8, 5 and 7, respectively. Statistical analysis between groups was performed using the Mann-Whitney U-test.

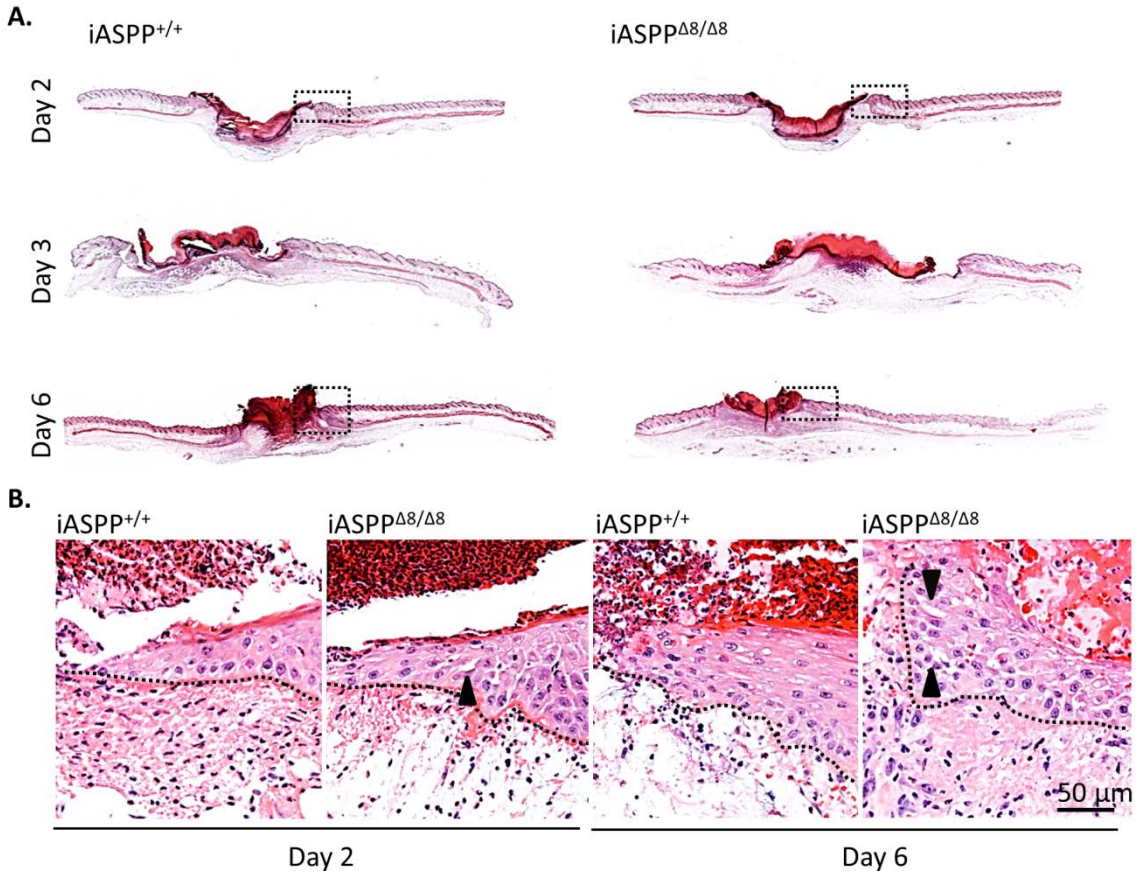

Figure 4.3 Widened intercellular spaces in the advancing epithelia of wounded iASPPΔ8/Δ8 mice

A. Representative haematoxylin and eosin-stained sections of wounds from iASPP$^{+/+}$ and iASPP$^{\Delta 8/\Delta 8}$ mice at days 2, 3 and 6 post-wounding. Black boxes are regions that are enlarged and shown in panel B. **B.** Advancing epithelial tongues of wounds from iASPP$^{+/+}$ and iASPP$^{\Delta 8/\Delta 8}$ mice at days 2 and 6, as indicated. Black arrowheads point to increased intercellular spaces observed in iASPP$^{\Delta 8/\Delta 8}$ wounded epidermis. Dashed lines indicate the dermal-epidermal boundary.

4.2.3 Proliferation and apoptosis do not contribute to delayed wound healing in iASPP$^{\Delta 8/\Delta 8}$ mice

The cause for delayed wound healing in iASPP$^{\Delta 8/\Delta 8}$ mice was further investigated. Given that keratinocyte proliferation is one of the first steps in re-epithelisation, and iASPP$^{\Delta 8/\Delta 8}$ mice showed a delay in the initial stages of wound closure, whether abnormalities in keratinocyte proliferation could be responsible for the hindered healing process was examined. Using a BrdU incorporation assay, epithelial cell proliferation was assessed at the wound site in iASPP$^{+/+}$ and iASPP$^{\Delta 8/\Delta 8}$ mice at days 2, 3 and 6 post-wounding. The percentage of BrdU-positive nuclei in cells expressing K6, a marker for proliferative and activated keratinocytes, was determined. The combination of BrdU staining with staining for K6 allowed the quantification and comparison of proliferation specifically in keratinocytes participating in wound healing. Results showed that proliferation was equivalent between iASPP$^{+/+}$ and iASPP$^{\Delta 8/\Delta 8}$ wounds at days 2, 3 and 6 (Figure 4.4A). BrdU is a structural analogue of thymidine and gets incorporated into DNA during the synthesis (S) phase of the cell cycle as a substitute for thymidine. To verify that the observed results were not due to cells entering the S phase, and not progressing through other phases of the cell cycle, staining was performed for Ki67 (a proliferation marker that is present throughout all active phases of the cell cycle). At day 3 post-wounding, no significant difference in the percentage of Ki67-positive wound edge keratinocytes was observed between iASPP$^{+/+}$ and iASPP$^{\Delta 8/\Delta 8}$ mice (Figure 4.4B).

Although the keratinocyte proliferation was unaffected by a lack of iASPP, this aspect of re-epithelisation could still be affected by increased epithelial apoptosis. In addition to the above mentioned staining, the wound sections at day 3 post-wounding were also stained for cleaved caspase 3, a marker for apoptosis. Staining for cleaved caspase 3 revealed limited epithelial apoptosis, with no difference between iASPP$^{+/+}$ and iASPP$^{\Delta 8/\Delta 8}$ wounds (Figure 4.5). In summary,

these results suggest that altered levels of proliferation or apoptosis are not responsible for delayed wound healing in iASPP$^{\Delta 8/\Delta 8}$ mice.

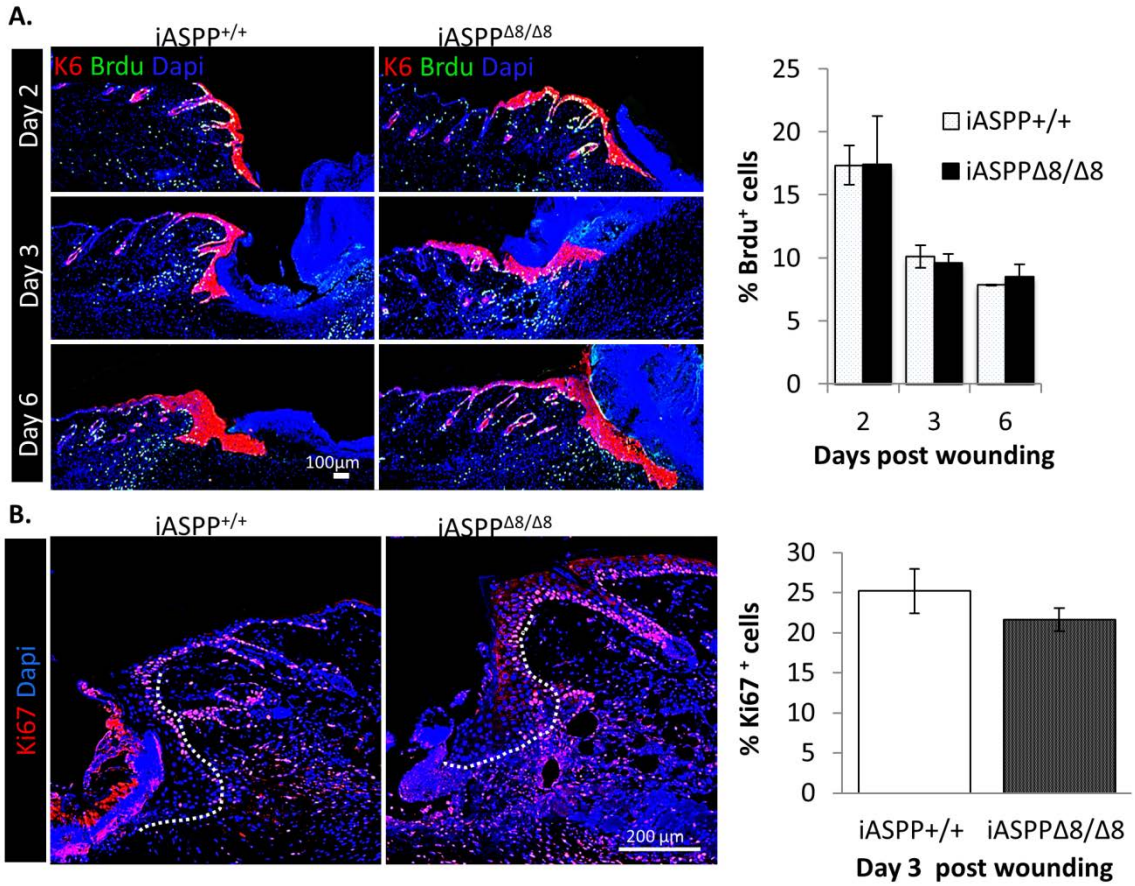

Figure 4.4 iASPP$^{\Delta 8/\Delta 8}$ migrating keratinocytes do not exhibit hampered proliferation during wound re-epithelisation

A. Representative images for BrdU (green) and K6 (red) staining in wound sections from iASPP$^{+/+}$ and iASPP$^{\Delta 8/\Delta 8}$ mice at days 2, 3, and 6 post-wounding are shown on the left. Quantification of cell proliferation within the K6-positive epithelial sheet domain (red) is shown on the right. Bars represent mean ± SE. **B.** Ki67-stained day 3 wound sections from iASPP$^{+/+}$ and iASPP$^{\Delta 8/\Delta 8}$ mice. Quantification of the percentage of Ki67-positive cells at the wound edge epidermis 3 days post-wounding is shown on the right. Dotted line marks the basement membrane separating the epidermis from the dermis.

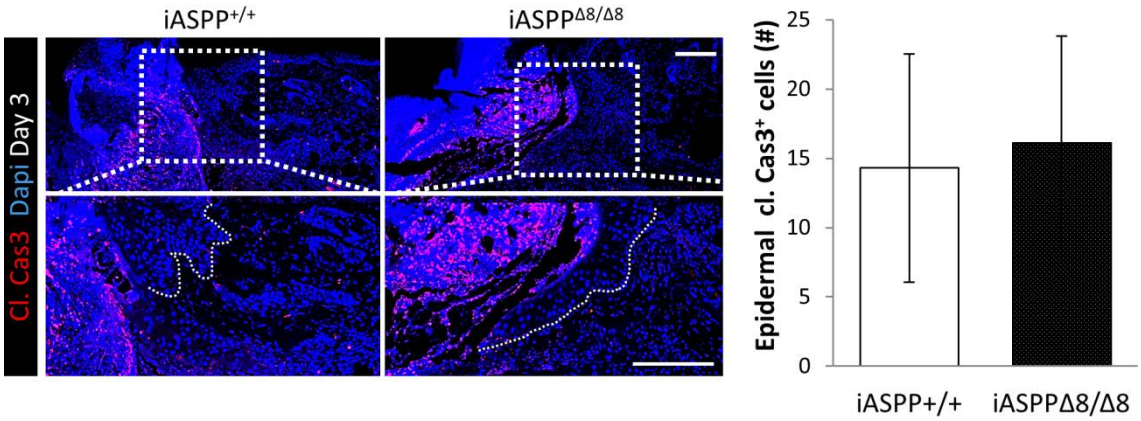

Figure 4.5 iASPP$^{\Delta 8/\Delta 8}$ migrating keratinocytes do not show altered apoptosis

Staining for cleaved caspase 3 (cl. Cas3, red) to detect apoptotic cells in day 3 wounded epidermis from iASPP$^{+/+}$ and iASPP$^{\Delta 8/\Delta 8}$ mice. Bottom panel represents magnification of the boxed region in the panel above. Dotted line demarcates the basement membrane, which separates the epidermis (above the line) from the dermis (below the line). In the right panel, quantification of number of cleaved caspase 3 (red)-positive epithelial cells at the wound edge is shown. Scale bar is 200 µm.

4.2.4 Loss of iASPP leads to increased keratinocyte migration

As the impaired wound healing observed in iASPP$^{\Delta 8/\Delta 8}$ mice was not due to deficits in proliferation, whether or not compromised keratinocyte migration was the culprit for the delayed healing observed was investigated. The migration of keratinocytes from iASPP$^{+/+}$ and iASPP$^{\Delta 8/\Delta 8}$ mice was compared using an *in vitro* wound scratch assay. Briefly, keratinocytes were grown in HCM for 24 hours, confluent monolayers were subjected to a scratch wound, and the extent of wound closure monitored and calculated using ImageJ software. iASPP$^{\Delta 8/\Delta 8}$ keratinocytes were able to migrate a longer distance and close the wound to a greater extent than iASPP$^{+/+}$ keratinocytes (Figure 4.6A). Specifically, cells lacking iASPP closed 40%, while control keratinocytes closed 25%, of the initial wound area within 8 hours of wound induction (Figure 4.6B, Mann-Whitney's U test, $p<0.001$). These results suggest that a loss of iASPP enhances cell migration. Interestingly, loss of the desmosome component Perp leads to a delayed wound healing process with no alteration in proliferation or apoptosis. Instead, the impaired wound healing process in Perp-deficient mice has been attributed to enhanced and chaotic keratinocyte migration due to compromised cell-cell adhesion (Beaudry *et al.*, 2010). The results observed in iASPP$^{\Delta 8/\Delta 8}$ mice and cells are in keeping with a loss of Perp, which exhibits delayed wound healing *in vivo* and increased cell migration *in vitro*, suggesting that iASPP might regulate wound healing through regulation of cell-cell adhesions such as desmosomes.

In order to ensure that the increased closure of the scratch wound in *in vitro* conditions was not caused by increased proliferation, the keratinocytes from iASPP$^{+/+}$ and iASPP$^{\Delta 8/\Delta 8}$ mice were tested for proliferation and apoptosis using the same markers as in *in vivo* conditions. Briefly, keratinocytes were synchronised by serum starvation, stimulated to enter the cell cycle by the addition of growth media containing BrdU for 4 hours and then stained for BrdU, Ki67, and

cleaved caspase 3. As judged by the percentage of cells that were positive for BrdU or Ki67, iASPP$^{+/+}$ and iASPP$^{\Delta 8/\Delta 8}$ keratinocytes had similar proliferation profiles (Figure 4.7A). Intriguingly, apoptosis was enhanced in cells lacking iASPP compared to control cells, and a significantly higher percentage of iASPP$^{\Delta 8/\Delta 8}$ cells were positive for cleaved caspase 3 (Figure 4.7B, *t*-test, p=0.04). This is at odds with the *in vivo* data. A potential explanation for this discrepancy is that in *in vitro* conditions apoptosis were examined 4 hours after release from serum starvation. This suggests that iASPP deficiency *in vitro* makes cells more susceptible to apoptosis under stress conditions, and that the *in vivo* conditions might not have been as stressful. These findings also raise questions about apoptotic pathways that lead to cell death in the absence of iASPP. In the previous chapter, weakened cell-cell adhesion upon iASPP loss was shown. Whether these cells also die as a result of weakened cell-matrix adhesion and subsequent detachment remains to be determined. All together, these results suggest that iASPP$^{\Delta 8/\Delta 8}$ keratinocytes are more migratory than iASPP$^{+/+}$ keratinocytes. Increased intercellular spaces at the leading edge of the epithelial sheet (Figure 4.3B) and weakened cell-cell adhesion (Figure 3.11) associating with a loss of iASPP suggests that delayed wound healing in iASPP$^{\Delta 8/\Delta 8}$ mice is probably due to inefficient migration of keratinocytes.

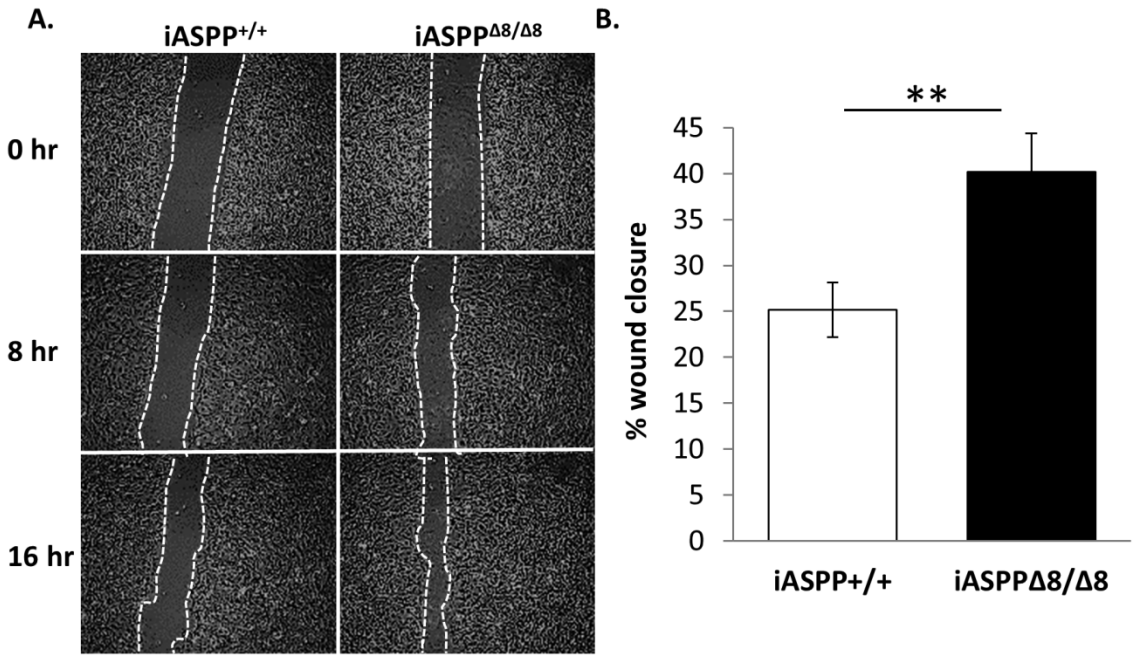

Figure 4.6 In vitro keratinocyte migration is enhanced upon iASPP excision

A. Primary keratinocytes isolated from newborn iASPP CreER mice were grown with or without 1 µM 4-OHT for 4 days to induce the deletion of iASPP. Upon reaching confluence, the cells were subjected to *in vitro* wound scratch. *In vitro* cell migration and wound closure were assessed by measuring how far the layer of cells migrated into the scratch every 20 minutes at 8 different wound areas. Representative images at 0, 8, or 16 hours post wound scratching are shown. Dashed lines indicate wound edges. **B.** Quantification of the average percentage of wound area closed in iASPP$^{+/+}$ or 4OHT-induced iASPP$^{\Delta 8/\Delta 8}$keratinocytes within 8 hours of wound closure is shown. Statistical analysis was done using a Mann-Whitney's U test, p<0.001.

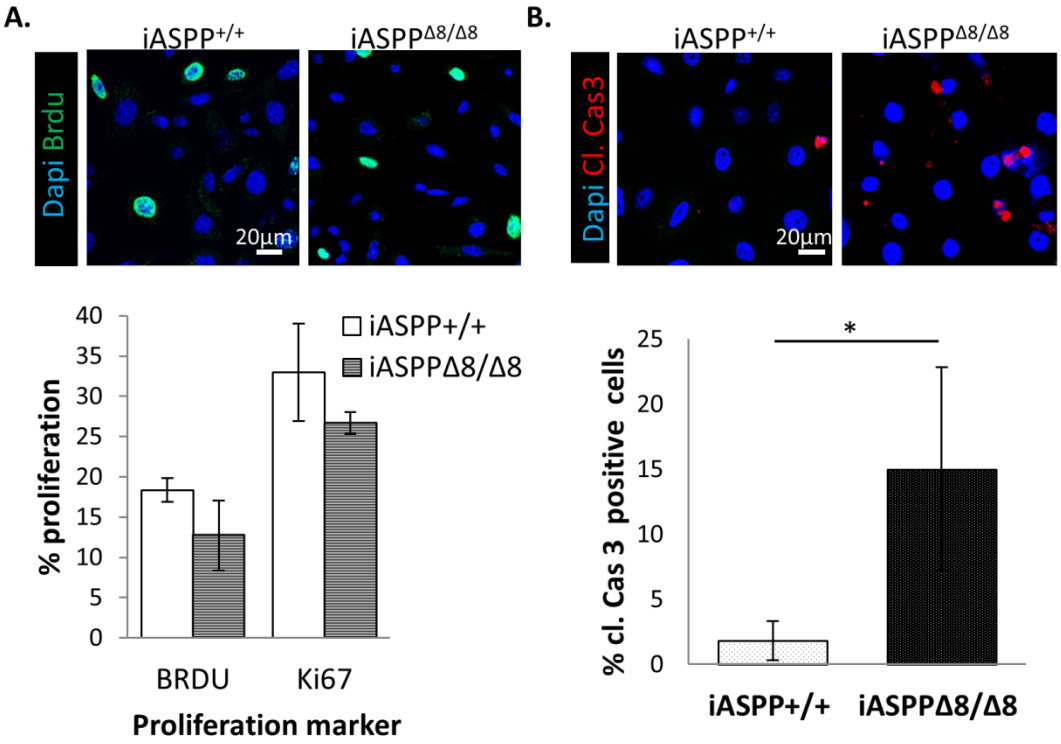

Figure 4.7 Loss of iASPP results in unaltered cell proliferation and enhanced apoptosis
A. Cell proliferation is modestly reduced in iASPP$^{\Delta 8/\Delta 8}$ cells. Lower panel is a graphical representation showing quantification of the percentage of cells that have incorporated BrdU or are positive for the Ki67 proliferation marker. **B**. Cell death is increased in iASPP$^{\Delta 8/\Delta 8}$ cells. Dying cells were identified via immunostaining for cleaved caspase 3, and quantification of the percentage of cells that are positive for cleaved caspase 3 is represented in the graph. Statistical analysis was done using the *t*-test, p=0.04. Error bars denote ± 2SEM in all graphical representations.

4.2.5 Loss of iASPP enhances disorganised cell migration *in vitro*

The components of motility behaviour that are affected by iASPP were further investigated. Live-cell imaging and tracking of individual iASPP$^{+/+}$ and iASPP$^{\Delta 8/\Delta 8}$ keratinocytes within a cell cluster was carried out. Briefly, keratinocytes were grown in growth-factor rich conditions to encourage the formation of cell contacts and therefore cell clusters (Figure 4.8A). To exclude the effect of proliferation on the migratory behaviour of the cells, proliferation was blocked by the addition of mitomycin C to the cell media. Analysis of individual cell motility paths showed that iASPP$^{\Delta 8/\Delta 8}$ keratinocytes moved in random directions without attempting to remain within the cell cluster (Figure 4.8C). Conversely, iASPP$^{+/+}$ keratinocyte movement was more directional and cells maintained contacts. The average distance travelled by iASPP$^{\Delta 8/\Delta 8}$ keratinocytes was over three-fold greater compared to iASPP$^{+/+}$ keratinocytes (Figure 4.8B; *t*-test, p=0.001). Thus, these data suggest that iASPP plays a role in controlling the directionality of keratinocyte migration by facilitating the cohesion between cells. Given the role of iASPP in maintaining the integrity of junctions reported previously (chapter III), and the more disorganised motility of keratinocytes in the absence of iASPP, it is likely that the wound closure defect in iASPP$^{\Delta 8/\Delta 8}$ mice is due to the disorganised migration of keratinocytes that might cause them to detach and die, thus disrupting the collective epithelial sheet migration.

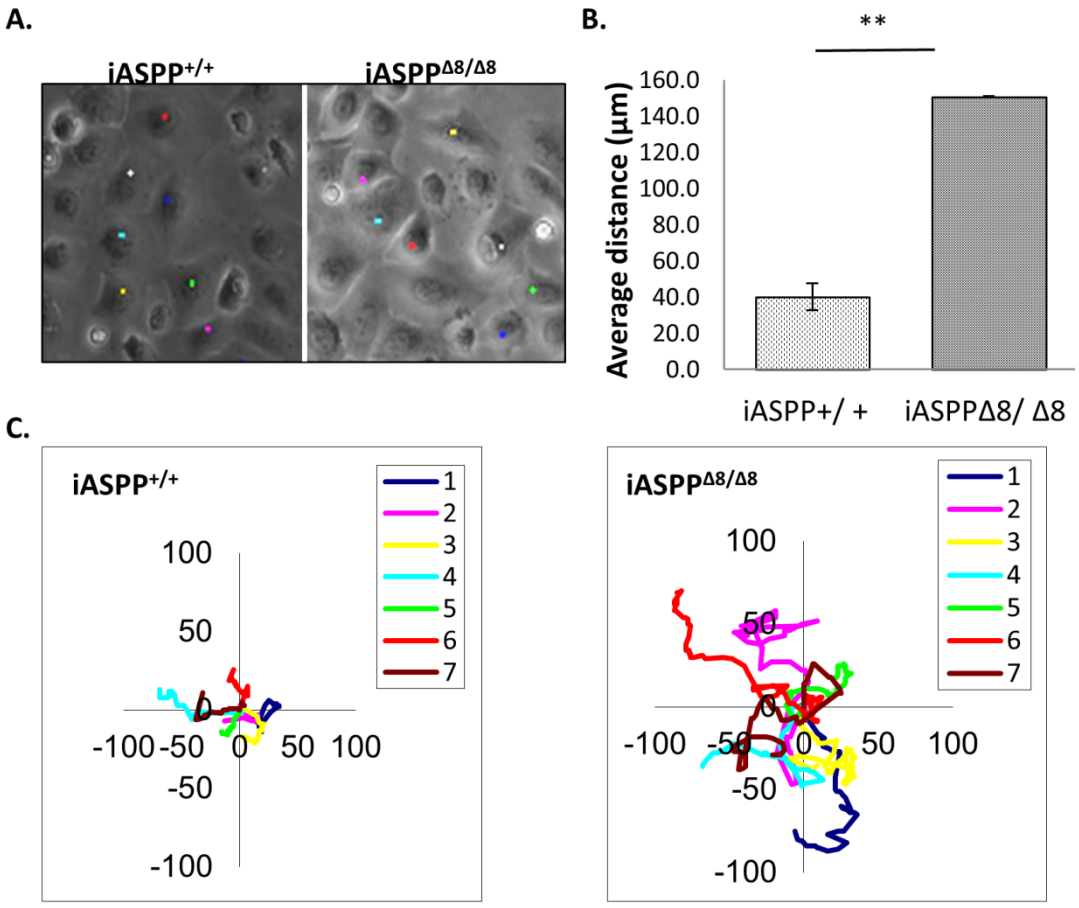

Figure 4.8 iASPP regulates the motile behaviour of murine primary keratinocytes
A. Representative image of cells whose motile behaviour was examined. Keratinocytes isolated from newborn iASPP CreER mice were grown for 4 days with or without 1 µM 4-OHT to induce the deletion of iASPP. Subsequently, the motility of individual cells within a cell cluster was tracked to examine their motile behaviour and tendency to remain in the cluster. **B.** Graph showing average distance (µm) travelled by iASPP$^{+/+}$ or 4OHT-induced iASPP$^{\Delta 8/\Delta 8}$ cells. Significance was assessed using a *t*-test (p=0.001). Error bars represent ± 2SEM. **C.** Representative migratory tracks showing the motile behaviour of selected cells.

4.2.6 Loss of iASPP results in an altered expression pattern of desmosome components

Wound closure depends on the ability of cells to proliferate and collectively migrate over the wound bed. This coordinated collective cell migration is mediated by the maintenance of cell-cell adhesions. Given the observed disorganised migration of iASPP$^{\Delta 8/\Delta 8}$ keratinocytes *in vitro*, whether or not the expression of desmosome components is altered in the absence of iASPP was determined. Day 2 and day 6 wound sections from iASPP$^{+/+}$ and iASPP$^{\Delta 8/\Delta 8}$ mice were immunostained for the expression of desmoglein 1 and 2, using an antibody that detects both proteins simultaneously. Immunostaining for desmoglein 1 and 2 should detect desmosomes throughout the wounded epidermis, as desmoglein 1 is expressed in the suprabasal layer while desmoglein 2 is expressed in the basal layers (Garrod and Chidgey, 2008). To mark basal cells, wound sections were also immunostained for p63. The results for iASPP$^{+/+}$ mice were consistent with the published literature (Beaudry *et al.*, 2010; Garrod *et al.*, 2005). Namely, wound sections from iASPP$^{+/+}$ mice showed dynamic expression of desmogleins. Junctional expression of desmogleins in cells at the wound edge and in the basal layer was attenuated when compared to cells further away from the wound and in the upper epidermal layers (Figure 4.9, left panels and Figure 4.10, upper panels, green staining). A similar pattern of desmoglein 1 and 2 expression was observed in wound sections from iASPP$^{\Delta 8/\Delta 8}$ mice. However, it was noted that downregulation of desmogleins at the wound edge was more pronounced in iASPP$^{\Delta 8/\Delta 8}$ sections in comparison to iASPP$^{+/+}$ sections (Figure 4.9, right panels, white arrowheads). In these sections, a number of p63-expressing cells appeared to have lost desmoglein expression and detached from the leading edge of the wound (Figure 4.9, white arrowheads). Furthermore, in day 6 iASPP$^{\Delta 8/\Delta 8}$ wound sections, a clear disruption of cell-cell adhesions could be observed that was rarely seen in iASPP$^{+/+}$ control sections (Figure 4.10, lower rightmost panel, green staining). Additionally, p63 cells appeared sparser in iASPP$^{\Delta 8/\Delta 8}$

day 2 and day 6 wounds relative to iASPP$^{+/+}$ wounds. This is in keeping with previous reports in our laboratory showing that iASPP regulates p63 expression (Chikh *et al.*, 2011; Notari *et al.*, 2011). Previous studies have also shown that p63 regulates the expression of desmoglein 1 and 2 (Romano *et al.*, 2012). Whether, iASPP influences desmoglein expression through p63, or via its direct effect on desmoplakin phosphorylation, remains to be determined. Overall, these results suggest that cell-cell adhesions are weakened in wounds from iASPP$^{\Delta 8/\Delta 8}$ mice. The observed downregulation of desmogleins and the increased sparsity of p63 cells and their uncoupling from the leading edge could have important implications for the cohesive migration of the cell sheet during the re-epithelisation process, potentially delaying the wound healing process.

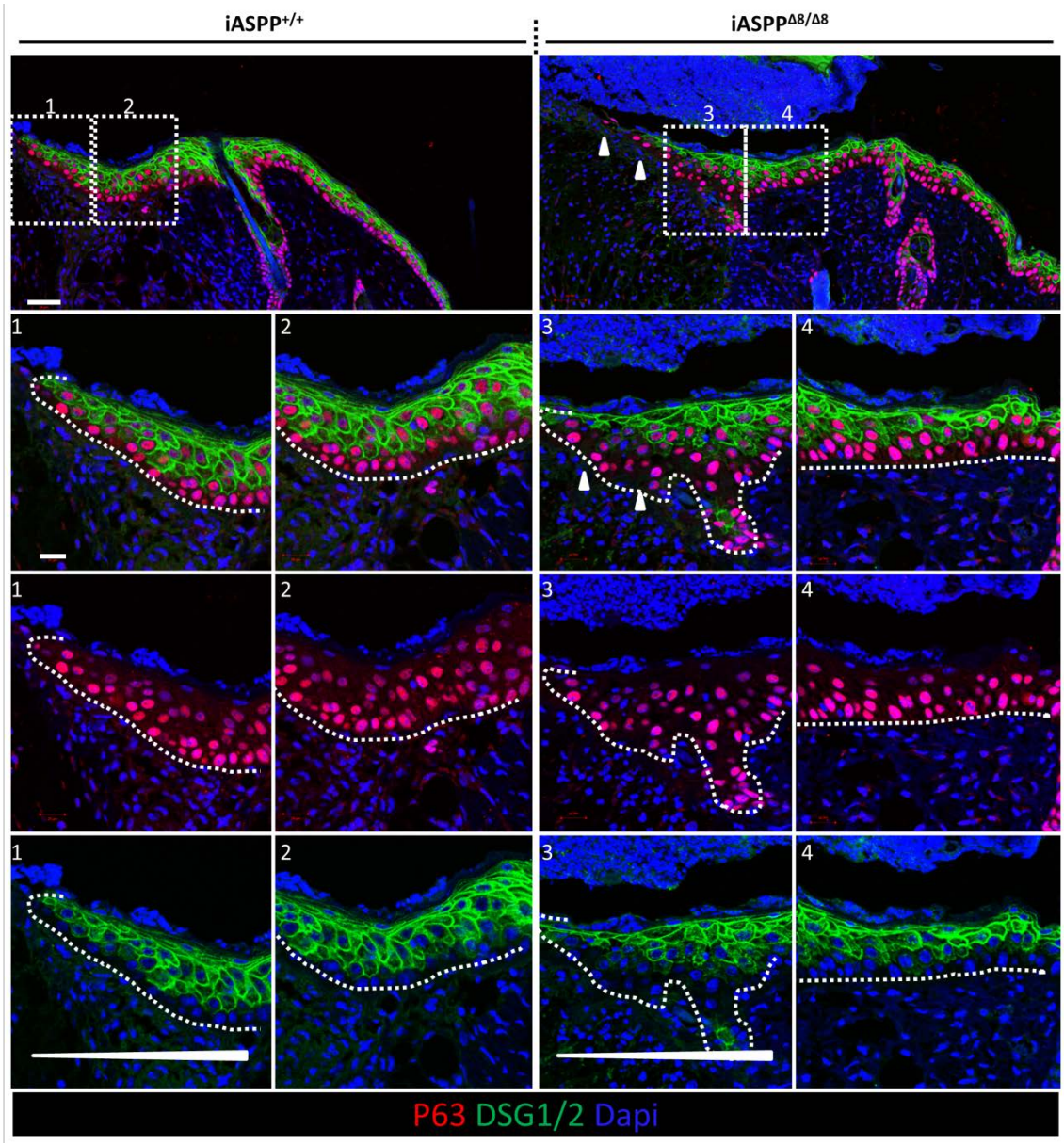

Figure 4.9 Loss of iASPP results in attenuated desmoglein expression at the wound edge
Immunoflorescence staining for p63 (red), desmoglein 1/2 (DSG, green) in day 2 wound sections from iASPP$^{+/+}$ and iASPP$^{\Delta 8/\Delta 8}$ mice. Regions in the numbered square boxes in the top panels are shown enlarged in the bottom panels. Small arrowheads indicate p63-expressing cells that have lost contact with the desmoglein-expressing cells above them. Dashed lines represent epidermal-dermal junction. Scale bars are 50 µm for the top panel images, and 20 µm for all other images.

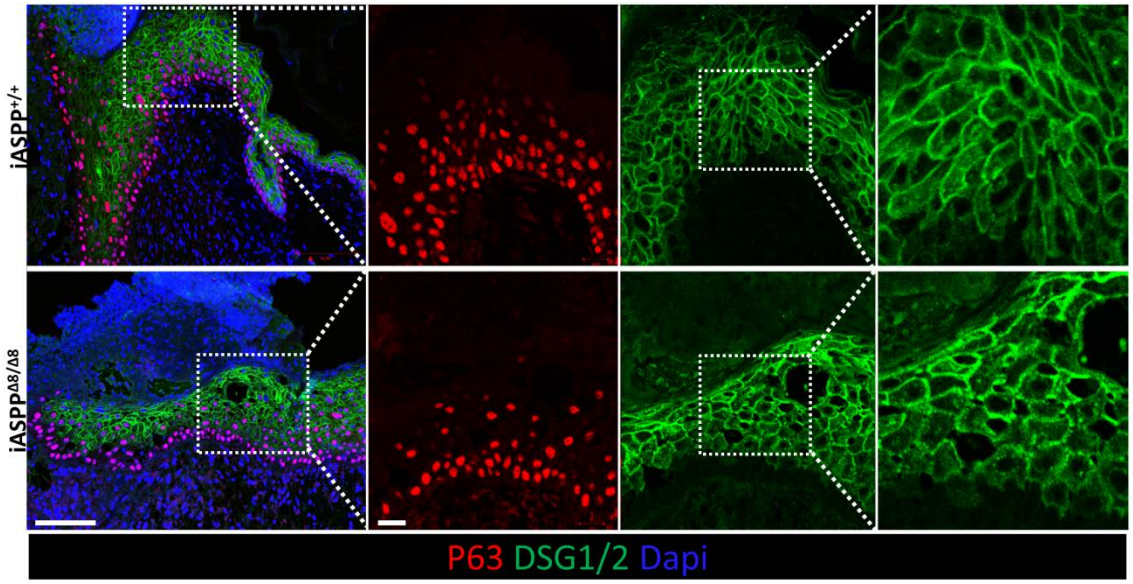

Figure 4.10 Loss of iASPP results in disrupted cell-cell adhesions
Immunofluorescence analysis of desmoglein 1/2 (green) and p63 (red) expression in day 6 wound sections from iASPP$^{+/+}$ and iASPP$^{\Delta 8/\Delta 8}$ mice. p63-positive cells appear sparser in iASPP$^{\Delta 8/\Delta 8}$ wounds relative to iASPP$^{+/+}$ wounds. Desmoglein staining shows disrupted cell-cell adhesions and tissue integrity in iASPP$^{\Delta 8/\Delta 8}$ wounded epidermis.

4.2.7 Loss of one copy of p63 does not alter the wound healing phenotype in iASPP-deficient mice

Given previous reports showing that iASPP regulates the proliferative potential of p63, and the supporting observations presented herein, whether iASPP's regulation of the wound healing process is p63 dependent was examined. As ablation of both copies of p63 results in lethality, whether the loss of one copy of p63 could alter the wound healing phenotype observed in iASPP$^{\Delta 8/\Delta 8}$ mice was tested. Therefore, three mice of each genotype (iASPP$^{+/+}$;p63$^{+/+}$, iASPP$^{+/+}$;p63$^{+/-}$, iASPP$^{\Delta 8/\Delta 8}$;p63$^{+/+}$and iASPP$^{\Delta 8/\Delta 8}$;p63$^{+/-}$) were subjected to the wound healing procedure described earlier and the progression of wound closure monitored. Interestingly, the results obtained from this study confirmed that wound healing was delayed in iASPP$^{\Delta 8/\Delta 8}$ mice compared to iASPP$^{+/+}$ controls (Figure 4.11). However, the wound healing phenotype in iASPP$^{\Delta 8/\Delta 8}$ mice was not exacerbated when a copy of the *p63* gene was deleted. Wound closure in p63 heterozygous mice was comparable to that of mice wild type for both iASPP and p63. These results show that the delay in wound healing in iASPP$^{\Delta 8/\Delta 8}$ mice is reproducible, but that the deletion of one copy of p63 is not sufficient to affect the progression of wound healing in these mice. Germline deletion of TAp63 has previously been reported to result in delayed wound healing (Su *et al.*, 2009). However, this study did not report whether the deletion of one copy of TAp63 impairs the wound healing process. The delay in wound healing in TAp63-deficient mice has been attributed to an exhaustion of stem/progenitor cells. As iASPP is known to regulate the proliferative potential of p63, it is likely that the stem cell pool is not properly maintained in iASPP$^{\Delta 8/\Delta 8}$ mice. Induction of repeated wounds could help address this in future experiments.

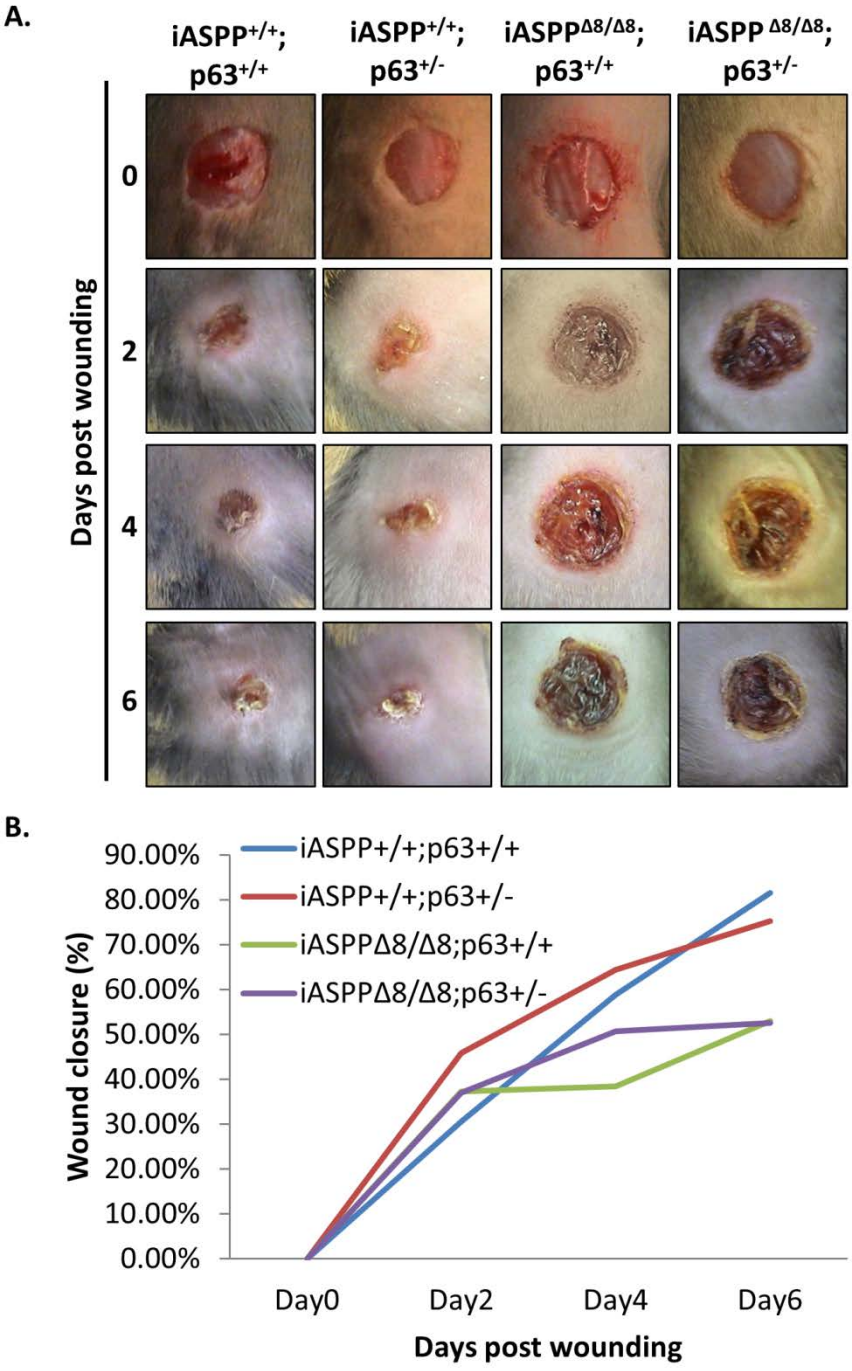

Figure 4.11 Loss of one copy of p63 does not alter wound healing in iASPP-deficient mice
A. Representative images of wound healing progress in iASPP$^{+/+}$;p63$^{+/+}$, iASPP$^{+/+}$;p63$^{+/-}$, iASPP$^{\Delta8/\Delta8}$;p63$^{+/+}$ and iASPP$^{\Delta8/\Delta8}$;p63$^{+/-}$mice. **B.** Graphical representation showing the average percentage of wound area closed in these mice. Three mice of each genotype were included at each time point.

4.3 Summary and brief discussion

In the previous chapter, it was reported that iASPP is a regulator of desmosomes and their adhesiveness. This chapter shows, for the first time, that iASPP is important for proper wound closure by demonstrating that iASPP$^{\Delta 8/\Delta 8}$ mice have delayed wound healing. This delay is not due to a defect in proliferation or apoptosis, but rather due to changes in the migratory behaviour of keratinocytes: iASPP$^{\Delta 8/\Delta 8}$ cells migrate faster and in a disorganised manner. Therefore, impeded wound healing in iASPP$^{\Delta 8/\Delta 8}$ mice is, at least in part, due to an inability of the epithelial sheet to migrate efficiently and cohesively over the wound site. Consistent with this, in addition to enhanced disorganised motility of iASPP$^{\Delta 8/\Delta 8}$ cells *in vitro*, increased intercellular spaces in the advancing epithelial sheets at the wound rim in iASPP$^{\Delta 8/\Delta 8}$ mice were observed, suggestive of weakened intercellular adhesions.

Remarkably, a notable similarity has been found between mice lacking iASPP and mice lacking Perp. Deficiency in either iASPP or Perp results in delayed wound healing *in vivo* with no differences in proliferation or apoptosis. Moreover, iASPP$^{\Delta 8/\Delta 8}$ cells, just like cells lacking Perp, display enhanced disorganised cell motility (Beaudry *et al.*, 2010). These results further support the notion that iASPP, like Perp, is a regulator of desmosomes. In contrast to the *in vivo* data, enhanced apoptosis was observed *in vitro* in iASPP$^{\Delta 8/\Delta 8}$ keratinocytes relative to control iASPP$^{+/+}$ keratinocytes. The discrepancy between the *in vivo* and *in vitro* apoptosis data presented here could be explained by the fact that the *in vitro* apoptosis study was done under stress conditions, while the *in vivo* assay was done under basal (non-stress) conditions. The phenotypes observed in iASPP$^{\Delta 8/\Delta 8}$ mice and cells are in keeping with previous studies showing that a loss of desmosome components such as desmoplakin, plakoglobin, plakophilin 1 and 3 results in enhanced cell migration and unaltered cell proliferation (Setzer *et al.*, 2004; South *et al.*, 2003; Yin *et al.*, 2005b).

The studies presented in this chapter querying the role of iASPP in wound healing have implications for other morphological and pathological conditions. This is because the cellular processes taking place during wound healing (e.g. migration and the dynamic regulation of cell-cell adhesions) are reminiscent of the developmental and tumourigenic process of epithelial-mesenchymal transition (EMT). Accordingly, Slug, a zinc finger transcriptional repressor, known for its role in triggering EMT and contributing towards tumour invasiveness (Shih and Yang, 2011), is also important for wound closure (Savagner *et al.*, 2005). During wound healing, Slug is thought to regulate desmosome dissociation and the subsequent induction of keratinocyte migration, facilitating the movement of the epithelial sheet over the wound site (Savagner *et al.*, 2005; Savagner *et al.*, 1997). Therefore, investigation into the regulation and regulators of desmosomes during wound healing may help further elucidate pathways involved in tumour progression and development.

Interestingly, iASPP is overexpressed in many cancers, including squamous cell carcinoma of the cervix and the head and neck. Its elevated expression is associated with tumour invasiveness and poor clinical outcome (Cao *et al.*, 2013; Liu *et al.*, 2012). Intriguingly, both Liu *et al.*and Cao *et al.*reported that increased nuclear iASPP in patients' tumour samples was associated with worse prognosis. Hence, in future studies, it would be interesting to explore whether a loss of iASPP from cell-cell junctions and its gain in the nucleus contributes to tumour progression and invasiveness.

Taken together, the studies presented here show, for the first time, that iASPP regulates wound closure. iASPP appears to execute this role by participating in the regulation of cell-cell adhesion, which enables efficient cell migration during wound healing. In addition, this study

supports previous reports highlighting the need for precise spatiotemporal regulation of desmosome adhesion during wound healing.

Chapter V: iASPP regulates developmental eyelid epithelial sheet extension

Chapter V: iASPP regulates developmental eyelid epithelial sheet extension

5.1 Introduction

Common to all mammals is the formation of eyelids and their developmental fusion and subsequent disjunction. Some mammals, like mice, are born with their eyelids closed while other mammals, like humans, are born with their eyelids open. Whether a particular mammalian species exhibits eyelids open or closed at birth is dependent on the developmental stage of ocular structures at the time of birth (Findlater *et al.*, 1993). Transient developmental eyelid closure is thought to shield the morphologically and functionally maturing ocular structures from premature exposure to environmental stresses and toxins (Harris and McLeod, 1982). Once structures like the cornea and retina reach functional maturity, eyelid disjunction occurs. In humans, eyelid formation starts at about 6 weeks of gestational development with eyelid fusion occurring within the subsequent 3 weeks. The eyelids remain fused until the 20th week of gestational development (Byun *et al.*, 2011; Pearson, 1980). In mice, eyelid development follows a similar developmental pattern, except that mice are born with fused eyelids. Embryonic eyelid formation, fusion and reopening in mice has been characterised in great detail.

In mice, eyelid development starts at E11.5 with the appearance of eyelid buds consisting of loose periocular mesenchyme covered by undifferentiated ectoderm. This is followed by further growth of the eyelid buds, which results from the proliferation of epithelial and mesenchymal cells and leads to the formation of recognisable eyelid structures by E14.5. At E14.5, the epithelial cells at the leading edges of the apposed eyelids start to migrate across the cornea until they ultimately meet and fuse at about E16.5. Following this fusion, mesenchymal cells of the dermis also extend towards the fusion junction. The eyelids remain

fused with help from desmosome cell-cell adhesions until postpartum day 12 (Teraishi and Yoshioka, 2001). Apoptosis and desquamation of cells at the fusion junction are thought to lead to separation of the eyelids at postnatal day 12 (Findlater *et al.*, 1993; Mine *et al.*, 2005; Teraishi and Yoshioka, 2001).

During eyelid closure, the epithelium overlying the dermis differentiates into the palpebral epidermis (the epithelium on the outer eyelid surface) and conjunctival epidermis (the epithelium on the inner eyelid surface). After the eyelids fuse, the palpebral epidermis undergoes differentiation, stratification and keratinisation as part of the skin. Differentiation of eyelid epithelial cells and their subsequent desquamation is thought to facilitate the separation of the opposing eyelids. The formation of the eyelash hair follicles at the eyelid rims also occurs at this stage. The conjunctival epithelium, on the other hand, never keratinises and only stratifies after separation of the eyelids. This epithelium hosts goblet cells and Meibomian glands, which help to lubricate the eyes (Findlater *et al.*, 1993; Huang *et al.*, 2009).

Defects in eyelid growth and fusion lead to the open-eyelids at birth phenotype in mice, which can cause a variety of ocular pathologies including corneal inflammation and blindness (Li *et al.*, 2003; Weng *et al.*, 2008). The Mouse Genome Informatics (MGI) website lists 77 genes associated with open-eyelids at birth (http://www.informatics.jax.org/ (Blake *et al.*, 2014)). The loss or overexpression of these genes in mouse models is thought to disrupt cellular processes such as proliferation, differentiation, apoptosis, cell-cell adhesion and cell motility, resulting in the open-eyelids at birth phenotype (Chidgey *et al.*, 2001; Jin *et al.*, 2008; Sharov *et al.*, 2003; Tao *et al.*, 2005).

Chapter III of this thesis outlined gross developmental abnormalities that result from iASPP deficiency in mouse models. These abnormalities included eye defects. Such eye defects have

also been described in Wa3 mice, which carry a spontaneous mutation in the *iASPP* gene, and they are thought to be secondary to the open-eyelids at birth phenotype that these mice present with (Herron *et al.*, 2005). iASPP has a wide range of functions. It participates in p53-mediated apoptosis and p63-mediated epithelial stratification. Moreover, previous chapters have shown that iASPP regulates desmosome adhesion and cell motility (Bergamaschi *et al.*, 2003; Notari *et al.*, 2011). Therefore, the biological processes that are compromised in eyelid development as a result of iASPP deficiency remain to be elucidated. Furthermore, whether the open-eyelids at birth phenotype results from premature eyelid opening or a failure of eyelid extension and fusion needs to be determined. The work presented in this chapter aims to investigate the biological function of iASPP during eyelid development, focusing on whether defects in cellular processes such as proliferation, apoptosis, cell migration and cell-cell adhesion contribute to the open-eyelids at birth phenotype. Moreover, whether or not genetic interactions of iASPP with p63 and p53 contribute to eyelid development is investigated.

5.2 Results

5.2.1 Impaired eyelid epithelial sheet extension in iASPP-deficient embryos

To specify the role of iASPP in eyelid closure, mice with ubiquitous germline deletion of iASPP were used, as described in chapter III (Notari *et al.*, 2011). Histological examination of the developing eyelids in $iASPP^{+/+}$ and $iASPP^{\Delta 8/\Delta 8}$ embryos at various embryonic stages (E14.5, E15.5 and E16.5) was performed. At E14.5, no gross abnormalities in the eyelid morphology were observed in $iASPP^{\Delta 8/\Delta 8}$ embryos compared to $iASPP^{+/+}$ embryos, suggesting that iASPP does not play a role in the initial stages of eyelid development (Figure 5.1A). However, at E15.5, the progression of the eyelid epithelial sheet towards the centre of the cornea was delayed in $iASPP^{\Delta 8/\Delta 8}$ embryos (Figure 5.1A). By E16.5, the eyelid epithelial sheets fused in $iASPP^{+/+}$ embryos, while in $iASPP^{\Delta 8/\Delta 8}$ embryos they extended only slightly or not at all, and often no

leading edge was observed (Figure 5.1A). These results suggest that the extension of the eyelid epithelial sheets is impaired in iASPP$^{\Delta 8/\Delta 8}$ mice, and that the open-eyelids at birth phenotype results from a failure of eyelid extension, rather than premature eyelid opening. This is further supported by the lack of eyelid closure in E18.5 and P1 iASPP$^{\Delta 8/\Delta 8}$ mice (Figure 5.1B). The eyes of adult iASPP$^{\Delta 8/\Delta 8}$ mice are often small and opaque. Histological examination revealed neovascularisation of the corneal stroma and thickening of the corneal epithelium in iASPP$^{\Delta 8/\Delta 8}$ mice shortly after birth (Figure 5.2). Given that no defects were observed in the posterior segments of the eye, like the retina, it was postulated that defects in the cornea are secondary to the open-eyelids at birth phenotype.

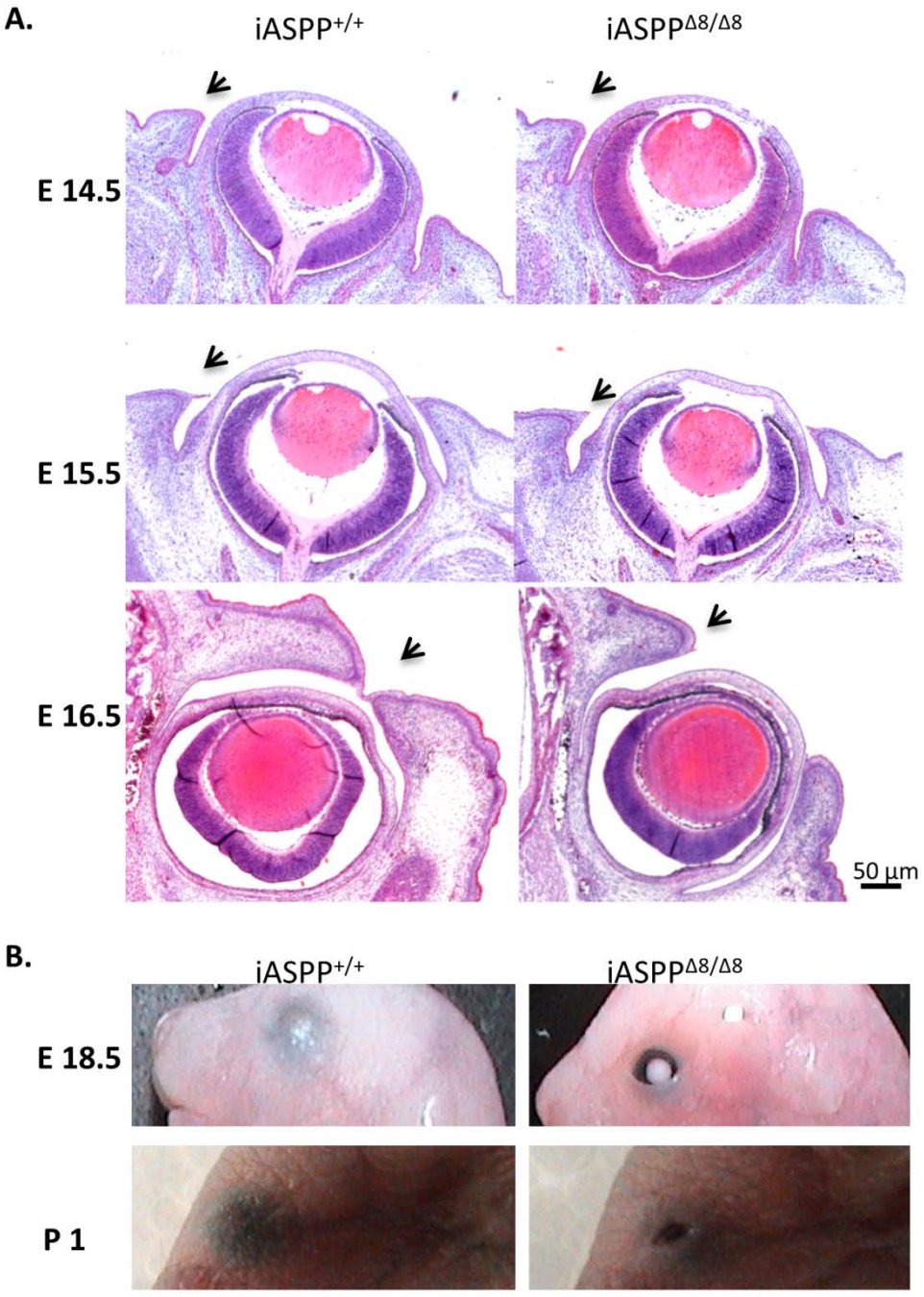

Figure 5.1 iASPP deficiency leads to impaired eyelid closure
A. Histological analysis (H&E staining) of eyelid sections from iASPP$^{+/+}$ and iASPP$^{\Delta 8/\Delta 8}$ embryos at E14.5, E15.5 and E16.5. The arrows point to the tips of the eyelid. **B.** Lack of eyelid closure in iASPP$^{+/+}$ and iASPP$^{\Delta 8/\Delta 8}$ mice at E18.5 and postnatal day P1.

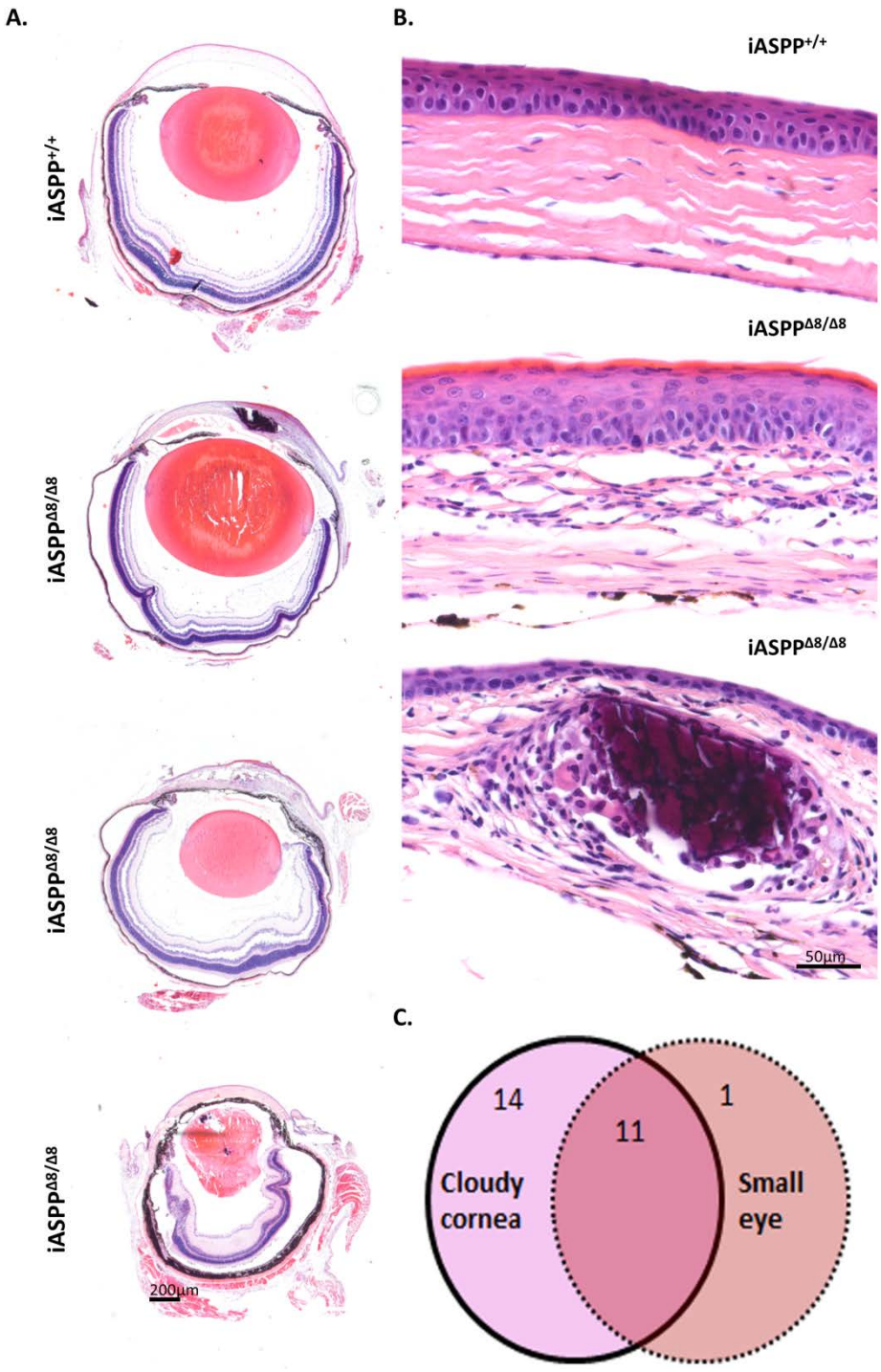

Figure 5.2 iASPP$^{\Delta 8/\Delta 8}$ mice present with a variety of ocular pathologies
A. Adult iASPP$^{\Delta 8/\Delta 8}$ mice present with cloudy corneas and often one small eye. iASPP$^{\Delta 8/\Delta 8}$ mice with the small eye phenotype display lens degradation. **B.** Representative histological sections of corneas from adult iASPP$^{+/+}$ and iASPP$^{\Delta 8/\Delta 8}$ mice. Thickening of the cornea and neovascularisation can be observed in iASPP$^{\Delta 8/\Delta 8}$mice. **C.** Number of iASPP$^{\Delta 8/\Delta 8}$mice exhibiting the indicated eye pathologies. 11 out of 26 mice had both the small eye and cloudy cornea phenotypes, while only 14 mice had the cloudy cornea phenotype. One mouse exhibited the small eye phenotype only.

5.2.2 iASPP is expressed in the eyelid epithelium

To determine the role of iASPP in eyelid development, its expression pattern in the developing eyelid was determined using immunofluorescence. At E14.5, iASPP was expressed at the surface ectoderm of the eyelid (Figure 5.3). Interestingly, iASPP staining was slightly more intense in the keratinocytes at the tip of eyelid epithelium, which are responsible for the formation of the leading edge. At E15.5, as the eyelid epithelial sheet migrated towards the centre of the cornea, iASPP expression was broadly distributed and abundant in the leading edge cells (Figure 5.3), indicating iASPP's role in leading edge extension during eyelid closure. At E16.5, when the opposing eyelid epithelia fused, iASPP expression was uniform in the surface ectoderm of the eyelid epithelia (Figure 5.3). iASPP appeared to have very limited expression in the mesenchyme underlying the eyelid epithelia. The expression pattern suggests that iASPP is involved in the extension of the eyelid epithelia, rather than the growth and migration of the underlying mesenchyme.

To show which eyelid epithelia cell types express iASPP, co-staining was performed for iASPP and various epithelial markers: K14, K1 and K6. K14, K1 and K6 are well-known markers for basal proliferative cells, suprabasal differentiated cells and leading edge migratory cells, respectively (Fuchs, 1990, 1996; Mazzalupo and Coulombe, 2001). The majority of iASPP positive cells in the eyelid epithelia were also positive for K14, K1 and K6 (Figure 5.4). These results confirm the role of iASPP in eyelid epithelia. Given that differentiation in eyelid epithelia proceeds after eyelid fusion (Findlater *et al.*, 1993), it is not surprising that the expression of iASPP is very broad and not confined to a particular cell type at the E15.5-16.5 developmental stage. Prominent co-expression of iASPP and K6 at the leading edge of the eyelid epithelia suggests that iASPP could be involved in the regulation of epithelial cell migration. In summary, iASPP expression is restricted to the eyelid epithelium. As no or very

limited iASPP expression was observed in the underlying mesenchyme, defects in eyelid epithelium specifically are likely to contribute to the open-eyelids at birth phenotype in iASPP$^{\Delta 8/\Delta 8}$ mice.

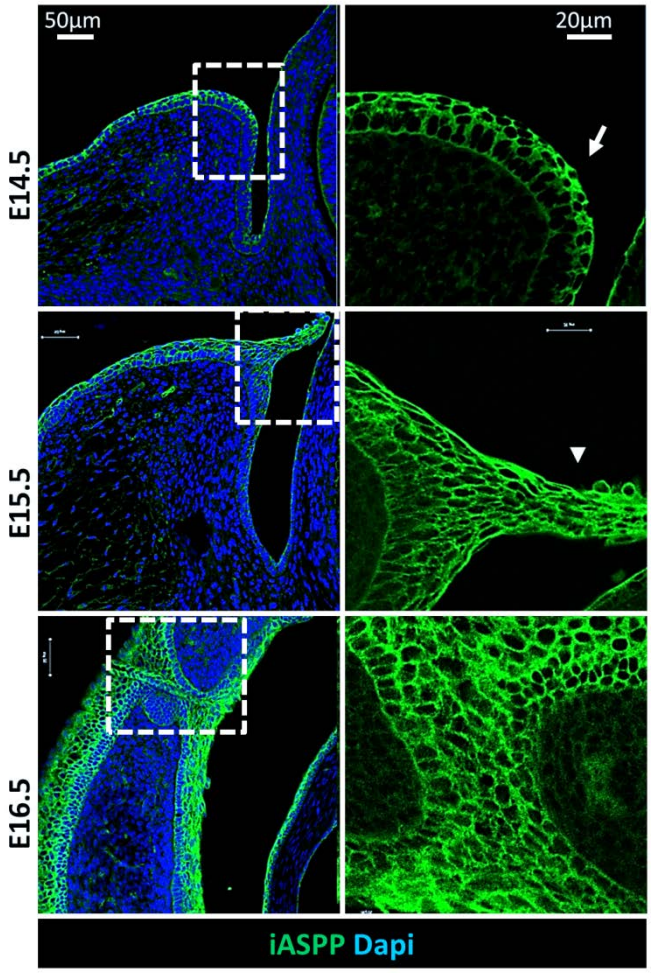

Figure 5.3 iASPP expression during eyelid development
Immunofluorescence analysis of iASPP expression in eyelids at E14.5, E15.5 and E16.5. Arrow points to the initiating leading edge at E14.5 where iASPP appears highly expressed. Arrowhead points to the advancing leading edge where iASPP is observed to have high expression. The white box represents the region that is enlarged and shown in the righthand panel.

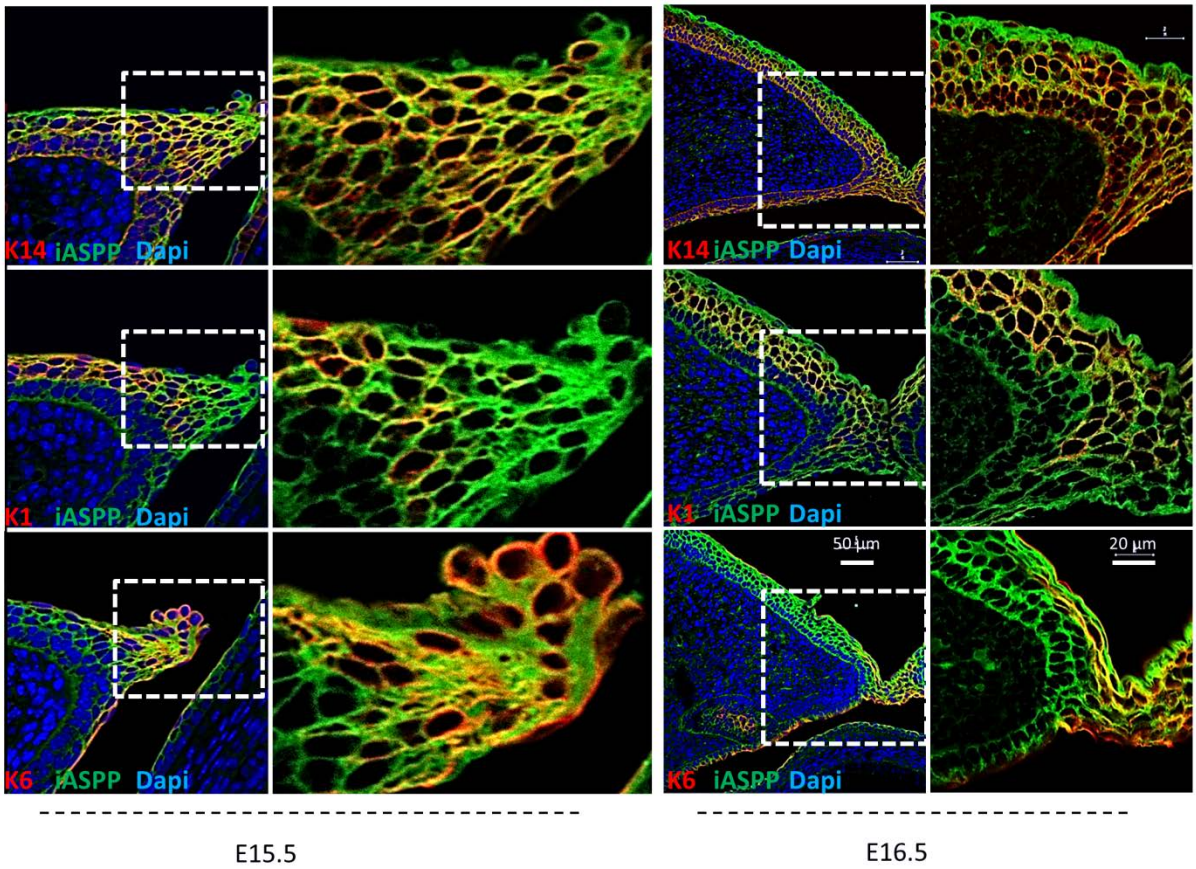

Figure 5.4 iASPP is robustly expressed in proliferating and migrating cells

Co-immunostaining for iASPP and various keratins (K14, K1 and K6) to determine which epithelial layers iASPP is expressed in at E15.5 and E16.5. The panels to the right of each image correspond to the magnification of boxed regions in the columns to the left. K14 is a marker for basal proliferating cells. K1 is a marker for differentiated suprabasal cells. K6 is a marker for migratory cells with proliferative potential.

5.2.3 Epithelial-specific deletion of iASPP leads to the open-eyelids at birth phenotype

The fact that the expression of iASPP was confined to the eyelid epithelia suggested that the role of iASPP is to control the extension of the eyelid epithelial sheets over the cornea. To confirm this, it was investigated whether or not epithelial-specific deletion of iASPP in mice would result in the open-eyelids at birth phenotype. Mice bearing *loxP*-flanked *iASPP* exon 8 were crossed with mice bearing K14-driven Cre to generate embryos in which iASPP was absent from epithelial organs. Eyelids from E16.5 K14-iASPP$^{+/+}$ and K14-iASPP$^{\Delta 8/\Delta 8}$ embryos were histologically examined. At E16.5, K14-iASPP$^{+/+}$ mice had closed eyelids while K14-iASPP$^{\Delta 8/\Delta 8}$ mice eyelids were open (Figure 5.5). The open-eyelids phenotype was not fully penetrant in K14-iASPP$^{\Delta 8/\Delta 8}$ and only 71% of embryos exhibited the phenotype. It is postulated that the decreased penetrance of the open-eyelids phenotype in K14-iASPP$^{\Delta 8/\Delta 8}$ embryos is due to the genetic background. K14-iASPP$^{\Delta 8/\Delta 8}$ mice were generated on a C57BL/6J background, while the iASPP$^{\Delta 8/\Delta 8}$ mice were generated on a mixed C57BL/6J and 129Sv background. Our group recently generated iASPP$^{\Delta 8/\Delta 8}$ mice on a C57BL/6J background, and the eye defects were not as penetrant and severe in these mice, supporting the idea that reduced penetrance of the open-eyelids phenotype was due to the genetic background (Miller, personal communication). Another possible explanation is that K14-Cre was not very efficient in deleting iASPP from all epithelial cells in the skin, and that the few remaining cells expressing iASPP could have facilitated eyelid closure in the 29% of K14-iASPP$^{\Delta 8/\Delta 8}$ mouse embryos that did not show the phenotype. In summary, the results presented so far indicate that the open-eyelids phenotype in iASPP$^{\Delta 8/\Delta 8}$ mice is due to a defect in the extension of the eyelid epithelial sheets.

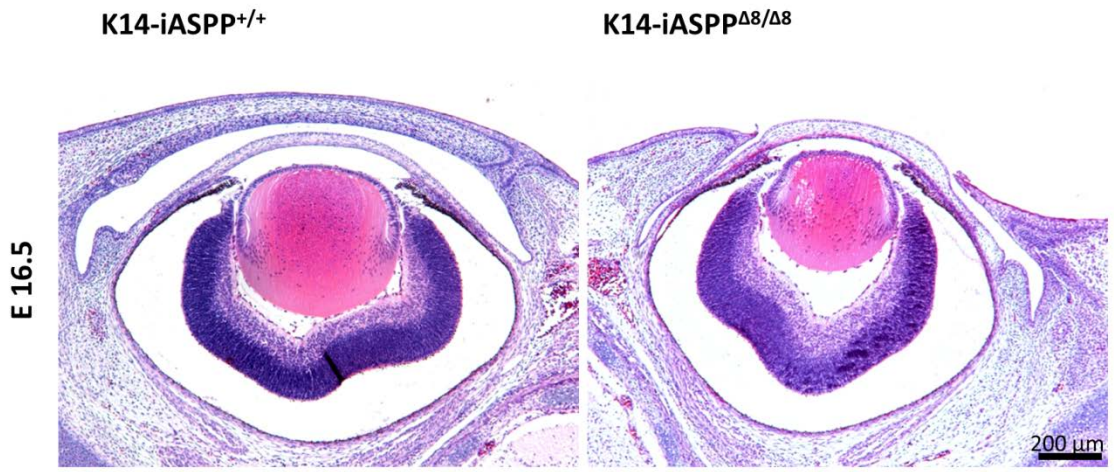

Genotype	Open-eyelid phenotype % (n)
K14-iASPP$^{+/+}$	0% (0/14)
K14-iASPP$^{\Delta 8/\Delta 8}$	71.4 % (10/14)

Figure 5.5 Epithelial-specific deletion of iASPP hinders eyelid extension
Histological examination of eyelids from E16.5 K14-iASPP$^{+/+}$and K14-iASPP$^{\Delta 8/\Delta 8}$ embryos reveals impaired eyelid extension in embryos lacking iASPP in the eyelid epithelia. The table presented as part of the image shows the number of K14-iASPP$^{\Delta 8/\Delta 8}$ embryos displaying the open-eyelids phenotype. The open-eyelids at birth phenotype is easily spotted, therefore, histological examination was performed on four embryos of each genotype only. The other 10 embryos were examined with the naked eye, and these 10 animals were part of the colony maintained in our laboratory by Kathryn Chung.

5.2.4 Loss of iASPP does not affect proliferation but leads to increased apoptosis in developing eyelids

To elucidate whether impaired eyelid closure in iASPP$^{\Delta 8/\Delta 8}$ embryos is due to altered cell proliferation, *in vivo* BrdU uptake was examined in iASPP$^{+/+}$ and iASPP$^{\Delta 8/\Delta 8}$ eyelids from E14.5 to E16.5 embryos. No significant difference in the percentage of cells that took up BrdU in iASPP$^{+/+}$ and iASPP$^{\Delta 8/\Delta 8}$ eyelids was observed at any embryonic stage (Figure 5.6A; *t*-test, E14.5 p=0.4, E15.5 p=0.7, E16.5 p=0.8), suggesting that iASPP is not involved in cell proliferation during eyelid closure. To verify that this was not due to cells entering the S phase and not progressing through other phases of the cell cycle, eyelid sections from E15.5 iASPP$^{+/+}$ and iASPP$^{\Delta 8/\Delta 8}$ embryos were stained for the proliferation marker Ki67. No difference in the percentage of cells positive for Ki67 was observed between iASPP$^{+/+}$ and iASPP$^{\Delta 8/\Delta 8}$ embryos (Figure 5.6B; *t*-test, p=0.4). This is in agreement with a recent paper by Heller and colleagues, which showed that eyelid closure between E15.5 and E16.5 is highly dependent on epithelial cell migration and not cell proliferation (Heller *et al.*, 2014).

To investigate whether increased apoptosis contributed to reduced eyelid extension in iASPP$^{\Delta 8/\Delta 8}$ embryos, TUNEL assays were performed on eyelid sections from iASPP$^{+/+}$ and iASPP$^{\Delta 8/\Delta 8}$ embryos at developmental stages E14.5 to E16.5. An increase in the percentage of TUNEL-positive cells was observed in eyelid sections from iASPP$^{\Delta 8/\Delta 8}$ embryos at E15.5 and E16.5, compared to iASPP$^{+/+}$ controls (Figure 5.7). The difference in apoptosis, however, did not reach statistical significance (Figure 5.7, *t*-test, E15.5 p=0.1, E16.5 p=0.1). This could be due to the small sample size, which included 5 embryos of each genotype at each developmental stage. Interestingly, the apoptotic cells in iASPP$^{\Delta 8/\Delta 8}$ eyelids at E15.5 and E16.5 were often observed within the leading edge, while apoptotic cells were rarely seen in this region in the eyelids of iASPP$^{+/+}$ embryos (Figure 5.7, white arrowheads). These results suggest that

increased apoptosis at the leading edge of the eyelid epithelial sheet is a contributing factor to defective eyelid closure in iASPP$^{\Delta 8/\Delta 8}$ embryos. These results were further confirmed by staining iASPP$^{+/+}$ and iASPP$^{\Delta 8/\Delta 8}$ E15.5 eyelid sections for the apoptotic marker cleaved caspase 3. A clear trend towards an increase in the percentage of apoptotic cells was observed in the eyelids of iASPP$^{\Delta 8/\Delta 8}$ embryos (Figure 5.8). Similar to the TUNEL assay data, apoptotic cells were seen at the leading edges of migrating epithelial sheets. The leading edge cells are thought to be the driving force for eyelid closure (Heller *et al.*, 2014), therefore, cell death at the leading edge could disrupt cell polarisation and cohesive movement across the cornea, leading the eyelids to be open at birth. However, the cause of cell death in the eyelids of iASPP$^{\Delta 8/\Delta 8}$ embryos warrants further investigation. Future experiments are needed to determine whether the elevated apoptosis in iASPP$^{\Delta 8/\Delta 8}$ embryos is p53-dependent. Additionally, studies are required to determine whether the death of cells at the migrating epithelial tip is due to a loss of cell-cell contacts or the inability of cells to withstand the shear forces.

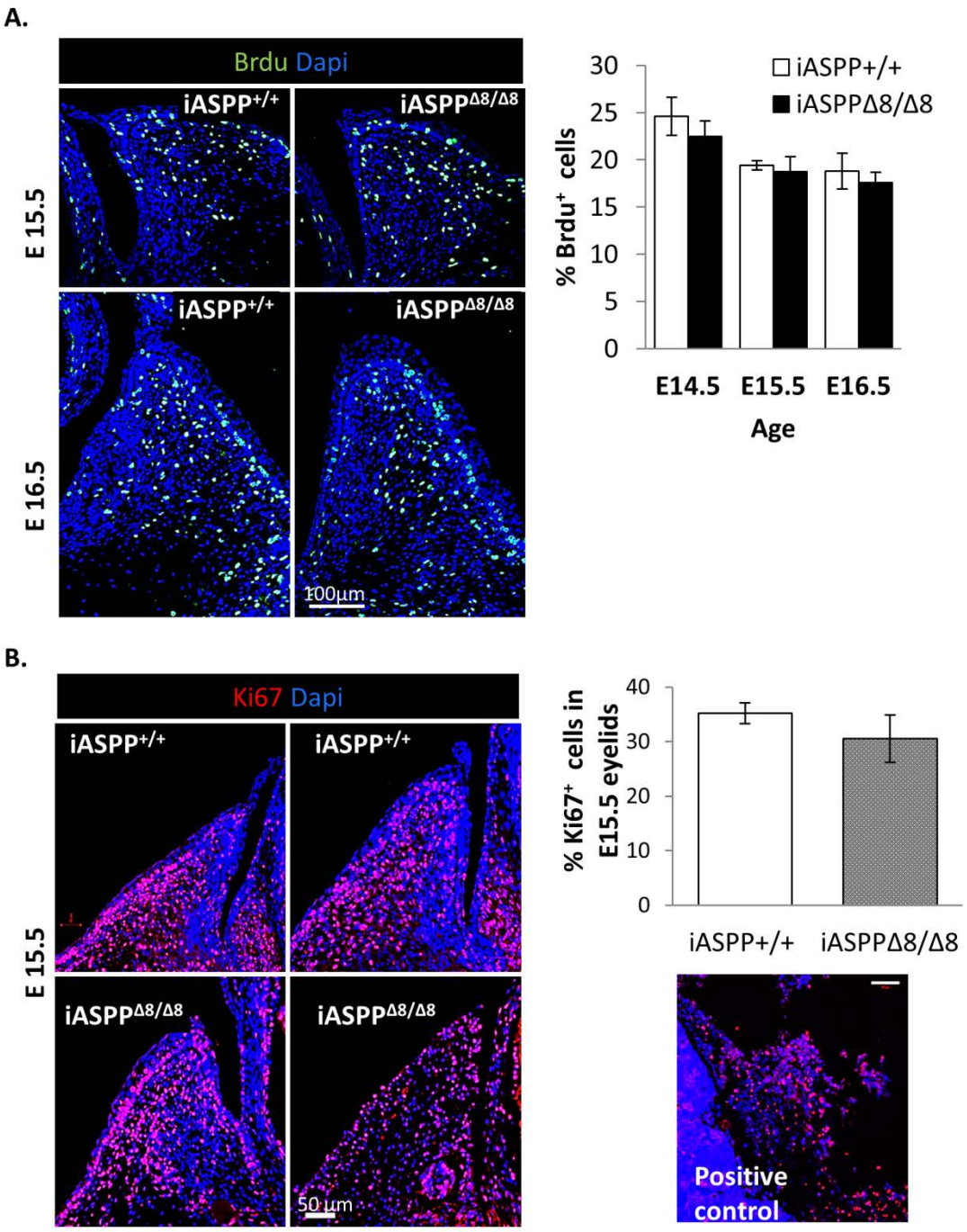

Figure 5.6 Cell proliferation is unaffected in the developing eyelids of iASPP$^{\Delta 8/\Delta 8}$ embryos
A. Immunofluorescence staining for incorporated BrdU in the eyelids of iASPP$^{+/+}$ and iASPP$^{\Delta 8/\Delta 8}$ embryos at E14.5, E15.5 and E16.5. Bar graphs show the percentage of the BrdU-positive cells in the eyelids of iASPP$^{+/+}$ and iASPP$^{\Delta 8/\Delta 8}$ embryos at different embryonic stages. Error bars represent ± SEM. **B.** Immunofluorescence staining for the proliferation marker Ki67 in E15.5 eyelids of iASPP$^{+/+}$ and iASPP$^{\Delta 8/\Delta 8}$ embryos. Bar graph shows quantification of the percentage of Ki67 cells in the eyelids of iASPP$^{+/+}$ and iASPP$^{\Delta 8/\Delta 8}$ mice at E15.5.

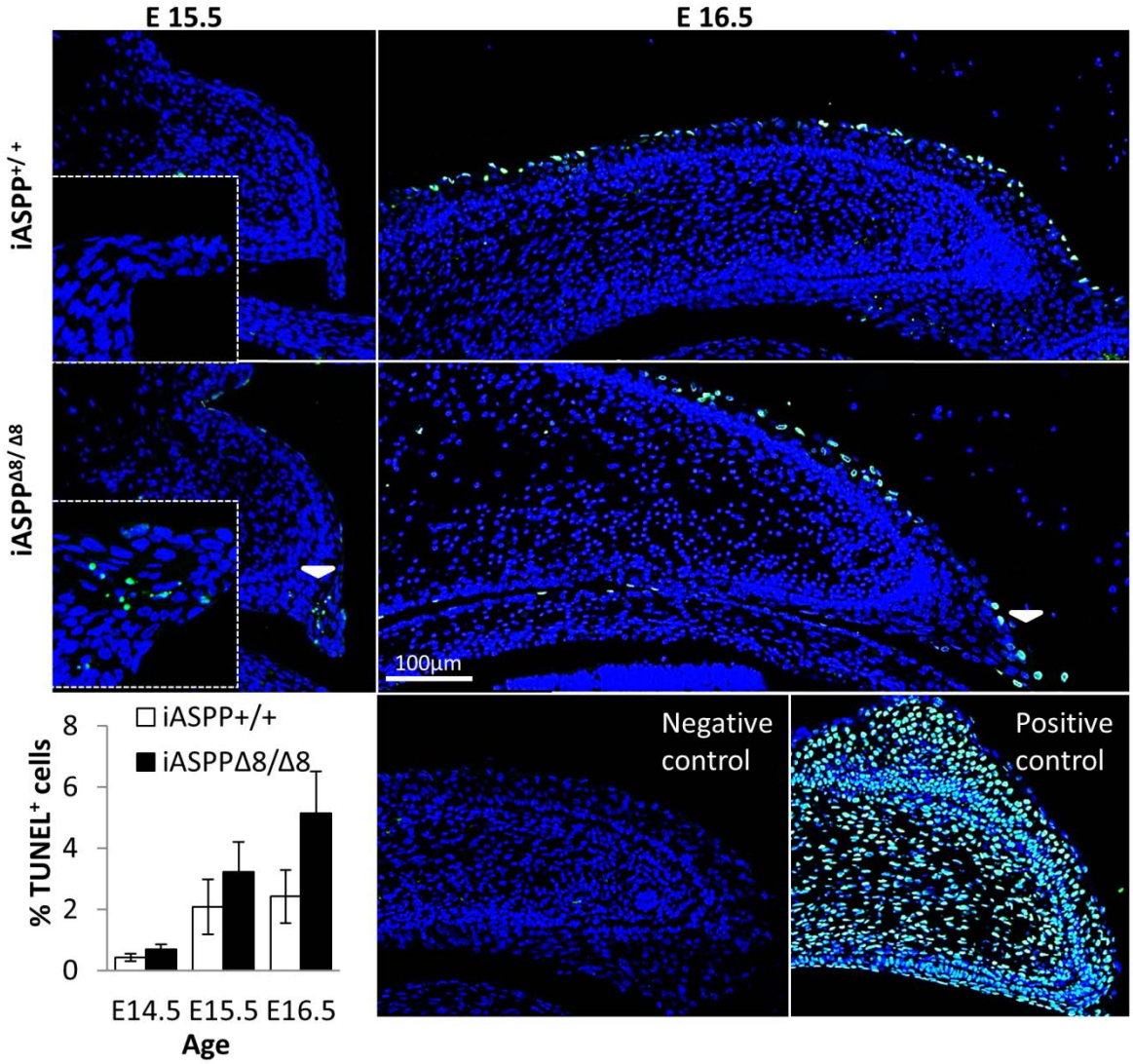

Figure 5.7 Increased apoptosis in the developing eyelids of iASPP$^{\Delta 8/\Delta 8}$ embryos

TUNEL assays were performed on eyelid sections from iASPP$^{+/+}$ and iASPP$^{\Delta 8/\Delta 8}$ embryos at E14.5, E15.5 and E16.5 to determine the extent of cell apoptosis. Bar graph shows the percentage of TUNEL-labelled apoptotic cells in the eyelids of iASPP$^{+/+}$ and iASPP$^{\Delta 8/\Delta 8}$ embryos at different embryonic stages. Augmented apoptosis is observed in the eyelids of iASPP$^{\Delta 8/\Delta 8}$ embryos at E15.5 and E16.5. Error bars represent ± SEM. Arrowhead points to the leading edge where apoptotic cells are more often observed in the eyelids of iASPP$^{\Delta 8/\Delta 8}$ embryos. Positive control eyelid sections were treated with DNaseI, and negative control sections were spared treatment with deoxyribonucleotidyl transferase.

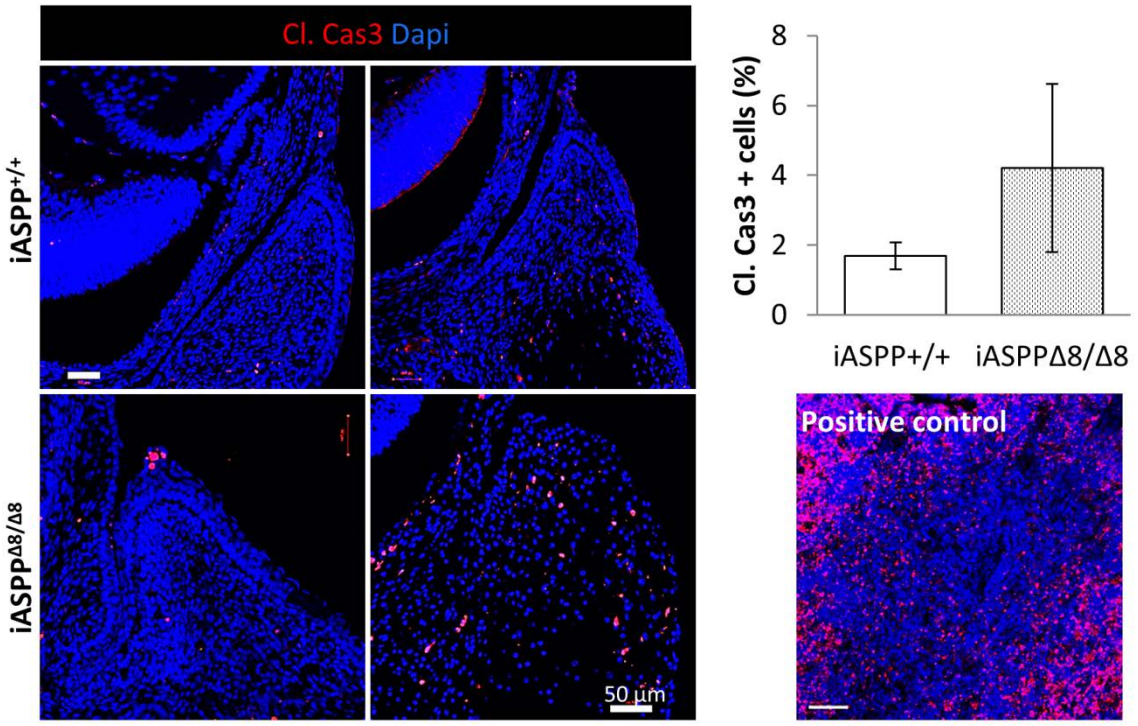

Figure 5.8 Apoptosis is augmented in the eyelids of E15.5 iASPP$^{\Delta 8/\Delta 8}$ embryos
E15.5 eyelid sections from iASPP$^{+/+}$ and iASPP$^{\Delta 8/\Delta 8}$ embryos stained for the apoptotic marker cleaved caspase 3. Bar graph shows the percentage of eyelid cells that stained positive for caspase 3 in iASPP$^{+/+}$ and iASPP$^{\Delta 8/\Delta 8}$ embryos. A thymus section from mice irradiated with X-rays was used as a positive control, as irradiation induces apoptosis.

5.2.5 Apoptosis in the eyelids of iASPP$^{\Delta 8/\Delta 8}$ mice is p53-independent

The previous section showed that a loss of iASPP results in increased apoptosis in the eyelids. iASPP is known for its inhibition of p53-mediated apoptosis. To determine whether impaired eyelid extension in iASPP$^{\Delta 8/\Delta 8}$ embryos was due to increased p53-mediated apoptosis, iASPP$^{+/\Delta 8}$;p53$^{+/-}$ mice were intercrossed to produce embryos of various p53 and iASPP genotypes. Histological examination of E16.5 embryos revealed that a loss of p53 was not able to rescue the open-eyelids phenotype in iASPP$^{\Delta 8/\Delta 8}$ embryos. Furthermore, the extent of eyelid opening in iASPP$^{\Delta 8/\Delta 8}$ embryos was not altered upon the loss of one or both alleles of p53 (Figure 5.9A). In support of this, examination of apoptosis in the eyelids of p53$^{+/+}$;iASPP$^{+/+}$, p53$^{+/+}$;iASPP$^{\Delta 8/\Delta 8}$, p53$^{-/-}$;iASPP$^{+/+}$, and p53$^{-/-}$;iASPP$^{\Delta 8/\Delta 8}$ mice showed no difference in the distribution of apoptotic cells between p53$^{+/+}$;iASPP$^{\Delta 8/\Delta 8}$ and p53$^{-/-}$;iASPP$^{\Delta 8/\Delta 8}$ eyelids (Figure 5.9B). Interestingly, apoptotic cells in p53$^{+/+}$;iASPP$^{\Delta 8/\Delta 8}$ and p53$^{-/-}$;iASPP$^{\Delta 8/\Delta 8}$ eyelids were present at the leading epithelial edge, which was consistent with the previous observations. These results suggest that apoptosis in iASPP$^{\Delta 8/\Delta 8}$ mice is p53-independent. This is further supported by the finding that a loss of p53 does not impair eyelid extension, and that eyelids closes appropriately in p53$^{-/-}$ embryos (Figure 5.9A). Moreover, immunohistochemical and immunofluorescence staining for p53 failed to detect any p53-positive cells in the eyelids (data not shown).

A.

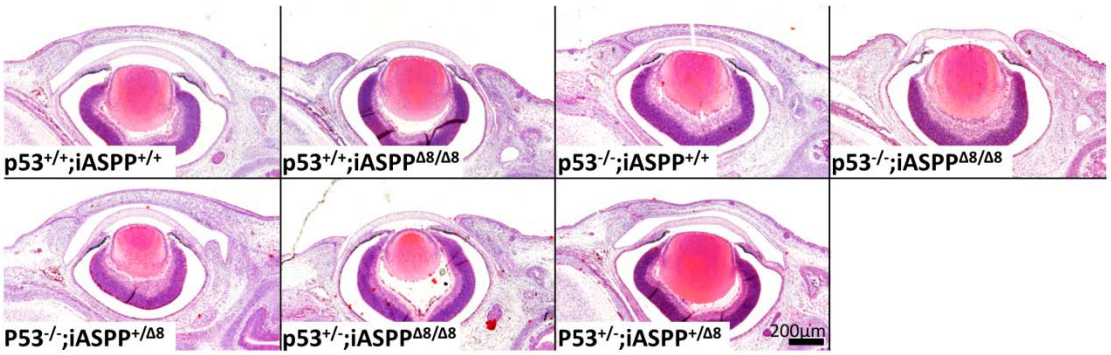

Genotype	Embryonic Eyelid Phenotype (n)
$p53^{+/+};iASPP^{+/+}$	No phenotype (7/7)
$p53^{+/+};iASPP^{\Delta8/\Delta8}$	Open eyelid (2/2)
$p53^{-/-};iASPP^{+/+}$	No phenotype (2/2)
$p53^{-/-};iASPP^{\Delta8/\Delta8}$	Open eyelid (1/1, 3 adult mice have eye phenotype resembling $iASPP^{\Delta8/\Delta8}$ phenotype)
$P53^{-/-};iASPP^{+/\Delta8}$	No phenotype (2/2)
$p53^{+/-};iASPP^{\Delta8/\Delta8}$	Open eyelid (7/7)
$p53^{+/-};iASPP^{+/\Delta8}$	No phenotype(12/12)

B.

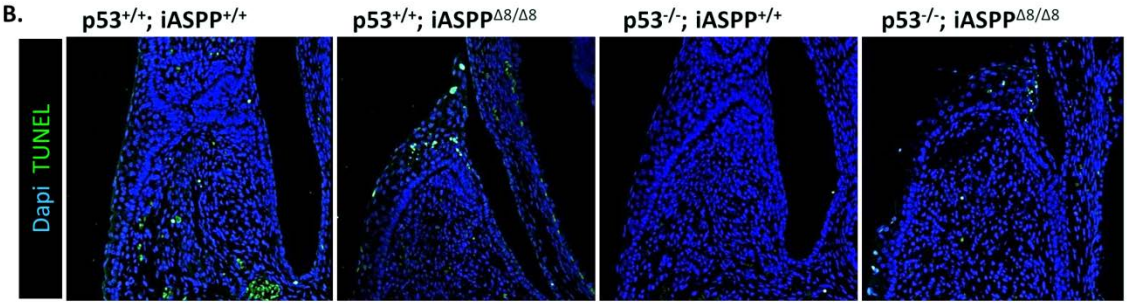

Figure 5.9 Impaired developmental eyelid closure in $iASPP^{\Delta8/\Delta8}$ mice is p53-independent
A. Histological examination of eyelids from E16.5 $p53^{+/+};iASPP^{+/+}$, $p53^{+/+};iASPP^{\Delta8/\Delta8}$, $p53^{-/-};iASPP^{+/+}$, $p53^{-/-};iASPP^{\Delta8/\Delta8}$, $p53^{-/-};iASPP^{+/\Delta8}$, $p53^{+/-};iASPP^{\Delta8/\Delta8}$ and $p53^{+/-};iASPP^{+/\Delta8}$ mice. Loss of one or both alleles of p53 has no effect on eyelid closure in $iASPP^{\Delta8/\Delta8}$ embryos. The table presented as part of the image summarises the number of embryos of each genotype analysed and the eyelid phenotype they present with. **B.** To determine whether p53 loss has an influence on apoptosis in $iASPP^{\Delta8/\Delta8}$ eyelids, TUNEL assays were performed on eyelid sections from $p53^{+/+};iASPP^{+/+}$, $p53^{+/+};iASPP^{\Delta8/\Delta8}$, $p53^{-/-};iASPP^{+/+}$ and $p53^{-/-};iASPP^{\Delta8/\Delta8}$ embryos at E16.5. Apoptotic cells can be observed at the leading edges of eyelids from $p53^{+/+};iASPP^{\Delta8/\Delta8}$ and $p53^{-/-};iASPP^{\Delta8/\Delta8}$ embryos. TUNEL-positive cells are green. Nuclear stain DAPI is in blue.

5.2.6 The open-eyelids phenotype in $p63^{-/-}$;$iASPP^{\Delta8/\Delta8}$ embryos parallels that observed in $p63^{-/-}$;$iASPP^{+/+}$ embryos

p63 is a member of the p53 family, and is essential for the regulation of epidermal stratification. In the absence of p63, stratified epithelia fail to develop. iASPP interacts with p63 and regulates the expression of genes involved in epidermal stratification (Notari *et al.*, 2011). iASPP is also able to interact with p63 and inhibit its transactivation of pro-apoptotic genes (Bergamaschi *et al.*, 2003). In view of this, it was investigated whether: 1. increased apoptosis in $iASPP^{\Delta8/\Delta8}$ embryos was p63-dependent; and 2. impaired eyelid closure in $iASPP^{\Delta8/\Delta8}$ embryos resulted from deficits in iASPP's regulation of p63 stratification. To address these aims, $iASPP^{+/\Delta8}$;$p63^{+/-}$ mice were intercrossed, producing embryos of various p63 and iASPP genotypes. Eyelid closure was examined histologically in E16.5 embryos with the following genotypes: $p63^{+/+}$;$iASPP^{+/+}$, $p63^{+/+}$;$iASPP^{\Delta8/\Delta8}$, $p63^{-/-}$;$iASPP^{+/+}$, $p63^{-/-}$;$iASPP^{\Delta8/\Delta8}$, $p63^{-/-}$;$iASPP^{+/\Delta8}$, $p63^{+/-}$;$iASPP^{\Delta8/\Delta8}$ and $p63^{+/-}$;$iASPP^{+/\Delta8}$. Interestingly, it was found that $p63^{-/-}$;$iASPP^{+/+}$embryos developed eyelids, although the eyelid groove and protrusion was smaller and the leading edge was absent. Eyelid closure failed to occur in $p63^{-/-}$;$iASPP^{+/+}$embryos (Figure 5.10A). In agreement with previous reports, these embryos also exhibited a single-layered surface epithelium instead of a stratified epidermis. In comparison to $p63^{-/-}$;$iASPP^{+/+}$ embryos, the open-eyelids phenotype observed in the absence of iASPP was milder. Eyelids in $p63^{+/+}$;$iASPP^{\Delta8/\Delta8}$embryos were larger and were of a typical cuboidal shape. Moreover, the eyelid mesenchyme was covered with multiple epidermal layers. Intriguingly, $p63^{-/-}$;$iASPP^{\Delta8/\Delta8}$ embryos with combined deficiency of p63 and iASPP showed no difference from $p63^{-/-}$;$iASPP^{+/+}$mice with respect to the extent of eyelid closure and the presence of epidermal stratification. Eyelid closure in the embryos heterozygous for iASPP and p63 was comparable to that of wild type embryos. Loss of one copy of p63 did not alter the extent of eyelid closure observed in the absence of iASPP. Therefore, these findings show no additive or synergistic

interaction between iASPP and p63 during eyelid closure. These results suggest that either p63 is downstream of iASPP, or that p63 and iASPP regulate eyelid development via distinct signalling pathways.

It was further investigated whether the increased apoptosis seen in the eyelids of iASPP$^{\Delta 8/\Delta 8}$ embryos was p63-dependent. The eyelid sections from p63$^{+/+}$;iASPP$^{+/+}$, p63$^{+/+}$;iASPP$^{\Delta 8/\Delta 8}$, p63$^{+/-}$;iASPP$^{\Delta 8/\Delta 8}$ and p63$^{-/-}$;iASPP$^{\Delta 8/\Delta 8}$ E16.5 embryos were subjected to TUNEL assay, and the distribution of apoptotic cells in the eyelids was examined. In a previous section, it was reported that apoptosis is increased and apoptotic cells can be observed at the leading edge in the absence of iASPP. Whether a combined loss of p63 and iASPP could ameliorate the apoptosis observed in the eyelids of iASPP$^{\Delta 8/\Delta 8}$ embryos was determined. It was found that the loss of one copy of p63 in iASPP$^{\Delta 8/\Delta 8}$embryos had no overt effect on apoptosis. The distribution of apoptotic cells in p63$^{+/-}$;iASPP$^{\Delta 8/\Delta 8}$ and p63$^{+/+}$;iASPP$^{\Delta 8/\Delta 8}$ embryos was comparable (Figure 5.10B). These results suggest that apoptosis in the eyelids of iASPP$^{\Delta 8/\Delta 8}$ embryos occurs via a p63-independent mechanism.

Collectively, these results indicate that the open-eyelids phenotype in iASPP$^{\Delta 8/\Delta 8}$ embryos likely occurs via a p63-independent mechanism. The analysis of p63 expression in eyelid sections from iASPP$^{+/+}$ and iASPP$^{\Delta 8/\Delta 8}$ embryos described here supports this. In the absence of iASPP, no notable difference in the expression pattern of p63 was observed (Figure 5.11).

A.

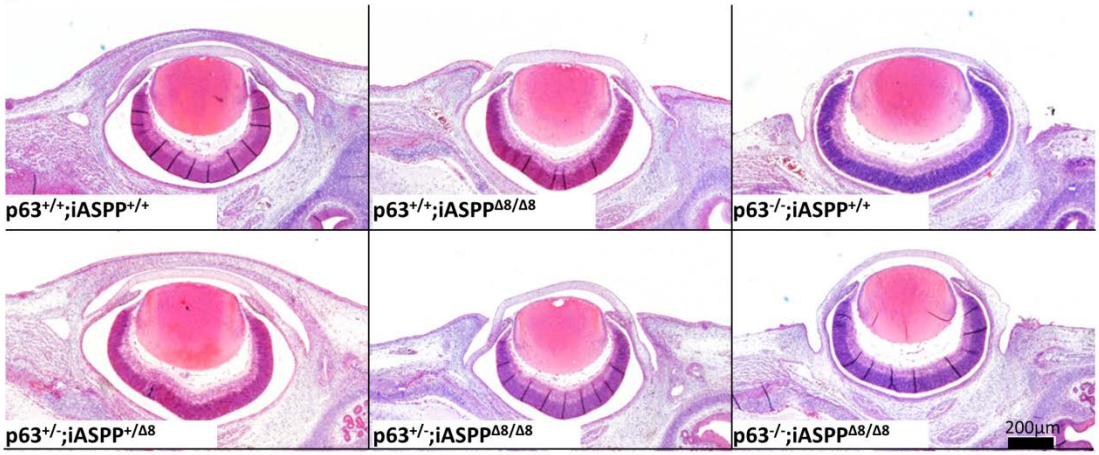

Genotype	Embryonic Eyelid Phenotype (n)
$p63^{+/+};iASPP^{+/+}$	No phenotype (n=6/6)
$p63^{+/+};iASPP^{\Delta8/\Delta8}$	Open eyelid (n=5/5)
$p63^{-/-};iASPP^{+/+}$	Underdeveloped and open eyelid (n=4/4)
$p63^{+/-};iASPP^{+/\Delta8}$	No phenotype (9/9)
$p63^{+/-};iASPP^{\Delta8/\Delta8}$	Open eyelid (5/5)
$p63^{-/-};iASPP^{\Delta8/\Delta8}$	Underdeveloped and open eyelid (n=4/4)

B.

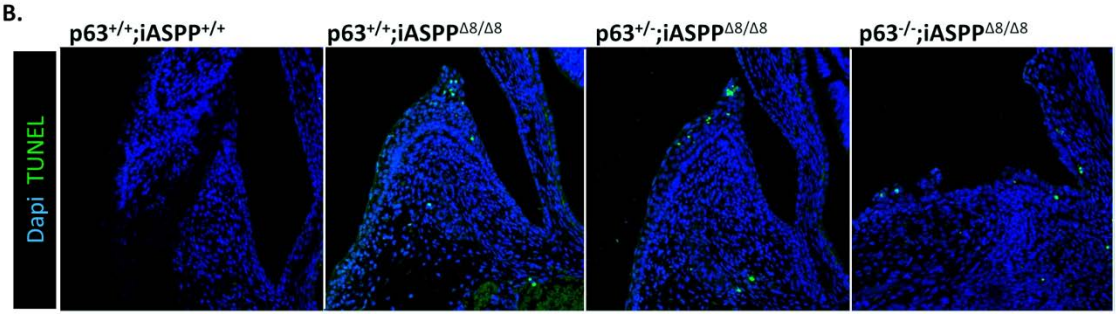

Figure 5.10 iASPP and p63 do not interact in the regulation of eyelid closure

A. Histological examination of eyelids from E16.5 $p63^{+/+};iASPP^{+/+}$, $p63^{+/+};iASPP^{\Delta8/\Delta8}$, $p63^{-/-};iASPP^{+/+}$, $p63^{-/-};iASPP^{\Delta8/\Delta8}$, $p63^{-/-};iASPP^{+/\Delta8}$, $p63^{+/-};iASPP^{\Delta8/\Delta8}$ and $p63^{+/-};iASPP^{+/\Delta8}$ mice. $p63^{-/-};iASPP^{+/+}$ embryos display an open-eyelids phenotype and show no epidermal stratification of the eyelids. $p63^{+/+};iASPP^{\Delta8/\Delta8}$ mice exhibit an open-eyelids phenotype but have multiple epithelial layers covering the eyelid surface. Loss of one allele of p63 has no effect on eyelid closure in $iASPP^{\Delta8/\Delta8}$ embryos. $p63^{-/-};iASPP^{\Delta8/\Delta8}$ embryos showed no difference from $p63^{-/-};iASPP^{+/+}$ embryos with respect to eyelid closure and the presence of epidermal layers. The table presented as part of the image summarises the number of embryos of each genotype analysed and the eyelid phenotype that they presented with. Note that eyelids of $p63^{-/-};iASPP^{+/+}$ mice are described as underdeveloped and open. Underdevelopment refers to lack of multiple epidermal layers. **B.** Apoptosis in the eyelids of $iASPP^{\Delta8/\Delta8}$ embryos is p63-independent. TUNEL assays were performed on eyelid sections from $p63^{+/+};iASPP^{+/+}$, $p63^{+/+};iASPP^{\Delta8/\Delta8}$, $p63^{+/-};iASPP^{\Delta8/\Delta8}$, and $p63^{-/-};iASPP^{\Delta8/\Delta8}$ embryos at E16.5. Apoptotic cells can be observed at the leading edges of eyelids from $p63^{+/-};iASPP^{\Delta8/\Delta8}$ and $p63^{-/-};iASPP^{\Delta8/\Delta8}$ embryos. TUNEL-positive cells are green. Nuclear stain DAPI is in blue.

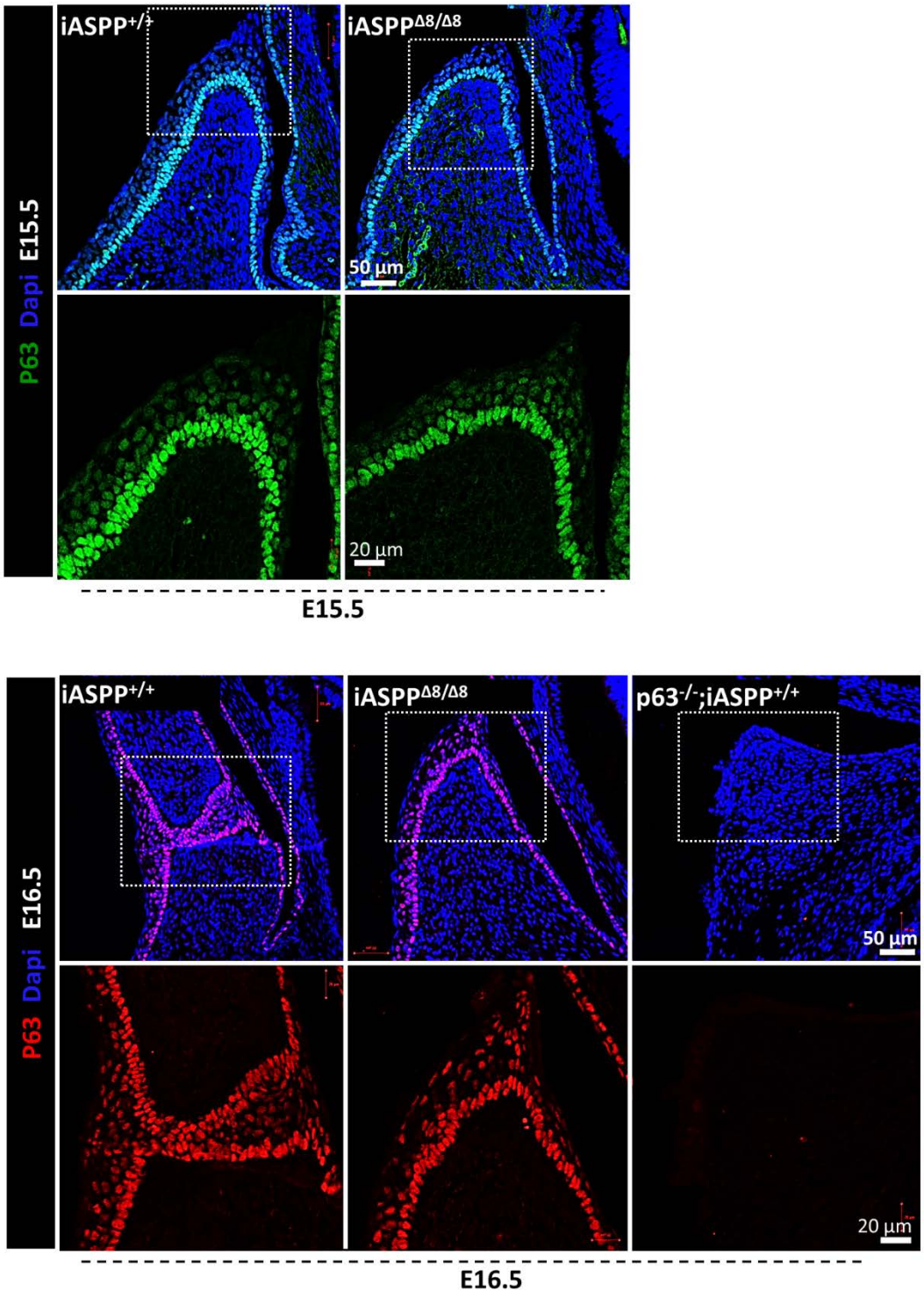

Figure 5.11 Loss of iASPP moderately affects p63 expression in embryonic eyelids
Immunofluorescence analysis of p63 expression in eyelid sections from iASPP$^{+/+}$ and iASPP$^{\Delta 8/\Delta 8}$ embryos at E15.5 (top 2 panels, p63 in green) and E16.5 (bottom 2 panels, p63 in red). Lower panels show enlarged areas of the white boxes in the above panels. Eyelid sections from p63$^{-/-}$;iASPP$^{+/+}$ (leftmost panel, 3rd and 4th row) mice were stained for p63 to confirm the specificity of the antibody. No p63 staining was observed.

5.2.6 iASPP deficiency results in sustained K6 expression at the leading edge

To further understand the mechanisms through which a loss of iASPP results in eyelid closure defects, the expression of markers of keratinocyte proliferation, differentiation and migration (K14, K1 and K6, respectively) were analysed in eyelid sections from iASPP$^{+/+}$ and iASPP$^{\Delta 8/\Delta 8}$ mouse embryos. At E15.5 to E16.5, the basal layers of the eyelid epithelia in both iASPP$^{+/+}$ and iASPP$^{\Delta 8/\Delta 8}$ embryos were negative for K1 and positive for K14 (Figure 5.12). This is indicative of a normal cell constituency of the basal layer at this embryonic stage (Shimizu *et al.*, 2005). Moreover, the cells in the eyelid basal layer were positive for BrdU and Ki67 in both iASPP$^{+/+}$ and iASPP$^{\Delta 8/\Delta 8}$ embryos, suggestive of unaltered proliferative behaviour in the basal epithelial layer in the eyelids of iASPP$^{\Delta 8/\Delta 8}$ embryos (Figure 5.6). These results suggest that overall cell type specificity is not altered upon the loss of iASPP and that impaired eyelid extension in iASPP$^{\Delta 8/\Delta 8}$ is not due to defects in the differentiation programme. This is in agreement with the previously outlined observation that showed that iASPP regulates eyelid closure independently of p63.

Analysis of K6 distribution in iASPP$^{+/+}$ and iASPP$^{\Delta 8/\Delta 8}$ eyelids was subsequently carried out to determine if impaired eyelid extension is due to defects in migration. At E15.5, the cells at the leading edge were positive for K6 in the eyelids of both iASPP$^{+/+}$ and iASPP$^{\Delta 8/\Delta 8}$ embryos (Figure 5.12A). However, K6 appeared to have a broader distribution in eyelid epithelia of E15.5 iASPP$^{\Delta 8/\Delta 8}$ embryos (Figure 5.12A, white arrowhead). Similarly, in E16.5 iASPP$^{\Delta 8/\Delta 8}$ embryos there was sustained expression of K6 at the eyelid leading edge, indicative of continuous and active migration of keratinocytes. In contrast, in E16.5 iASPP$^{+/+}$ embryos as eyelids fused, the expression of K6 ceased (Figure 5.12B). In summary, these results show that iASPP$^{\Delta 8/\Delta 8}$ keratinocytes express migration-specific keratins. A lack of eyelid extension in the absence of iASPP suggests that keratinocytes are unable to efficiently migrate across the cornea. The

cause of this inefficient migration of keratinocytes needs further examination. The morphology of cells in the eyelids of iASPP$^{\Delta 8/\Delta 8}$ embryos appeared rounded compared to the flattened and extended cell shape observed in the eyelids of iASPP$^{+/+}$ embryos (Figure 5.12). Given the shape of the migrating cells in the eyelids of iASPP$^{\Delta 8/\Delta 8}$ embryos, it is likely that these cells fail to polarise correctly. This is in agreement with *in vitro* migration data (Chapter IV, Figure 4.8), where it was shown that the loss of iASPP leads to disorganised and increased cellular migration. Therefore, it is proposed that the open-eyelids phenotype in iASPP$^{\Delta 8/\Delta 8}$ embryos is due to the impaired migration and increased apoptosis of epithelial cells.

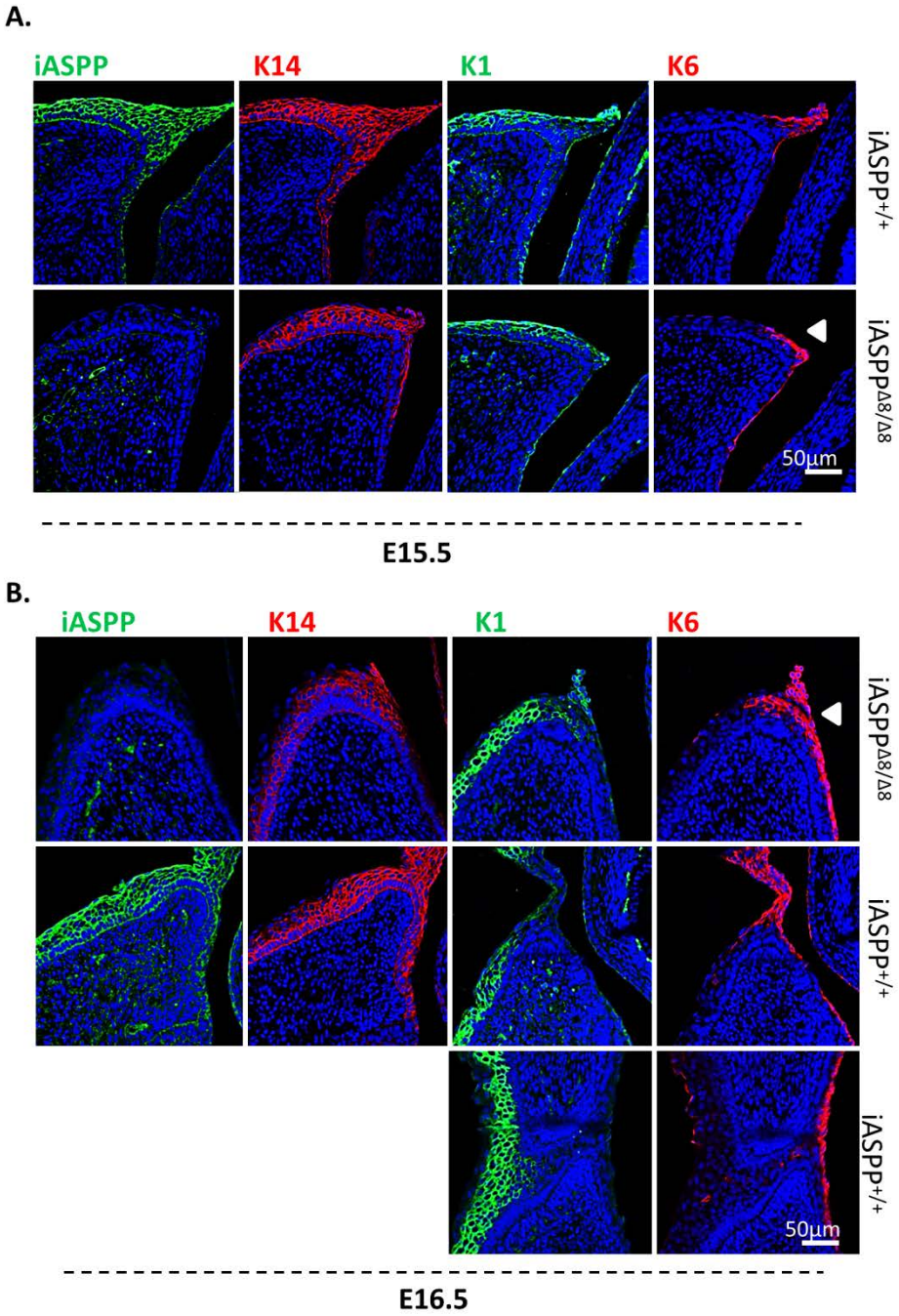

Figure 5.12 Sustained K6 expression in iASPP$^{\Delta 8/\Delta 8}$ embryos at E16.5
Immunofluorescence analysis of expression of K14, K1, and K6 in the eyelids of iASPP$^{+/+}$ and iASPP$^{\Delta 8/\Delta 8}$ embryos at **A.** E15.5 and **B.** E16.5. Continual expression of K6 can be observed in the eyelids of iASPP$^{\Delta 8/\Delta 8}$ embryos at E16.5. Cells at the leading edge appear more rounded in iASPP$^{\Delta 8/\Delta 8}$ embryos.

5.2.7 EGF stimulation leads to increased phospho-ERK levels in iASPP$^{\Delta 8/\Delta 8}$ keratinocytes

In view of the earlier observation showing that the loss of iASPP leads to sustained expression of K6, the molecular mechanisms by which this occurs were examined. EGFR signalling is critical for the induction of migration, and the loss of EGFR leads to an open-eyelids phenotype. EGFR is activated by various ligands including EGF, TGFα and HB-EGF. Ligand binding to the EGFR receptor activates downstream signalling cascades through phosphorylation. This includes the phosphorylation and activation of ERK1/2, which transduces the extracellular signal to the nucleus (Sibilia *et al.*, 2000). K6 is one of the target genes activated by EGFR signalling (Jiang *et al.*, 1993). Therefore, it was investigated whether EGFR signalling is altered in the absence of iASPP, and whether this could explain the broader expression of K6 in the eyelids of iASPP$^{\Delta 8/\Delta 8}$ embryos. EGFR signalling is active during processes that require cell migration, such as eyelid closure. Therefore, *in vitro* studies examining EGFR signalling needed to be done under EGFR stimulation with its ligands. EGFR signalling was activated in iASPP$^{+/+}$ and iASPP$^{\Delta 8/\Delta 8}$ keratinocytes by treatment with EGF, the levels of ERK2 and phyosphorylated-ERK1/2 (pERK1/2) were examined using western blotting techniques. The results showed the increased activation of pERK1/2 in iASPP$^{\Delta 8/\Delta 8}$ keratinocytes compared to iASPP$^{+/+}$ controls (Figure 5.13). Interestingly, activation of EGFR is thought to lead to decreased desmosome adhesive strength (Lacouture, 2006). Therefore, higher induction of ERK signalling could explain the increased cellular migration in keratinocytes that was reported in Chapter IV. Moreover, looser adhesion and increased migration could lead to cell detachment and death by anoikis. This could explain the impaired eyelid closure seen in iASPP$^{\Delta 8/\Delta 8}$ mice, and the increase in apoptosis at the eyelid leading edge.

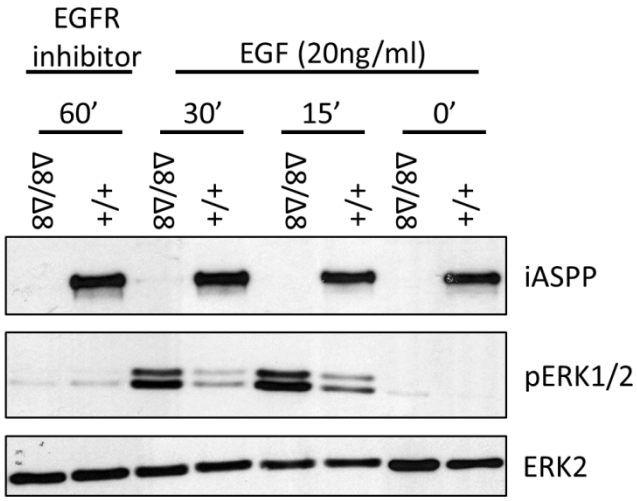

Figure 5.13 Increased pERK1/2 levels in iASPPΔ8/Δ8 cells upon stimulation with EGF
Primary keratinocytes isolated from conditional iASPP CreER mice were treated with vehicle or 4-OHT for four days to induce iASPP deletion. 4-OHT-induced iASPP$^{\Delta 8/\Delta 8}$ and vehicle-treated iASPP$^{+/+}$ keratinocytes were then stimulated with 20ng/ml EGF for the indicated amount of time in minutes. Cells stimulated with EGF for 15 minutes were treated with EGFR inhibitor for 60 minutes to confirm that the stimulation of ERK was EGFR-dependent.

5.3 Summary and brief discussion

In this chapter, it is shown that iASPP is an important regulator of developmental eyelid closure. In the absence of iASPP, eyelid epithelial sheet extension is impaired and the fusion of eyelids never occurs. It is demonstrated here that iASPP expression is restricted to the epithelial cells of the eyelid, suggesting that iASPP regulates the migration of epithelial sheets. Consistent with this, epithelial-specific deletion of iASPP recapitulates the open-eyelids phenotype observed when iASPP is deleted globally. Lack of eyelid sheet extension in $iASPP^{\Delta 8/\Delta 8}$ embryos is not due to decreased proliferation, as there was no difference in proliferation between the eyelids of $iASPP^{\Delta 8/\Delta 8}$ and $iASPP^{+/+}$ embryos. Instead, the eyelid phenotype in $iASPP^{\Delta 8/\Delta 8}$ mice arises from impaired epithelial sheet progression due to increased apoptosis. Our findings show that the observed apoptosis is p53- and p63-independent. This in agreement with a previous study that showed that p53-dependent apoptosis in developing eyelids only occurs following treatment with teratogen agents. Embryos treated with teratogen at E8 to activate p53-mediated apoptosis exhibited an open-eyelids phenotype at E17 in 3.9% of cases (Wubah *et al.*, 1996).

Death receptors of the Tumour Necrosis Factor Receptor (TNFR)-family signal apoptosis independently of p53 (Ashkenazi, 2002). TNFR1 has been implicated in the regulation of apoptosis of a variety of cells, including epithelial cells (Wehrli *et al.*, 2000). A study by Sharov *et al.* has shown that deregulated expression of the apoptotic receptors Fas and type 1 TNFR (TNFR1) can lead to impaired eyelid fusion (Sharov *et al.*, 2003). Direct targets of the Fas and TNFR1 signalling cascades are transcription factors of the NF-κB family. NF-κB proteins can promote the transcription of pro-apoptotic genes, leading to cell death. iASPP is known to bind to the NF-κB protein RelA and inhibit its transcriptional activities (Yang *et al.*, 1999). Therefore,

iASPP could also inhibit the induction of apoptosis by suppressing the pro-apoptotic NF-κB/RelA pathway. This requires future investigation.

Moreover, eyelid closure in iASPP$^{\Delta 8/\Delta 8}$ embryos was not due to impaired differentiation. This is unsurprising, as the differentiation and stratification processes start after eyelid fusion. Previous studies that have implicated iASPP in the regulation of stratification either used cell lines or adult mice (Chikh *et al.*, 2011; Notari *et al.*, 2011). In these studies, it was shown that a loss of iASPP leads to increased differentiation of the epidermis. In Chapter III in this thesis, deregulated differentiation in the palmoplantar epidermis of adult mice in the absence of iASPP was reported. Therefore, iASPP could be involved in the homeostasis of mature skin rather than the regulation of early epidermal development and differentiation. Future studies will be needed to clarify at what developmental stage iASPP begins to participate in the regulation of epidermal differentiation.

Furthermore, a broader and sustained expression pattern of K6 (a keratin expressed in migratory cells) was observed in the eyelid epithelia of iASPP$^{\Delta 8/\Delta 8}$ mice compared to iASPP$^{+/+}$ controls. Therefore, iASPP$^{\Delta 8/\Delta 8}$ cells have the expression profile of cells that are able to migrate. However, iASPP$^{\Delta 8/\Delta 8}$ cells are unable to efficiently migrate and close the eyelid. The reason for this inefficient movement might be an inability of the cells to remain cohesive due to a loss of cell-cell adhesion. This is supported by the previous data presented in chapters III and IV, showing that loss of iASPP results in weaker cell-cell adhesions and in more disorganised cell movement. Furthermore, this study has shown that, upon EGF induction, cells lacking iASPP have higher levels of pERK1/2 than control cells. Induction of ERK1/2 phosphorylation is associated with increased migration. Interestingly, increased EGFR stimulation is associated with weaker intercellular adhesion. Therefore, these data provide evidence that inefficient migration is likely due to increased cell migration and possibly cell detachment due to weaker

cell-cell adhesions, and hence increased apoptosis in the eyelid leading edge. As a consequence, whether the death of cells at the leading edge of the eyelid is due to a loss of cell-cell contacts or a detachment of cells from the substrate, anoikis requires further investigation.

In summary, the epithelial cells of the leading edge are thought to be necessary to direct the movement of succeeding epithelial cells across the cornea (Heller *et al.*, 2014). The results outlined in this chapter show that, in the absence of iASPP, leading edge epithelial cells are more prone to apoptosis. Therefore, loss of cells in this location can disrupt the polarity of movement, resulting in inefficient migration and the death of cells across the cornea.

Chapter VI: General discussion and future directions

Chapter VI: General discussion and future directions

Overview

The aim of this thesis was to investigate whether iASPP is a dual function protein that regulates desmosomal adhesion and couples it to intracellular signalling events and if, in the absence of iASPP, desmosome-related diseases develop.

iASPP was found to co-localise with the desmosomal complex by interacting with both desmoplakin and K5. iASPP deficiency resulted in increased phosphorylation and solubilisation of desmoplakin, and abnormal K5 aggregation. This culminated in decreased adhesive strength in iASPP$^{\Delta 8/\Delta 8}$ keratinocyte cultures, which facilitated enhanced cellular migration. iASPP's interaction with phosphatase PP1 facilitated the dephosphorylation of desmoplakin, and mutation of the PP1 binding site on iASPP resulted in increased desmoplakin phosphorylation. These results suggested that iASPP participates in the strengthening of desmosomal adhesion by mediating desmoplakin's phosphorylation and solubilisation and, hence, the maturation of desmosomes.

Consistent with the role of iASPP in the maintenance of desmosomal adhesion, focal palmoplantar keratoderma, a desmosome-related disorder, was observed in iASPP$^{\Delta 8/\Delta 8}$ mice. This was accompanied by altered differentiation of keratinocytes within affected areas. An increase in the thickness of K1-expressing cell layers was noted, and aberrant K5 and K6 expression was detected throughout the diseased palmoplantar epidermis. Altogether, these results showed that a loss of iASPP results in aberrant adhesion and misregulated cell signalling, suggesting that iASPP is a potential link between desmosomal adhesion and cell signalling events.

Impaired intercellular adhesion and migration had adverse effects on wound healing, and iASPP$^{\Delta 8/\Delta 8}$ mice exhibited delays in wound closure. Furthermore, it was found that a defect in eyelid closure in iASPP$^{\Delta 8/\Delta 8}$ mice was, in part, due to increased apoptosis. The localisation of apoptotic cells at the leading edge implicated that the apoptosis might have occurred due to the loss of cell-matrix or cell-cell contacts, i.e. anoikis.

From these studies, it is tempting to speculate that iASPP is a new regulator of desmosomal adhesion and a new candidate gene in cutaneous disorders. Furthermore, these results set the stage for future studies focusing on further characterising the interactions between iASPP with desmosomal components, and the delineation of the signalling events that trigger the translocation of iASPP from cell-cell junctions to the nucleus. The identification of iASPP as a regulator of desmoplakin phosphorylation and solubilisation, which governs the strength of intercellular adhesion, has exposed a potential molecular pathway for therapeutic targeting in the treatment of cutaneous disorders.

6.1 iASPP is a regulator of desmosomes and its deficiency leads to cutaneous disorders

6.1.1 Mapping of the interaction sites between iASPP, desmoplakin and K5, or other desmosome components

The results presented in this thesis show that iASPP interacts with desmosome components including desmoplakin and K5 filaments. Desmoplakin is known to interact with type II keratins other than K5, such as K1, K2 and K6. Since iASPP expression extends beyond the basal epidermal layer and includes layers expressing K1 and K6, future studies should examine whether or not iASPP is able to interact with these keratins and mediate their binding to desmoplakin. Furthermore, mapping of the interaction sites between iASPP, desmoplakin and K5 would offer further insight into how iASPP could be mediating the integrity of desmosomes. Generation of recombinant iASPP, desmoplakin and K5 proteins and their truncated forms would help to determine whether iASPP interacts with these proteins directly, and which protein domains mediate their interaction.

The hypothesis is that the N-terminus of iASPP interacts with desmoplakin, while its C-terminus interacts with PP1. The targeting of iASPP to cell-cell junctions via its N-terminus would be reminiscent of the regulation of the junctional localisation of ASPP2, a family member of iASPP. ASPP2's N-terminus has been shown to bind Par3, which directs it to the tight junctions of neuronal epithelia (Sottocornola, 2011). Interestingly, while the C-termini of iASPP and ASPP2 share high sequence homologies, their N-termini are divergent. Therefore, binding of desmoplakin to the N-terminus of iASPP would explain the lack of desmosome-related heart and skin phenotypes in ASPP2-deficient mice.

6.1.2 Defining the role of iASPP in desmoplakin phosphorylation, and its effect on desmosome adhesion and integrity

It was shown that a lack of iASPP increases desmoplakin solubilisation and phosphorylation in mouse keratinocytes, but not the solubilisation of other desmosome components such as plakoglobin. Cells containing iASPP$^{F811A/F811A}$, a PP1 binding mutant, had increased phosphorylation of desmoplakin S2849, suggesting that iASPP regulates desmoplakin phosphorylation by bringing phosphatase PP1 to desmoplakin. Interestingly, cells expressing iASPP$^{F811A/F811A}$ did not have increased desmoplakin solubility, suggesting that iASPP could be participating in desmosome regulation by stabilising the interactions of desmoplakin at the plasma membrane. Alternatively, binding of iASPP to desmoplakin could obscure kinase binding sites on desmoplakin and this could prevent its phosphorylation, solubilisation and dissociation from cell-cell adhesion sites.

Desmoplakin is a very large protein; its longest isoform is comprised of 2871 amino acids. Running the desmoplakin protein sequence against the PROSITE collection of motifs (Sigrist *et al.*, 2010) predicts multiple phosphorylation sites for a number of different kinases, including PKCα. The functions of these putative phosphorylation sites are not yet known. Given that the ability of desmosomes to switch between weakly and strongly adhesive states depends on phosphorylation by PKCα, future studies should aim to unravel the functions of these putative phosphorylation sites. This could be accomplished through mutagenesis studies in combination with functional assays testing the adhesiveness of desmosomes. By mapping the interaction sites between iASPP and desmoplakin, whether or not iASPP interferes with the interaction of kinases with desmoplakin will be determined. The hypothesis is that iASPP affects the phosphorylation of sites other than desmoplakin S2849. This is supported by the

observation that the iASPP$^{F811A/F811A}$ mutant does not affect desmoplakin S2849 phosphorylation and solubility to the same extent as iASPP$^{\Delta8/\Delta8}$.

6.1.3 Understanding the regulation of the subcellular expression of iASPP in the epidermis

Focal thickening of palmoplantar epidermis was observed in iASPP$^{\Delta8/\Delta8}$ mice. This thickening possibly resulted from the aberrant regulation of epidermal differentiation in response to mechanical stress. An increased number of cell layers expressing K1 was observed, and sporadic K5 and K6-expressing cells were found in K1-expressing layers. These observations are in agreement with previous findings showing that iASPP is an important regulator of the p63-mediated stratification programme, repressing its transactivation of genes involved in differentiation, such as K1 and envoplakin, while maintaining the expression of basal cell markers such as K14 and K5 (Notari *et al.*, 2011). p63 consists of TA and ΔN isoforms, where ΔNp63 isoforms regulate the expression of proliferation markers such as K14 and K5, while TAp63 isoforms regulate the expression of differentiation markers such as K1, K10 and loricrin. TAp63 also has a crucial role in the maintenance of adult stem cells and its loss results in hyperproliferation of stem cells, their differentiation and ultimately exhaustion of the stem cell pool (Su *et al.*, 2009). Whether iASPP regulates TAp63 or ΔNp63, or both isoforms, has not been investigated before. Given the epidermal thickening as well as loss of p63 from some regions of palmoplantar epidermis in iASPP$^{\Delta8/\Delta8}$ mice, it is possible that iASPP participates in the regulation of adult stem cell maintenance mediated by TAp63. Therefore, in future studies, it would be interesting to investigate whether impairing the translocation of iASPP to cell-cell junctions or to the nucleus influences the proliferation and differentiation of adult stem cells.

Previous studies have shown that the C-terminus of iASPP contains a nuclear localisation signal, whereas its N-terminus is necessary for its cytoplasmic localisation (Slee *et al.*, 2004). A recent study showed that phosphorylation of iASPP on serines 84 and 113 by cyclin B/cyclin-dependent kinase 1 prevents the dimerisation of iASPP, and exposes its RanGDP binding site in the C-terminus, facilitating its nuclear entry via the newly identified RaDAR-mediated nuclear import pathway (Lu *et al.*, 2013; Lu *et al.*, 2014). In addition, the unmasking of iASPP's C-terminus also enables iASPP to interact with p53, p63 and PP1. Therefore, iASPP's interaction with PP1 could be one of the signals that triggers its translocation to the cell membrane, while its interaction with RanGDP facilitates its nuclear entry. It is possible that the interaction of iASPP with desmoplakin prevents iASPP from going into the nucleus. Future research should address whether truncation of iASPP's N-terminus alters the dynamics of iASPP and its regulation with regard to cell adhesion and nuclear cell signalling.

6.1.4 Investigating whether dysregulation of Wnt signalling facilitates the development of palmoplantar keratoderma and ARVC in iASPP$^{\Delta 8/\Delta 8}$ mice

Enhanced activation of the EGFR-ERK signalling pathway was observed in iASPP$^{\Delta 8/\Delta 8}$ cells, demonstrating additional mechanisms by which iASPP can influence desmosomal adhesion and couple it to cell signalling. EGFR activation has been shown to regulate desmosomal adhesion by participating in the cleavage and internalisation of desmoglein 2, and by mediating plakoglobin phosphorylation and its dissociation from desmoplakin (Lorch *et al.*, 2004; Yin *et al.*, 2005a). Plakoglobin's dissociation from cell-cell adhesion sites can result in its accumulation in the nucleus, where it can repress Wnt signalling and stimulate pro-adipogenic gene expression, which can lead to ARVC pathogenesis (Garcia-Gras *et al.*, 2006; Lombardi *et al.*, 2009; Wankell *et al.*, 2001). Wnt signalling is also necessary for keratinisation of the plamoplantar epidermis, and its misregulation can lead to palmoplantar keratoderma, a

disorder that can be observed in conjunction with ARVC. In future studies, it will be important to address whether the ARVC and palmoplantar keratoderma observed in iASPP$^{\Delta 8/\Delta 8}$ mice is due to disruption of the Wnt signalling pathway. TOP-flash assays (a quantitative technique that can determine β-catenin's induction of Wnt signalling) should be performed in the absence or presence of iASPP to determine whether iASPP can regulate Wnt signalling. In addition, iASPP should be cotransfected with the TOP-flash construct to determine if iASPP can regulate its activity. Furthermore, iASPP should be downregulated in cardiac muscle cells such as HL1, and the ability of these cells to differentiate into adipocytes should be examined. This experiment has already been attempted, but failed due to an inability to achieve sustained iASPP downregulation. However, it was found that iASPP$^{\Delta 8/\Delta 8}$ mouse embryonic fibroblasts (MEFs) are more easily induced to differentiate into adipocytes than control iASPP$^{+/+}$ MEFs (Figure A1). These results indicate that a loss of iASPP can lead to the induction of pro-adipogenic genes which, if it occurs in cardiac progenitor cells, can have severe consequences and can lead to ARVC and sudden death.

6.1.5 Investigating whether the subcellular localisation of iASPP has implications regarding tumour progression

iASPP is upregulated in several cancers. Its nuclear and cytoplasmic overexpression in head and neck squamous cell carcinoma (HNSCC) has been associated with poor clinical prognosis (Liu *et al.*, 2012). Whether iASPP could be used as a prognostic biomarker requires further investigation. Given the observations made in this study that implicate iASPP in the regulation of desmosomal adhesion, it will be interesting to investigate whether the loss of iASPP from cell-cell junctions and its translocation into the nucleus is associated with a worse clinical outcome in cancer patients overexpressing iASPP.

iASPP in the progression of oesophageal squamous cell carcinoma

It will be important to investigate the role of iASPP and its subcellular localisation in the progression of oesophageal squamous cell carcinoma. Palmoplantar keratoderma was first associated with the progression of oesophageal squamous cell carcinoma in 1958 and, since then, the association has received further backing (Ellis *et al.*, 1994; Howel-Evans *et al.*, 1958; Kelsell *et al.*, 1996). Given that a loss of iASPP leads to palmoplantar keratoderma, it would worthwhile to explore the role that iASPP plays in the progression of this type of oesophageal carcinoma.

iASPP in the progression of oesophageal adenocarcinoma

Oesophageal adenocarcinoma (EAC) is another well suited model with which to explore whether iASPP's subcellular localisation is associated with cancer progression. EAC arises from Barrett's oesophagus, a premalignant condition that is characterised by the replacement of normal squamous epithelium with metaplastic intestinal-like columnar epithelium. EAC develops through multistep metaplasia-dysplasia-adenocarcinoma malignant conversion (Spechler, 2002). If EAC is not diagnosed early, metastasis to the lymph nodes with poor clinical outcome proceeds. A few biomarkers for predicting the progression of Barrett's oesophagus to adenocarcinoma have emerged in recent years, including p53 positivity (Ong *et al.*, 2010). More recently, reduced desmosome assembly through the methylation and downregulation of plakophilin 1 has been implicated in the malignant transition of Barrett's oesophagus into EAC (Kaz *et al.*, 2012). Studies examining the role of desmosomes in cancer progression have elucidated that a loss of desmosome adhesion is a prerequisite for malignant conversion. iASPP stabilises desmosome adhesion and, in the nucleus, represses p53-mediated apoptotic activity, making it an ideal early candidate biomarker for the malignant conversion of

Barrett's oesophagus. Therefore, the question of whether iASPP's expression pattern is altered at various stages of the conversion of Barrett's oesophagus into EAC warrants future investigation. These studies have already been started, using patient samples in which disease progression to malignancy can be followed. Preliminary data shows that junctional iASPP is lost during disease progression and transition to malignancy (Figure A2 and A3). The number of samples used in the study will need to be increased substantially if any firmer conclusions are to be made. Dr Lai Mun Wang, with whom collaboration has been made, will provide additional samples from the Oxford Centre for Histopathology Research Biobank. Ideally, hundreds of unaffected and affected samples should be used.

6.1.6 Determining the expression of iASPP in human palmoplantar keratoderma samples

If the proposed role of iASPP in cardiocutaneous disorders is to be strengthened, a link to human patients should be established. Therefore, palmoplantar keratoderma and ARVC patients should be tested for mutations in iASPP. Specifically, patients suffering from ARVC and palmoplantar keratoderma without any mutations in desmosome components should be screened for mutations in iASPP. These include two Arab families and a Spanish patient presenting with a phenotypic triad of ARVC, palmoplantar keratoderma and woolly hair, who lack mutations in known desmosomal components (Alonso-Orgaz *et al.*, 2007; Djabali *et al.*, 2002). Furthermore, when possible, iASPP's subcellular localisation should be examined in diseased tissue samples from patients suffering from desmosome-related disorders.

6.2 iASPP regulates wound healing *in vivo* and *in vitro*

It was elucidated in this study that iASPP is important in the regulation of wound healing *in vivo*. In the absence of iASPP, wound healing was delayed and this was not due to alterations in the proliferation or apoptosis of epithelial cells. Cells lacking iASPP migrated in a disorganised manner, failing to maintain the cohesiveness of the epithelial sheet. This suggested that delayed wound healing in the absence of iASPP was a consequence of impaired intercellular adhesion of epithelial cells during migration. It is not unusual that a loss of desmosome components or their regulators results in delayed wound healing and/or enhanced disorganisation of cell migration (Garrod *et al.*, 2005; Thomason *et al.*, 2012). Loss of the desmosome component PERP leads to impaired wound healing, and it was suggested that this is not due to impaired keratinocyte proliferation, but rather due to enhanced albeit inefficient and incohesive migration of keratinocytes across the wound bed (Beaudry *et al.*, 2010). Similarly, loss of plakoglobin leads to increased cell migration and this is not linked to cell proliferation (Yin *et al.*, 2005b).

6.2.1 Delineating whether fibroblasts and other cell types contribute to delayed wound healing in iASPP$^{\Delta 8/\Delta 8}$ mice

In concert with keratinocyte proliferation and migration, fibroblast contraction is essential for successful wound re-epithelisation. However, delayed wound healing in iASPP$^{\Delta 8/\Delta 8}$mice is probably not due to impaired fibroblast contraction, as the expression of iASPP in fibroblasts appears to be very limited. Furthermore, preliminary results obtained from analysing wound closure in K14-iASPP$^{\Delta 8/\Delta 8}$ mice support this claim. Relative to K14-iASPP$^{+/+}$, K14-iASPP$^{\Delta 8/\Delta 8}$ mice also exhibited delayed wound healing. This data has not been shown as these experiments are at an early stage and are still ongoing. Upon their completion, it will also be determined

whether deficits in the recruitment of inflammatory cells to the wound site contribute to hindered wound closure in iASPP$^{\Delta 8/\Delta 8}$mice.

An *ex vivo* assay developed by Mazzalupo and associates (Wang *et al.*, 2013), which assesses the potential of mouse keratinocytes for wound epithelisation, is also in progress. In this assay, full skin explants from iASPP$^{+/+}$ and iASPP$^{\Delta 8/\Delta 8}$mice are excised and grown *ex vivo* with subsequent monitoring of the outgrowth of keratinocytes. As the epidermis can be separated from the dermis, this assay can be applied to a full skin explants versus epidermis-only explants. This will help to evaluate whether dermal cells such as fibroblasts influence the keratinocyte potential.

6.2.2 Evaluating the role of iASPP in chronic wounds and malignant tumours

Chronic wounds such as pressure ulcers, venous leg ulcers and diabetic ulcers affect hundreds of thousands of patients each year, and impose immense economic burden on health systems globally (Sen *et al.*, 2009). A secondary complication is that malignant tumours often arise at the sites of chronic injuries (Schafer and Werner, 2008). It has been established that a key feature of chronic wounds is the impaired re-epithelisation and restoration of the epidermal barrier (Stojadinovic *et al.*, 2008; Thomason *et al.*, 2012). Inadequate targeting of primary causes of impaired healing is a major cause of treatment failure for chronic wound patients. Hence, understanding the molecular mechanisms that go awry in non-healing wounds is needed in order to promote the development of better treatment strategies. Deregulation of desmosome components has been reported to occur in non-healing venous ulcers (Stojadinovic *et al.*, 2008). In this study, it is shown that iASPP is a regulator of desmosomes and wound healing is delayed in the absence of iASPP. It cannot be excluded that the focal palmoplantar keratoderma that occurs in iASPP$^{\Delta 8/\Delta 8}$ mice may not result from an inability of the palmoplantar epidermis to repair itself. In future studies, it will be interesting to examine the

expression of iASPP in samples collected from patients suffering from chronic wounds and palmoplantar keratoderma. Furthermore, iASPP is overexpressed in many cancers and wound healing is impaired in the absence of iASPP. A recently revisited hypothesis is that cancer is an over-healing wound. Hence, overexpression of iASPP could trigger constant induction of the molecular pathways involved in the regulation of wound healing, initiating the formation of tumours. Therefore, larger studies examining the distribution of iASPP staining in chronic wounds and tumours undergoing the transition from benign to malignant are needed. The status of iASPP and its subcellular localisation might prove to be a useful indicator of the invasive states of cancers, and the severity of chronic wounds.

6.3 iASPP regulates eyelid epithelial sheet extension during development

Movement of epithelial sheets is a process that occurs in many pathological, physiological and developmental processes such as cancer metastasis, wound healing and eyelid closure. In light of the finding that wound healing is delayed in the absence of iASPP, it is not surprising that impaired embryonic eyelid extension in iASPP$^{\Delta 8/\Delta 8}$ mice was also detected. This is also true for many other genes that have been implicated in wound closure. For example, impaired c-Jun, TGFα, EGFR and activin signalling results in the delayed healing of wounded skin and impaired embryonic eyelid closure (Wankell *et al.*, 2001; Xia and Kao, 2004). Furthermore, overexpression of cell signalling molecules implicated in wound and eyelid closure has been reported in cancer patients. In human patients, overexpression of EGFR or iASPP has been associated with worse prognosis and the development of more aggressive tumour types that are resistant to cancer therapies. Thus, delineation of the signals important for eyelid closure might help to identify potential pharmaceutical targets for new cancer treatments.

6.3.1 Elucidating the mechanisms by which loss of iASPP causes increased apoptosis: a link to hemidesmosomes?

It was demonstrated that impaired eyelid extension is, in part, due to increased apoptosis at the leading edge of the eyelid epidermis. iASPP is a known inhibitor of the apoptotic function of the p53 family of proteins. However, apoptosis in the eyelids of iASPP$^{\Delta 8/\Delta 8}$ embryos observed in this study appeared to be p53- and p63-independent, prompting speculation that apoptosis must occur via alternative pathways. iASPP can also repress the transcriptional activities of the NF-κB protein RelA (Yang *et al.*, 1999). NF-κB proteins can promote the transcription of pro-apoptotic genes, leading to cell death. Therefore, iASPP could also inhibit the induction of apoptosis by suppressing the NF-κB/RelA pathway in developing eyelids. This requires further investigation. The localisation of apoptotic cells at the leading edge of the migrating epidermis

is very intriguing. It could be an indicator of detachment-induced apoptosis, i.e. anoikis. Interestingly, the NF-κB/RelA pathway has been implicated in anoikis pathways (Toruner *et al.*, 2006; Yan *et al.*, 2005), therefore, iASPP could suppress cell death via the NF-κB/RelA anoikis pathway.

Another possible explanation for cell detachment and subsequent apoptosis could be weakened adhesion of hemidesmosomes to the basement membrane. Given that iASPP is expressed in basal keratinocytes, and it was shown that iASPP is a regulator of desmosomes, interaction of iASPP with hemidesmosomes cannot be excluded. Hence, future research should address whether iASPP participates in the establishment of stable hemidesmosome adhesion to the basement membrane.

6.3.2 Exploring the mechanisms by which loss of iASPP enhances migration

The delayed wound and eyelid closure phenotype in iASPP$^{\Delta 8/\Delta 8}$ embryos, and the increased migration of iASPP$^{\Delta 8/\Delta 8}$ keratinocytes *in vitro,* may be perceived to be at odds. Fast and disorganised motility and the loss of cell-cell contacts in iASPP-deficient cells could contribute to impaired epidermal closures. As has been seen in the eyelids of iASPP$^{\Delta 8/\Delta 8}$embryos, such disorganised migratory behaviour could lead to increased apoptosis, impairing the closure process. In agreement with increased migration of keratinocytes, increased phosphorylation (i.e. activation) of ERK1/2 was observed in keratinocytes lacking iASPP in response to EGF stimulation. Activated ERK can induce migration by 1) reducing the stability of hemidesmosomes, 2) increasing the turnover of focal adhesions and 3) regulating actin-myosin contractions. ERK regulates hemidesmosome stability by mediating the phosphorylation of its component integrin β4. This results in disrupted interaction of this integrin with the cytoskeletal linker protein plectin, and leads to the decreased interaction of hemidesmosomes with basement membrane protein laminin 322 (Frijns *et al.*, 2010). A second action of

activated ERK is to regulate actin-myosin contractions and membrane protrusions by phosphorylating the Myosin Light Chain (MLC). A third branch of ERK function is to mediate focal adhesion turnover by phosphorylating Focal Adhesion Kinase (FAK), Paxillin and Calpain. Phosphorylation of these proteins regulates their activity, subsequently mediating their migration. To determine by which mechanisms iASPP influences keratinocyte migration, the effect of iASPP deficiency on the phosphorylation status of integrin β4, MLC, FAK and Calpain should be examined. Moreover, whether or not actin-myosin and focal adhesion dynamics are altered in iASPP$^{\Delta 8/\Delta 8}$ keratinocytes should be investigated.

6.3.3 Confirming a loss of directional migration in the absence of iASPP

It was demonstrated that cell motility is disorganised, and intercellular connections are disrupted, in the absence of iASPP. To further examine the role of iASPP in controlling directional migration, wounds should be introduced to confluent layers of cells to induce the reorientation and polarisation of the cells towards the wound. Cells normally respond to this induction by positioning the golgi and centrosome in front of the nucleus in the 120° sector facing the wound, and extending protrusions driven by actin polymerisation. At 0, 12, 24 and 36 hours post wound induction, iASPP$^{+/+}$ and iASPP$^{\Delta 8/\Delta 8}$ cells should be fixed and stained for the golgi marker GM120, as well as for actin. The orientation of the golgi should be examined and compared between iASPP$^{+/+}$ and iASPP$^{\Delta 8/\Delta 8}$ cells. Moreover, the orientation of actin filaments and the formation of actin ruffles at the wound edge should be compared between iASPP$^{+/+}$ and iASPP$^{\Delta 8/\Delta 8}$ cells.

6.4 Prospective remarks

The evidence presented in this thesis and the current literature demonstrates the importance of iASPP in normal development and the control of cancer progression. Its overexpression is observed in many cancer types and contributes to cancer malignancy, while its downregulation results in the development of cardiocutaneous disorders including ARVC, palmoplantar keratoderma and delayed wound healing. Thus, the correct maintenance of iASPP levels is pivotal for managing/preventing the progression of pathological and physiological conditions. The question that necessitates immediate attention, therefore, is what are the regulators of iASPP's expression and its subcellular localisation? The answer to this question will facilitate the development of specific therapeutic agents that specifically target iASPP's localisation or levels. In addition, it should be investigated how current cancer therapies influence iASPP dynamics. This needs to be addressed, because a major complication of modern anticancer treatments is cardiotoxicity, which can alter cardiac rhythms, blood pressure, cause ischemia and, in some cases, heart failure. iASPP$^{\Delta 8/\Delta 8}$ mice have abnormal cardiac rhythms and die from heart failure, so whether anticancer drugs cause cardiovascular side effects by influencing iASPP expression warrants further investigation. Future work will undoubtedly answer many questions regarding the regulation of iASPP's expression, and the molecular mechanisms by which iASPP participates in the regulation of biological processes.

Literature cited

AGIRRE, X., ROMAN-GOMEZ, J., JIMENEZ-VELASCO, A., GARATE, L., MONTIEL-DUARTE, C., NAVARRO, G., VAZQUEZ, I., ZALACAIN, M., CALASANZ, M. J., HEINIGER, A., TORRES, A., MINNA, J. D., & PROSPER, F. (2006). ASPP1, a common activator of TP53, is inactivated by aberrant methylation of its promoter in acute lymphoblastic leukemia. *Oncogene, 25*(13), 1862-1870. doi: 10.1038/sj.onc.1209236

AL-AMOUDI, A., DIEZ, D. C., BETTS, M. J., & FRANGAKIS, A. S. (2007). The molecular architecture of cadherins in native epidermal desmosomes. *Nature, 450*(7171), 832-837. doi: 10.1038/nature05994

AL-JASSAR, C., BIKKER, H., OVERDUIN, M., & CHIDGEY, M. (2013). Mechanistic basis of desmosome-targeted diseases. *J Mol Biol, 425*(21), 4006-4022. doi: 10.1016/j.jmb.2013.07.035

AL-SABEQ, B., KRAHN, A. D., CONACHER, S., KLEIN, G. J., & LAKSMAN, Z. (2014). Arrhythmogenic right ventricular cardiomyopathy with recessive inheritance related to a new homozygous desmocollin-2 mutation. *Can J Cardiol, 30*(6), 696 e691-693. doi: 10.1016/j.cjca.2014.01.014

ALCALAI, R., METZGER, S., ROSENHECK, S., MEINER, V., & CHAJEK-SHAUL, T. (2003). A recessive mutation in desmoplakin causes arrhythmogenic right ventricular dysplasia, skin disorder, and woolly hair. *J Am Coll Cardiol, 42*(2), 319-327.

ALONSO-ORGAZ, S., ZAMORANO-LEON, J. J., FERNANDEZ-ARQUERO, M., VILLACASTIN, J., PEREZ-CASTELLANOS, N., GARCIA-TORRENT, M. J., MACAYA, C., & LOPEZ FARRE, A. J. (2007). Case report of a Spanish patient with arrhythmogenic right ventricular cardiomyopathy and palmoplantar keratoderma without plakoglobin and desmoplakin gene modifications. *Int J Cardiol, 118*(2), 275-277. doi: 10.1016/j.ijcard.2006.06.065

ALPATOV, R., MUNGUBA, G. C., CATON, P., JOO, J. H., SHI, Y., SHI, Y., HUNT, M. E., & SUGRUE, S. P. (2004). Nuclear speckle-associated protein Pnn/DRS binds to the transcriptional corepressor CtBP and relieves CtBP-mediated repression of the E-cadherin gene. *Mol Cell Biol, 24*(23), 10223-10235. doi: 10.1128/MCB.24.23.10223-10235.2004

AMAGAI, M., MATSUYOSHI, N., WANG, Z. H., ANDL, C., & STANLEY, J. R. (2000). Toxin in bullous impetigo and staphylococcal scalded-skin syndrome targets desmoglein 1. *Nat Med, 6*(11), 1275-1277. doi: 10.1038/81385

AMAR, L. S., SHABANA, A. H., OBOEUF, M., MARTIN, N., & FOREST, N. (1999). Involvement of desmoplakin phosphorylation in the regulation of desmosomes by protein kinase C, in HeLa cells. *Cell Adhes Commun, 7*(2), 125-138.

ANGST, B. D., NILLES, L. A., & GREEN, K. J. (1990). Desmoplakin II expression is not restricted to stratified epithelia. *J Cell Sci, 97 (Pt 2)*, 247-257.

ARMSTRONG, D. K., MCKENNA, K. E., PURKIS, P. E., GREEN, K. J., EADY, R. A., LEIGH, I. M., & HUGHES, A. E. (1999). Haploinsufficiency of desmoplakin causes a striate subtype of palmoplantar keratoderma. *Hum Mol Genet, 8*(1), 143-148.

ARTEAGA, L. A., PRISAYANH, P. S., WARREN, S. J., LIU, Z., DIAZ, L. A., LIN, M. S., & COOPERATIVE GROUP ON FOGO SELVAGEM, RESEARCH. (2002). A subset of pemphigus foliaceus patients exhibits pathogenic autoantibodies against both desmoglein-1 and desmoglein-3. *J Invest Dermatol, 118*(5), 806-811. doi: 10.1046/j.1523-1747.2002.01743.x

ASHKENAZI, A. (2002). Targeting death and decoy receptors of the tumour-necrosis factor superfamily. *Nat Rev Cancer, 2*(6), 420-430. doi: 10.1038/nrc821

ASIMAKI, A., SYRRIS, P., WICHTER, T., MATTHIAS, P., SAFFITZ, J. E., & MCKENNA, W. J. (2007). A novel dominant mutation in plakoglobin causes arrhythmogenic right ventricular cardiomyopathy. *Am J Hum Genet, 81*(5), 964-973. doi: 10.1086/521633

AWAD, M. M., CALKINS, H., & JUDGE, D. P. (2008). Mechanisms of disease: molecular genetics of arrhythmogenic right ventricular dysplasia/cardiomyopathy. *Nat Clin Pract Cardiovasc Med, 5*(5), 258-267. doi: 10.1038/ncpcardio1182

AWAD, M. M., DALAL, D., CHO, E., AMAT-ALARCON, N., JAMES, C., TICHNELL, C., TUCKER, A., RUSSELL, S. D., BLUEMKE, D. A., DIETZ, H. C., CALKINS, H., & JUDGE, D. P. (2006a). DSG2 mutations contribute to arrhythmogenic right ventricular dysplasia/cardiomyopathy. *Am J Hum Genet, 79*(1), 136-142. doi: 10.1086/504393

AWAD, M. M., DALAL, D., TICHNELL, C., JAMES, C., TUCKER, A., ABRAHAM, T., SPEVAK, P. J., CALKINS, H., & JUDGE, D. P. (2006b). Recessive arrhythmogenic right ventricular dysplasia due to novel cryptic splice mutation in PKP2. *Hum Mutat, 27*(11), 1157. doi: 10.1002/humu.9461

AYUB, M., BASIT, S., JELANI, M., UR REHMAN, F., IQBAL, M., YASINZAI, M., & AHMAD, W. (2009). A homozygous nonsense mutation in the human desmocollin-3 (DSC3) gene underlies hereditary hypotrichosis and recurrent skin vesicles. *Am J Hum Genet, 85*(4), 515-520. doi: 10.1016/j.ajhg.2009.08.015

BASS-ZUBEK, A. E., GODSEL, L. M., DELMAR, M., & GREEN, K. J. (2009). Plakophilins: multifunctional scaffolds for adhesion and signaling. *Curr Opin Cell Biol, 21*(5), 708-716. doi: 10.1016/j.ceb.2009.07.002

BASS-ZUBEK, A. E., HOBBS, R. P., AMARGO, E. V., GARCIA, N. J., HSIEH, S. N., CHEN, X., WAHL, J. K., 3RD, DENNING, M. F., & GREEN, K. J. (2008). Plakophilin 2: a critical scaffold for PKC alpha that regulates intercellular junction assembly. *J Cell Biol, 181*(4), 605-613. doi: 10.1083/jcb.200712133

BAUCE, B., BASSO, C., RAMPAZZO, A., BEFFAGNA, G., DALIENTO, L., FRIGO, G., MALACRIDA, S., SETTIMO, L., DANIELI, G., THIENE, G., & NAVA, A. (2005). Clinical profile of four families with arrhythmogenic right ventricular cardiomyopathy caused by dominant desmoplakin mutations. *Eur Heart J, 26*(16), 1666-1675. doi: 10.1093/eurheartj/ehi341

BAZZI, H., & CHRISTIANO, A. M. (2007). Broken hearts, woolly hair, and tattered skin: when desmosomal adhesion goes awry. *Curr Opin Cell Biol, 19*(5), 515-520. doi: 10.1016/j.ceb.2007.08.001

BEAUDRY, V. G., IHRIE, R. A., JACOBS, S. B., NGUYEN, B., PATHAK, N., PARK, E., & ATTARDI, L. D. (2010). Loss of the desmosomal component perp impairs wound healing in vivo. *Dermatol Res Pract, 2010*, 759731. doi: 10.1155/2010/759731

BERGAMASCHI, D., SAMUELS, Y., JIN, B., DURAISINGHAM, S., CROOK, T., & LU, X. (2004). ASPP1 and ASPP2: common activators of p53 family members. *Mol Cell Biol, 24*(3), 1341-1350.

BERGAMASCHI, D., SAMUELS, Y., O'NEIL, N. J., TRIGIANTE, G., CROOK, T., HSIEH, J. K., O'CONNOR, D. J., ZHONG, S., CAMPARGUE, I., TOMLINSON, M. L., KUWABARA, P. E., & LU, X. (2003). iASPP oncoprotein is a key inhibitor of p53 conserved from worm to human. *Nat Genet, 33*(2), 162-167. doi: 10.1038/ng1070

BERGAMASCHI, D., SAMUELS, Y., SULLIVAN, A., ZVELEBIL, M., BREYSSENS, H., BISSO, A., DEL SAL, G., SYED, N., SMITH, P., GASCO, M., CROOK, T., & LU, X. (2006). iASPP preferentially binds p53 proline-rich region and modulates apoptotic function of codon 72-polymorphic p53. *Nat Genet, 38*(10), 1133-1141. doi: 10.1038/ng1879

BERKOWITZ, E. A., SEROOGY, K. B., SCHROEDER, J. A., RUSSELL, W. E., EVANS, E. P., RIEDEL, R. F., PHILLIPS, H. K., HARRISON, C. A., LEE, D. C., & LUETTEKE, N. C. (1996). Characterization of the mouse transforming growth factor alpha gene: its expression during eyelid development and in waved 1 tissues. *Cell Growth Differ, 7*(9), 1271-1282.

BERONJA, S., JANKI, P., HELLER, E., LIEN, W. H., KEYES, B. E., OSHIMORI, N., & FUCHS, E. (2013). RNAi screens in mice identify physiological regulators of oncogenic growth. *Nature, 501*(7466), 185-190. doi: 10.1038/nature12464

BIEDERMANN, K., VOGELSANG, H., BECKER, I., PLASCHKE, S., SIEWERT, J. R., HOFLER, H., & KELLER, G. (2005). Desmoglein 2 is expressed abnormally rather than mutated in familial and sporadic gastric cancer. *J Pathol, 207*(2), 199-206. doi: 10.1002/path.1821

BIERKAMP, C., MCLAUGHLIN, K. J., SCHWARZ, H., HUBER, O., & KEMLER, R. (1996). Embryonic heart and skin defects in mice lacking plakoglobin. *Dev Biol, 180*(2), 780-785. doi: 10.1006/dbio.1996.0346

BLAKE, J. A., BULT, C. J., EPPIG, J. T., KADIN, J. A., RICHARDSON, J. E., & MOUSE GENOME DATABASE, GROUP. (2014). The Mouse Genome Database: integration of and access to knowledge about the laboratory mouse. *Nucleic Acids Res, 42*(Database issue), D810-817. doi: 10.1093/nar/gkt1225

BLANPAIN, C., & FUCHS, E. (2006). Epidermal stem cells of the skin. *Annu Rev Cell Dev Biol, 22*, 339-373. doi: 10.1146/annurev.cellbio.22.010305.104357

BLANPAIN, C., & FUCHS, E. (2009). Epidermal homeostasis: a balancing act of stem cells in the skin. *Nat Rev Mol Cell Biol, 10*(3), 207-217. doi: 10.1038/nrm2636

BLANPAIN, C., HORSLEY, V., & FUCHS, E. (2007). Epithelial stem cells: turning over new leaves. *Cell, 128*(3), 445-458. doi: 10.1016/j.cell.2007.01.014

BLAYDON, D. C., BIANCHERI, P., DI, W. L., PLAGNOL, V., CABRAL, R. M., BROOKE, M. A., VAN HEEL, D. A., RUSCHENDORF, F., TOYNBEE, M., WALNE, A., O'TOOLE, E. A., MARTIN, J. E., LINDLEY, K., VULLIAMY, T., ABRAMS, D. J., MACDONALD, T. T., HARPER, J. I., & KELSELL, D. P. (2011). Inflammatory skin and bowel disease linked to ADAM17 deletion. *N Engl J Med, 365*(16), 1502-1508. doi: 10.1056/NEJMoa1100721

BOLLING, M. C., & JONKMAN, M. F. (2009). Skin and heart: une liaison dangereuse. *Exp Dermatol, 18*(8), 658-668. doi: 10.1111/j.1600-0625.2009.00908.x

BORNSLAEGER, E. A., GODSEL, L. M., CORCORAN, C. M., PARK, J. K., HATZFELD, M., KOWALCZYK, A. P., & GREEN, K. J. (2001). Plakophilin 1 interferes with plakoglobin binding to desmoplakin, yet together with plakoglobin promotes clustering of desmosomal plaque complexes at cell-cell borders. *J Cell Sci, 114*(Pt 4), 727-738.

BRANCOLINI, C., SGORBISSA, A., & SCHNEIDER, C. (1998). Proteolytic processing of the adherens junctions components beta-catenin and gamma-catenin/plakoglobin during apoptosis. *Cell Death Differ, 5*(12), 1042-1050. doi: 10.1038/sj.cdd.4400443

BRANDL, K., SUN, L., NEPPL, C., SIGGS, O. M., LE GALL, S. M., TOMISATO, W., LI, X., DU, X., MAENNEL, D. N., BLOBEL, C. P., & BEUTLER, B. (2010). MyD88 signaling in nonhematopoietic cells protects mice against induced colitis by regulating specific EGF receptor ligands. *Proc Natl Acad Sci U S A, 107*(46), 19967-19972. doi: 10.1073/pnas.1014669107

BROOKE, M. A., NITOIU, D., & KELSELL, D. P. (2012). Cell-cell connectivity: desmosomes and disease. *J Pathol, 226*(2), 158-171. doi: 10.1002/path.3027

BUKHARI, I., & JUMA'A, N. (2004). Naxos disease in Saudi Arabia. *J Eur Acad Dermatol Venereol, 18*(5), 614-616. doi: 10.1111/j.1468-3083.2004.01010.x

BURDETT, I. D., & SULLIVAN, K. H. (2002). Desmosome assembly in MDCK cells: transport of precursors to the cell surface occurs by two phases of vesicular traffic and involves major changes in centrosome and Golgi location during a Ca(2+) shift. *Exp Cell Res, 276*(2), 296-309. doi: 10.1006/excr.2002.5509

BYUN, T. H., KIM, J. T., PARK, H. W., & KIM, W. K. (2011). Timetable for upper eyelid development in staged human embryos and fetuses. *Anat Rec (Hoboken), 294*(5), 789-796. doi: 10.1002/ar.21366

CABRAL, R. M., LIU, L., HOGAN, C., DOPPING-HEPENSTAL, P. J., WINIK, B. C., ASIAL, R. A., DOBSON, R., MEIN, C. A., BASELAGA, P. A., MELLERIO, J. E., NANDA, A., BOENTE MDEL, C., KELSELL, D. P., MCGRATH, J. A., & SOUTH, A. P. (2010a). Homozygous mutations in the 5' region of the JUP gene result in cutaneous disease but normal heart development in children. *J Invest Dermatol, 130*(6), 1543-1550. doi: 10.1038/jid.2010.7

CABRAL, R. M., TATTERSALL, D., PATEL, V., MCPHAIL, G. D., HATZIMASOURA, E., ABRAMS, D. J., SOUTH, A. P., & KELSELL, D. P. (2012). The DSPII splice variant is crucial for desmosome-mediated adhesion in HaCaT keratinocytes. *J Cell Sci, 125*(Pt 12), 2853-2861. doi: 10.1242/jcs.084152

CABRAL, R. M., WAN, H., COLE, C. L., ABRAMS, D. J., KELSELL, D. P., & SOUTH, A. P. (2010b). Identification and characterization of DSPIa, a novel isoform of human desmoplakin. *Cell Tissue Res, 341*(1), 121-129. doi: 10.1007/s00441-010-0989-1

CANDI, E., RUFINI, A., TERRINONI, A., DINSDALE, D., RANALLI, M., PARADISI, A., DE LAURENZI, V., SPAGNOLI, L. G., CATANI, M. V., RAMADAN, S., KNIGHT, R. A., & MELINO, G. (2006). Differential roles of p63 isoforms in epidermal development: selective genetic complementation in p63 null mice. *Cell Death Differ, 13*(6), 1037-1047. doi: 10.1038/sj.cdd.4401926

CANDI, E., SCHMIDT, R., & MELINO, G. (2005). The cornified envelope: a model of cell death in the skin. *Nat Rev Mol Cell Biol, 6*(4), 328-340. doi: 10.1038/nrm1619

CAO, L., HUANG, Q., HE, J., LU, J., & XIONG, Y. (2013). Elevated expression of iASPP correlates with poor prognosis and chemoresistance/radioresistance in FIGO Ib1-IIa squamous cell cervical cancer. *Cell Tissue Res, 352*(2), 361-369. doi: 10.1007/s00441-013-1569-y

CAPUTO, R., & PELUCHETTI, D. (1977). The junctions of normal human epidermis. A freeze-fracture study. *J Ultrastruct Res, 61*(1), 44-61.

CARROLL, D. K., CARROLL, J. S., LEONG, C. O., CHENG, F., BROWN, M., MILLS, A. A., BRUGGE, J. S., & ELLISEN, L. W. (2006). p63 regulates an adhesion programme and cell survival in epithelial cells. *Nat Cell Biol, 8*(6), 551-561. doi: 10.1038/ncb1420

CELLI, A., SANCHEZ, S., BEHNE, M., HAZLETT, T., GRATTON, E., & MAURO, T. (2010). The epidermal Ca(2+) gradient: Measurement using the phasor representation of fluorescent lifetime imaging. *Biophys J, 98*(5), 911-921. doi: 10.1016/j.bpj.2009.10.055

CELLI, J., DUIJF, P., HAMEL, B. C., BAMSHAD, M., KRAMER, B., SMITS, A. P., NEWBURY-ECOB, R., HENNEKAM, R. C., VAN BUGGENHOUT, G., VAN HAERINGEN, A., WOODS, C. G., VAN ESSEN, A. J., DE WAAL, R., VRIEND, G., HABER, D. A., YANG, A., MCKEON, F., BRUNNER, H. G., & VAN BOKHOVEN, H. (1999). Heterozygous germline mutations in the p53 homolog p63 are the cause of EEC syndrome. *Cell, 99*(2), 143-153.

CHEN, D., PADIERNOS, E., DING, F., LOSSOS, I. S., & LOPEZ, C. D. (2005). Apoptosis-stimulating protein of p53-2 (ASPP2/53BP2L) is an E2F target gene. *Cell Death Differ, 12*(4), 358-368. doi: 10.1038/sj.cdd.4401536

CHEN, J., XIE, F., ZHANG, L., & JIANG, W. G. (2010). iASPP is over-expressed in human non-small cell lung cancer and regulates the proliferation of lung cancer cells through a p53 associated pathway. *BMC Cancer, 10*, 694. doi: 10.1186/1471-2407-10-694

CHEN, X., BONNE, S., HATZFELD, M., VAN ROY, F., & GREEN, K. J. (2002). Protein binding and functional characterization of plakophilin 2. Evidence for its diverse roles in desmosomes and beta -catenin signaling. *J Biol Chem, 277*(12), 10512-10522. doi: 10.1074/jbc.M108765200

CHIDGEY, M., BRAKEBUSCH, C., GUSTAFSSON, E., CRUCHLEY, A., HAIL, C., KIRK, S., MERRITT, A., NORTH, A., TSELEPIS, C., HEWITT, J., BYRNE, C., FASSLER, R., & GARROD, D. (2001). Mice lacking desmocollin 1 show epidermal fragility accompanied by barrier defects and abnormal differentiation. *J Cell Biol, 155*(5), 821-832. doi: 10.1083/jcb.200105009

CHIDGEY, M., & DAWSON, C. (2007). Desmosomes: a role in cancer? *Br J Cancer, 96*(12), 1783-1787. doi: 10.1038/sj.bjc.6603808

CHIKH, A., MATIN, R. N., SENATORE, V., HUFBAUER, M., LAVERY, D., RAIMONDI, C., OSTANO, P., MELLO-GRAND, M., GHIMENTI, C., BAHTA, A., KHALAF, S., AKGUL, B., BRAUN, K. M., CHIORINO, G., PHILPOTT, M. P., HARWOOD, C. A., & BERGAMASCHI, D. (2011). iASPP/p63 autoregulatory feedback loop is required for the homeostasis of stratified epithelia. *EMBO J, 30*(20), 4261-4273. doi: 10.1038/emboj.2011.302

CHOI, H. J., PARK-SNYDER, S., PASCOE, L. T., GREEN, K. J., & WEIS, W. I. (2002). Structures of two intermediate filament-binding fragments of desmoplakin reveal a unique repeat motif structure. *Nat Struct Biol, 9*(8), 612-620. doi: 10.1038/nsb818

CHRISTIANO, A. M. (1997). Frontiers in keratodermas: pushing the envelope. *Trends Genet, 13*(6), 227-233. doi: 10.1016/S0168-9525(97)01104-9

CHUN, M. G., & HANAHAN, D. (2010). Genetic deletion of the desmosomal component desmoplakin promotes tumor microinvasion in a mouse model of pancreatic neuroendocrine carcinogenesis. *PLoS Genet, 6*(9), e1001120. doi: 10.1371/journal.pgen.1001120

CIRILLO, N., FEMIANO, F., GOMBOS, F., & LANZA, A. (2007). Metalloproteinase 9 is the outer executioner of desmoglein 3 in apoptotic keratinocytes. *Oral Dis, 13*(3), 341-345. doi: 10.1111/j.1601-0825.2006.01287.x

COBLEIGH, M. A., TABESH, B., BITTERMAN, P., BAKER, J., CRONIN, M., LIU, M. L., BORCHIK, R., MOSQUERA, J. M., WALKER, M. G., & SHAK, S. (2005). Tumor gene expression and prognosis in breast cancer patients with 10 or more positive lymph nodes. *Clin Cancer Res, 11*(24 Pt 1), 8623-8631. doi: 10.1158/1078-0432.CCR-05-0735

CONACCI-SORRELL, M. E., BEN-YEDIDIA, T., SHTUTMAN, M., FEINSTEIN, E., EINAT, P., & BEN-ZE'EV, A. (2002). Nr-CAM is a target gene of the beta-catenin/LEF-1 pathway in melanoma and colon cancer and its expression enhances motility and confers tumorigenesis. *Genes Dev, 16*(16), 2058-2072. doi: 10.1101/gad.227502

COULOMBE, P. A. (2003). Wound epithelialization: accelerating the pace of discovery. *J Invest Dermatol, 121*(2), 219-230. doi: 10.1046/j.1523-1747.2003.12387.x

CROFT, C. B., & TARIN, D. (1970). Ultrastructural studies of wound healing in mouse skin. I. Epithelial behaviour. *J Anat, 106*(Pt 1), 63-77.

DAVIES, E. L., GEE, J. M., COCHRANE, R. A., JIANG, W. G., SHARMA, A. K., NICHOLSON, R. I., & MANSEL, R. E. (1999). The immunohistochemical expression of desmoplakin and its role in vivo in the progression and metastasis of breast cancer. *Eur J Cancer, 35*(6), 902-907.

DEHNER, C., ROTZER, V., WASCHKE, J., & SPINDLER, V. (2014). A desmoplakin point mutation with enhanced keratin association ameliorates pemphigus vulgaris autoantibody-mediated loss of cell cohesion. *Am J Pathol, 184*(9), 2528-2536. doi: 10.1016/j.ajpath.2014.05.016

DELMAR, M., & MCKENNA, W. J. (2010). The cardiac desmosome and arrhythmogenic cardiomyopathies: from gene to disease. *Circ Res, 107*(6), 700-714. doi: 10.1161/CIRCRESAHA.110.223412

DELVA, E., TUCKER, D. K., & KOWALCZYK, A. P. (2009). The desmosome. *Cold Spring Harb Perspect Biol, 1*(2), a002543. doi: 10.1101/cshperspect.a002543

DEN HAAN, A. D., TAN, B. Y., ZIKUSOKA, M. N., LLADO, L. I., JAIN, R., DALY, A., TICHNELL, C., JAMES, C., AMAT-ALARCON, N., ABRAHAM, T., RUSSELL, S. D., BLUEMKE, D. A., CALKINS, H., DALAL, D., & JUDGE, D. P. (2009). Comprehensive desmosome mutation analysis in north americans with arrhythmogenic right ventricular dysplasia/cardiomyopathy. *Circ Cardiovasc Genet, 2*(5), 428-435. doi: 10.1161/CIRCGENETICS.109.858217

DEN, Z., CHENG, X., MERCHED-SAUVAGE, M., & KOCH, P. J. (2006). Desmocollin 3 is required for pre-implantation development of the mouse embryo. *J Cell Sci, 119*(Pt 3), 482-489. doi: 10.1242/jcs.02769

DESAI, B. V., HARMON, R. M., & GREEN, K. J. (2009). Desmosomes at a glance. *J Cell Sci, 122*(Pt 24), 4401-4407. doi: 10.1242/jcs.037457

DESCARGUES, P., DERAISON, C., BONNART, C., KREFT, M., KISHIBE, M., ISHIDA-YAMAMOTO, A., ELIAS, P., BARRANDON, Y., ZAMBRUNO, G., SONNENBERG, A., & HOVNANIAN, A. (2005). Spink5-deficient mice mimic Netherton syndrome through degradation of

desmoglein 1 by epidermal protease hyperactivity. *Nat Genet, 37*(1), 56-65. doi: 10.1038/ng1493

DESCARGUES, P., DERAISON, C., PROST, C., FRAITAG, S., MAZEREEUW-HAUTIER, J., D'ALESSIO, M., ISHIDA-YAMAMOTO, A., BODEMER, C., ZAMBRUNO, G., & HOVNANIAN, A. (2006). Corneodesmosomal cadherins are preferential targets of stratum corneum trypsin- and chymotrypsin-like hyperactivity in Netherton syndrome. *J Invest Dermatol, 126*(7), 1622-1632. doi: 10.1038/sj.jid.5700284

DJABALI, K., MARTINEZ-MIR, A., HOREV, L., CHRISTIANO, A. M., & ZLOTOGORSKI, A. (2002). Evidence for extensive locus heterogeneity in Naxos disease. *J Invest Dermatol, 118*(3), 557-560. doi: 10.1046/j.0022-202x.2001.01627.x

DUIJF, P. H., VANMOLKOT, K. R., PROPPING, P., FRIEDL, W., KRIEGER, E., MCKEON, F., DOTSCH, V., BRUNNER, H. G., & VAN BOKHOVEN, H. (2002). Gain-of-function mutation in ADULT syndrome reveals the presence of a second transactivation domain in p63. *Hum Mol Genet, 11*(7), 799-804.

DUSEK, R. L., & ATTARDI, L. D. (2011). Desmosomes: new perpetrators in tumour suppression. *Nat Rev Cancer, 11*(5), 317-323. doi: 10.1038/nrc3051

DUSEK, R. L., GETSIOS, S., CHEN, F., PARK, J. K., AMARGO, E. V., CRYNS, V. L., & GREEN, K. J. (2006). The differentiation-dependent desmosomal cadherin desmoglein 1 is a novel caspase-3 target that regulates apoptosis in keratinocytes. *J Biol Chem, 281*(6), 3614-3624. doi: 10.1074/jbc.M508258200

DUSEK, R. L., GODSEL, L. M., CHEN, F., STROHECKER, A. M., GETSIOS, S., HARMON, R., MULLER, E. J., CALDELARI, R., CRYNS, V. L., & GREEN, K. J. (2007a). Plakoglobin deficiency protects keratinocytes from apoptosis. *J Invest Dermatol, 127*(4), 792-801. doi: 10.1038/sj.jid.5700615

DUSEK, R. L., GODSEL, L. M., & GREEN, K. J. (2007b). Discriminating roles of desmosomal cadherins: beyond desmosomal adhesion. *J Dermatol Sci, 45*(1), 7-21. doi: 10.1016/j.jdermsci.2006.10.006

ECKERT, R. L., STURNIOLO, M. T., BROOME, A. M., RUSE, M., & RORKE, E. A. (2005). Transglutaminase function in epidermis. *J Invest Dermatol, 124*(3), 481-492. doi: 10.1111/j.0022-202X.2005.23627.x

ELIAS, P. M., MATSUYOSHI, N., WU, H., LIN, C., WANG, Z. H., BROWN, B. E., & STANLEY, J. R. (2001). Desmoglein isoform distribution affects stratum corneum structure and function. *J Cell Biol, 153*(2), 243-249.

ELLIS, A., FIELD, J. K., FIELD, E. A., FRIEDMANN, P. S., FRYER, A., HOWARD, P., LEIGH, I. M., RISK, J., SHAW, J. M., & WHITTAKER, J. (1994). Tylosis associated with carcinoma of the oesophagus and oral leukoplakia in a large Liverpool family--a review of six generations. *Eur J Cancer B Oral Oncol, 30B*(2), 102-112.

ERKEN, H., YARIZ, K. O., DUMAN, D., KAYA, C. T., SAYIN, T., HEPER, A. O., & TEKIN, M. (2011). Cardiomyopathy with alopecia and palmoplantar keratoderma (CAPK) is caused by a JUP mutation. *Br J Dermatol, 165*(4), 917-921. doi: 10.1111/j.1365-2133.2011.10455.x

ESHKIND, L., TIAN, Q., SCHMIDT, A., FRANKE, W. W., WINDOFFER, R., & LEUBE, R. E. (2002). Loss of desmoglein 2 suggests essential functions for early embryonic development and proliferation of embryonal stem cells. *Eur J Cell Biol, 81*(11), 592-598. doi: 10.1078/0171-9335-00278

FINDLATER, G. S., MCDOUGALL, R. D., & KAUFMAN, M. H. (1993). Eyelid development, fusion and subsequent reopening in the mouse. *J Anat, 183 (Pt 1)*, 121-129.

FOGAL, V., KARTASHEVA, N. N., TRIGIANTE, G., LLANOS, S., YAP, D., VOUSDEN, K. H., & LU, X. (2005). ASPP1 and ASPP2 are new transcriptional targets of E2F. *Cell Death Differ, 12*(4), 369-376. doi: 10.1038/sj.cdd.4401562

FOMENKOV, A., HUANG, Y. P., TOPALOGLU, O., BRECHMAN, A., OSADA, M., FOMENKOVA, T., YURIDITSKY, E., TRINK, B., SIDRANSKY, D., & RATOVITSKI, E. (2003). P63 alpha

mutations lead to aberrant splicing of keratinocyte growth factor receptor in the Hay-Wells syndrome. *J Biol Chem, 278*(26), 23906-23914. doi: 10.1074/jbc.M300746200

FRIJNS, E., SACHS, N., KREFT, M., WILHELMSEN, K., & SONNENBERG, A. (2010). EGF-induced MAPK signaling inhibits hemidesmosome formation through phosphorylation of the integrin {beta}4. *J Biol Chem, 285*(48), 37650-37662. doi: 10.1074/jbc.M110.138818

FUCHS, E. (1990). Epidermal differentiation: the bare essentials. *J Cell Biol, 111*(6 Pt 2), 2807-2814.

FUCHS, E. (1996). The cytoskeleton and disease: genetic disorders of intermediate filaments. *Annu Rev Genet, 30*, 197-231. doi: 10.1146/annurev.genet.30.1.197

FUCHS, E. (2007). Scratching the surface of skin development. *Nature, 445*(7130), 834-842. doi: 10.1038/nature05659

FUCHS, E., & GREEN, H. (1980). Changes in keratin gene expression during terminal differentiation of the keratinocyte. *Cell, 19*(4), 1033-1042.

FUCHS, E., & RAGHAVAN, S. (2002). Getting under the skin of epidermal morphogenesis. *Nat Rev Genet, 3*(3), 199-209. doi: 10.1038/nrg758

FUCHS, E., & WEBER, K. (1994). Intermediate filaments: structure, dynamics, function, and disease. *Annu Rev Biochem, 63*, 345-382. doi: 10.1146/annurev.bi.63.070194.002021

GALLICANO, G. I., BAUER, C., & FUCHS, E. (2001). Rescuing desmoplakin function in extra-embryonic ectoderm reveals the importance of this protein in embryonic heart, neuroepithelium, skin and vasculature. *Development, 128*(6), 929-941.

GALLICANO, G. I., KOUKLIS, P., BAUER, C., YIN, M., VASIOUKHIN, V., DEGENSTEIN, L., & FUCHS, E. (1998). Desmoplakin is required early in development for assembly of desmosomes and cytoskeletal linkage. *J Cell Biol, 143*(7), 2009-2022.

GARCIA-GRAS, E., LOMBARDI, R., GIOCONDO, M. J., WILLERSON, J. T., SCHNEIDER, M. D., KHOURY, D. S., & MARIAN, A. J. (2006). Suppression of canonical Wnt/beta-catenin signaling by nuclear plakoglobin recapitulates phenotype of arrhythmogenic right ventricular cardiomyopathy. *J Clin Invest, 116*(7), 2012-2021. doi: 10.1172/JCI27751

GARROD, D. (2010). Desmosomes in vivo. *Dermatol Res Pract, 2010*, 212439. doi: 10.1155/2010/212439

GARROD, D., & CHIDGEY, M. (2008). Desmosome structure, composition and function. *Biochim Biophys Acta, 1778*(3), 572-587. doi: 10.1016/j.bbamem.2007.07.014

GARROD, D. R., BERIKA, M. Y., BARDSLEY, W. F., HOLMES, D., & TABERNERO, L. (2005). Hyper-adhesion in desmosomes: its regulation in wound healing and possible relationship to cadherin crystal structure. *J Cell Sci, 118*(Pt 24), 5743-5754. doi: 10.1242/jcs.02700

GARROD, D. R., MERRITT, A. J., & NIE, Z. (2002). Desmosomal adhesion: structural basis, molecular mechanism and regulation (Review). *Mol Membr Biol, 19*(2), 81-94. doi: 10.1080/09687680210132476

GARROD, D., & TABERNERO, L. (2014). Hyper-adhesion: A Unique Property of Desmosomes. *Cell Commun Adhes*, 1-8. doi: 10.3109/15419061.2014.930133

GERULL, B., HEUSER, A., WICHTER, T., PAUL, M., BASSON, C. T., MCDERMOTT, D. A., LERMAN, B. B., MARKOWITZ, S. M., ELLINOR, P. T., MACRAE, C. A., PETERS, S., GROSSMANN, K. S., DRENCKHAHN, J., MICHELY, B., SASSE-KLAASSEN, S., BIRCHMEIER, W., DIETZ, R., BREITHARDT, G., SCHULZE-BAHR, E., & THIERFELDER, L. (2004). Mutations in the desmosomal protein plakophilin-2 are common in arrhythmogenic right ventricular cardiomyopathy. *Nat Genet, 36*(11), 1162-1164. doi: 10.1038/ng1461

GODSEL, L. M., GETSIOS, S., HUEN, A. C., & GREEN, K. J. (2004). The molecular composition and function of desmosomes. *Handb Exp Pharmacol*(165), 137-193. doi: 10.1007/978-3-540-68170-0_6

GODSEL, L. M., HOBBS, R. P., & GREEN, K. J. (2008). Intermediate filament assembly: dynamics to disease. *Trends Cell Biol, 18*(1), 28-37. doi: 10.1016/j.tcb.2007.11.004

GODSEL, L. M., HSIEH, S. N., AMARGO, E. V., BASS, A. E., PASCOE-MCGILLICUDDY, L. T., HUEN, A. C., THORNE, M. E., GAUDRY, C. A., PARK, J. K., MYUNG, K., GOLDMAN, R. D., CHEW, T. L., & GREEN, K. J. (2005). Desmoplakin assembly dynamics in four dimensions: multiple phases differentially regulated by intermediate filaments and actin. *J Cell Biol, 171*(6), 1045-1059. doi: 10.1083/jcb.200510038

GREEN, K. J., GETSIOS, S., TROYANOVSKY, S., & GODSEL, L. M. (2010). Intercellular junction assembly, dynamics, and homeostasis. *Cold Spring Harb Perspect Biol, 2*(2), a000125. doi: 10.1101/cshperspect.a000125

GREEN, K. J., PARRY, D. A., STEINERT, P. M., VIRATA, M. L., WAGNER, R. M., ANGST, B. D., & NILLES, L. A. (1990). Structure of the human desmoplakins. Implications for function in the desmosomal plaque. *J Biol Chem, 265*(5), 2603-2612.

GREEN, K. J., & SIMPSON, C. L. (2007). Desmosomes: new perspectives on a classic. *J Invest Dermatol, 127*(11), 2499-2515. doi: 10.1038/sj.jid.5701015

GREEN, K. J., STAPPENBECK, T. S., PARRY, D. A., & VIRATA, M. L. (1992). Structure of desmoplakin and its association with intermediate filaments. *J Dermatol, 19*(11), 765-769.

GROSSMANN, K. S., GRUND, C., HUELSKEN, J., BEHREND, M., ERDMANN, B., FRANKE, W. W., & BIRCHMEIER, W. (2004). Requirement of plakophilin 2 for heart morphogenesis and cardiac junction formation. *J Cell Biol, 167*(1), 149-160. doi: 10.1083/jcb.200402096

HAINAUT, P., & HOLLSTEIN, M. (2000). p53 and human cancer: the first ten thousand mutations. *Adv Cancer Res, 77*, 81-137.

HAINES, R. L., & LANE, E. B. (2012). Keratins and disease at a glance. *J Cell Sci, 125*(Pt 17), 3923-3928. doi: 10.1242/jcs.099655

HAKIMELAHI, S., PARKER, H. R., GILCHRIST, A. J., BARRY, M., LI, Z., BLEACKLEY, R. C., & PASDAR, M. (2000). Plakoglobin regulates the expression of the anti-apoptotic protein BCL-2. *J Biol Chem, 275*(15), 10905-10911.

HANAHAN, D., & WEINBERG, R. A. (2000). The hallmarks of cancer. *Cell, 100*(1), 57-70.

HARMON, R. M., SIMPSON, C. L., JOHNSON, J. L., KOETSIER, J. L., DUBASH, A. D., NAJOR, N. A., SARIG, O., SPRECHER, E., & GREEN, K. J. (2013). Desmoglein-1/Erbin interaction suppresses ERK activation to support epidermal differentiation. *J Clin Invest, 123*(4), 1556-1570. doi: 10.1172/JCI65220

HARRIS, M. J., & MCLEOD, M. J. (1982). Eyelid growth and fusion in fetal mice. A scanning electron microscope study. *Anat Embryol (Berl), 164*(2), 207-220.

HASHIMOTO, T., KIYOKAWA, C., MORI, O., MIYASATO, M., CHIDGEY, M. A., GARROD, D. R., KOBAYASHI, Y., KOMORI, K., ISHII, K., AMAGAI, M., & NISHIKAWA, T. (1997). Human desmocollin 1 (Dsc1) is an autoantigen for the subcorneal pustular dermatosis type of IgA pemphigus. *J Invest Dermatol, 109*(2), 127-131.

HASSEMER, E. L., LE GALL, S. M., LIEGEL, R., MCNALLY, M., CHANG, B., ZEISS, C. J., DUBIELZIG, R. D., HORIUCHI, K., KIMURA, T., OKADA, Y., BLOBEL, C. P., & SIDJANIN, D. J. (2010). The waved with open eyelids (woe) locus is a hypomorphic mouse mutation in Adam17. *Genetics, 185*(1), 245-255. doi: 10.1534/genetics.109.113167

HATZFELD, M. (2007). Plakophilins: Multifunctional proteins or just regulators of desmosomal adhesion? *Biochim Biophys Acta, 1773*(1), 69-77. doi: 10.1016/j.bbamcr.2006.04.009

HELLER, E., KUMAR, K. V., GRILL, S. W., & FUCHS, E. (2014). Forces generated by cell intercalation tow epidermal sheets in mammalian tissue morphogenesis. *Dev Cell, 28*(6), 617-632. doi: 10.1016/j.devcel.2014.02.011

HENNINGS, H., & HOLBROOK, K. A. (1983). Calcium regulation of cell-cell contact and differentiation of epidermal cells in culture. An ultrastructural study. *Exp Cell Res, 143*(1), 127-142.

HENNINGS, H., HOLBROOK, K., STEINERT, P., & YUSPA, S. (1980). Growth and differentiation of mouse epidermal cells in culture: effects of extracellular calcium. *Curr Probl Dermatol, 10*, 3-25.

HERREN, T., GERBER, P. A., & DURU, F. (2009). Arrhythmogenic right ventricular cardiomyopathy/dysplasia: a not so rare "disease of the desmosome" with multiple clinical presentations. *Clin Res Cardiol, 98*(3), 141-158. doi: 10.1007/s00392-009-0751-4

HERRMANN, H., BAR, H., KREPLAK, L., STRELKOV, S. V., & AEBI, U. (2007). Intermediate filaments: from cell architecture to nanomechanics. *Nat Rev Mol Cell Biol, 8*(7), 562-573. doi: 10.1038/nrm2197

HERRON, B. J., RAO, C., LIU, S., LAPRADE, L., RICHARDSON, J. A., OLIVIERI, E., SEMSARIAN, C., MILLAR, S. E., STUBBS, L., & BEIER, D. R. (2005). A mutation in NFkB interacting protein 1 results in cardiomyopathy and abnormal skin development in wa3 mice. *Hum Mol Genet, 14*(5), 667-677. doi: 10.1093/hmg/ddi063

HEUSER, A., PLOVIE, E. R., ELLINOR, P. T., GROSSMANN, K. S., SHIN, J. T., WICHTER, T., BASSON, C. T., LERMAN, B. B., SASSE-KLAASSEN, S., THIERFELDER, L., MACRAE, C. A., & GERULL, B. (2006). Mutant desmocollin-2 causes arrhythmogenic right ventricular cardiomyopathy. *Am J Hum Genet, 79*(6), 1081-1088. doi: 10.1086/509044

HIRASHIMA, M., BERNSTEIN, A., STANFORD, W. L., & ROSSANT, J. (2004). Gene-trap expression screening to identify endothelial-specific genes. *Blood, 104*(3), 711-718. doi: 10.1182/blood-2004-01-0254

HIRASHIMA, M., SANO, K., MORISADA, T., MURAKAMI, K., ROSSANT, J., & SUDA, T. (2008). Lymphatic vessel assembly is impaired in Aspp1-deficient mouse embryos. *Dev Biol, 316*(1), 149-159. doi: 10.1016/j.ydbio.2008.01.023

HOWEL-EVANS, W., MC, CONNELL RB, CLARKE, C. A., & SHEPPARD, P. M. (1958). Carcinoma of the oesophagus with keratosis palmaris et plantaris (tylosis): a study of two families. *Q J Med, 27*(107), 413-429.

HU, P., BERKOWITZ, P., O'KEEFE, E. J., & RUBENSTEIN, D. S. (2003). Keratinocyte adherens junctions initiate nuclear signaling by translocation of plakoglobin from the membrane to the nucleus. *J Invest Dermatol, 121*(2), 242-251. doi: 10.1046/j.1523-1747.2003.12376.x

HUANG, J., DATTILO, L. K., RAJAGOPAL, R., LIU, Y., KAARTINEN, V., MISHINA, Y., DENG, C. X., UMANS, L., ZWIJSEN, A., ROBERTS, A. B., & BEEBE, D. C. (2009). FGF-regulated BMP signaling is required for eyelid closure and to specify conjunctival epithelial cell fate. *Development, 136*(10), 1741-1750. doi: 10.1242/dev.034082

HUNT, D. M., RICKMAN, L., WHITTOCK, N. V., EADY, R. A., SIMRAK, D., DOPPING-HEPENSTAL, P. J., STEVENS, H. P., ARMSTRONG, D. K., HENNIES, H. C., KUSTER, W., HUGHES, A. E., ARNEMANN, J., LEIGH, I. M., MCGRATH, J. A., KELSELL, D. P., & BUXTON, R. S. (2001). Spectrum of dominant mutations in the desmosomal cadherin desmoglein 1, causing the skin disease striate palmoplantar keratoderma. *Eur J Hum Genet, 9*(3), 197-203. doi: 10.1038/sj.ejhg.5200605

IHRIE, R. A., MARQUES, M. R., NGUYEN, B. T., HORNER, J. S., PAPAZOGLU, C., BRONSON, R. T., MILLS, A. A., & ATTARDI, L. D. (2005). Perp is a p63-regulated gene essential for epithelial integrity. *Cell, 120*(6), 843-856. doi: 10.1016/j.cell.2005.01.008

ITIN, P. H., & FISTAROL, S. K. (2005). Palmoplantar keratodermas. *Clin Dermatol, 23*(1), 15-22. doi: 10.1016/j.clindermatol.2004.09.005

IWABUCHI, K., LI, B., MASSA, H. F., TRASK, B. J., DATE, T., & FIELDS, S. (1998). Stimulation of p53-mediated transcriptional activation by the p53-binding proteins, 53BP1 and 53BP2. *J Biol Chem, 273*(40), 26061-26068.

IWAMOTO, R., YAMAZAKI, S., ASAKURA, M., TAKASHIMA, S., HASUWA, H., MIYADO, K., ADACHI, S., KITAKAZE, M., HASHIMOTO, K., RAAB, G., NANBA, D., HIGASHIYAMA, S.,

HORI, M., KLAGSBRUN, M., & MEKADA, E. (2003). Heparin-binding EGF-like growth factor and ErbB signaling is essential for heart function. *Proc Natl Acad Sci U S A, 100*(6), 3221-3226. doi: 10.1073/pnas.0537588100

JAULIN-BASTARD, F., ARSANTO, J. P., LE BIVIC, A., NAVARRO, C., VELY, F., SAITO, H., MARCHETTO, S., HATZFELD, M., SANTONI, M. J., BIRNBAUM, D., & BORG, J. P. (2002). Interaction between Erbin and a Catenin-related protein in epithelial cells. *J Biol Chem, 277*(4), 2869-2875. doi: 10.1074/jbc.M109652200

JIANG, C. K., MAGNALDO, T., OHTSUKI, M., FREEDBERG, I. M., BERNERD, F., & BLUMENBERG, M. (1993). Epidermal growth factor and transforming growth factor alpha specifically induce the activation- and hyperproliferation-associated keratins 6 and 16. *Proc Natl Acad Sci U S A, 90*(14), 6786-6790.

JIMENEZ-JAIMEZ, J., LOPEZ MORENO, E., BARRIO LOPEZ, M. T., GONZALEZ-MOLINA, M., ALVAREZ, M., & TERCEDOR, L. (2014). A recessive inheritance pattern contributes to arrhythmogenic biventricular cardiomyopathy. *Rev Esp Cardiol (Engl Ed), 67*(9), 772-774. doi: 10.1016/j.rec.2014.04.012

JIN, C., YIN, F., LIN, M., LI, H., WANG, Z., WENG, J., LIU, M., DA DONG, X., QU, J., & TU, L. (2008). GPR48 regulates epithelial cell proliferation and migration by activating EGFR during eyelid development. *Invest Ophthalmol Vis Sci, 49*(10), 4245-4253. doi: 10.1167/iovs.08-1860

JONCA, N., GUERRIN, M., HADJIOLOVA, K., CAUBET, C., GALLINARO, H., SIMON, M., & SERRE, G. (2002). Corneodesmosin, a component of epidermal corneocyte desmosomes, displays homophilic adhesive properties. *J Biol Chem, 277*(7), 5024-5029. doi: 10.1074/jbc.M108438200

JONKMAN, M. F., PASMOOIJ, A. M., PASMANS, S. G., VAN DEN BERG, M. P., TER HORST, H. J., TIMMER, A., & PAS, H. H. (2005). Loss of desmoplakin tail causes lethal acantholytic epidermolysis bullosa. *Am J Hum Genet, 77*(4), 653-660. doi: 10.1086/496901

KALININ, A. E., KAJAVA, A. V., & STEINERT, P. M. (2002). Epithelial barrier function: assembly and structural features of the cornified cell envelope. *Bioessays, 24*(9), 789-800. doi: 10.1002/bies.10144

KAMPA, K. M., ACOBA, J. D., CHEN, D., GAY, J., LEE, H., BEEMER, K., PADIERNOS, E., BOONMARK, N., ZHU, Z., FAN, A. C., BAILEY, A. S., FLEMING, W. H., CORLESS, C., FELSHER, D. W., NAUMOVSKI, L., & LOPEZ, C. D. (2009). Apoptosis-stimulating protein of p53 (ASPP2) heterozygous mice are tumor-prone and have attenuated cellular damage-response thresholds. *Proc Natl Acad Sci U S A, 106*(11), 4390-4395. doi: 10.1073/pnas.0809080106

KAZ, A. M., LUO, Y., DZIECIATKOWSKI, S., CHAK, A., WILLIS, J. E., UPTON, M. P., LEIDNER, R. S., & GRADY, W. M. (2012). Aberrantly methylated PKP1 in the progression of Barrett's esophagus to esophageal adenocarcinoma. *Genes Chromosomes Cancer, 51*(4), 384-393. doi: 10.1002/gcc.21923

KELLER, D. I., STEPOWSKI, D., BALMER, C., SIMON, F., GUENTHARD, J., BAUER, F., ITIN, P., DAVID, N., DROUIN-GARRAUD, V., & FRESSART, V. (2012). De novo heterozygous desmoplakin mutations leading to Naxos-Carvajal disease. *Swiss Med Wkly, 142*, w13670. doi: 10.4414/smw.2012.13670

KELSELL, D. P., RISK, J. M., LEIGH, I. M., STEVENS, H. P., ELLIS, A., HENNIES, H. C., REIS, A., WEISSENBACH, J., BISHOP, D. T., SPURR, N. K., & FIELD, J. K. (1996). Close mapping of the focal non-epidermolytic palmoplantar keratoderma (PPK) locus associated with oesophageal cancer (TOC). *Hum Mol Genet, 5*(6), 857-860.

KILIC, T., BABAOGLU, K., AYGUN, F., VURAL, A., URAL, D., AGACDIKEN, A., ANIK, Y., & KOMSUOGLU, B. (2007). Biventricular involvement in a Turkish boy with palmoplantar hyperkeratosis and curly hair, an unusual presentation of Naxos-Carvajal syndrome. *Int J Cardiol, 115*(3), e122-125. doi: 10.1016/j.ijcard.2006.08.097

KIMURA, T. E., MERRITT, A. J., & GARROD, D. R. (2007). Calcium-independent desmosomes of keratinocytes are hyper-adhesive. *J Invest Dermatol, 127*(4), 775-781. doi: 10.1038/sj.jid.5700643

KIMURA, T. E., MERRITT, A. J., LOCK, F. R., ECKERT, J. J., FLEMING, T. P., & GARROD, D. R. (2012). Desmosomal adhesiveness is developmentally regulated in the mouse embryo and modulated during trophectoderm migration. *Dev Biol, 369*(2), 286-297. doi: 10.1016/j.ydbio.2012.06.025

KLESSNER, J. L., DESAI, B. V., AMARGO, E. V., GETSIOS, S., & GREEN, K. J. (2009). EGFR and ADAMs cooperate to regulate shedding and endocytic trafficking of the desmosomal cadherin desmoglein 2. *Mol Biol Cell, 20*(1), 328-337. doi: 10.1091/mbc.E08-04-0356

KLJUIC, A., BAZZI, H., SUNDBERG, J. P., MARTINEZ-MIR, A., O'SHAUGHNESSY, R., MAHONEY, M. G., LEVY, M., MONTAGUTELLI, X., AHMAD, W., AITA, V. M., GORDON, D., UITTO, J., WHITING, D., OTT, J., FISCHER, S., GILLIAM, T. C., JAHODA, C. A., MORRIS, R. J., PANTELEYEV, A. A., NGUYEN, V. T., & CHRISTIANO, A. M. (2003a). Desmoglein 4 in hair follicle differentiation and epidermal adhesion: evidence from inherited hypotrichosis and acquired pemphigus vulgaris. *Cell, 113*(2), 249-260.

KLJUIC, A., GILEAD, L., MARTINEZ-MIR, A., FRANK, J., CHRISTIANO, A. M., & ZLOTOGORSKI, A. (2003b). A nonsense mutation in the desmoglein 1 gene underlies striate keratoderma. *Exp Dermatol, 12*(4), 523-527.

KOCH, P. J., MAHONEY, M. G., COTSARELIS, G., ROTHENBERGER, K., LAVKER, R. M., & STANLEY, J. R. (1998). Desmoglein 3 anchors telogen hair in the follicle. *J Cell Sci, 111 (Pt 17)*, 2529-2537.

KOCH, P. J., MAHONEY, M. G., ISHIKAWA, H., PULKKINEN, L., UITTO, J., SHULTZ, L., MURPHY, G. F., WHITAKER-MENEZES, D., & STANLEY, J. R. (1997). Targeted disruption of the pemphigus vulgaris antigen (desmoglein 3) gene in mice causes loss of keratinocyte cell adhesion with a phenotype similar to pemphigus vulgaris. *J Cell Biol, 137*(5), 1091-1102.

KOLLIGS, F. T., KOLLIGS, B., HAJRA, K. M., HU, G., TANI, M., CHO, K. R., & FEARON, E. R. (2000). gamma-catenin is regulated by the APC tumor suppressor and its oncogenic activity is distinct from that of beta-catenin. *Genes Dev, 14*(11), 1319-1331.

KOSTER, M. I. (2010). p63 in skin development and ectodermal dysplasias. *J Invest Dermatol, 130*(10), 2352-2358. doi: 10.1038/jid.2010.119

KOSTER, M. I., & ROOP, D. R. (2007). Mechanisms regulating epithelial stratification. *Annu Rev Cell Dev Biol, 23*, 93-113. doi: 10.1146/annurev.cellbio.23.090506.123357

KOTTKE, M. D., DELVA, E., & KOWALCZYK, A. P. (2006). The desmosome: cell science lessons from human diseases. *J Cell Sci, 119*(Pt 5), 797-806. doi: 10.1242/jcs.02888

KOUKLIS, P. D., HUTTON, E., & FUCHS, E. (1994). Making a connection: direct binding between keratin intermediate filaments and desmosomal proteins. *J Cell Biol, 127*(4), 1049-1060.

KOWALCZYK, A. P., BORNSLAEGER, E. A., BORGWARDT, J. E., PALKA, H. L., DHALIWAL, A. S., CORCORAN, C. M., DENNING, M. F., & GREEN, K. J. (1997). The amino-terminal domain of desmoplakin binds to plakoglobin and clusters desmosomal cadherin-plakoglobin complexes. *J Cell Biol, 139*(3), 773-784.

KOWALCZYK, A. P., HATZFELD, M., BORNSLAEGER, E. A., KOPP, D. S., BORGWARDT, J. E., CORCORAN, C. M., SETTLER, A., & GREEN, K. J. (1999). The head domain of plakophilin-1 binds to desmoplakin and enhances its recruitment to desmosomes. Implications for cutaneous disease. *J Biol Chem, 274*(26), 18145-18148.

KRAWCZYK, W. S., & WILGRAM, G. F. (1973). Hemidesmosome and desmosome morphogenesis during epidermal wound healing. *J Ultrastruct Res, 45*(1), 93-101.

KREPLAK, L., & FUDGE, D. (2007). Biomechanical properties of intermediate filaments: from tissues to single filaments and back. *Bioessays, 29*(1), 26-35. doi: 10.1002/bies.20514

KURZEN, H., MUNZING, I., & HARTSCHUH, W. (2003). Expression of desmosomal proteins in squamous cell carcinomas of the skin. *J Cutan Pathol, 30*(10), 621-630.

LACOUTURE, M. E. (2006). Mechanisms of cutaneous toxicities to EGFR inhibitors. *Nat Rev Cancer, 6*(10), 803-812. doi: 10.1038/nrc1970

LAI-CHEONG, J. E., ARITA, K., & MCGRATH, J. A. (2007). Genetic diseases of junctions. *J Invest Dermatol, 127*(12), 2713-2725. doi: 10.1038/sj.jid.5700727

LAI CHEONG, J. E., WESSAGOWIT, V., & MCGRATH, J. A. (2005). Molecular abnormalities of the desmosomal protein desmoplakin in human disease. *Clin Exp Dermatol, 30*(3), 261-266. doi: 10.1111/j.1365-2230.2005.01736.x

LAURIKKALA, J., MIKKOLA, M. L., JAMES, M., TUMMERS, M., MILLS, A. A., & THESLEFF, I. (2006). p63 regulates multiple signalling pathways required for ectodermal organogenesis and differentiation. *Development, 133*(8), 1553-1563. doi: 10.1242/dev.02325

LECHLER, T., & FUCHS, E. (2007). Desmoplakin: an unexpected regulator of microtubule organization in the epidermis. *J Cell Biol, 176*(2), 147-154. doi: 10.1083/jcb.200609109

LECLERC, E. A., HUCHENQ, A., MATTIUZZO, N. R., METZGER, D., CHAMBON, P., GHYSELINCK, N. B., SERRE, G., JONCA, N., & GUERRIN, M. (2009). Corneodesmosin gene ablation induces lethal skin-barrier disruption and hair-follicle degeneration related to desmosome dysfunction. *J Cell Sci, 122*(Pt 15), 2699-2709. doi: 10.1242/jcs.050302

LETAI, A., COULOMBE, P. A., & FUCHS, E. (1992). Do the ends justify the mean? Proline mutations at the ends of the keratin coiled-coil rod segment are more disruptive than internal mutations. *J Cell Biol, 116*(5), 1181-1195.

LEWIS, J. E., WAHL, J. K., 3RD, SASS, K. M., JENSEN, P. J., JOHNSON, K. R., & WHEELOCK, M. J. (1997). Cross-talk between adherens junctions and desmosomes depends on plakoglobin. *J Cell Biol, 136*(4), 919-934.

LI, F., CHONG, Z. Z., & MAIESE, K. (2006). Winding through the WNT pathway during cellular development and demise. *Histol Histopathol, 21*(1), 103-124.

LI, G., GUSTAFSON-BROWN, C., HANKS, S. K., NASON, K., ARBEIT, J. M., POGLIANO, K., WISDOM, R. M., & JOHNSON, R. S. (2003). c-Jun is essential for organization of the epidermal leading edge. *Dev Cell, 4*(6), 865-877.

LICHTI, U., ANDERS, J., & YUSPA, S. H. (2008). Isolation and short-term culture of primary keratinocytes, hair follicle populations and dermal cells from newborn mice and keratinocytes from adult mice for in vitro analysis and for grafting to immunodeficient mice. *Nat Protoc, 3*(5), 799-810. doi: 10.1038/nprot.2008.50

LIU, W. K., JIANG, X. Y., REN, J. K., & ZHANG, Z. X. (2010). Expression pattern of the ASPP family members in endometrial endometrioid adenocarcinoma. *Onkologie, 33*(10), 500-503. doi: 10.1159/000319692

LIU, Z. J., LU, X., ZHANG, Y., ZHONG, S., GU, S. Z., ZHANG, X. B., YANG, X., & XIN, H. M. (2005). Downregulated mRNA expression of ASPP and the hypermethylation of the 5'-untranslated region in cancer cell lines retaining wild-type p53. *FEBS Lett, 579*(7), 1587-1590. doi: 10.1016/j.febslet.2005.01.069

LIU, Z. J., ZHANG, Y., ZHANG, X. B., & YANG, X. (2004). Abnormal mRNA expression of ASPP members in leukemia cell lines. *Leukemia, 18*(4), 880. doi: 10.1038/sj.leu.2403300

LIU, Z., ZHANG, X., HUANG, D., LIU, Y., ZHANG, X., LIU, L., LI, G., DAI, Y., TAN, H., XIAO, J., & TIAN, Y. (2012). Elevated expression of iASPP in head and neck squamous cell carcinoma and its clinical significance. *Med Oncol, 29*(5), 3381-3388. doi: 10.1007/s12032-012-0306-9

LLANOS, S., ROYER, C., LU, M., BERGAMASCHI, D., LEE, W. H., & LU, X. (2011). Inhibitory member of the apoptosis-stimulating proteins of the p53 family (iASPP) interacts with protein phosphatase 1 via a noncanonical binding motif. *J Biol Chem, 286*(50), 43039-43044. doi: 10.1074/jbc.M111.270751

LLOYD, C., YU, Q. C., CHENG, J., TURKSEN, K., DEGENSTEIN, L., HUTTON, E., & FUCHS, E. (1995). The basal keratin network of stratified squamous epithelia: defining K15 function in the absence of K14. *J Cell Biol, 129*(5), 1329-1344.

LOMBARDI, R., DONG, J., RODRIGUEZ, G., BELL, A., LEUNG, T. K., SCHWARTZ, R. J., WILLERSON, J. T., BRUGADA, R., & MARIAN, A. J. (2009). Genetic fate mapping identifies second heart field progenitor cells as a source of adipocytes in arrhythmogenic right ventricular cardiomyopathy. *Circ Res, 104*(9), 1076-1084. doi: 10.1161/CIRCRESAHA.109.196899

LORCH, J. H., KLESSNER, J., PARK, J. K., GETSIOS, S., WU, Y. L., STACK, M. S., & GREEN, K. J. (2004). Epidermal growth factor receptor inhibition promotes desmosome assembly and strengthens intercellular adhesion in squamous cell carcinoma cells. *J Biol Chem, 279*(35), 37191-37200. doi: 10.1074/jbc.M405123200

LOSSOS, I. S., NATKUNAM, Y., LEVY, R., & LOPEZ, C. D. (2002). Apoptosis stimulating protein of p53 (ASPP2) expression differs in diffuse large B-cell and follicular center lymphoma: correlation with clinical outcome. *Leuk Lymphoma, 43*(12), 2309-2317. doi: 10.1080/1042819021000040017

LU, B., GUO, H., ZHAO, J., WANG, C., WU, G., PANG, M., TONG, X., BU, F., LIANG, A., HOU, S., FAN, X., DAI, J., WANG, H., & GUO, Y. (2010). Increased expression of iASPP, regulated by hepatitis B virus X protein-mediated NF-kappaB activation, in hepatocellular carcinoma. *Gastroenterology, 139*(6), 2183-2194 e2185. doi: 10.1053/j.gastro.2010.06.049

LU, M., BREYSSENS, H., SALTER, V., ZHONG, S., HU, Y., BAER, C., RATNAYAKA, I., SULLIVAN, A., BROWN, N. R., ENDICOTT, J., KNAPP, S., KESSLER, B. M., MIDDLETON, M. R., SIEBOLD, C., JONES, E. Y., SVIDERSKAYA, E. V., CEBON, J., JOHN, T., CABALLERO, O. L., GODING, C. R., & LU, X. (2013). Restoring p53 function in human melanoma cells by inhibiting MDM2 and cyclin B1/CDK1-phosphorylated nuclear iASPP. *Cancer Cell, 23*(5), 618-633. doi: 10.1016/j.ccr.2013.03.013

LU, M., ZAK, J., CHEN, S., SANCHEZ-PULIDO, L., SEVERSON, D. T., ENDICOTT, J., PONTING, C. P., SCHOFIELD, C. J., & LU, X. (2014). A code for RanGDP binding in ankyrin repeats defines a nuclear import pathway. *Cell, 157*(5), 1130-1145. doi: 10.1016/j.cell.2014.05.006

LUETTEKE, N. C., QIU, T. H., PEIFFER, R. L., OLIVER, P., SMITHIES, O., & LEE, D. C. (1993). TGF alpha deficiency results in hair follicle and eye abnormalities in targeted and waved-1 mice. *Cell, 73*(2), 263-278.

LUMPKIN, E. A., & CATERINA, M. J. (2007). Mechanisms of sensory transduction in the skin. *Nature, 445*(7130), 858-865. doi: 10.1038/nature05662

MAEDA, O., USAMI, N., KONDO, M., TAKAHASHI, M., GOTO, H., SHIMOKATA, K., KUSUGAMI, K., & SEKIDO, Y. (2004). Plakoglobin (gamma-catenin) has TCF/LEF family-dependent transcriptional activity in beta-catenin-deficient cell line. *Oncogene, 23*(4), 964-972. doi: 10.1038/sj.onc.1207254

MAK, V. C., LEE, L., SIU, M. K., WONG, O. G., LU, X., NGAN, H. Y., WONG, E. S., & CHEUNG, A. N. (2011). Downregulation of ASPP1 in gestational trophoblastic disease: correlation with hypermethylation, apoptotic activity and clinical outcome. *Mod Pathol, 24*(4), 522-532. doi: 10.1038/modpathol.2010.216

MAK, V. C., LEE, L., SIU, M. K., WONG, O. G., LU, X., NGAN, H. Y., WONG, E. S., & CHEUNG, A. N. (2013). Downregulation of ASPP2 in choriocarcinoma contributes to increased migratory potential through Src signaling pathway activation. *Carcinogenesis, 34*(9), 2170-2177. doi: 10.1093/carcin/bgt161

MANN, G. B., FOWLER, K. J., GABRIEL, A., NICE, E. C., WILLIAMS, R. L., & DUNN, A. R. (1993). Mice with a null mutation of the TGF alpha gene have abnormal skin architecture, wavy hair, and curly whiskers and often develop corneal inflammation. *Cell, 73*(2), 249-261.

MARCUS, F. I., EDSON, S., & TOWBIN, J. A. (2013). Genetics of arrhythmogenic right ventricular cardiomyopathy: a practical guide for physicians. *J Am Coll Cardiol, 61*(19), 1945-1948. doi: 10.1016/j.jacc.2013.01.073

MARQUES, M. R., IHRIE, R. A., HORNER, J. S., & ATTARDI, L. D. (2006). The requirement for perp in postnatal viability and epithelial integrity reflects an intrinsic role in stratified epithelia. *J Invest Dermatol, 126*(1), 69-73. doi: 10.1038/sj.jid.5700032

MARTIN, P. (1997). Wound healing--aiming for perfect skin regeneration. *Science, 276*(5309), 75-81.

MAZZALUPO, S., & COULOMBE, P. A. (2001). A reporter transgene based on a human keratin 6 gene promoter is specifically expressed in the periderm of mouse embryos. *Mech Dev, 100*(1), 65-69.

MAZZALUPO, S., WONG, P., MARTIN, P., & COULOMBE, P. A. (2003). Role for keratins 6 and 17 during wound closure in embryonic mouse skin. *Dev Dyn, 226*(2), 356-365. doi: 10.1002/dvdy.10245

MCGRATH, J. A. (2005). Inherited disorders of desmosomes. *Australas J Dermatol, 46*(4), 221-229. doi: 10.1111/j.1440-0960.2005.00188.x

MCGRATH, J. A., HOEGER, P. H., CHRISTIANO, A. M., MCMILLAN, J. R., MELLERIO, J. E., ASHTON, G. H., DOPPING-HEPENSTAL, P. J., LAKE, B. D., LEIGH, I. M., HARPER, J. I., & EADY, R. A. (1999). Skin fragility and hypohidrotic ectodermal dysplasia resulting from ablation of plakophilin 1. *Br J Dermatol, 140*(2), 297-307.

MCGRATH, J. A., MCMILLAN, J. R., SHEMANKO, C. S., RUNSWICK, S. K., LEIGH, I. M., LANE, E. B., GARROD, D. R., & EADY, R. A. (1997). Mutations in the plakophilin 1 gene result in ectodermal dysplasia/skin fragility syndrome. *Nat Genet, 17*(2), 240-244. doi: 10.1038/ng1097-240

MCKOY, G., PROTONOTARIOS, N., CROSBY, A., TSATSOPOULOU, A., ANASTASAKIS, A., COONAR, A., NORMAN, M., BABOONIAN, C., JEFFERY, S., & MCKENNA, W. J. (2000). Identification of a deletion in plakoglobin in arrhythmogenic right ventricular cardiomyopathy with palmoplantar keratoderma and woolly hair (Naxos disease). *Lancet, 355*(9221), 2119-2124. doi: 10.1016/S0140-6736(00)02379-5

MERRITT, A. J., BERIKA, M. Y., ZHAI, W., KIRK, S. E., JI, B., HARDMAN, M. J., & GARROD, D. R. (2002). Suprabasal desmoglein 3 expression in the epidermis of transgenic mice results in hyperproliferation and abnormal differentiation. *Mol Cell Biol, 22*(16), 5846-5858.

MERRITT, A. J., SCOTHERN, A., & BHATTACHARYYA, T. (2006). Assays for the calcium sensitivity of desmosomes. *Methods Mol Biol, 341*, 167-183. doi: 10.1385/1-59745-113-4:167

MESE, G., RICHARD, G., & WHITE, T. W. (2007). Gap junctions: basic structure and function. *J Invest Dermatol, 127*(11), 2516-2524. doi: 10.1038/sj.jid.5700770

MILLS, A. A., ZHENG, B., WANG, X. J., VOGEL, H., ROOP, D. R., & BRADLEY, A. (1999). p63 is a p53 homologue required for limb and epidermal morphogenesis. *Nature, 398*(6729), 708-713. doi: 10.1038/19531

MINE, N., IWAMOTO, R., & MEKADA, E. (2005). HB-EGF promotes epithelial cell migration in eyelid development. *Development, 132*(19), 4317-4326. doi: 10.1242/dev.02030

MIRAVET, S., PIEDRA, J., CASTANO, J., RAURELL, I., FRANCI, C., DUNACH, M., & GARCIA DE HERREROS, A. (2003). Tyrosine phosphorylation of plakoglobin causes contrary effects on its association with desmosomes and adherens junction components and modulates beta-catenin-mediated transcription. *Mol Cell Biol, 23*(20), 7391-7402.

MOLL, I., KURZEN, H., LANGBEIN, L., & FRANKE, W. W. (1997). The distribution of the desmosomal protein, plakophilin 1, in human skin and skin tumors. *J Invest Dermatol, 108*(2), 139-146.

MORI, S., ITO, G., USAMI, N., YOSHIOKA, H., UEDA, Y., KODAMA, Y., TAKAHASHI, M., FONG, K. M., SHIMOKATA, K., & SEKIDO, Y. (2004). p53 apoptotic pathway molecules are

frequently and simultaneously altered in nonsmall cell lung carcinoma. *Cancer, 100*(8), 1673-1682. doi: 10.1002/cncr.20164

MORRIS, E. (2013) Investigating the role of iASPP in normal prostate development and prostate tumourigenesis. DPhil thesis. *University of Oxford, UK*

MORITA, K., & MIYACHI, Y. (2003). Tight junctions in the skin. *J Dermatol Sci, 31*(2), 81-89.

NAGAO, S., KITAJIMA, Y., NAGATA, K., INOUE, S., YAOITA, H., & NOZAWA, Y. (1989). Correlation between cell-cell contact formation and activation of protein kinase C in a human squamous cell carcinoma cell line. *J Invest Dermatol, 92*(2), 175-178.

NAUMOVSKI, L., & CLEARY, M. L. (1996). The p53-binding protein 53BP2 also interacts with Bc12 and impedes cell cycle progression at G2/M. *Mol Cell Biol, 16*(7), 3884-3892.

NEUBER, S., MUHMER, M., WRATTEN, D., KOCH, P. J., MOLL, R., & SCHMIDT, A. (2010). The desmosomal plaque proteins of the plakophilin family. *Dermatol Res Pract, 2010*, 101452. doi: 10.1155/2010/101452

NIESSEN, C. M. (2007). Tight junctions/adherens junctions: basic structure and function. *J Invest Dermatol, 127*(11), 2525-2532. doi: 10.1038/sj.jid.5700865

NITOIU, D., ETHERIDGE, S. L., & KELSELL, D. P. (2014). Insights into desmosome biology from inherited human skin disease and cardiocutaneous syndromes. *Cell Commun Adhes, 21*(3), 129-140. doi: 10.3109/15419061.2014.908854

NORGETT, E. E., HATSELL, S. J., CARVAJAL-HUERTA, L., CABEZAS, J. C., COMMON, J., PURKIS, P. E., WHITTOCK, N., LEIGH, I. M., STEVENS, H. P., & KELSELL, D. P. (2000). Recessive mutation in desmoplakin disrupts desmoplakin-intermediate filament interactions and causes dilated cardiomyopathy, woolly hair and keratoderma. *Hum Mol Genet, 9*(18), 2761-2766.

NORTH, A. J., BARDSLEY, W. G., HYAM, J., BORNSLAEGER, E. A., CORDINGLEY, H. C., TRINNAMAN, B., HATZFELD, M., GREEN, K. J., MAGEE, A. I., & GARROD, D. R. (1999). Molecular map of the desmosomal plaque. *J Cell Sci, 112 (Pt 23)*, 4325-4336.

NOTARI, M., HU, Y., KOCH, S., LU, M., RATNAYAKA, I., ZHONG, S., BAER, C., PAGOTTO, A., GOLDIN, R., SALTER, V., CANDI, E., MELINO, G., & LU, X. (2011). Inhibitor of apoptosis-stimulating protein of p53 (iASPP) prevents senescence and is required for epithelial stratification. *Proc Natl Acad Sci U S A, 108*(40), 16645-16650. doi: 10.1073/pnas.1102292108

NOTARI, M. (2012) Investigation of the biological role of iASPP *in vivo*. DPhil thesis. *University of Oxford, UK*

NOVAK, A., & DEDHAR, S. (1999). Signaling through beta-catenin and Lef/Tcf. *Cell Mol Life Sci, 56*(5-6), 523-537.

O'KEEFE, E. J., ERICKSON, H. P., & BENNETT, V. (1989). Desmoplakin I and desmoplakin II. Purification and characterization. *J Biol Chem, 264*(14), 8310-8318.

ODLAND, G., & ROSS, R. (1968). Human wound repair. I. Epidermal regeneration. *J Cell Biol, 39*(1), 135-151.

OMARY, M. B., COULOMBE, P. A., & MCLEAN, W. H. (2004). Intermediate filament proteins and their associated diseases. *N Engl J Med, 351*(20), 2087-2100. doi: 10.1056/NEJMra040319

ONG, C. A., LAO-SIRIEIX, P., & FITZGERALD, R. C. (2010). Biomarkers in Barrett's esophagus and esophageal adenocarcinoma: predictors of progression and prognosis. *World J Gastroenterol, 16*(45), 5669-5681.

OUYANG, P., & SUGRUE, S. P. (1996). Characterization of pinin, a novel protein associated with the desmosome-intermediate filament complex. *J Cell Biol, 135*(4), 1027-1042.

PARIKH, N., NAGARAJAN, P., SEI-ICHI, M., SINHA, S., & GARRETT-SINHA, L. A. (2008). Isolation and characterization of an immortalized oral keratinocyte cell line of mouse origin. *Arch Oral Biol, 53*(11), 1091-1100. doi: 10.1016/j.archoralbio.2008.07.002

PARK, S. W., AN, C. H., KIM, S. S., YOO, N. J., & LEE, S. H. (2010). Mutational Analysis of ASPP1 and ASPP2 Genes, a p53-related Gene, in Gastric and Cololorectal Cancers with Microsatellite Instability. *Gut Liver, 4*(2), 292-293. doi: 10.5009/gnl.2010.4.2.292

PASDAR, M., KRZEMINSKI, K. A., & NELSON, W. J. (1991). Regulation of desmosome assembly in MDCK epithelial cells: coordination of membrane core and cytoplasmic plaque domain assembly at the plasma membrane. *J Cell Biol, 113*(3), 645-655.

PASDAR, M., & NELSON, W. J. (1988). Kinetics of desmosome assembly in Madin-Darby canine kidney epithelial cells: temporal and spatial regulation of desmoplakin organization and stabilization upon cell-cell contact. II. Morphological analysis. *J Cell Biol, 106*(3), 687-695.

PASDAR, M., & NELSON, W. J. (1989). Regulation of desmosome assembly in epithelial cells: kinetics of synthesis, transport, and stabilization of desmoglein I, a major protein of the membrane core domain. *J Cell Biol, 109*(1), 163-177.

PEARSON, A. A. (1980). The development of the eyelids. Part I. External features. *J Anat, 130*(Pt 1), 33-42.

PENN, E. J., BURDETT, I. D., HOBSON, C., MAGEE, A. I., & REES, D. A. (1987). Structure and assembly of desmosome junctions: biosynthesis and turnover of the major desmosome components of Madin-Darby canine kidney cells in low calcium medium. *J Cell Biol, 105*(5), 2327-2334.

PENN, E. J., HOBSON, C., REES, D. A., & MAGEE, A. I. (1989). The assembly of the major desmosome glycoproteins of Madin-Darby canine kidney cells. *FEBS Lett, 247*(1), 13-16.

PESCHON, J. J., SLACK, J. L., REDDY, P., STOCKING, K. L., SUNNARBORG, S. W., LEE, D. C., RUSSELL, W. E., CASTNER, B. J., JOHNSON, R. S., FITZNER, J. N., BOYCE, R. W., NELSON, N., KOZLOSKY, C. J., WOLFSON, M. F., RAUCH, C. T., CERRETTI, D. P., PAXTON, R. J., MARCH, C. J., & BLACK, R. A. (1998). An essential role for ectodomain shedding in mammalian development. *Science, 282*(5392), 1281-1284.

PETERS, B., KIRFEL, J., BUSSOW, H., VIDAL, M., & MAGIN, T. M. (2001). Complete cytolysis and neonatal lethality in keratin 5 knockout mice reveal its fundamental role in skin integrity and in epidermolysis bullosa simplex. *Mol Biol Cell, 12*(6), 1775-1789.

PILICHOU, K., NAVA, A., BASSO, C., BEFFAGNA, G., BAUCE, B., LORENZON, A., FRIGO, G., VETTORI, A., VALENTE, M., TOWBIN, J., THIENE, G., DANIELI, G. A., & RAMPAZZO, A. (2006). Mutations in desmoglein-2 gene are associated with arrhythmogenic right ventricular cardiomyopathy. *Circulation, 113*(9), 1171-1179. doi: 10.1161/CIRCULATIONAHA.105.583674

PROTONOTARIOS, N., TSATSOPOULOU, A., PATSOURAKOS, P., ALEXOPOULOS, D., GEZERLIS, P., SIMITSIS, S., & SCAMPARDONIS, G. (1986). Cardiac abnormalities in familial palmoplantar keratosis. *Br Heart J, 56*(4), 321-326.

RAMANI, V. C., HENNINGS, L., & HAUN, R. S. (2008). Desmoglein 2 is a substrate of kallikrein 7 in pancreatic cancer. *BMC Cancer, 8*, 373. doi: 10.1186/1471-2407-8-373

REICHELT, J., BAUER, C., PORTER, R., LANE, E., & MAGIN, V. (1997). Out of balance: consequences of a partial keratin 10 knockout. *J Cell Sci, 110 (Pt 18)*, 2175-2186.

RESING, K. A., DALE, B. A., & WALSH, K. A. (1985). Multiple copies of phosphorylated filaggrin in epidermal profilaggrin demonstrated by analysis of tryptic peptides. *Biochemistry, 24*(15), 4167-4175.

RICKMAN, L., SIMRAK, D., STEVENS, H. P., HUNT, D. M., KING, I. A., BRYANT, S. P., EADY, R. A., LEIGH, I. M., ARNEMANN, J., MAGEE, A. I., KELSELL, D. P., & BUXTON, R. S. (1999). N-terminal deletion in a desmosomal cadherin causes the autosomal dominant skin disease striate palmoplantar keratoderma. *Hum Mol Genet, 8*(6), 971-976.

RISEK, B., KLIER, F. G., & GILULA, N. B. (1992). Multiple gap junction genes are utilized during rat skin and hair development. *Development, 116*(3), 639-651.

ROBINSON, R. A., LU, X., JONES, E. Y., & SIEBOLD, C. (2008). Biochemical and structural studies of ASPP proteins reveal differential binding to p53, p63, and p73. *Structure, 16*(2), 259-268. doi: 10.1016/j.str.2007.11.012

ROMANO, R. A., SMALLEY, K., MAGRAW, C., SERNA, V. A., KURITA, T., RAGHAVAN, S., & SINHA, S. (2012). DeltaNp63 knockout mice reveal its indispensable role as a master regulator of epithelial development and differentiation. *Development, 139*(4), 772-782. doi: 10.1242/dev.071191

ROSS, S. E., HEMATI, N., LONGO, K. A., BENNETT, C. N., LUCAS, P. C., ERICKSON, R. L., & MACDOUGALD, O. A. (2000). Inhibition of adipogenesis by Wnt signaling. *Science, 289*(5481), 950-953.

RUHRBERG, C., HAJIBAGHERI, M. A., PARRY, D. A., & WATT, F. M. (1997). Periplakin, a novel component of cornified envelopes and desmosomes that belongs to the plakin family and forms complexes with envoplakin. *J Cell Biol, 139*(7), 1835-1849.

RUIZ, P., BRINKMANN, V., LEDERMANN, B., BEHREND, M., GRUND, C., THALHAMMER, C., VOGEL, F., BIRCHMEIER, C., GUNTHERT, U., FRANKE, W. W., & BIRCHMEIER, W. (1996). Targeted mutation of plakoglobin in mice reveals essential functions of desmosomes in the embryonic heart. *J Cell Biol, 135*(1), 215-225.

RUNSWICK, S. K., O'HARE, M. J., JONES, L., STREULI, C. H., & GARROD, D. R. (2001). Desmosomal adhesion regulates epithelial morphogenesis and cell positioning. *Nat Cell Biol, 3*(9), 823-830. doi: 10.1038/ncb0901-823

SAFFITZ, J. E. (2009). Desmosome mutations in arrhythmogenic right ventricular cardiomyopathy: important insight but only part of the picture. *Circ Cardiovasc Genet, 2*(5), 415-417. doi: 10.1161/CIRCGENETICS.109.909366

SAMUELOV, L., SARIG, O., HARMON, R. M., RAPAPORT, D., ISHIDA-YAMAMOTO, A., ISAKOV, O., KOETSIER, J. L., GAT, A., GOLDBERG, I., BERGMAN, R., SPIEGEL, R., EYTAN, O., GELLER, S., PELEG, S., SHOMRON, N., GOH, C. S., WILSON, N. J., SMITH, F. J., POHLER, E., SIMPSON, M. A., MCLEAN, W. H., IRVINE, A. D., HOROWITZ, M., MCGRATH, J. A., GREEN, K. J., & SPRECHER, E. (2013). Desmoglein 1 deficiency results in severe dermatitis, multiple allergies and metabolic wasting. *Nat Genet, 45*(10), 1244-1248. doi: 10.1038/ng.2739

SAMUELS-LEV, Y., O'CONNOR, D. J., BERGAMASCHI, D., TRIGIANTE, G., HSIEH, J. K., ZHONG, S., CAMPARGUE, I., NAUMOVSKI, L., CROOK, T., & LU, X. (2001). ASPP proteins specifically stimulate the apoptotic function of p53. *Mol Cell, 8*(4), 781-794.

SAVAGNER, P., KUSEWITT, D. F., CARVER, E. A., MAGNINO, F., CHOI, C., GRIDLEY, T., & HUDSON, L. G. (2005). Developmental transcription factor slug is required for effective re-epithelialization by adult keratinocytes. *J Cell Physiol, 202*(3), 858-866. doi: 10.1002/jcp.20188

SAVAGNER, P., YAMADA, K. M., & THIERY, J. P. (1997). The zinc-finger protein slug causes desmosome dissociation, an initial and necessary step for growth factor-induced epithelial-mesenchymal transition. *J Cell Biol, 137*(6), 1403-1419.

SAVIGNAC, M., EDIR, A., SIMON, M., & HOVNANIAN, A. (2011). Darier disease : a disease model of impaired calcium homeostasis in the skin. *Biochim Biophys Acta, 1813*(5), 1111-1117. doi: 10.1016/j.bbamcr.2010.12.006

SCHAFER, M., & WERNER, S. (2008). Cancer as an overhealing wound: an old hypothesis revisited. *Nat Rev Mol Cell Biol, 9*(8), 628-638. doi: 10.1038/nrm2455

SCHITTENHELM, M. M., ILLING, B., AHMUT, F., RASP, K. H., BLUMENSTOCK, G., DOHNER, K., LOPEZ, C. D., & KAMPA-SCHITTENHELM, K. M. (2013). Attenuated expression of apoptosis stimulating protein of p53-2 (ASPP2) in human acute leukemia is associated with therapy failure. *PLoS One, 8*(11), e80193. doi: 10.1371/journal.pone.0080193

SCHMIDT, A., & KOCH, P. J. (2007). Desmosomes: just cell adhesion or is there more? *Cell Adh Migr, 1*(1), 28-32.

SCHMITTGEN, T. D., & LIVAK, K. J. (2008). Analyzing real-time PCR data by the comparative C(T) method. *Nat Protoc, 3*(6), 1101-1108.

SEGRE, J. (2003). Complex redundancy to build a simple epidermal permeability barrier. *Curr Opin Cell Biol, 15*(6), 776-782.

SEN, C. K., GORDILLO, G. M., ROY, S., KIRSNER, R., LAMBERT, L., HUNT, T. K., GOTTRUP, F., GURTNER, G. C., & LONGAKER, M. T. (2009). Human skin wounds: a major and snowballing threat to public health and the economy. *Wound Repair Regen, 17*(6), 763-771. doi: 10.1111/j.1524-475X.2009.00543.x

SETZER, S. V., CALKINS, C. C., GARNER, J., SUMMERS, S., GREEN, K. J., & KOWALCZYK, A. P. (2004). Comparative analysis of armadillo family proteins in the regulation of a431 epithelial cell junction assembly, adhesion and migration. *J Invest Dermatol, 123*(3), 426-433. doi: 10.1111/j.0022-202X.2004.23319.x

SEVILLA, L. M., NACHAT, R., GROOT, K. R., & WATT, F. M. (2008). Kazrin regulates keratinocyte cytoskeletal networks, intercellular junctions and differentiation. *J Cell Sci, 121*(Pt 21), 3561-3569. doi: 10.1242/jcs.029538

SGROI, D. C., TENG, S., ROBINSON, G., LEVANGIE, R., HUDSON, J. R., JR., & ELKAHLOUN, A. G. (1999). In vivo gene expression profile analysis of human breast cancer progression. *Cancer Res, 59*(22), 5656-5661.

SHAROV, A. A., WEINER, L., SHAROVA, T. Y., SIEBENHAAR, F., ATOYAN, R., REGINATO, A. M., MCNAMARA, C. A., FUNA, K., GILCHREST, B. A., BRISSETTE, J. L., & BOTCHKAREV, V. A. (2003). Noggin overexpression inhibits eyelid opening by altering epidermal apoptosis and differentiation. *EMBO J, 22*(12), 2992-3003. doi: 10.1093/emboj/cdg291

SHEU, H. M., KITAJIMA, Y., & YAOITA, H. (1989). Involvement of protein kinase C in translocation of desmoplakins from cytosol to plasma membrane during desmosome formation in human squamous cell carcinoma cells grown in low to normal calcium concentration. *Exp Cell Res, 185*(1), 176-190.

SHI, W., CHEN, H., SUN, J., BUCKLEY, S., ZHAO, J., ANDERSON, K. D., WILLIAMS, R. G., & WARBURTON, D. (2003). TACE is required for fetal murine cardiac development and modeling. *Dev Biol, 261*(2), 371-380.

SHIH, J. Y., & YANG, P. C. (2011). The EMT regulator slug and lung carcinogenesis. *Carcinogenesis, 32*(9), 1299-1304. doi: 10.1093/carcin/bgr110

SHIMIZU, Y., THUMKEO, D., KEEL, J., ISHIZAKI, T., OSHIMA, H., OSHIMA, M., NODA, Y., MATSUMURA, F., TAKETO, M. M., & NARUMIYA, S. (2005). ROCK-I regulates closure of the eyelids and ventral body wall by inducing assembly of actomyosin bundles. *J Cell Biol, 168*(6), 941-953. doi: 10.1083/jcb.200411179

SHIRAKATA, Y., KIMURA, R., NANBA, D., IWAMOTO, R., TOKUMARU, S., MORIMOTO, C., YOKOTA, K., NAKAMURA, M., SAYAMA, K., MEKADA, E., HIGASHIYAMA, S., & HASHIMOTO, K. (2005). Heparin-binding EGF-like growth factor accelerates keratinocyte migration and skin wound healing. *J Cell Sci, 118*(Pt 11), 2363-2370. doi: 10.1242/jcs.02346

SIBILIA, M., FLEISCHMANN, A., BEHRENS, A., STINGL, L., CARROLL, J., WATT, F. M., SCHLESSINGER, J., & WAGNER, E. F. (2000). The EGF receptor provides an essential survival signal for SOS-dependent skin tumor development. *Cell, 102*(2), 211-220.

SIGRIST, C. J., CERUTTI, L., DE CASTRO, E., LANGENDIJK-GENEVAUX, P. S., BULLIARD, V., BAIROCH, A., & HULO, N. (2010). PROSITE, a protein domain database for functional characterization and annotation. *Nucleic Acids Res, 38*(Database issue), D161-166. doi: 10.1093/nar/gkp885

SIMON, M., JONCA, N., GUERRIN, M., HAFTEK, M., BERNARD, D., CAUBET, C., EGELRUD, T., SCHMIDT, R., & SERRE, G. (2001). Refined characterization of corneodesmosin proteolysis during terminal differentiation of human epidermis and its relationship to desquamation. *J Biol Chem, 276*(23), 20292-20299. doi: 10.1074/jbc.M100201200

SIMPSON, C. L., PATEL, D. M., & GREEN, K. J. (2011). Deconstructing the skin: cytoarchitectural determinants of epidermal morphogenesis. *Nat Rev Mol Cell Biol, 12*(9), 565-580. doi: 10.1038/nrm3175

SIMPSON, M. A., COOK, R. W., SOLANKI, P., PATTON, M. A., DENNIS, J. A., & CROSBY, A. H. (2009a). A mutation in NFkappaB interacting protein 1 causes cardiomyopathy and woolly haircoat syndrome of Poll Hereford cattle. *Anim Genet, 40*(1), 42-46. doi: 10.1111/j.1365-2052.2008.01796.x

SIMPSON, M. A., MANSOUR, S., AHNOOD, D., KALIDAS, K., PATTON, M. A., MCKENNA, W. J., BEHR, E. R., & CROSBY, A. H. (2009b). Homozygous mutation of desmocollin-2 in arrhythmogenic right ventricular cardiomyopathy with mild palmoplantar keratoderma and woolly hair. *Cardiology, 113*(1), 28-34. doi: 10.1159/000165696

SKERROW, C. J., CLELLAND, D. G., & SKERROW, D. (1989). Changes to desmosomal antigens and lectin-binding sites during differentiation in normal human epidermis: a quantitative ultrastructural study. *J Cell Sci, 92 (Pt 4)*, 667-677.

SLEE, E. A., GILLOTIN, S., BERGAMASCHI, D., ROYER, C., LLANOS, S., ALI, S., JIN, B., TRIGIANTE, G., & LU, X. (2004). The N-terminus of a novel isoform of human iASPP is required for its cytoplasmic localization. *Oncogene, 23*(56), 9007-9016. doi: 10.1038/sj.onc.1208088

SMITH, E. A., & FUCHS, E. (1998). Defining the interactions between intermediate filaments and desmosomes. *J Cell Biol, 141*(5), 1229-1241.

SONNENBERG, A., & LIEM, R. K. (2007). Plakins in development and disease. *Exp Cell Res, 313*(10), 2189-2203. doi: 10.1016/j.yexcr.2007.03.039

SOTTOCORNOLA, R., ROYER, C., VIVES, V., TORDELLA, L., ZHONG, S., WANG, Y., RATNAYAKA, I., SHIPMAN, M., CHEUNG, A., GASTON-MASSUET, C., FERRETTI, P., MOLNAR, Z., & LU, X. (2010). ASPP2 binds Par-3 and controls the polarity and proliferation of neural progenitors during CNS development. *Dev Cell, 19*(1), 126-137. doi: 10.1016/j.devcel.2010.06.003

SOUTH, A. P., WAN, H., STONE, M. G., DOPPING-HEPENSTAL, P. J., PURKIS, P. E., MARSHALL, J. F., LEIGH, I. M., EADY, R. A., HART, I. R., & MCGRATH, J. A. (2003). Lack of plakophilin 1 increases keratinocyte migration and reduces desmosome stability. *J Cell Sci, 116*(Pt 16), 3303-3314. doi: 10.1242/jcs.00636

SPECHLER, S. J. (2002). Clinical practice. Barrett's Esophagus. *N Engl J Med, 346*(11), 836-842. doi: 10.1056/NEJMcp012118

STADELI, R., HOFFMANS, R., & BASLER, K. (2006). Transcription under the control of nuclear Arm/beta-catenin. *Curr Biol, 16*(10), R378-385. doi: 10.1016/j.cub.2006.04.019

STAPPENBECK, T. S., BORNSLAEGER, E. A., CORCORAN, C. M., LUU, H. H., VIRATA, M. L., & GREEN, K. J. (1993). Functional analysis of desmoplakin domains: specification of the interaction with keratin versus vimentin intermediate filament networks. *J Cell Biol, 123*(3), 691-705.

STAPPENBECK, T. S., LAMB, J. A., CORCORAN, C. M., & GREEN, K. J. (1994). Phosphorylation of the desmoplakin COOH terminus negatively regulates its interaction with keratin intermediate filament networks. *J Biol Chem, 269*(47), 29351-29354.

STOCKINGER, A., EGER, A., WOLF, J., BEUG, H., & FOISNER, R. (2001). E-cadherin regulates cell growth by modulating proliferation-dependent beta-catenin transcriptional activity. *J Cell Biol, 154*(6), 1185-1196. doi: 10.1083/jcb.200104036

STOJADINOVIC, O., PASTAR, I., VUKELIC, S., MAHONEY, M. G., BRENNAN, D., KRZYZANOWSKA, A., GOLINKO, M., BREM, H., & TOMIC-CANIC, M. (2008). Deregulation of keratinocyte differentiation and activation: a hallmark of venous ulcers. *J Cell Mol Med, 12*(6B), 2675-2690. doi: 10.1111/j.1582-4934.2008.00321.x

STRAUB, W. E., WEBER, T. A., SCHAFER, B., CANDI, E., DURST, F., OU, H. D., RAJALINGAM, K., MELINO, G., & DOTSCH, V. (2010). The C-terminus of p63 contains multiple regulatory elements with different functions. *Cell Death Dis, 1*, e5. doi: 10.1038/cddis.2009.1

SU, M., GU, Y., SU, S., & LU, B. (2014). [Expression of ASPP gene family and its relationship with survival of patients with non-small cell lung cancer]. *Zhonghua Zhong Liu Za Zhi, 36*(4), 268-272.

SU, X., PARIS, M., GI, Y. J., TSAI, K. Y., CHO, M. S., LIN, Y. L., BIERNASKIE, J. A., SINHA, S., PRIVES, C., PEVNY, L. H., MILLER, F. D., & FLORES, E. R. (2009). TAp63 prevents premature aging by promoting adult stem cell maintenance. *Cell Stem Cell, 5*(1), 64-75. doi: 10.1016/j.stem.2009.04.003

SWARTZENDRUBER, D. C., WERTZ, P. W., KITKO, D. J., MADISON, K. C., & DOWNING, D. T. (1989). Molecular models of the intercellular lipid lamellae in mammalian stratum corneum. *J Invest Dermatol, 92*(2), 251-257.

SYRRIS, P., WARD, D., ASIMAKI, A., EVANS, A., SEN-CHOWDHRY, S., HUGHES, S. E., & MCKENNA, W. J. (2007). Desmoglein-2 mutations in arrhythmogenic right ventricular cardiomyopathy: a genotype-phenotype characterization of familial disease. *Eur Heart J, 28*(5), 581-588. doi: 10.1093/eurheartj/ehl380

SYRRIS, P., WARD, D., EVANS, A., ASIMAKI, A., GANDJBAKHCH, E., SEN-CHOWDHRY, S., & MCKENNA, W. J. (2006). Arrhythmogenic right ventricular dysplasia/cardiomyopathy associated with mutations in the desmosomal gene desmocollin-2. *Am J Hum Genet, 79*(5), 978-984. doi: 10.1086/509122

SZEVERENYI, I., CASSIDY, A. J., CHUNG, C. W., LEE, B. T., COMMON, J. E., OGG, S. C., CHEN, H., SIM, S. Y., GOH, W. L., NG, K. W., SIMPSON, J. A., CHEE, L. L., ENG, G. H., LI, B., LUNNY, D. P., CHUON, D., VENKATESH, A., KHOO, K. H., MCLEAN, W. H., LIM, Y. P., & LANE, E. B. (2008). The Human Intermediate Filament Database: comprehensive information on a gene family involved in many human diseases. *Hum Mutat, 29*(3), 351-360. doi: 10.1002/humu.20652

TAKAHASHI, N., KOBAYASHI, S., JIANG, X., KITAGORI, K., IMAI, K., HIBI, Y., & OKAMOTO, T. (2004). Expression of 53BP2 and ASPP2 proteins from TP53BP2 gene by alternative splicing. *Biochem Biophys Res Commun, 315*(2), 434-438. doi: 10.1016/j.bbrc.2004.01.079

TAO, H., SHIMIZU, M., KUSUMOTO, R., ONO, K., NOJI, S., & OHUCHI, H. (2005). A dual role of FGF10 in proliferation and coordinated migration of epithelial leading edge cells during mouse eyelid development. *Development, 132*(14), 3217-3230. doi: 10.1242/dev.01892

TERAISHI, T., & YOSHIOKA, M. (2001). Electron-microscopic and immunohistochemical studies of eyelid reopening in the mouse. *Anat Embryol (Berl), 204*(2), 101-107.

THOMASON, H. A., COOPER, N. H., ANSELL, D. M., CHIU, M., MERRIT, A. J., HARDMAN, M. J., & GARROD, D. R. (2012). Direct evidence that PKCalpha positively regulates wound re-epithelialization: correlation with changes in desmosomal adhesiveness. *J Pathol, 227*(3), 346-356. doi: 10.1002/path.4016

THOMASON, H. A., SCOTHERN, A., MCHARG, S., & GARROD, D. R. (2010). Desmosomes: adhesive strength and signalling in health and disease. *Biochem J, 429*(3), 419-433. doi: 10.1042/BJ20100567

TOIVOLA, D. M., GOLDMAN, R. D., GARROD, D. R., & ERIKSSON, J. E. (1997). Protein phosphatases maintain the organization and structural interactions of hepatic keratin intermediate filaments. *J Cell Sci, 110 (Pt 1)*, 23-33.

TORUNER, M., FERNANDEZ-ZAPICO, M., SHA, J. J., PHAM, L., URRUTIA, R., & EGAN, L. J. (2006). Antianoikis effect of nuclear factor-kappaB through up-regulated expression of osteoprotegerin, BCL-2, and IAP-1. *J Biol Chem, 281*(13), 8686-8696. doi: 10.1074/jbc.M512178200

TOSTI, A., MISCIALI, C., PIRACCINI, B. A., FANTI, P. A., BARBARESCHI, M., & FERRETTI, R. M. (1994). Woolly hair, palmoplantar keratoderma, and cardiac abnormalities: report of a family. *Arch Dermatol, 130*(4), 522-524.

TRIGIANTE, G., & LU, X. (2006). ASPP [corrected] and cancer. *Nat Rev Cancer, 6*(3), 217-226. doi: 10.1038/nrc1818

TRUONG, A. B., KRETZ, M., RIDKY, T. W., KIMMEL, R., & KHAVARI, P. A. (2006). p63 regulates proliferation and differentiation of developmentally mature keratinocytes. *Genes Dev, 20*(22), 3185-3197. doi: 10.1101/gad.1463206

TSELEPIS, C., CHIDGEY, M., NORTH, A., & GARROD, D. (1998). Desmosomal adhesion inhibits invasive behavior. *Proc Natl Acad Sci U S A, 95*(14), 8064-8069.

TSURUTA, D., HASHIMOTO, T., HAMILL, K. J., & JONES, J. C. (2011). Hemidesmosomes and focal contact proteins: functions and cross-talk in keratinocytes, bullous diseases and wound healing. *J Dermatol Sci, 62*(1), 1-7. doi: 10.1016/j.jdermsci.2011.01.005

TURNQUIST, C., WANG, Y., SEVERSON, D. T., ZHONG, S., SUN, B., MA, J., CONSTANINESCU, S. N., ANSORGE, O., STOLP, H. B., MOLNAR, Z., SZELE, F. G., & LU, X. (2014). STAT1-induced ASPP2 transcription identifies a link between neuroinflammation, cell polarity, and tumor suppression. *Proc Natl Acad Sci U S A, 111*(27), 9834-9839. doi: 10.1073/pnas.1407898111

UZUMCU, A., NORGETT, E. E., DINDAR, A., UYGUNER, O., NISLI, K., KAYSERILI, H., SAHIN, S. E., DUPONT, E., SEVERS, N. J., LEIGH, I. M., YUKSEL-APAK, M., KELSELL, D. P., & WOLLNIK, B. (2006). Loss of desmoplakin isoform I causes early onset cardiomyopathy and heart failure in a Naxos-like syndrome. *J Med Genet, 43*(2), e5. doi: 10.1136/jmg.2005.032904

VASIOUKHIN, V. (2012). Adherens junctions and cancer. *Subcell Biochem, 60*, 379-414. doi: 10.1007/978-94-007-4186-7_16

VASIOUKHIN, V., BOWERS, E., BAUER, C., DEGENSTEIN, L., & FUCHS, E. (2001). Desmoplakin is essential in epidermal sheet formation. *Nat Cell Biol, 3*(12), 1076-1085. doi: 10.1038/ncb1201-1076

VIVES, V., SU, J., ZHONG, S., RATNAYAKA, I., SLEE, E., GOLDIN, R., & LU, X. (2006). ASPP2 is a haploinsufficient tumor suppressor that cooperates with p53 to suppress tumor growth. *Genes Dev, 20*(10), 1262-1267. doi: 10.1101/gad.374006

VOOIJS, M., JONKERS, J., & BERNS, A. (2001). A highly efficient ligand-regulated Cre recombinase mouse line shows that LoxP recombination is position dependent. *EMBO Rep, 2*(4), 292-297. doi: 10.1093/embo-reports/kve064

WAHL, J. K., SACCO, P. A., MCGRANAHAN-SADLER, T. M., SAUPPE, L. M., WHEELOCK, M. J., & JOHNSON, K. R. (1996). Plakoglobin domains that define its association with the desmosomal cadherins and the classical cadherins: identification of unique and shared domains. *J Cell Sci, 109 (Pt 5)*, 1143-1154.

WALLIS, S., LLOYD, S., WISE, I., IRELAND, G., FLEMING, T. P., & GARROD, D. (2000). The alpha isoform of protein kinase C is involved in signaling the response of desmosomes to wounding in cultured epithelial cells. *Mol Biol Cell, 11*(3), 1077-1092.

WAN, H., DOPPING-HEPENSTAL, P. J., GRATIAN, M. J., STONE, M. G., ZHU, G., PURKIS, P. E., SOUTH, A. P., KEANE, F., ARMSTRONG, D. K., BUXTON, R. S., MCGRATH, J. A., & EADY, R. A. (2004). Striate palmoplantar keratoderma arising from desmoplakin and desmoglein 1 mutations is associated with contrasting perturbations of desmosomes and the keratin filament network. *Br J Dermatol, 150*(5), 878-891. doi: 10.1111/j.1365-2133.2004.05996.x

WAN, H., SOUTH, A. P., & HART, I. R. (2007). Increased keratinocyte proliferation initiated through downregulation of desmoplakin by RNA interference. *Exp Cell Res, 313*(11), 2336-2344. doi: 10.1016/j.yexcr.2007.01.010

WANG, P., LOU, P. J., LEU, S., & OUYANG, P. (2002). Modulation of alternative pre-mRNA splicing in vivo by pinin. *Biochem Biophys Res Commun, 294*(2), 448-455. doi: 10.1016/S0006-291X(02)00495-3

WANG, Y., GODIN-HEYMANN, N., DAN WANG, X., BERGAMASCHI, D., LLANOS, S., & LU, X. (2013). ASPP1 and ASPP2 bind active RAS, potentiate RAS signalling and enhance p53 activity in cancer cells. *Cell Death Differ, 20*(4), 525-534. doi: 10.1038/cdd.2013.3

WANKELL, M., MUNZ, B., HUBNER, G., HANS, W., WOLF, E., GOPPELT, A., & WERNER, S. (2001). Impaired wound healing in transgenic mice overexpressing the activin antagonist follistatin in the epidermis. *EMBO J, 20*(19), 5361-5372. doi: 10.1093/emboj/20.19.5361

WARREN, S. J., LIN, M. S., GIUDICE, G. J., HOFFMANN, R. G., HANS-FILHO, G., AOKI, V., RIVITTI, E. A., SANTOS, V., & DIAZ, L. A. (2000). The prevalence of antibodies against desmoglein 1 in endemic pemphigus foliaceus in Brazil. Cooperative Group on Fogo Selvagem Research. *N Engl J Med, 343*(1), 23-30. doi: 10.1056/NEJM200007063430104

WATT, F. M. (2002). Role of integrins in regulating epidermal adhesion, growth and differentiation. *EMBO J, 21*(15), 3919-3926. doi: 10.1093/emboj/cdf399

WATT, F. M., MATTEY, D. L., & GARROD, D. R. (1984). Calcium-induced reorganization of desmosomal components in cultured human keratinocytes. *J Cell Biol, 99*(6), 2211-2215.

WEHRLI, P., VIARD, I., BULLANI, R., TSCHOPP, J., & FRENCH, L. E. (2000). Death receptors in cutaneous biology and disease. *J Invest Dermatol, 115*(2), 141-148. doi: 10.1046/j.1523-1747.2000.00037.x

WEISKE, J., SCHONEBERG, T., SCHRODER, W., HATZFELD, M., TAUBER, R., & HUBER, O. (2001). The fate of desmosomal proteins in apoptotic cells. *J Biol Chem, 276*(44), 41175-41181. doi: 10.1074/jbc.M105769200

WENG, J., LUO, J., CHENG, X., JIN, C., ZHOU, X., QU, J., TU, L., AI, D., LI, D., WANG, J., MARTIN, J. F., AMENDT, B. A., & LIU, M. (2008). Deletion of G protein-coupled receptor 48 leads to ocular anterior segment dysgenesis (ASD) through down-regulation of Pitx2. *Proc Natl Acad Sci U S A, 105*(16), 6081-6086. doi: 10.1073/pnas.0708257105

WHITE, F. H., & GOHARI, K. (1984). Desmosomes in hamster cheek pouch epithelium: their quantitative characterization during epithelial differentiation. *J Cell Sci, 66*, 411-429.

WHITTOCK, N. V. (2003). Genomic sequence analysis of the mouse desmoglein cluster reveals evidence for six distinct genes: characterization of mouse DSG4, DSG5, and DSG6. *J Invest Dermatol, 120*(6), 970-980.

WHITTOCK, N. V., ASHTON, G. H., DOPPING-HEPENSTAL, P. J., GRATIAN, M. J., KEANE, F. M., EADY, R. A., & MCGRATH, J. A. (1999). Striate palmoplantar keratoderma resulting from desmoplakin haploinsufficiency. *J Invest Dermatol, 113*(6), 940-946. doi: 10.1046/j.1523-1747.1999.00783.x

WHITTOCK, N. V., HAFTEK, M., ANGOULVANT, N., WOLF, F., PERROT, H., EADY, R. A., & MCGRATH, J. A. (2000). Genomic amplification of the human plakophilin 1 gene and detection of a new mutation in ectodermal dysplasia/skin fragility syndrome. *J Invest Dermatol, 115*(3), 368-374. doi: 10.1046/j.1523-1747.2000.00082.x

WOJCIK, S. M., LONGLEY, M. A., & ROOP, D. R. (2001). Discovery of a novel murine keratin 6 (K6) isoform explains the absence of hair and nail defects in mice deficient for K6a and K6b. *J Cell Biol, 154*(3), 619-630. doi: 10.1083/jcb.200102079

WONG, P., COLUCCI-GUYON, E., TAKAHASHI, K., GU, C., BABINET, C., & COULOMBE, P. A. (2000). Introducing a null mutation in the mouse K6alpha and K6beta genes reveals their essential structural role in the oral mucosa. *J Cell Biol, 150*(4), 921-928.

WUBAH, J. A., IBRAHIM, M. M., GAO, X., NGUYEN, D., PISANO, M. M., & KNUDSEN, T. B. (1996). Teratogen-induced eye defects mediated by p53-dependent apoptosis. *Curr Biol, 6*(1), 60-69.

XIA, Y., & KAO, W. W. (2004). The signaling pathways in tissue morphogenesis: a lesson from mice with eye-open at birth phenotype. *Biochem Pharmacol, 68*(6), 997-1001. doi: 10.1016/j.bcp.2004.05.028

YAMAZAKI, S., IWAMOTO, R., SAEKI, K., ASAKURA, M., TAKASHIMA, S., YAMAZAKI, A., KIMURA, R., MIZUSHIMA, H., MORIBE, H., HIGASHIYAMA, S., ENDOH, M., KANEDA, Y., TAKAGI, S., ITAMI, S., TAKEDA, N., YAMADA, G., & MEKADA, E. (2003). Mice with defects in HB-EGF ectodomain shedding show severe developmental abnormalities. *J Cell Biol, 163*(3), 469-475. doi: 10.1083/jcb.200307035

YAN, S. R., JOSEPH, R. R., ROSEN, K., REGINATO, M. J., JACKSON, A., ALLAIRE, N., BRUGGE, J. S., JOBIN, C., & STADNYK, A. W. (2005). Activation of NF-kappaB following detachment delays apoptosis in intestinal epithelial cells. *Oncogene, 24*(43), 6482-6491. doi: 10.1038/sj.onc.1208810

YANG, A., KAGHAD, M., WANG, Y., GILLETT, E., FLEMING, M. D., DOTSCH, V., ANDREWS, N. C., CAPUT, D., & MCKEON, F. (1998). p63, a p53 homolog at 3q27-29, encodes multiple products with transactivating, death-inducing, and dominant-negative activities. *Mol Cell, 2*(3), 305-316.

YANG, A., ZHU, Z., KAPRANOV, P., MCKEON, F., CHURCH, G. M., GINGERAS, T. R., & STRUHL, K. (2006). Relationships between p63 binding, DNA sequence, transcription activity, and biological function in human cells. *Mol Cell, 24*(4), 593-602. doi: 10.1016/j.molcel.2006.10.018

YANG, J. P., HORI, M., SANDA, T., & OKAMOTO, T. (1999). Identification of a novel inhibitor of nuclear factor-kappaB, RelA-associated inhibitor. *J Biol Chem, 274*(22), 15662-15670.

YANG, L., CHEN, Y., CUI, T., KNOSEL, T., ZHANG, Q., ALBRING, K. F., HUBER, O., & PETERSEN, I. (2012). Desmoplakin acts as a tumor suppressor by inhibition of the Wnt/beta-catenin signaling pathway in human lung cancer. *Carcinogenesis, 33*(10), 1863-1870. doi: 10.1093/carcin/bgs226

YASHIRO, M., NISHIOKA, N., & HIRAKAWA, K. (2006). Decreased expression of the adhesion molecule desmoglein-2 is associated with diffuse-type gastric carcinoma. *Eur J Cancer, 42*(14), 2397-2403. doi: 10.1016/j.ejca.2006.03.024

YIN, T., GETSIOS, S., CALDELARI, R., GODSEL, L. M., KOWALCZYK, A. P., MULLER, E. J., & GREEN, K. J. (2005a). Mechanisms of plakoglobin-dependent adhesion: desmosome-specific functions in assembly and regulation by epidermal growth factor receptor. *J Biol Chem, 280*(48), 40355-40363. doi: 10.1074/jbc.M506692200

YIN, T., GETSIOS, S., CALDELARI, R., KOWALCZYK, A. P., MULLER, E. J., JONES, J. C., & GREEN, K. J. (2005b). Plakoglobin suppresses keratinocyte motility through both cell-cell adhesion-dependent and -independent mechanisms. *Proc Natl Acad Sci U S A, 102*(15), 5420-5425. doi: 10.1073/pnas.0501676102

YIN, T., & GREEN, K. J. (2004). Regulation of desmosome assembly and adhesion. *Semin Cell Dev Biol, 15*(6), 665-677. doi: 10.1016/j.semcdb.2004.09.005

ZHANG, B., XIAO, H. J., CHEN, J., TAO, X., & CAI, L. H. (2011). Inhibitory member of the apoptosis-stimulating protein of p53 (ASPP) family promotes growth and tumorigenesis in human p53-deficient prostate cancer cells. *Prostate Cancer Prostatic Dis, 14*(3), 219-224. doi: 10.1038/pcan.2011.25

ZHANG, X., WANG, M., ZHOU, C., CHEN, S., & WANG, J. (2005). The expression of iASPP in acute leukemias. *Leuk Res, 29*(2), 179-183. doi: 10.1016/j.leukres.2004.07.001

ZHAO, J., WU, G., BU, F., LU, B., LIANG, A., CAO, L., TONG, X., LU, X., WU, M., & GUO, Y. (2010). Epigenetic silence of ankyrin-repeat-containing, SH3-domain-containing, and proline-rich-region- containing protein 1 (ASPP1) and ASPP2 genes promotes tumor growth in hepatitis B virus-positive hepatocellular carcinoma. *Hepatology, 51*(1), 142-153. doi: 10.1002/hep.23247

ZHU, Z., RAMOS, J., KAMPA, K., ADIMOOLAM, S., SIRISAWAD, M., YU, Z., CHEN, D., NAUMOVSKI, L., & LOPEZ, C. D. (2005). Control of ASPP2/(53BP2L) protein levels by proteasomal degradation modulates p53 apoptotic function. *J Biol Chem, 280*(41), 34473-34480. doi: 10.1074/jbc.M503736200

ZHURINSKY, J., SHTUTMAN, M., & BEN-ZE'EV, A. (2000). Plakoglobin and beta-catenin: protein interactions, regulation and biological roles. *J Cell Sci, 113 (Pt 18)*, 3127-3139.

Appendix

A1 Loss of iASPP leads to increased adipogenic differentiation of MEFs

The pathogenic hallmarks of ARVC include desmosome instability, cardiomyocyte loss and their replacement by fibroblasts and adipocytes. The cellular origin of the cardiac adipocytes in ARVC mouse models has been recently addressed using genetic fate mapping. It has been suggested that, during ARVC pathogenesis, the cardiac progenitors of the second heart field are more predisposed to an adipogenic fate due to suppressed Wnt signalling, which ensues from increased nuclear plakoglobin (Lombardi *et al.*, 2009; Wankell *et al.*, 2001). The ability of nuclear plakoglobin to provoke cardiac cells to undergo adipogenic differentiation has also been shown in the cardiac cell line HL1, in which downregulation of desmoplakin using sequence-specific siRNA resulted in increased nuclear plakoglobin (Garcia-Gras *et al.*, 2006). To examine whether iASPP participates in signalling pathways that control the differentiation of cardiac cells, a similar experiment was attempted in HL1 cells using siRNA against iASPP. However, these experiments were unsuccessful due to an inability to establish HL1 cells with sustained downregulation of iASPP. Future experiments will aim to circumvent this problem through the usage of CRISPR (clustered regularly interspaced short palindromic repeats) gene-editing technology.

To gain at least some insight into whether a loss of iASPP can facilitate adipogenic differentiation, MEFs isolated from iASPP$^{+/+}$ and iASPP$^{\Delta 8/\Delta 8}$ embryos were isolated and differentiated into adipocytes using a previously described protocol (Ross *et al.*, 2000; Schafer and Werner, 2008). Interestingly, compared to iASPP$^{+/+}$ MEFs, differentiation of iASPP$^{\Delta 8/\Delta 8}$ MEFs into adipocytes was more enhanced. Increased numbers of iASPP$^{\Delta 8/\Delta 8}$cells expressed adipocyte markers (PPARγ and adiponectin) and contained Oil Red-stained lipid droplets

(Figure A1). These results suggest that a loss of iASPP may influence the signalling cascades that drive adipogenic differentiation. Pursuing this line of research using cardiac cells will be important in the future if the molecular mechanisms behind ARVC pathogenesis in iASPP$^{\Delta 8/\Delta 8}$ mice are to be delineated. Nonetheless, these are very interesting findings, and show that iASPP may link the desmosomes to cell signalling in both the skin and heart.

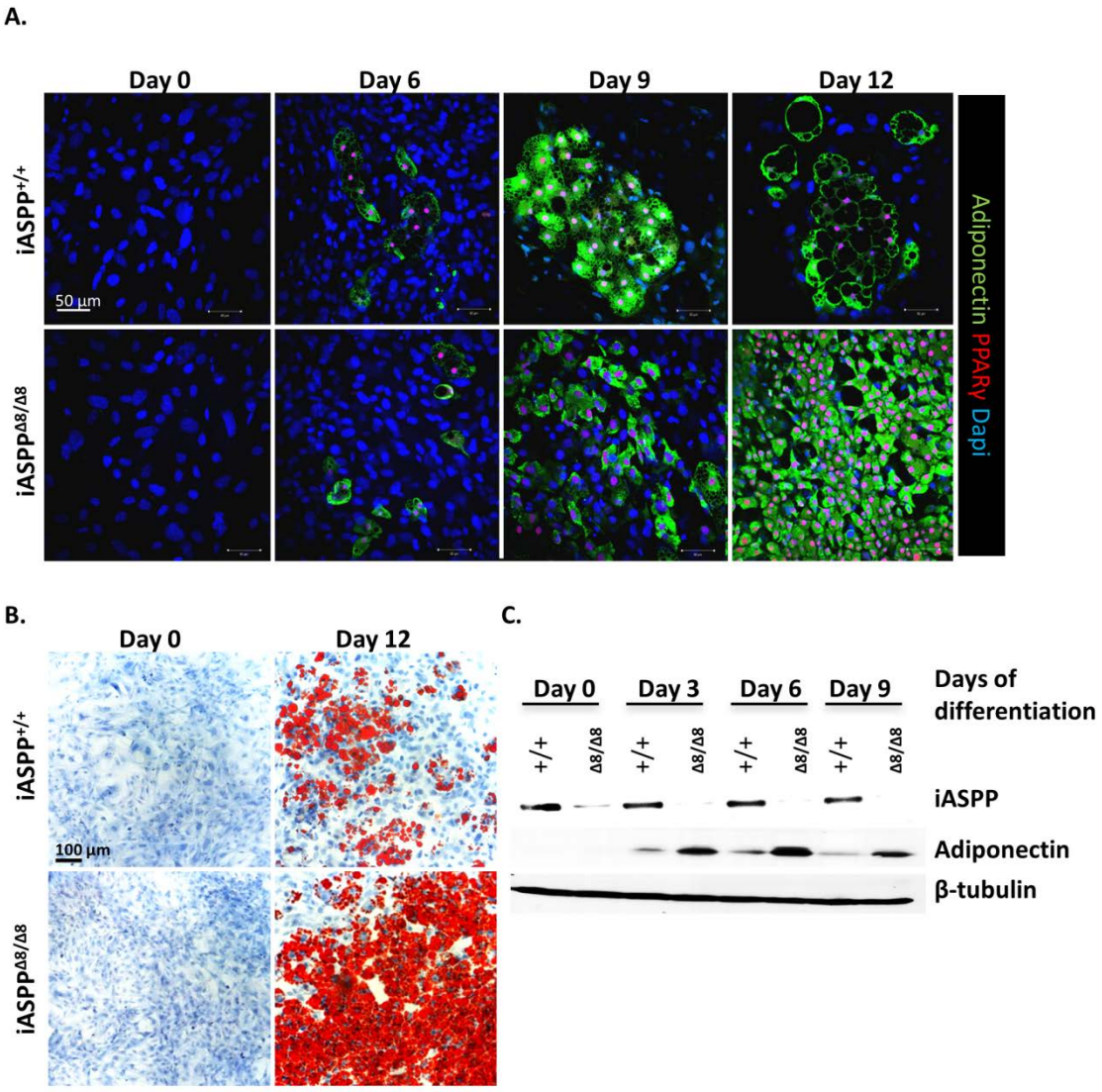

Figure A1 Enhanced adipogenic differentiation in iASPP$^{\Delta 8/\Delta 8}$ MEFs

iASPP$^{+/+}$ and iASPP$^{\Delta 8/\Delta 8}$ MEFs were maintained in DMEM with 10% FBS, and allowed to reach confluence. 2 days post confluence, they were induced to differentiate into adipocytes in growth media containing 5 µM dexamethasone, 500 µM 3-isobutyl-1-methylxanthine, 10 µg/ml insulin and 1 µM Rosiglitazone **A.** On days 0, 6, 9, 12 after differentiation was induced, cells were fixed and stained for early and late adipogenic markers PPARγ and adiponectin, respectively. **B.** On day 0 and 12 post-induction of adipogenic differentiation, the presence of cytoplasmic lipid droplets was observed by staining for Oil Red using a protocol previously described (Garcia-Gras *et al.*, 2006). **C.** Lysates from cells undergoing differentiation were collected on the indicated days and subjected to immunoblotting with antibodies against iASPP and adiponectin. For loading control, immunoblotting for β-tubulin was performed. Relative to iASPP$^{+/+}$ MEFs, exacerbated adipogenic potential in iASPP$^{\Delta 8/\Delta 8}$ MEFs can be observed.

A2 Junctional iASPP is decreased during the progression of Barrett's oesophagus to adenocarcinoma

To gain insight into whether it is worth exploring the role of iASPP during the malignant conversion of Barrett's oesophagus to adenocarcinoma, the expression of iASPP was examined in a small panel of samples taken from human patients with Barrett's oesophagus that went on to suffer from adenocarcinoma. One such sample is shown below (Figure A2 and A3). Preliminary data shows that during the malignant conversion of normal squamous epithelium to adenocarcinoma, junctional expression of iASPP is reduced while its cytoplasmic expression is increased.

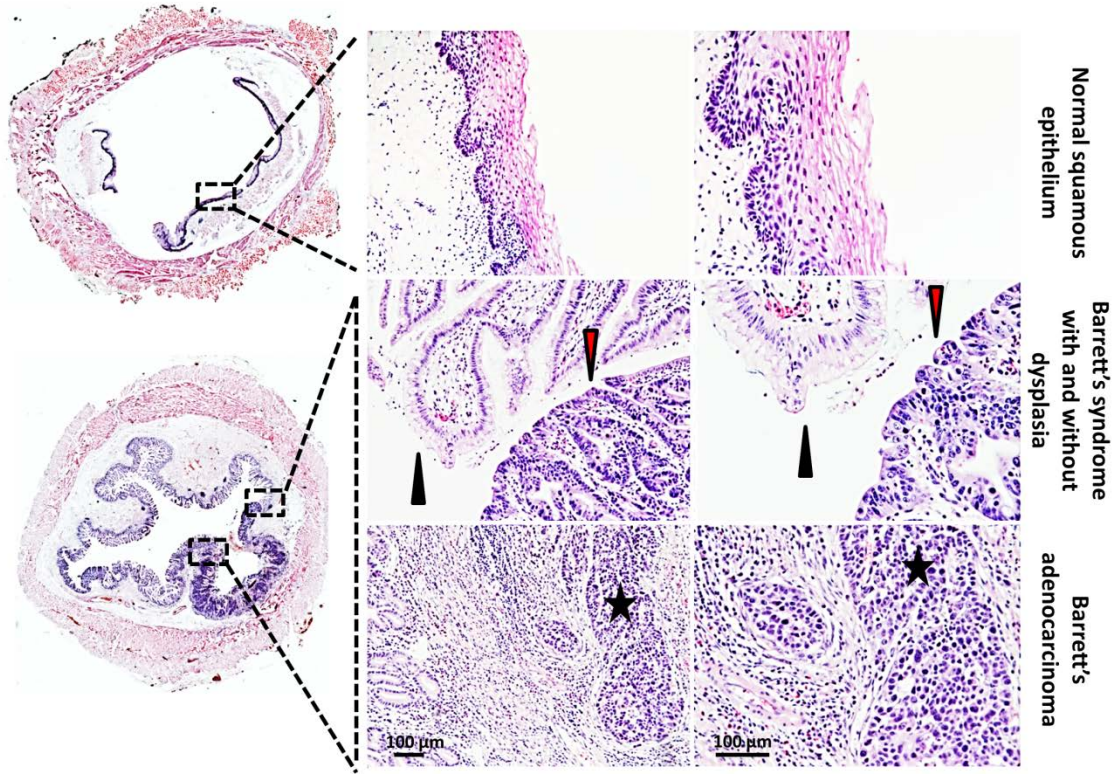

Figure A2 Conversion of oesophageal squamous epithelium to intestinal metaplasia, dysplasia and adenocarcinoma
The uppermost panels show normal stratified squamous epithelium. The panels in the second row show Barrett's oesophagus (note the characteristic intestinal goblet cells in the oesophageal squamous epithelium) without dysplasia (indicated by black arrowheads) and with dysplasia (red arrowheads). The bottom panels show adenocarcinoma (black star).

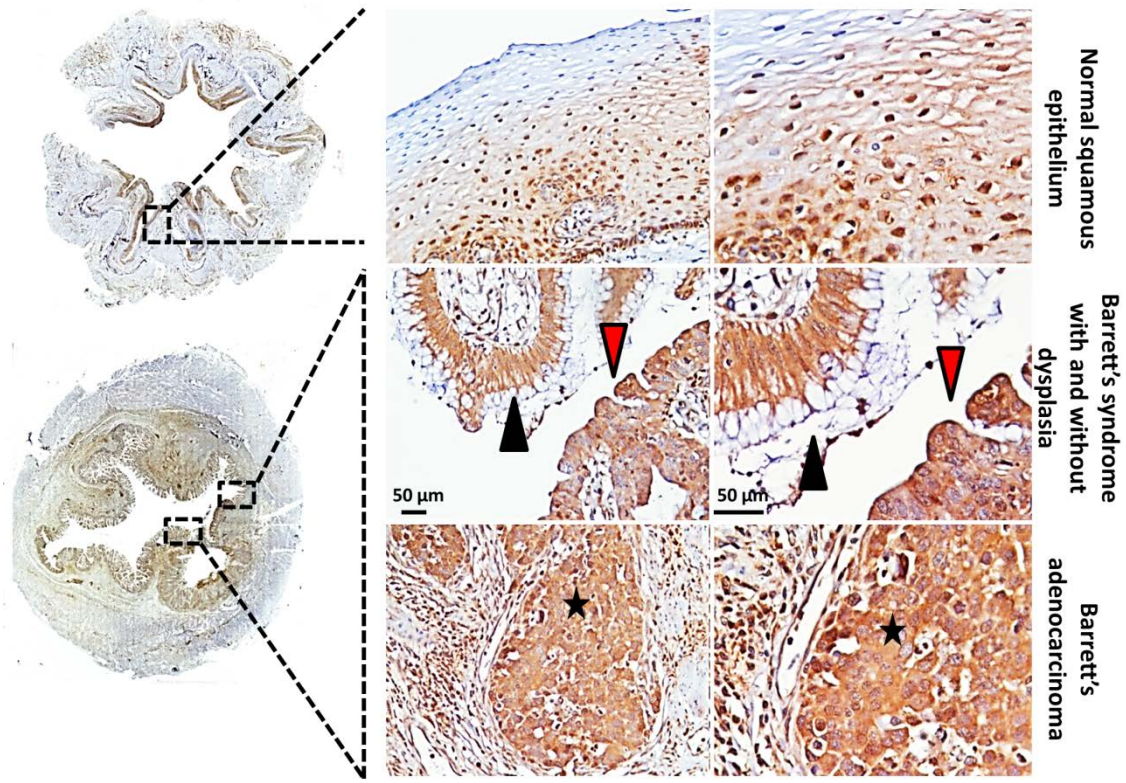

Figure A3 Loss of junctional iASPP during the conversion of oesophageal squamous epithelium to intestinal metaplasia, dysplasia and adenocarcinoma

iASPP expression was investigated during the malignant conversion of Barrett's intestinal metaplasia to adenocarcinoma. The uppermost panels show the expression of iASPP in normal stratified squamous epithelium. The panels in the second row show the expression of iASPP in Barrett's oesophagus without dysplasia (indicated by black arrowheads) and in Barrett's oesophagus with dysplasia (red arrowheads). The bottom panels show the subcellular localisation of iASPP in adenocarcinoma (black star).